POLITECNICO DI TORINO

Collegio di Ingegneria Chimica e dei Materiali

Corso di Laurea Magistrale
in Ingegneria Chimica e dei Processi Sostenibili

Tesi di Laurea Magistrale

Modified Acid Treated Bentonites as Catalysts in Selective Catalytic Reduction of Nitrogen Oxides by Ammonia
(SCR-NH_3)

Relatore

Prof.ssa Stefania Specchia

Candidato

Corinne Trabbia

Marzo 2020

Summary

The research for MSc thesis was carried out within Erasmus+ Programme at Faculty of Energy and Fuels, AGH University of Science and Technology (Kraków, Poland) in the Group of Prof. M. Motak - The Group for Catalytic and Adsorption Processes in Energy and Environmental Protection

Riassunto in italiano

1. Introduzione

La rapida crescita della concentrazione di inquinanti causa impatti negativi sull'atmosfera, sull'ambiente e sulla salute umana a livello locale, regionale e globale. Gli inquinanti vengono suddivisi in primari e secondari. I primi vengono emessi nell'ambiente direttamente dopo essere stati originati da processi di natura umana o naturale. I secondi sono, invece, sostanze che si formano a seguito di cambiamenti di vario genere, come reazioni chimico-fisiche tra gli inquinanti primari stessi o con l'atmosfera. Gli inquinanti maggiormente presenti nell'atmosfera sono: CO, CO_2, NO_x, SO_2, idrocarburi, particolato e ozono. In genere vengono anche distinte le sorgenti di emissione: sorgenti naturali o antropologiche. La concentrazione di inquinanti atmosferici emessi nell'ambiente è sufficientemente elevata da causare un aumento della mortalità, deficit polmonari e problemi cardiovascolari. Le organizzazioni sanitarie mondiali hanno stimato che l'inquinamento atmosferico urbano, generato da veicoli, industrie e fonti energetiche, uccide oltre 800'000 persone all'anno. Nel 1972 a Stoccolma, The World Health Organizations iniziò a sensibilizzare le coscienze per quanto concerne i problemi di inquinamento ambientale globale. Venne istituito il Programma Ambientale delle Nazioni Unite (UNEP), che iniziò a collaborare con l'Organizzazione Mondiale della Sanità (OMS) all'avvio di un sistema di monitoraggio ambientale globale (GEMS). Questo sistema ha permesso di creare una rete di monitoraggio dell'inquinamento atmosferico (Fig 1.1, Fig 1.2). Si stima che il numero di morti causate dall'inquinamento atmosferico sia destinato ad aumentare nei prossimi trent'anni a causa della crescita della popolazione mondiale, principalmente nelle città e nei paesi più poveri. Oggigiorno, i paesi maggiormente sviluppati hanno cercato di preservare l'ambiente dall'inquinamento atmosferico stabilendo limiti e valori target molto restrittivi al fine di migliorare la qualità dell'aria e ridurre le emissioni. L'Europa ad esempio ha messo in atto politiche sempre più restrittive che limitano le singole fonti, ma anche il totale nazionale delle emissioni in atmosfera dei principali inquinanti (Fig.1.3). Tra gli inquinanti precedentemente citati gli ossidi di azoto conosciuti come NO_x sono causa di gravi e significativi impatti negativi sull'uomo e sull'ambiente. Sono responsabili dell'inquinamento dell'aria attraverso la loro partecipazione a una serie di reazioni fotochimiche e vengono considerati come uno dei principali fattori dell'inquinamento atmosferico, in quanto, in presenza della luce solare possono venire trasformati in inquinanti acidi e sono il principale fattore della formazione dell'ozono e delle piogge acide. Sulla riduzione di questi inquinanti viene rivolta l'attenzione in questo lavoro di tesi.

La famiglia degli NO_x consiste in sei ossidi di azoto (Tab. 1.1) anche se l'attenzione viene riposta principalemte su NO e NO_2. L'elemento Azoto (N) fu scoperto nel XVII secolo e descritto da Carl Willhelm Scheel e Daniel Rutherford per la prima volta. La molecola di azoto diatomica (N_2) è molto stabile con un'energia di legame intorno ai 950 kJ/mol e rappresenta il 78% della composizione dell'aria. Il monossido di azoto (NO) è un gas incolore e altamente reattivo. Si origina dalla reazione tra ossigeno e azoto durante un qualsiasi processo di combustione ad alte temperature (1200 °C). (Eq. 1.1). Un'ulteriore ossidazione di NO può anche produrre tracce di biossido di azoto (NO_2), che generalmente non supera il 5 % del totale degli NO_x emessi. (Eq. 1.2).

Il rapporto NO_2/NO aumenta con il diminuire della temperatura. Durante un processo di combustine infatti le temperature superano i 1000°C e questo spiega il motivo del 95% di produzione di NO. NO dopo il processo di combustione tenderà a trasformarsi in NO_2: processo termodinamicamente favorito ma cineticamente molto lento. Tre meccanismi di reazione vengono riportati per la produzione di NO_x: NO_x termici, NO_x del combustibile e NO_x veloci (o prompt). Le tre diverse fonti di NO_x sono riportate in Fig. 1.4 in funzione della temperatura. A temperature molto basse gli NO_x termici sono praticamente assenti e non danno alcun contributo. NO_x prompt, derivanti dall'HC radicale, hanno un valore quasi costante indipendente dalla temperatura. Gli NO_x del combustibile contribuiscono in misura sempre minore all'aumento della temperatura. Fig 1.5 presenta le trasformazioni chimiche che causano l'inquinamento (PAN, O_3, piogge acide). Le emissioni di NO_x hanno per lo più origine antropica, solo piccole percentuali di NO_x emessi sono collegate a fonti naturali (Fig. 1.6). Il settore dei trasporti che costituisce quasi la metà del totale delle emissioni di NO_x è stato ampiamente colpito dalle restrizioni introdotte con una riduzione di di oltre il 40% negli ultimi anni (Fig. 1.7). La riduzione delle emissioni di inquinanti è diventata una sfida particolarmente complessa per la Polonia a causa dell'uso massiccio del carbone come fonte energetica e dell'obsolescenza delle infrastrutture per la produzione, trasmissione e trasporto dell'energia. La politica energetica della nazione mira a ridurre queste emissioni del 20% entro il 2030. Il carbone è il combustibile primario per il settore energetico polacco e come riportato in Fig. 1.8 è anche il principale settore della produzione di NO_x.

I metodi di riduzione delle emissioni di ossido di azoto possono essere suddivisi in due categorie principali: primari e secondari. I metodi secondari avvengono nella fase successiva alla combustione con il tentativo di ridurre gli NO_x dopo la loro emissione con la presenza di un reagente riducente. I metodi primari, invece, mirano a ridurne l'emissione durante il processo di combustione. I metodi primari (flue gas recirculation, low excess of air, fuel switching, staged combustion, fuel reburning and water/steam injection) sono più economici dei metodi secondari, anche se offrono minori efficienze di riduzione. La quantità dell'agente riducente dipende dalla potenza della caldaia e quindi i costi di funzionamento di una centrale elettrica possono aumentare in modo significativo. Due diversi processi possono essere distinti tra i metodi secondari: SNCR (Selective non-Catalytic Reduction) and SCR (Selective Catalytic Reduction). In questo lavoro di tesi l'attenzione viene riposta principalmente su SCR- NH_3 (Selective Catalytic Reduction con ammoniaca) che verrà utilizzato per testare i catalizzatori preparati. Il processo SCR è molto simile a quello SNCR in quanto utilizza allo stesso modo ammoniaca o urea come agenti riducenti, ma introduce l'applicazione di un catalizzatore al fine di abbassare l'energia di attivazione della reazione e farla avvenire a temperature più basse (170 °C - 510 °C). Le reazioni di riduzione sono riportate in Eq. 1.12, 1.13, 1.14, 1.15 e quelle indesiderate in Eq. 1.16, 1.17, 1.18, in cui l'ammoniaca viene ossidata e produce NO, N_2 e N_2O. Questa tecnologia fu inventata nel 1974 e introdotta commercialmente negli anni '80. Gli agenti riducenti più utilizzati sono urea e ammoniaca, iniettati attraverso un sistema di ugelli per garantire una miscela omogenea con il gas combustibile. Tuttavia, per motivi ambientali ed economici, la perdita di NH_3 (NH3-slip) deve essere contenuta al di sotto di un certo valore (Tab. 1.4). A causa del suo costo ridotto per kg, l'ammoniaca è l'agente più comunemente utilizzato e presenta una maggiore selettività rispetto ad altri agenti che possono essere impiegati nel processo. Tre diverse configurazioni possono presentarsi per il processo SCR: high dust, in cui il catalizzatore viene posto a valle della caldaia e opera in presenza di polvere, low dust, in cui è installato un depolveratore ad alta temperatura a monte del catalizzatore e tail end in cui il catalizzatore è posto a valle di filtrazione e desolforazione e i fumi devo essere riscaldati per il funzionamento del catalizzatore. (Fig 1.11). Sebbene il processo SCR presenti alcuni svantaggi, quali NH_3-slip e costi più elevati rispetto al processo SNCR, rimane ancora considerata la tecnologia principale e più efficiente per ridurre l'emissione di NOx. Dal momento che il processo SCR richiede l'applicazione di un catalizzatore, grandi sforzi per svilupparne di sempre maggiormente efficienti e resistenti all'avvelenamento sono stati fatti e continuano ad essere fatti in questi ultimi anni. La forte acidità e le proprietà redox sono due fattori cruciali per aumentarne le proprietà, in un'ampia finestra di temperature, che ottimizzano la formazione dei prodotti desiderati (N_2 e H_2O) e influenzano l'adsorbimento/attivazione di NH_3 e NO_x. La catalisi viene definita come un processo in cui una piccola quantità di sostanza (catalizzatore) incrementa la velocità della reazione, forma intermedi di reazione e ritorna nella sua forma originale. La prima definizione di catalizzatore fu fornita da Berzelius nel 1836: "*Un catalizzatore è una sostanza che incrementa la velocità con cui una reazione chimica raggiunge il suo equilibrio senza essere consumata in modo apprezzabile*". Un catalizzatore può aumentare solo le reazioni che sono termodinamicamente favorite, aumenta la reazione diretta e quella inversa allo stesso tempo e quando sono possibili vie di reazione multiple, il catalizzatore ne aumenta solo alcune con un incremento di selettività. La scelta del catalizzatore più adatto è quindi molto importante, ma tuttavia non esiste una teoria unificata sulla scelta del catalizzatore, la catalisi, dunque, può essere considerata una sorta di "arte", in quanto ogni industria sviluppa il suo sistema catalitico con principi basati principalmente su valutazioni empiriche. Si può inoltre distinguere tra catalisi eterogenea o omogenea. La catalisi eterogenea implica che il catalizzatore si trovi in una fase fisica diversa da quella dei reagenti; di solito il catalizzatore è un solido e i reagenti sono gassosi o liquidi. D'altra parte, la catalisi omogenea richiede che i reagenti e il catalizzatore siano nella stessa fase fisica, generalmente liquidi o gassosi. La catalisi ambientale contribuisce alla protezione ambientale e alla necessità di ridurre l'inquinamento atmosferico per poter garantire un migliore tenore di vita. Il mercato dei catalizzatori è suddiviso in quattro settori: prodotti chimici, polimeri, raffinazione, ambiente. (Fig 1.14). Dal 1995 al 2005 l'impiego di catalizzatori è cresciuto del 4% annuo, soprattutto in Nord America e in Europa.

La produzione di NO_x da gas di scarico è uno dei problemi più rilevanti e impegnativi del XXI secolo. Gli NO_x sono ancora considerati una delle sostanze più pericolose rilasciate nell'atmosfera da industrie e trasporti. Anche se gli obiettivi legislativi sono diventati sempre più restrittivi e le emissioni di NO_x sono diminuite negli ultimi decenni, il problema della loro riduzione è ancora sotto esame. Attualmente i tre catalizzatori commerciali più utilizzati nel processo SCR sono: quelli di tipo Pt a basse temperature (175-250°C), zeoliti ad alte temperature (350-600 °C) e V_2O_5/ WO_3 /TiO_2 a temperature intermedie (300-450 °C). I più usati in assoluto per processi SCR con ammoniaca sono quelli V_2O_5 / WO_3 /TiO_2, anche se non riescono a fronteggiare le nuove richieste. Risulta infatti essere il catalizzatore più utilizzato ma non quello ideale e questo implica la necessità di migliorarne alcune proprietà quali una maggiore attività in una gamma più ampia di temperature (per temperature più basse 250°C e per temperature più elevate > 400 °C), una maggiore resistenza all'acqua e SO_2, la possibilità di impiegare altri agenti riducenti (idrocarburi: metano, propano, propene e altri) e soluzioni più economiche. Molte riviste scientifiche hanno rivolto l'interesse proprio sulla ricerca di nuovi catalizzatori quali idrotalciti, cenosfere o carboni attivi. Spiccano le argille stratificate che sembrano essere ottimi candidati e per questo motivo vengono spesso utilizzate in catalisi, ma a causa della loro grande varietà continuano ad essere studiate e indagate. Rappresentano infatti una grande classe di materiali molto abbondanti in natura, a buon mercato, posso essere trattate e modificate e preparate in forma di monolite, come V_2O_5 / WO_3 /TiO_2. Le argille stratificate trattate con acido sono state i primi catalizzatori utilizzati per la catalisi di cracking e sono tuttora studiate per la loro applicazione nell'industria organica e protezione ambientale. Tra tutte le argille investigate nel corso degli anni come possibili soluzioni al problema della rimozione degli NO_x è stata prestata particolare attenzione al gruppo delle smectiti, per lo più le montmorilloniti. Queste si sono dimostrate interessanti materiali che, trattate con diversi metodi, possono modificare la loro attività, selettività, proprietà acide/basiche e strutturali. La montmorillonite era un rifiuto industriale, utilizzato per l'assorbimento e per la pulizia di oli da composti organici. Tuttavia, mediante diversi trattamenti si è dimostrata attiva e selettiva nel processo SCR a basse temperature. Pertanto, questo materiale rappresenta una fonte riutilizzabile e una buona alternativa ai comuni catalizzatori.

Fonti bibliografiche hanno dimostrato che argille in cui viene fatto il pillaring con titanio su vanadio hanno prestazioni migliori in ampie finestre di temperatura, rispetto a vanadio/TiO_2 commerciale (Fig. 1.16). Per questo motivo un catalizzatore supportato con argilla modificata potrebbe presentare anche migliori attività catalitiche. Il catalizzatore commerciale a base di vanadio, inoltre, può anche rilasciare vanadio nell'ambiente, che porta ad una possibile contaminazione secondaria nel suolo. La scelta del supporto deve essere quindi ben ponderata. Esso deve disporre di sistemi porosi ben sviluppati per facilitare l'accesso delle molecole da convertire, deve avere un'elevata stabilità termica e durata di vita. Non è stato ancora raggiunto un accordo generale sul meccanismo di rimozione degli NO_x applicando argille stratificate. In effetti, i principali siti acidi necessari per la reazione e le specie intermedie NO non sono stati ancora identificati in modo soddisfacente. Questo lavoro di tesi affronta proprio questa sfida, al fine di trovare un catalizzatore alternativo a quelli commercialmente impiegati e attivo a basse temperature. Le argille naturali sono distribuite irregolarmente nella litosfera e sono soggette a modificazioni e trasformazioni spontanee, si formano da diverse rocce in diverse condizioni, variando nella struttura, composizione chimica e proprietà. Le particelle di argilla sono sensibili ai trattamenti meccanici e chimici. Le condizioni di prova possono dar luogo a discrepanze nei risultati delle misurazioni analizzate in laboratori diversi e con tecniche di indagine diverse. Per questo motivo, i risultati delle ricerche su questi materiali sono ancora per lo più sconosciuti, possono reagire in modi diversi e le analisi non portano a risultati unici quando vengono studiate gli stessi minerali argillosi. La scienza delle argille (science clay) ha acquisito sempre maggiore rilevanza nel corso degli anni. Ogni anno sono state pubblicate diverse centinaia di relazioni scientifiche, brevetti, abstract e relazioni tecniche sulle argille ed il loro rapido sviluppo è stato sostenuto dalla formazione di comunità scientifiche correlate in diversi paesi. Ad esempio, "Clays and Clay Minerals" è la pubblicazione ufficiale di The Clay Minerals Society (Fig. 1.17). Anche se l'interesse scientifico è aumentato solamente nel corso di questi ultimi anni, l'uso pratico dell'argilla risale ai primi antichi insediamenti agrari. Gli esseri umani hanno da sempre impiegato questi materiali per costruire utensili o mattoni, anche prima di acquisire un livello di competenze sulle loro proprietà fisico-chimiche. Col tempo, le tecnologie empiriche sono state convertite in metodi scientifici basati su studi teorici. Due caratteristiche principali hanno suscitato il crescente interesse nello studio di questi materiali: le loro straordinarie proprietà e facile accessibilità. In effetti, nessun altro gruppo di materiali inorganici ha altrettanti componenti diversi che mostrano una gamma di reattività particolarmente ampia e una capacità di venire modificati allo stesso modo.

Le argille e minerali argillosi sono riconosciuti come i materiali del XXI secolo per queste tre principali caratteristiche: abbondanza, basso costo di produzione e rispetto dell'ambiente. Quando si parla di questi materiali bisogna fare una distinzione tra argille e minerali argillosi. Georgius Agricula introdusse per la prima volta il termine argilla (1494-1555). Cinque secoli dopo, Joint Nomenclature Committees (JNC) dell'Associazione internazionale per lo studio delle argille (AIPEA) e della Società dei minerali argillosi (CMS) hanno definito il termine 'clay' (argilla) come un materiale naturale composto principalmente da minerali a grana fine, generalmente con elevate proprietà plastiche con un adeguato contenuto di acqua e che si indurisce se essiccato o cotto. Tab 1.1 mostra le varie denominazioni di argilla attualmente adottate, anche se quattro tipi di argilla (bentonite, caolini, palygorskite, sepiolite e argille comuni) vengono principalmente indagate per applicazioni industriali. Secondo la definizione approvata dalla JNC, i minerali argillosi sono, invece, minerali e minerali fillosilicati che conferiscono plasticità alle argille e che si induriscono all'essiccazione o alla cottura". I minerali argillosi non si distinguono per le loro dimensioni come le argille, possono essere naturali o sintetici e possono contenere o non contenere fillosilicati (Tab 1.2).

La struttura atomica delle argille minerali è costituita da due unità base ripetute diversamente nello spazio: i fogli ottaedrici e tetraedrici (Fig 1.19). La diversificazione delle argille minerali si basa sulla diversa configurazione e disposizione di queste unità. L'unità base del foglio tetraedrico è l'unità tetraedrica in cui il silicio (Si^{4+}) condivide la sua carica con quattro ossigeni (O^{2-}). Lungo il foglio tetraedrico i tre ossigeni basali di ciascun tetraedro sono condivisi con l'unità adiacente e disposti a formare anelli esagonali. Gli atomi sono dislocati su tre livelli. Il foglio ottaedrico invece è formato da ioni Al^{3+} al centro dell'unità ottaedrica circondati da sei ioni ossidrilici. La struttura è definita diottaedrica se due dei tre siti ottaedrici sono occupati, la configurazione viene invece chiamata triottaedrica se tutte e tre le posizioni centrali sono occupate per bilanciare la carica. I due fogli (tetraedro e ottaedro) sono assemblati e condividono gli ossigeni o idrossili apicali. Da questa unione si possono distinguere due tipi di strati: lo strato 1:1 e quello 2:1. Nello strato di tipo 1:1, ci sono due piani composti da un foglio tetraedrico e un foglio ottaedrico. Un piano del foglio è costituito unicamente da ossigeni basali che appartiene al foglio tetraedrico, il secondo è costituito dagli ossigeni apicali in comune ai fogli tetraedrici e ottaedrici oltre agli idrossili appartenenti al foglio ottaedrico, mentre il terzo è costituito unicamente da idrossili appartenenti al foglio ottaedrico. Nello strato 2:1, ci sono quattro piani di anioni composti da due fogli tetraedrici e un foglio ottaedrico. Le due superfici esterne sono composte dagli ossigeni basali appartenenti alle lastre tetraedriche, mentre le due interne sono formate dagli ossigeni apicali condivisi con le lastre ottaedriche e tetraedriche, oltre agli idrossili appartenenti alla lastra ottaedrica.

Diverse specie minerali appartengono al tipo 2:1, mentre solo due minerali principali presentano strutture a strato 1:1. Inoltre, vi sono anche i minerali argillosi 2:1:1, che sono composti da un foglio ottaedrico adiacente ad uno strato 2:1. Quando i diversi strati sono collegati insieme, la struttura risultante può essere elettricamente neutra o negativamente caricata.

Il termine "bentonite" è abbastanza ambiguo. Altri nomi sono spesso utilizzati al posto della bentonite per indicare lo stesso materiale: terreno sbiancante, terreno adsorbente, argilla adsorbente o argilla vulcanica. Il termine bentonite fu utilizzato per la prima volta nel 1898 da Knight per descrivere un minerale argilloso risalente all'unità di Fort Benton delle formazioni cretacee del Wyoming. Nel 1917 Wherry e Hewitt definiscono questa argilla come un prodotto di alterazione della cenere vulcanica. Nel 1926, Ross e Shannon presentarono la seguente definizione: "La bentonite è una roccia composta essenzialmente da un minerale argilloso cristallino formato dalla devitrificazione e dalla conseguente alterazione chimica di un materiale igneo vetroso, di solito un tufo o cenere vulcanica". Bentonite è un termine geologico per materiali ad alto contenuto di minerali, è altamente plastica, può espandersi notevolmente quando assorbe acqua (fino a 12-15 volte la sua massa secca) e ha un'elevata capacità di scambio cationico. È composta da smectiti, principalmente montmorillonite. Quarzo, feldspato, gesso, calcite, pirite, ossidi di ferro e idrossidi posso anche essere presenti nella bentonite. Le proprietà della bentonite sono dovute alla struttura cristallina del gruppo delle smectiti. Le variazioni nell'acqua interstiziale e i cationi scambiabili negli spazi intercalari influenzano le proprietà della bentonite. In questo progetto di tesi, alcune modifiche su questo materiale vengono fatte per aumentare alcune proprietà e migliorarne l'attività catalitica. La distinzione tra due diversi tipi di bentonite dipende dal principale minerale argilloso presente: la montmorillonite. Se il minerale di base è Na-Montmorillonite, la bentonite è chiamata bentonite sodica (Na-Bent), mentre se il minerale di base è Ca-Montmorillonite si parla di bentonite calcica (Ca-Bent). La Meta-Bentonite contiene sia Ca-Bentonite che Na-Bentonite. Na- Bentonite è stata adottata durante tutto questo lavoro di tesi. Il primo passo nella preparazione dei campioni è quindi quello di ottenere Na- Bentonite. A questo scopo, uno scambio con NaCl viene effettuato. La bentonite ha una struttura a strati paragonabile a foglie contorte, particolarmente evidente nei punti più scuri. (Fig. 1.31). La montmorillonite fa parte del gruppo delle smectiti diottaedriche ed è la componente principale della bentonite. Esistono numerose possibilità differenti per modificare la struttura e le proprietà fisico-chimiche delle argille naturali. L'attenzione in questo lavoro è focalizzata principalmente su: trattamenti con acidi e intercalazione (pillaring).

2. Materiali e metodi di preparazione

Come materiale di partenza è stata utilizzata bentonite pura (Fisher Scientific UK), CAS: 1302-78-9. La bentonite di partenza contiene solo acqua interstiziale. Per questo motivo il primo step al fine di modificarne la struttura è quello di trattarla con una soluzione di NaCl (1 M). Gli step seguiti nel trattamento della bentonite sono i seguenti:

- Preparazione di Na- Bentonite
- Trattamenti acidi con HNO_3 e HCl
- Pillaring (intercalazione)
- Deposizione della fase attiva

Alla bentonite pura di partenza viene fatto uno scambio ionico con una soluzione di NaCl (1M) per ottenerne Na-Bentonite (Fig. 2.2). Lo scambio viene condotto per 24h a temperatura ambiente. 20 grammi di materiale vengono scambiati con 200 ml di soluzione di NaCl. La separazione delle fasi viene fatta per centrifugazione, il materiale viene poi filtrato, esiccato a 110 °C per 24h e calcinato per 2h a 450°C. Successivamente per il trattamento acido, soluzioni di HCl e HNO_3 vengono preparate a diversa concentrazione (0,4; 0,6; 0,8 e 1 M). Il trattamento acido viene effettuato sulla bentonite pura e su quella sodica per tutte le concentrazioni di acido ottenute. L'attenzione verrà però riposta principalmente sui campioni trattati con concentrazioni di acido pari a 0.6 e 0.8 M al fine di non utilizzare trattamenti acidi troppo forti che potrebbero far collassare la struttura. Il trattamento acido dura 24 h a 100°C. 20 g di campione vengono introdotti in 200 cm^3 di acido. Dopo il trattamento i campioni vengono lavati con acqua distillata, esiccati e successivamente calcinati. Successivamente la calcinazione e i trattamenti acidi tutti, i campioni preparati vengono sottoposti al pillaring (intercalazione). La soluzione è preparata a partire da due soluzioni di $AlCl_3 \cdot 6H_2O$ e NaOH entrambe 0,4 M. Il rapporto molare di OH/Al nella soluzione finale è 2,5. La soluzione di NaOH viene lentamente aggiunta a $AlCl_3 \cdot 6H_2O$ miscelata con un agitatore magnetico a 70°C. Ci vogliono alcuni giorni per terminare questa preparazione. La stessa procedura viene eseguita per la preparazione della soluzione al 50% molare di cobalto. Oltre a NaOH e $AlCl_3 \cdot 6H_2O$ viene utilizzata anche una soluzione di $CoCl_2 \cdot 6H_2O$ (0,4 M). Una volta preparate le due soluzioni viene svolto il processo del pillaring (intercalazione). Il rapporto di 12 mmol Al/1 g campione è stato utilizzato, mescolando per 24h a 70°C. Il campione viene poi filtrato, esiccato per 24h a 120°C e poi calcinato per 2h a 450°C. Lo stesso procedimento viene fatto con la soluzione contenente cobalto. Per tutti i campioni trattati con acido viene fatta l'intercalazione. Solo i campioni scambiati con 0,6 M di HNO3 e HCl vengono anche intercalati con la soluzione di Al e Co. La deposizione della fase attiva avviene mediante Incipient Wetness Impregnation (IWI) che garantisce un'ottima dispersione della fase attiva sul supporto. I precursori delle specie di Fe e Ce derivano rispettivamente dalle soluzioni acquose di $Fe(NO_3)_3 \cdot 9 H_2O$ e $Ce(NO_3)_3 \cdot 6 H_2O$, al fine di ottenere 4 wt% di Fe e 0,12 wt% di Ce. La quantità calcolata della soluzione di nitrato viene aggiunta ad una quantità adeguata di bentonite (1g). I campioni vengono essiccati per 24 ore a 120°C e calcinati a 450°C per 2 ore. Dopo ogni fase di preparazione (preparazione di Na-Bentonite, trattamento acido con HNO3 e HCl, pillaring e deposizione della fase attiva), essiccazione (generalmente a 120°C per 24 h) e calcinazione (450°C per 2 h) vengono condotti. L'elenco dei campioni preparati è riportato nella tabella 2.2.

Quattro tecniche di caratterizzazione vengono condotte prima di svolgere i test catalitici, in questo lavoro di tesi XRD, FT-IR, UV-vis e TG vengono analizzati.

3. Risultati e discussioni

La diffrazione dei raggi X (XRD) viene impiegata come prima tecnica di caratterizzazione. Permette di identificare le fasi cristalline in campioni di polvere, aggregati policristallini e campioni a film sottile e di determinarne le dimensioni dei cristalli. Gli spettri dei campioni analizzati sono molto simili nelle direzioni X e Y. La direzione che presenta invece maggiori cambiamenti nell'analisi dei minerali argillosi è quella lungo Z. Il primo passo dell'analisi è il confronto con un modello di riferimento tratto da letteratura per confermare la formazione di Na-

Bentonite, dopo lo scambio con la soluzione di NaCl (1 M). Comparando i due spettri la presenza di Na- Bentonite è confermata. (Fig. 3.16 e Fig 3.17). I componenti principali della Na-Bentonite sono: Montmorillonite (M), Quarzo (Q) e Feldspati (F). Na-Bentonite è composta principalmente da montmorillonite e gli altri picchi rappresentano i riflessi delle impurità (come quarzo e feldspati). Il reference pattern di Na-Montmorillonite componente principale presente nella bentonite trattata è riportato in Tab 3.1. Oltre al picco 001 con FWHM= 0,51° a $2\theta = 19{,}77°$ in figura sono riportati anche altri picchi caratteristici della montmorillonite 100 e 060. 100 (M) a 2θ (°) = 19,77 (Intensità (arb.u.) = 501,02 e FWHM (°) = 0,43) e 060 (M) a 2θ (°) = 61,97 (Intensità (arb.u.) = 222.11 and FWHM (°) = 0,59). Picchi di quarzo e feldspato sono in accordo con il modello di riferimento. Quarzo (codice di riferimento: 01-089-1961) picco più intenso a 2θ (°) = 26,59° (Intensità (arb.u.) = 733,46 e FWHM (°) = 0,19). L'aumento dell'intensità dei trattamenti acidi può causare una perdita di cristallinità, Al presenti nella struttura possono essere tirati fuori con un aumento dei siti acidi. Il collasso della struttura può verificarsi con la formazione di SiO_2 amorfo non visibile in XRD. Il trattamento acido non deve, però, essere troppo aggressivo altrimenti la struttura dell'argilla potrebbe collassare completamente e la concentrazione amorfa aumentare drammaticamente. Questo è visibile in Fig. 3.18 e Fig. 3.19, il trattamento acido non ha cambiato i riflessi principali di montmorillonite e quarzo finché i trattamenti acidi sono stati poco aggressivi (fino a concentrazioni acide 0,8 M). Per NaB0.8HClAl, solo una leggera diminuzione della cristallinità è confermata e la struttura non collassa completamente. La direzione X è rimasta invariata (100 (M): 2θ (°) = 19,77°, l'intensità (arb. u.) = 510, FWHM (°) = 0,43) e in direzione Y sono visibili solo piccoli cambiamenti. Possono essere collegati ad un leggero collasso parziale di Al (060 (M): 2θ (°) = 61,97°, intensità (arb.u.) = 222,30 e FWHM (°) = 0,31). In direzione Z i cambiamenti nella struttura a causa di trattamenti acidi e pillaring sono più visibili. A causa del trattamento acido l'intensità di 001 è inferiore (114,11 arb.u.) e la forma del picco è più ampio (0,58 °). Con l'incremento della concentrazione di acido è visibile in Fig 3.19 la formazione di una struttura delaminata. Il picco 001 è stato completamente distrutto e la struttura ha mantenuto solo l'ordine nelle direzioni X e Y. L'impossibilità di calcolare d_{001} suggerisce solo la possibile formazione di pseudo pillars. In Fig. 3.21 è mostrata una rappresentazione schematica della struttura del campione (NaB1HClAl) con la presenza dei possibili pseudo pillars. Questo determina la possibilità di aver un maggior numero di siti acidi e una maggiore S_{BET} fornendo, così, una migliore accessibilità alle molecole con un aumento delle prestazioni catalitiche. Mediante i trattamenti acidi, FWHM del picco 001 aumenta e ne diminuisce di intensità. La perdita di intensità avviene per la distorsione lamellare che crea una decomposizione della struttura originaria. È evidente che i trattamenti acidi con diverse concentrazioni di acido (0,4; 0,6; 0,8 M di HCl) hanno mantenuto il carattere cristallino dei campioni, solo per NaB1HClAl la struttura è collassata nella direzione Z. Da letteratura è stato trovato che il valore minimo per il quale corrisponde il collasso totale del primo picco di bentonite pura è per concentrazione di HCl > 2,5 M. La presenza di Na^+ sembra dunque favorire l'effetto del trattamento acido. Il picco 001 appare più ampio dopo l'attivazione acida a causa della distruzione parziale della struttura. Tutti gli altri rimangono pressoché invariati. L'attivazione acida mostra che i trattamenti acidi hanno influenzato principalmente i picchi 00l come 001 (basali). I picchi non basali (riflessi prismatici) non cambiano significativamente dopo il trattamento (100, 060). La lista di tutti i campioni sottoposti al pillaring è riportata in Tab 3.2. In questo modo è possibile osservare laddove l'intercalazione sia avvenuta con o meno successo. Se d_{001} (Å) dopo il processo di intercalazione presenta un valore maggiore di 11,28 Å della Na-Bentonite di partenza si ha che il pillaring è avvenuto con successo, viceversa che questo non è avvenuto. La deposizione della fase attiva (con precursori di ferro e cerio) non ha modificato la posizione di 001 per tutti i campioni, non ha quindi determinato alcun cambiamento strutturale. Per tutti i campioni, come è visibile nelle figure riportate rappresentati gli spettri XRD dei campioni prima della deposizione della fase attiva e in seguito a questa, le stesse conclusioni sulla presenza di ossidi di cerio e di ferro possono essere condotte. Ossido di Cerio (codice di riferimento: 00-043-1002), α-Fe2O3 (codice di riferimento: 01-089-8104), Fe3O4 (codice di riferimento: 00-011-0614) e FeO (codice di riferimento: 00-002-1186) vengono riconosciuti, i loro picchi tuttavia sono sovrapposti a quelli dei principali componenti della bentonite. Per questo motivo non si possono escludere forme amorfe di ossidi di ferro e cerio, ma non possono essere identificate le loro forme cristalline. Solamente per il campione B0.6HNO3AlFe viene confermata la presenza di una forma cristallina di α-Fe2O3. Il raggio atomico dell'elemento cobalto è più grande di quello dell'alluminio. Per questo motivo, quando viene fatto il pillaring con la soluzione contenente cobalto, d_{001} deve aumentare. La quantità di cobalto introdotta, tuttavia, è particolarmente piccola, per cui non possono essere riconoscibili forme cristalline di ossidi di cobalto, come CoO or Co_3O_4. Da fonti bibliografiche si considera che Na-Bentonite mostra una superficie di circa 31,23 m^2/g mentre Al-Bentonite presenta una superficie superiore di 40,62 m^2/g. Tuttavia, è proprio grazie alla presenza di una soluzione di agenti misti per l'intercalazione che è possibile aumentare maggiormente l'area superficiale incrementandone così l'attività catalitica del campione.

La spettroscopia a infrarossi è una tecnologia utile per studiare le proprietà chimiche, i legami e la struttura dei composti come i minerali argillosi. Le argille in natura possono essere trovate come polveri o solidi e facilmente analizzate con analisi IR. La spettroscopia a trasformata di Fourier viene quindi utilizzata come seconda tecnica di caratterizzazione ed è possibile focalizzare l'attenzione sulle conseguenze dei trattamenti acidi che possono creare uno spopolamento del foglio ottaedrico e la formazione di silice amorfa. Dal confronto tra lo spettro FT-IR trovato in letteratura e quello ottenuto mediante lo scambio con la soluzione di NaCl (1M) viene verificato l'ottenimento della forma di bentonite desiderata. In Tab 3.4, vengono riportati i principali legami caratteristici della Na- Bentonite. In Fig 3.47 inoltre è possibile notare che lo spettro FT-IR di NaB e B è lo stesso. Non possono essere fatte considerazioni per quanto concerne la deposizione della fase attiva in FT-IR. Gli ossidi di ferro e di cerio non sono visibili nell'intervallo 4000-500 nm. FT-IR ha confermato che l'introduzione di specie di ferro e di cerio non ha introdotto differenze visibili negli spettri rispetto a quelli privi della fase attiva. Tutte le figure riportate da Fig. 3.48 a Fig. 3.53 mostrano questo. Considerazioni per quanto concerne il tipo di acido (HNO_3 o HCl) vengono condotte in Fig. 3.54 e Fig 3.55, gli spettri sono stati confrontati per mostrare che non ci sono differenze visibili negli spettri confrontando i due diversi tipi di acido. L'assenza di NO_3^- , che potrebbero essere visibili nell'intervallo 1500-1300 cm^{-1} per i campioni trattati con HNO_3, suggerisce che i campioni sono stati completamente lavati dopo il trattamento acido e gli ioni rimossi. Le bande vicino a 3446 e 1643 corrispondono all'acqua assorbita. Essicazione e calcinazione sono state effettuate dopo ogni fase di preparazione dei campioni. Le bande corrispondenti all'assorbimento di acqua rivelano una perdita di intensità con l'aumento della concentrazione acida dovuto alla rimozione dei cationi ottaedrici che causano la perdita di acqua e gruppi idrossilici coordinati. Queste considerazioni concordano con quanto riportato in letteratura, ma la presenza di acqua è molto sensibile, il bromuro di potassio in polvere utilizzato per la preparazione dei campioni per l'analisi FT-IR assorbe molta umidità (è igroscopico). Inoltre, la calcinazione e essicazione non sono sufficienti per rimuovere l'acqua. L'assenza di evacuazione dell'acqua rende i picchi più ampi e interferisce con le bande. La finestra da 3000 a 4000 cm^{-1} è influenzata da molti parametri e deve quindi essere trattata con cautela, i risultati possono essere più affidabili e non influenzati dal contenuto di acqua in un range inferiore (1500- 500 cm^{-1}) come presentato in Figura 3.57. I legami Si-O non cambiano con l'aumento del trattamento acido. Il trattamento acido mantiene un certo ordine lungo l'asse X e Y che è stato confermato anche nella diffrazione dei raggi X anche laddove la struttura era collassata lungo l'asse Z. Fig 3.59, 3.60, 3.61, 3.62 mostrano gli spettri di NaB confrontati con NaB0.6HNO3AlFe, NaB0.8HNO3AlFe, NaB0.6HClAlFe, NaB0.8HClAlFe. Il pillaring non ha modificato la struttura. Piccoli cambiamenti nella forma dei picchi nel range 1500-500 cm^{-1} implicano l'interazione dei pillars con il gruppo Si-O nel piano tetraedrico e con Al-OH nel piano ottaedrico. L'introduzione del cobalto non modifica gli spettri FT-IR analizzati, tuttavia, alcuni cambiamenti potrebbero essere osservati per una maggiore concentrazione di cobalto, una banda appare a 662 cm^{-1} per la presenza di composti di cobalto, ma questo sarebbe visibile per concentrazioni di cobalto superiori a quello esaminato.

La spettroscopia ultravioletta/visibile (UV-vis) viene utilizzata in questo lavoro di tesi per la determinazione delle varie forme di ferro introdotte con la deposizione della fase attiva. Questo avviene mediante l'osservazione di bande caratteristiche, tipiche di queste specie ($Fe^{3+} \leftarrow O$). Lo spettro di NaB non presenta alcuna banda di assorbimento tipica del ferro, questo è in accordo infatti con il fatto di avere una bentonite pura di partenza. Gli intervalli rilevanti per le specie contenti ferro sono: Fe^{3+} isolati (ioni Fe^{3+} mononucleari) in posizione tetraedrica, Fe^{3+} isolati (ioni Fe^{3+} mononucleari) in posizione ottaedrica e piccoli cluster di Fe_xO_y oligonucleari e particelle di Fe_2O_3 disperse. Fig. 3.70, 3.71, 3.72, 3.73, mostrano e confermano la presenza di tutte le forme citate di ferro (presenza di ioni Fe^{3+} isolati (200-300 nm), di cluster FexOy oligonucleari (300-400 nm) e di particelle Fe_2O_3 oltre 450 nm). Non ci sono differenze visibili dal campione trattato con bentonite pura o dai campioni trattati con Na-Bentonite. Differenze nello spettro sono visibili per B0.6HNO3AlFe dove nell'intervallo maggiore a 450 nm l'intensità è superiore a quella degli altri campioni, questo campione ha una quantità maggiore di particelle Fe_2O_3 disperse nel campione. Inoltre, per questo campione il pillaring è stato inefficiente e la presenza di particelle di Fe_2O_3 può bloccare i micropori e ridurne l'area creando conseguenze negative sulle attività catalitiche. NaB0.6HClAlFe indica la presenza di una maggiore quantità di cluster Fe_xO_y. Le stesse conclusioni possono essere fatte per i campioni trattati con una concentrazione di acido maggiore (0,8 M). L'aggiunta di una ulteriore fase attiva contenente precursori di cerio può modificare lo stato di ossidazione del ferro. La sovrapposizione delle bande nella stessa posizione di quelle del ferro impedisce tuttavia di trarre delle conclusioni.

Il trattamento termico ad alta temperatura sui minerali argillosi fornisce informazioni sull'evoluzione delle proprietà fisiche delle argille. La variazione della massa viene presa in considerazione durante la termogravimetria, identificando due regioni principali di perdita dell'acqua. In Fig. 3.38 sono riportate le curve TG di Na-Bentonite e di quella pura. Entrambe presentano due zone ben distinte di perdita d'acqua. In questo lavoro verranno proprio identificate queste due principali regioni di perdita di massa: la perdita d'acqua a bassa temperatura inferiore a 180 °C (Δm_l (%)) relativa all'acqua fisisorbita e la perdita d'acqua ad alta temperatura superiore a 180 °C (Δm_h (%)). Tab. 3.5 riporta tutti i campioni analizzati attraverso TG e la distinzione delle due principali aree di perdita di acqua. Le percentuali di perdita di massa sono molto basse per tutti i campioni. I campioni risultano molto stabili ad alte temperature: Δm_h (%) è sempre prossimo all'unità, eccetto per il campione B0.6HClAlFe che risulta il meno stabile. Non sono presenti differenze nelle curve significative con l'introduzione della fase attiva. Per quanto concerne, invece, l'introduzione di una soluzione per il pillaring con un agente misto quale il cobalto si verifica un leggero incremento della stabilità termica del campione. (Fig. 3.89)

Molti differenti metodi possono essere utilizzati per testare l'efficienza catalitica dei campioni ottenuti in laboratorio al fine di abbattere NO_x. 200 mg di campione vengono utilizzati, una concentrazione di NO iniziale pari a 800 ppm. Il primo risultato è stato quello di testare l'attività catalitica della pura bentonite e di Na-Bentonite, considerando gli errori sperimentali (± 3%), i valori di conversione ottenuti sono relativamente molto bassi, non è possibile attribuire alcuna attività a questo materiale, ma potrebbe essere un efficiente supporto in seguito a trattamenti e deposizione di una fase attiva. Nei capitoli successivi (4.2.2, 4.2.3, 4.2.4 e 4.2.5) vengono comparati i vari catalizzatori, in generale: B0.6ACIDAlFe/NaB0.6ACIDAlFe<B0.6ACIDAl/CoFe/NaB0.6ACIDAl/CoFe<B0.6ACIDAlFe Ce/NaB0.6ACIDAlFeCe. Indistintamente dall'acido utilizzato la deposizione di un'ulteriore fase attiva quale il cerio incrementa l'attività catalitica. Anche l'introduzione del cobalto ha un impatto positivo sulla conversione di NO se confrontato con il rispettivo campione in cui è stato fatto il pillaring solamente con alluminio. Tutti i campioni presentano una massima attività nel range di temperatura compreso tra i 350 °C, a 450 °C invece l'attività sembra diminuire e questo potrebbe essere dovuto alla reazione indesiderata di ossidazione dell'ammoniaca che porta alla formazione di prodotti indesiderati con una diminuzione della selettività rispetto a N_2. Elevate attività vengono attribuite a NaB1HClAlFe, questo dimostra che la presenza di una struttura delaminata con la formazione di pseudo pillars può aumentarne l'attività. Un'altra analisi catalitica è stata quella relativa all'attività del supporto senza la deposizione della fase attiva la cui conversione è incrementata e raggiunge il 30 % rispetto al 7% di conversione della pura bentonite. La selettività è confermata, l'emissione di N_2O è molto bassa considerando gli errori sperimentali di 30 ppm.

4. Conclusioni

Lo scopo di questo lavoro è stata la preparazione di catalizzatori attivi per la rimozione di NO in SCR-NH3. Un'argilla naturale quale la bentonite è stata modificata in seguito alle fasi di preparazione in laboratorio. La deposizione della fase attiva con precursori di ferro e cerio è stata studiata mediante XRD e UV-vis. La quantità di queste specie, tuttavia, è molto bassa e la diffrazione a raggi X non può confermare alcuna forma cristallina di ossidi di ferro (solo per B0.6HNO3AlFe è stata confermata la presenza di Fe_2O_3). Soltanto la presenza di questi ossidi in forma amorfa può non essere esclusa. Se il pillaring non è stato efficace la posizione del picco 001 rimane invariata viceversa si sposta a valori di 2θ sempre inferiori conseguenza di un incremento di d_{001}. Con l'incremento del trattamento acido si forma una struttura delaminata con la presenza di possibili pseudo pillars, la presenza di un maggior numero di siti acidi che offrono una migliore accessibilità alle molecole e un aumento delle prestazioni catalitiche del campione. Questo è confermato per NaB1HClAlFe. Gli spettri UV-vis identificano la posizione di Fe^{3+}, per tutti i campioni sono stati confermati tutti gli intervalli possibili per la presenza di specie ferrose: Fe^{3+} isolati (ioni Fe^{3+} mononucleari) in posizione tetraedrica, Fe^{3+} isolati (ioni Fe^{3+} mononucleari) in posizione ottaedrica e piccoli cluster di Fe_xO_y oligonucleari e particelle di Fe_2O_3 disperse. L'analisi FT-IR mostra che le diverse fasi di preparazione dei campioni (trattamento acido, pillaring e deposizione della fase attiva) non hanno modificato i principali legami presenti nella bentonite pura. Mediante termogravimetria i campioni hanno rilevato di essere termicamente stabili. Con il test catalitico, tutti i campioni trattati con la soluzione NaCl (1 M) presentano attività catalitiche più elevate. La presenza di Na^+ favorisce lo scambio cationico con un'efficienza maggiore del trattamento acido. Per la preparazione di un'argilla satura "acida" è importante la pre-saturazione dell'argilla con Na^+. I cationi H^+ dell'acido sostituiscono facilmente gli Na^+, un elevato grado di saturazione di Na^+ è infatti importante permette risultati migliori nella saturazione dell'argilla con H^+ e maggiore attività catalitica. Il trattamento con due tipi di acido (HNO_3 e HCl) non ha determinato differenze visibili nell'attività catalitica. Gli spettri FT-IR dei campioni trattati con HNO_3 non mostrano alcuna presenza di NO_3^-. Ciò significa che il campione è stato completamente lavato dagli anioni dell'acido. Inoltre, i campioni trattati con HNO_3 e HCl con concentrazioni di 0,6 M e 0,8M non presentano le stesse attività rispetto al tipo di acido. Diverse conclusioni si sarebbero potute trarre se la bentonite di partenza non fosse stata pura. Nella bentonite è possibile la presenza di sostituzioni nel foglio ottaedrico della montmorillonite con atomi diversi all'alluminio quali il ferro. Secondo quanto riportato in letteratura, la rimozione del ferro è più efficace con HCl che con HNO_3, ma per l'attività catalitica è il contrario. Le bentoniti naturali che hanno una maggiore concentrazione di ferro iniziale presentano una maggiore attività catalitica. Per questo motivo, il trattamento con HNO_3 sarebbe potuto essere più efficiente se la bentonite di partenza non fosse stata extra pura. L'introduzione del cobalto oltre all'alluminio per il processo del pillaring aumenta la stabilità termica e le attività catalitiche principalmente a 400°C. La presenza di cobalto garantisce buone prestazioni in NH_3-SCR. L'aggiunta di cerio può aumentare l'accumulo e lo scambio di ossigeno a basse temperature. CeO_2 ha una notevole capacità di accumulo di ossigeno, l'aggiunta di CeOx come fase attiva incrementa notevolmente l'attività catalitica per tutti i campioni. Il miglior catalizzatore preparato è NaB0.6HNO3AlFeCe a 350°C con 93 % di conversione di NO. Questo lavoro di tesi ha dimostrato che, con diverse fasi di modifica, la bentonite pura e quella sodica, che non presentano alcuna attività catalitica (7% di rimozione di NO come valore massimo), possono essere trasformate in buoni catalizzatori per la rimozione di NO_x, raggiungendo conversioni di NO superiori al 90%. I materiali scelti si sono dimostrati dunque attivi nella conversione di NO e selettivi a N_2 evidenziando buone potenzialità per sostituire i catalizzatori commerciali attualmente impiegati in SCR-NH3

Abstract

The emission of NO_x is one of the most dangerous environmental problem. The European Union has introduced strict standards for the reduction of emissions. Technologies based on selective catalytic reduction have been developed to follow the standards level allowed.

In this work, modified acid treated bentonites have been studied as catalysts for the removal of nitrogen oxides (NOx) in the selective catalytic reduction of NOx by ammonia (SCR-NH3). Clays and clay minerals are recognized as the materials of the 21st century for being abundant, inexpensive and environmentally friendly; therefore, they appear to be good candidates for their application in SCR- NH_3 to overcome the limits of commercial catalysts.

Modified bentonites have been here investigated following different steps of preparation: acid treatment and pillaring resulted to be the best methods of modification of these clays. The first step for the preparation of an acid-saturated clay is its pre-saturation with Na^+; for this reason, pure bentonite has been treated with a solution of NaCl. Acid treatments have been conducted with different concentrations of acid solutions (0.4, 0.6, 0.8, 1M) to investigate the different attacks to the layered structure of clays. Treatments with HNO_3 and HCl give good results.

On the other hand, pillaring allows the creation of an additional porous structure and increases the specific surface area with the introduction of inorganic polymer hydroxycations, whose sizes are bigger than the original exchangeable cations. In addition to aluminium, also cobalt has been introduced as a pillaring agent. The addition of different fractions of another cation for pillaring improves the thermal, adsorptive and catalytic properties of the catalyst. As catalytically active metals, iron and cerium have been added with incipient wetness impregnation to improve the removal of NOx. NaB0.6HNO3AlFeCe presents the highest catalytic performance among all the samples examined (93% of NO conversion). This work demonstrated that, with different modifications, pure bentonite and Na-Bentonite, which do not present any catalytic activities (7% of NO removal as the maximum value), can be transformed into a good catalyst for the removal of NOx, reaching NO conversions above 90%.

The main steps of this work have been the preparation of samples, characterization of samples (by XRD, FT-IR, UV-vis and TG) and the application of the obtained catalysts in SCR-NH_3.

Chapter 1 – Introduction

1.1 Pollutants and environmental problems

The rapid growth in the concentration of toxic pollutants, and its increasing emission, is causing negative impacts on the atmosphere, environment and human health at both a local, a regional and a global level. This has become an ecologically serious problem.

Pollutants are divided into primary pollutants and secondary pollutants. The former are emitted into the environment directly after being originated by processes related to human and natural processes. The latter are substances which are formed as a result of changes of various kinds, such as chemical-physical reactions among the primary pollutants themselves or with the atmosphere. They can be activated by solar energy and often involve atmospheric oxygen. The most present pollutants in the atmosphere are: CO, CO_2, NO_x, SO_2, hydrocarbons, particulate and ozone. It is also necessary to consider the kind of sources that emit pollutants:

- Natural sources : dust and various gases emitted by volcanoes and forest fires; ozone that is a secondary pollutant, formed near the soil as a result of a series of chemical reactions catalysed by the light, particulate originated from volcanoes and sandstorms, many volatile organic compounds (VOCs) are naturally produced by plants, like isoprene. Natural sources of sulphur dioxides include volcanoes, organic decomposition and forest fires and natural sources of nitrogen oxides include volcanoes, oceans, organic decomposition and action of lightning.

- Anthropologic sources: many of these anthropologic sources are closely linked to the production and consumption of energy, such as large permanent sources (industries, power plants and incinerators), small permanent sources (systems for domestic heating installations) and moving sources (urban traffic). Humans have always exploited natural resources without considering the consequences of their actions and producing the greatest air pollution to satisfy their civil and industrial needs.

The impact of pollutants depends on their production. Dispersion and concentration in the air is determined by several factors: the distance from the sources, the number and the concentration of the pollutant sources, the amount of contaminants in the emissions, the chemical-physical transformations undergone by the emitted substances, the morphological situation of the areas and the local and large-scale weather conditions. [1] The presence of pollutants generates catastrophic effects on the humans and on the environment. On the one hand, the growth of the exposure to various atmospheric irritants causes dysfunction of the lungs, respiratory diseases, mostly in children, and acute bronchitis attacks. This leads to an increase in the number of deaths among those most sensitive to certain pollutants, such as old people or those affected by cardiovascular respiratory diseases. On the other hand, the inexorable decline of animal, forest and agricultural heritage, the degradation of ecosystems, the damage caused to metal structures, the buildings, art works and the reduction of visibility.

The concentration of ambient air pollutants is sufficiently high to cause increased mortality, deficits in pulmonary function and cardiovascular and neuro-behavioural effects [2],[3]. The World Health Organizations has estimated that the urban air pollution, generated by vehicles, industries and energy production kills about 800,000 people annually.

In 1972 the UN Conference on the Environment in Stockholm wanted to increase the general awareness of the many global environmental pollution problems. The United Nations Environment Programme (UNEP) was created and started to collaborate with the World Health Organization (WHO) in the initiation of a Global Environment Monitoring System (GEMS). This system gave the possibility to create an air pollution monitoring network.[4]

The amount of deaths monitored by this network is increasing, as it is shown in Fig.1.1 and Fig. 1.2 from 2004 to 2016, attributable to ambient air pollution. These values have been estimated by the World Health Organization in the world death distribution map. [5]

Deaths from urban air pollution are estimated to grow over the next 30 years because of the world's population growth, mostly in cities and towns of the poorer countries. In Asia, for example, the region will see an overall increase by a billion people in urban areas over the next 3 decades.

Nowadays, the most developed countries are trying to preserve the environment from the air pollution. With this aim, strict limits and target values for the air quality are being set in order to reduce emissions. Europe, for example, has policies in place limiting individual sources, but also national totals of atmospheric emissions of the key five pollutants: sulphur dioxide, nitrogen oxides, volatile organic compounds, ammonia and fine particulate matter.

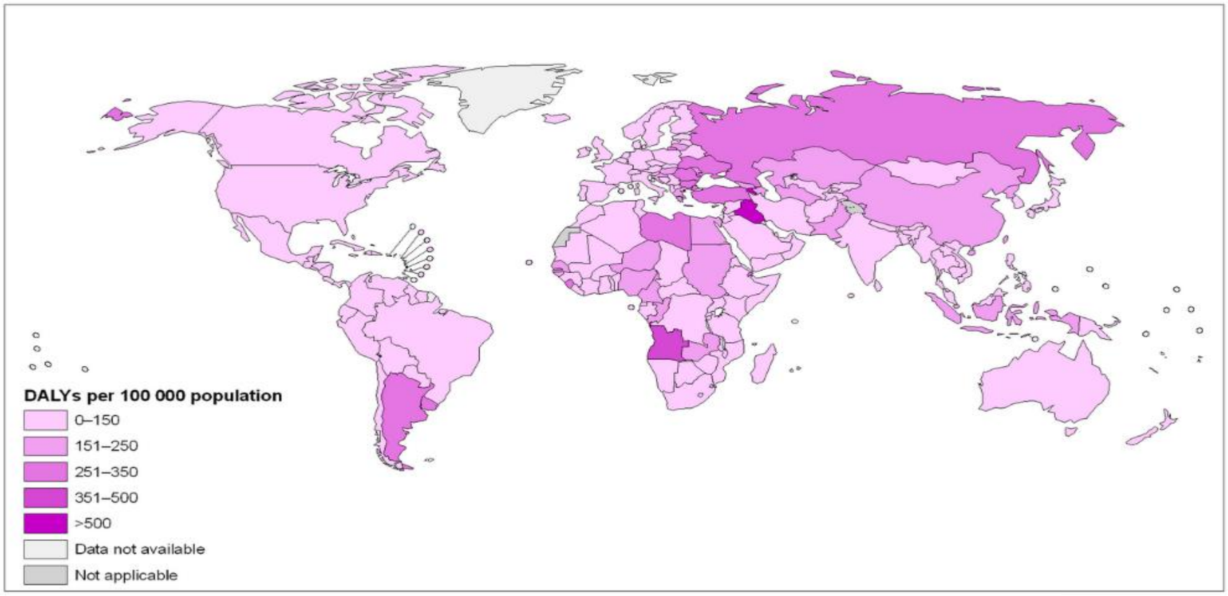

The boundaries and names shown and the designations used on this map do not imply the expression of any opinion whatsoever on the part of the World Health Organization concerning the legal status of any country, territory, city or area or of its authorities, or concerning the delimitation of its frontiers or boundaries. Dotted lines on maps represent approximate border lines for which there may not yet be full agreement.

Data Source: World Health Organization
Map Production: Public Health Information and Geographic Information Systems (GIS)
World Health Organization

World Health Organization

© WHO 2011. All rights reserved.

Figure 1.1: Deaths attributable to ambient air pollution (age- standardized, per 100 000 population), 2004

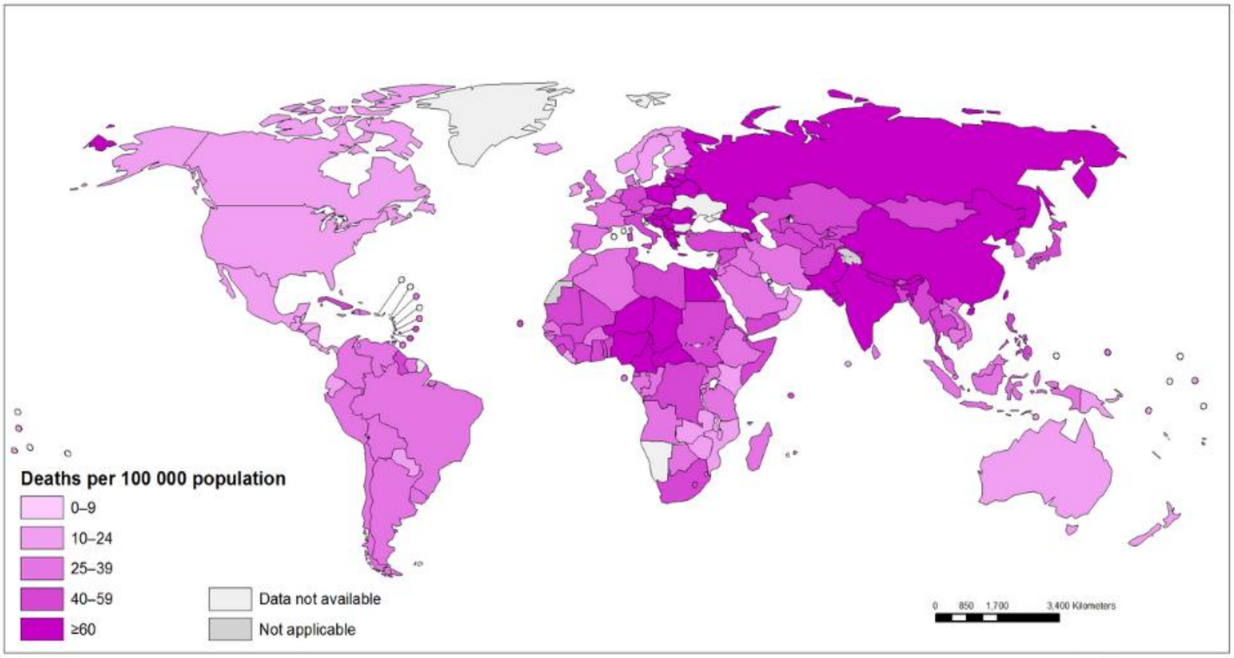

The boundaries and names shown and the designations used on this map do not imply the expression of any opinion whatsoever on the part of the World Health Organization concerning the legal status of any country, territory, city or area or of its authorities, or concerning the delimitation of its frontiers or boundaries. Dotted and dashed lines on maps represent approximate border lines for which there may not yet be full agreement.

Data Source: World Health Organization
Map Production: Information Evidence and Research (IER)
World Health Organization

World Health Organization

Figure 1.2: Deaths attributable to ambient air pollution (age- standardized, per 100 000 population), 2016

In 2011-2013 the Commission proposed a Clean Air Programme for Europe updating the 2005 Thematic Strategy on Air Pollution to set new objectives for the EU air policy for 2020 and 2030. To achieve these targets, the main legislative instrument is Directive 2016/2284. This Directive also considers the reduction commitments for 2020 established under the Gothenburg Protocol by the EU and its Member states and it imposes more restrict objectives as of 2030 to cut by half the health impacts of air pollution compared to 2005.[6]

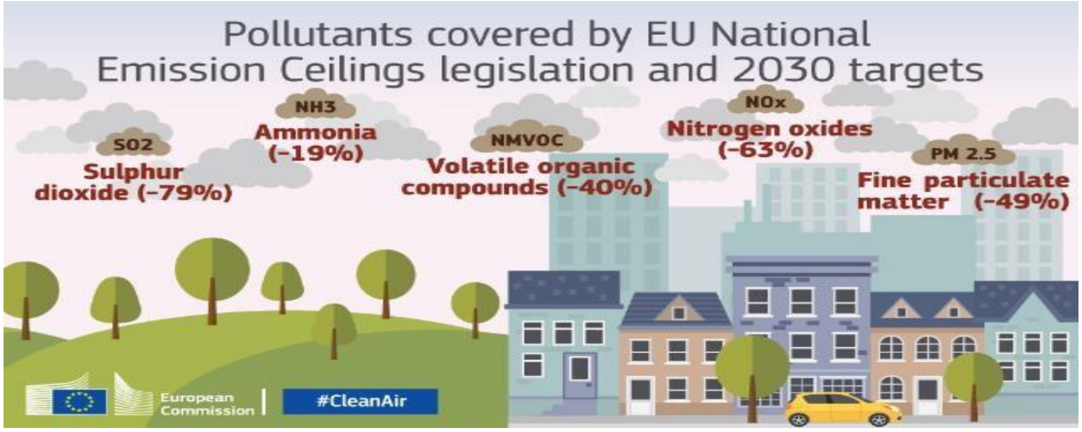

Figure 1.3: Pollutants covered by EU National Emission Ceilings legislation

1.1.1 NO_x as pollutants

Among the main pollutants, mentioned in 1.1, the Nitrogen Oxides (NO_x) lead to significant negative impacts on the human health and the environment. They belong to a different group of chemical compounds in terms of structure and properties. They are considered more harmful than sulphur oxide and carbon monoxide. NO_x are responsible for the air pollution through their participation in a series of photochemical reactions.

They are considered the main factor of air pollution, because in the presence of sunlight they can transform into acid pollutants, such as nitrate particles. [7] Furthermore, they are also the main factor of the formation of the ozone. Following their emissions in the air, they are converted into small particles and can also form acid rains.

These pollutants are the main focus of this project. After a thorough examination, it will analyse their causes and find out which techniques may be used to reduce them and limit their impact on the human health and the environment. VOC and NO_x are in fact the main causes of smog, which results in an increase in breathing problems and the amount of people suffering from asthma and bronchitis. [8]

The chemical element nitrogen (N) is a single atom with ionization levels ranging from plus one to five. N can therefore be in different valence states, hence being reactive and able to form different chemical compounds. The family of NO_x consists of six compounds, as shown. (Table 1.1).

Table 1.1. Nitrogen oxides and their properties

Name	Formula	Properties
Nitrous oxide	N_2O	colourless gas, water soluble
Nitric oxide	NO	colourless gas, slightly water soluble
Dinitrogen trioxide	N_2O_3	Black solid, water soluble, decomposes in water
Nitrogen dioxide **Dinitrogen tetroxide**	NO_2 N_2O_4	Red-brown gas, very water soluble, decomposes in water
Dinitrogen pentoxide	N_2O_5	White solid, very water soluble, decomposes in water

Nitrogen was discovered in the XVII century and described by Carl Wilhelm Scheel and Daniel Rutherford for the first time. It is colourless, tasteless and odourless. It is present in chlorophyll, proteins, nucleic acids (DNA and RNA) and is therefore a vital element for all the living organisms [9].

Molecular diatomic nitrogen (N_2) is very stable, in fact it has a binding energy of about 950 kJ/mol. It represents the 78% of the air. $C \equiv N$ has a binding energy of about 750 kJ/mol, $C = N$ has a binding energy of about 715 kJ/mol and C-N has a binding energy of about 270 kJ/mol. It is harder to break a N_2 molecule than a carbon inside any organic structure. Such a strong bond makes it very difficult to break, since it requires a great amount of energy. There are some species of germs that can convert the N_2 molecule into other compounds in the presence of biocatalysts. More generally, living organisms make use of nitrogen in the form of nitrate or proteins. Fritz Haber invented the technology of the ammonia production in the presence of Fe catalyst. The production of ammonia has found industrial applications since 1916. The reaction is: $N_2 + 3H_2 = 2NH_3$. A lot of energy is required to break N_2, the temperature needed to break the triple bond is 1000-1500 °C. These temperatures are easily reached in a flame, so it is necessary to know that in a combustion process N_2 can participate with a certain chemical reactivity. In a combustion process, the O_2 generally comes from the presence of oxygen in the air, where there is a big amount of N_2. [10] From the list of different compounds showed in Tab.1, the two main oxides considered as pollutants are NO and NO_2, jointly known as NO_x. Nitrogen oxide concentrations and species in the air may vary greatly depending on the place, time and season.

Nitric oxide (NO) is a colourless and highly reactive gas. It originates from the reaction of oxygen with nitrogen during any combustion process taking place in the air and at high temperatures (1200 °C). Further oxidation of NO may also produce traces of nitrogen dioxide, which generally does not exceed 5% of the total NO_x emitted.

$$N_2 + O_2 \rightarrow 2NO \tag{1.1}$$

$$2NO + O_2 \rightarrow 2NO_2 \tag{1.2}$$

The formation of nitrogen dioxide (NO_2) has an important role in the ozone formation process, it takes place because of the oxidation of nitric oxide in the atmosphere. Nitrogen dioxide is considered as a secondary pollutant, during the reaction phase NO is formed and then this is converted into NO_2.

NO can be oxidized by the molecule of ozone O_3:

$$NO + O_3 \rightarrow NO_2 + O_2 \tag{1.3}$$

Among the air pollutants, nitrogen dioxide absorbs most of the UV.

$$NO_2 + hv \rightarrow NO + O^* \tag{1.4}$$

This is a photochemical reaction. Oxygen radical produced in this reaction is going to react in the following reaction with a molecular oxygen, whose product is O_3:

$$O^* + O_2 \rightarrow O_3 \tag{1.5}$$

The ratio NO_2/NO increase as the temperature decreases. Accordingly, the higher the temperature, the more thermodynamically stable is NO. During combustion processes, in fact, the temperatures are higher than 1000 °C, which explains why a combustion results in 95% of NO and only few percentages of NO_2. NO_2 is more problematic than NO as a pollutant, and after the combustion with the decrease of the temperature NO will tend to become NO_2. This process is thermodynamically favoured, but kinetically low [11]

1.1.2 Kinetic of NO_x

There are three different reaction mechanisms that lead to the formation of nitric oxide[11]:

- Thermal NO_x
- Fuel NO_x
- Prompt NO_x

Thermal NO_x are controlled by the nitrogen and oxygen molecular concentrations and by the temperature of the combustion. At high temperatures, N_2 and O_2 present in the combustion air dissociate and participate in a series of reactions. The main reactions governing thermal NO_x formation are:

$$O^* + N_2 \leftrightarrow NO + N^* \tag{1.6}$$

$$N^* + O_2 \leftrightarrow NO + O^* \tag{1.7}$$

$$N^* + OH^* \leftrightarrow NO + O^* \tag{1.8}$$

The first two reactions were proposed in 1946 by Zeldovich, while the last one was added by Lavoie, Heywood and Keck. All the reactions are also known as the mechanism of extensive Zeldovich. The kinetic of these reactions is very fast and depends on the temperature: the higher the gases remain at high temperature the higher will be the production of NO_x. The best way to decrease the amount of thermal NO_x is the reduction of the residence time at high temperature and low content of oxygen.

Fuel NOx results from oxidation of the already-ionized nitrogen which is contained by the fuel. Whenever Nitrogen is bound to the fuel atoms of C and H, it is oxidized much more easily than the atmospheric nitrogen. These bonds are present in the oil fuel (such as pyridine or piperidine), in the coal, while they are absent in the natural gas. The nitrogen present in the fuel can be released as free radicals and yields the formation of NO and N_2. The fuel NO_x represent the 50 % of the release of NO_x from oil fuel and the 80% from the coal. The reactions leading to the formation of these NO_x can be related to the volatile species or to the nitrogen contained in the carbon matrix of the fuel. The nitrogen present in volatile species of the fuel may be oxidized during the first step of the combustion and can form intermediate species from oxidized to NO.

Prompt NO_x derive from the reaction between HC/ hydrocarbon radicals and the atmospheric nitrogen with the formation of hydrocyanic acid (HCN) as an intermediate that will be oxidized to NO_x, CO_2 and H_2O. HCN is only a reaction intermediate. The triple bond of the nitrogen molecule is destabilised by organic radicals (C, CH and CH_2 fragments) derived from the fuel. The reaction for the prompt NO_x is the following:

$$HC^* + N_2 \leftrightarrow HCN + N^* \tag{1.9}$$

These hydrocarbon radicals are especially present when there is not enough oxygen to oxide all the fuel with a certain number of unburnt hydrocarbons. The background of emissions is approximately between 15 ppm and 30 ppm.

Three different sources of NO_x are reported in the Fig.1.4 as a function of the temperature. At very low temperature, thermal NO_x are practically absent and they do not give any contribution. NO_x prompts, deriving from the radical HC, have an almost constant value independent from the temperature. Fuel NO_x have an increasingly less important contribution as the temperature increases. This is because the thermal NO_x are gradually predominant. [12]

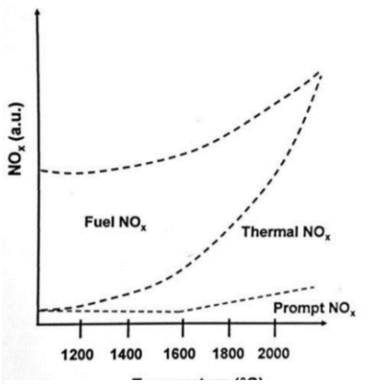

Figure 1.4: Different sources of NO_x

1.1.3 Environmental effects and emission sources of NO_x

Nitrogen oxides can damage both the respiratory systems and the environment (photochemical smog and ozone). Fig. 1.5 shows the chemical transformations that create air pollution. [13]

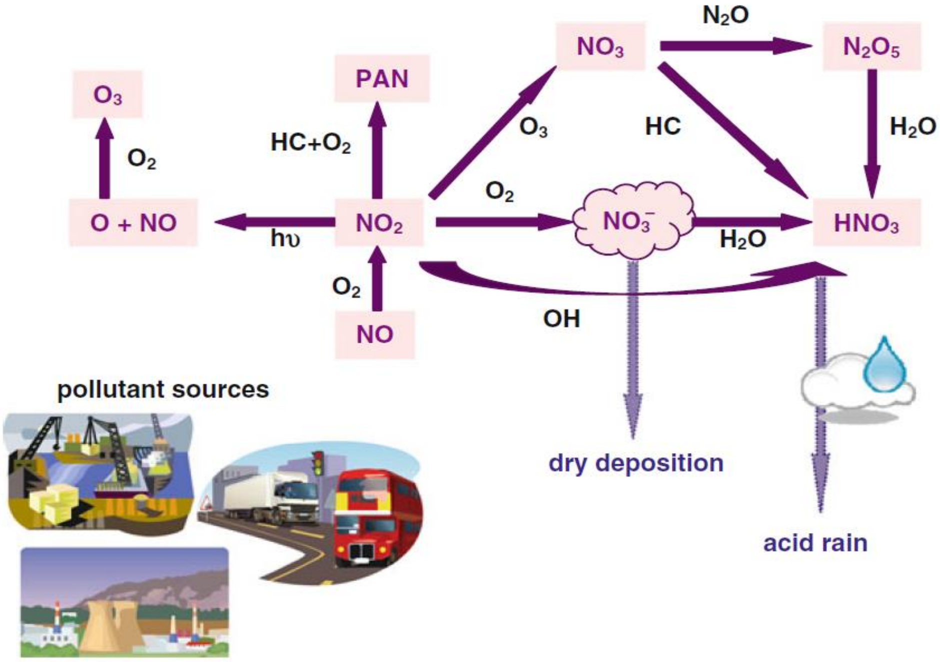

Figure 1.5: Chemical transformations suffered by NOx related to air

The formation of O_3 is a ground-level ozone, one of the most hazardous pollutants for the health. PAN (peroxyacetyl nitrate) a nitro-organic compound produced by photochemical oxidation of carbonyl compounds with NO_x. These organic compounds create damages and PAN is very soluble in water and its removal is very difficult. HNO_3 may be produced by different kinds of reactions: oxidation by O_2 and solubility in water, oxidation by -OH, reaction of NO_3 with HC or reaction of NO_3 with N_2O and then solubility in water. As HNO_3 is formed, its high solubility in water yields the formation of acid rains, which have negative impacts on the environment and buildings. [13]

NO_x emissions have mostly anthropogenic origins, only small percentages of the released NO_x are related to natural sources, such as from the nitrifying bacteria. As it is shown in Fig 1.6. the main anthropogenic sources are stationary sources (heat power generation, incineration, process industry), burning of fossil fuels (coal, oil and diesel) and road transports. The road transports sector, which contributes to nearly half of all the emissions of NO_x, has been widely affected by the legal restrictions limiting the emissions of NO_x.. [14]

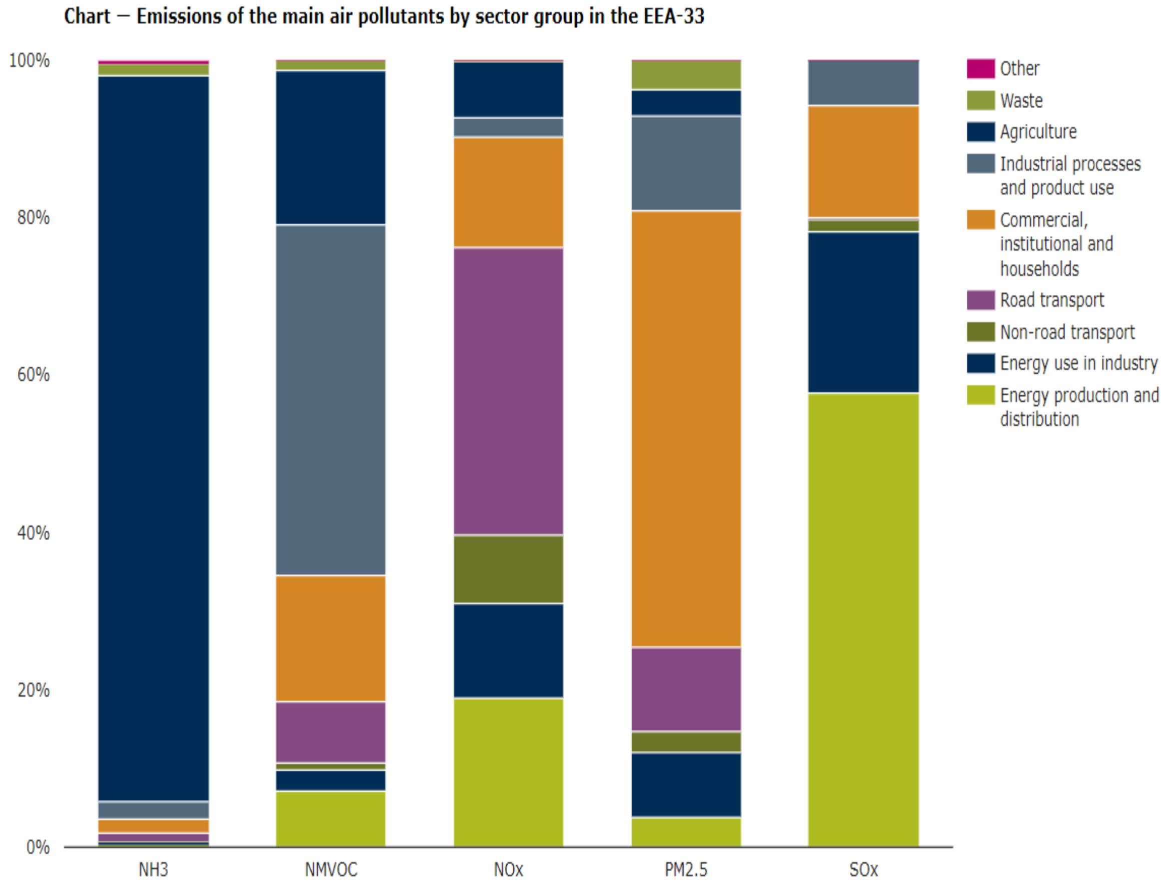
Chart — Emissions of the main air pollutants by sector group in the EEA-33

Figure 1.6: Emissions of main air pollutants provided by European Environment Agency (EEA)

The NO_x emissions also decreased in the sector of energy production. These results were achieved due to combustion modification (the introduction of low-NO_x burners), the introduction of flue-gas technologies (NO_x scrubbers, selective catalytic reduction or non -catalytic reduction technologies) and the changing from coal to gas as fuel; coal contains a significant amount of nitrogen, hence emissions of NO_x are higher from coal-fired power plants. (Tab1.2)

Table 1.2 Fuel bound nitrogen

Fuel	Fuel bound nitrogen (weight%, dry, ash-free basis)
Coal	0.5-2
Biomass (wood)	< 0.5
Peat	1.5-2.5
Fuel oil	<1
Natural gas	0
Derived gases	0.1-1

However, the sector which contributed the most to the total reduction in NO_x emissions is the road transports sector, having reduced these emissions by over 40 % in the last years, despite the general increase in transport activity.[15] Increasingly stringent regulations have led to the development of various abatement systems. This decrease is due to different reasons: some variations in the driving cycle, which has become more dynamic. In addition to the driving cycle, the RDE is introduced to test the emissions of vehicles on the road, taking into account different factors such as more real conditions, the traffic, climbs and descents. The composition of the outlet gases is monitored by the PEM (Portable Emissions Measurement Systems). It is assumed that a large portion of nitrogen in the atmosphere is released by diesel- vehicles, especially heavy trucks.

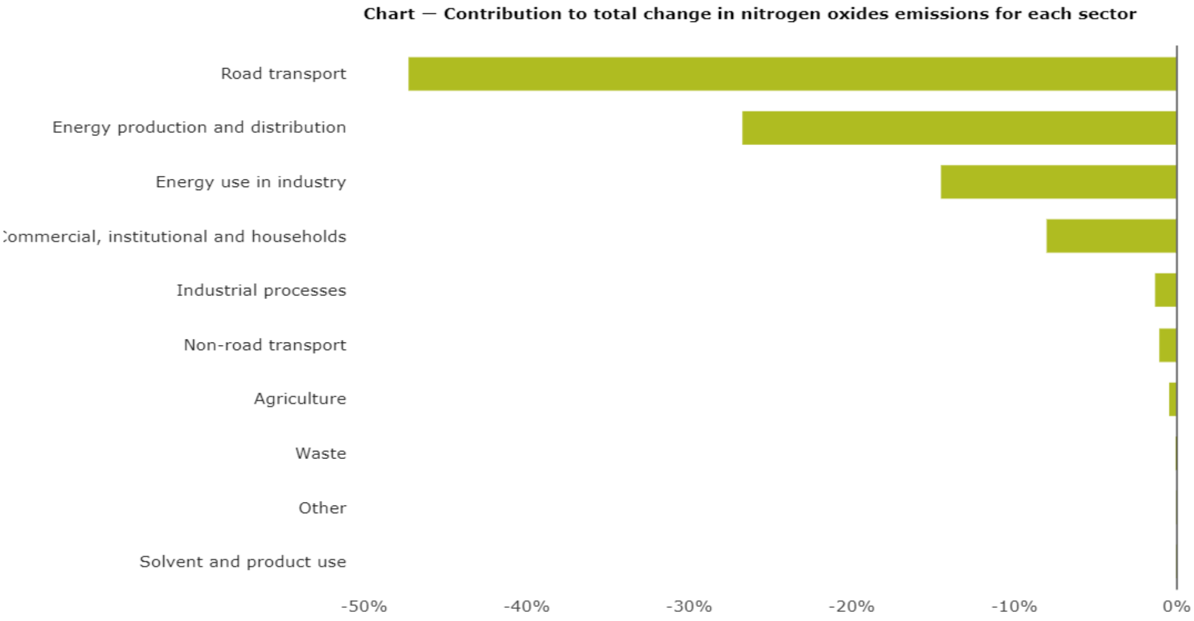

Figure 1.7 The contribution made by each sector to the total change in nitrogen oxide (NOx) emissions between 1990 and 2011.

The demand for these vehicles has been rising gradually, since they are characterized by 20-30% better fuel efficiency than the gasoline ones. They produce less CO_2, although they also form other main air pollutants such as particulate matter and NO_x. According to the China Vehicle Emission Control Annual Report, heavy-duty diesel vehicles produce about 66.2% of the atmosphere pollution.

1.1.4 NO_x emission in Poland

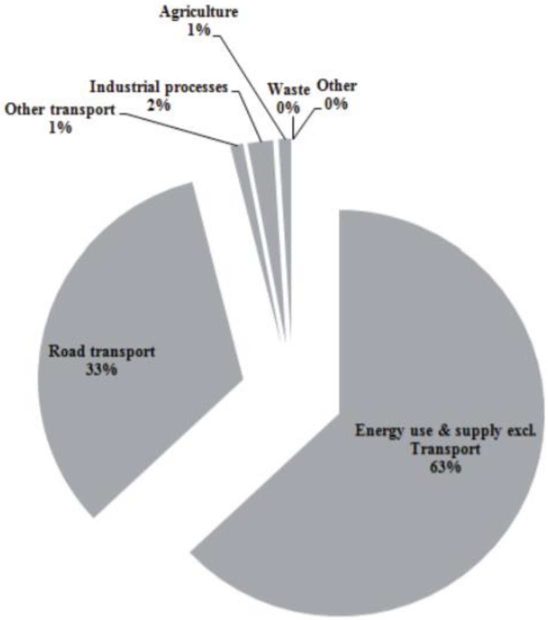

Figure 1.8: NOx emission by sector in Poland – 2011

The reduction of pollutant emissions has become a particularly complex challenge for Poland due to the massive use of coal as an energy source and the obsolescence of the infrastructures for the production, transmission and transport of energy. The energy policy of the nation, issued in 2005, aims at reducing these emissions by 20 % by 2030. These objectives are expected to be achieved thanks to the contributions of several actions aimed at promoting renewable energy sources, the cogeneration systems and those focussed on the reduction of the coal. Coal is the primary fuel for the Polish energy sector, since it is the main sector producing NO_x. Coal currently represents the 88% of all the structure of primary energy demand, and it is expected to be the main energy source in Poland in the coming years. (Fig 1.8) [16] This explains why the reduction of toxic compounds in exhaust gases is of great importance. [17]

1.1.5 NO_x Reduction Ways

The continuously implemented restrictive standards force the introduction of novel technologies. The methods for reducing nitrogen oxide emissions may be divided into two main categories:

- Primary methods (combustion control)
- Secondary methods (post combustion control)

The latter methods take place in the post combustion phase, proposing to reduce the NO_x after their emissions, while the former methods target the reduction of the NOx during the combustion. [13] The primary methods include optimisation of the amount of air directed to the boiler, stepwise combustion, the reduction of the exhaust gases temperatures or the recirculation of the exhaust gases. The primary methods are cheaper than the secondary ones, nonetheless they offer lower reduction efficiencies. Secondary methods are based on chemical reactions to reduce NO_x which is already emitted by the use of a reducing agent. The amount of the reducing agent depends on the boiler power and thus the running costs of a power plant can increase significantly. Therefore, although these secondary ways are more expensive, they allow more efficiency performances.

1.1.6 Primary methods

There are several primary methods developed to reduce the influence of combustion plants on the environment:

- Flue gas recirculation (FGR), which involves the recirculation of a portion of relatively cool exhaust gases back in the combustion process, aimed at decreasing the flame temperature. This results both in the reduction of fuel nitrogen conversion and in the formation of fewer thermal NO_x [18]. Around 20% - 30% of the flue gas is taken from the main seam at temperature of 350- 400 °C, before being injected back to the combustion zone. This method requires that the flue gas is cleaned from particulates and additionally it may require the application of special burners designs. The estimated amount of 30% should not be exceeded, otherwise corrosion or efficiency losses may occur.

- Low excess of air, which involves the decrease of the nitrogen oxide emission. By decreasing the amount of oxygen in the combustion (down to the minimum value for a complete combustion) , the thermal NO_x are reduced. Limiting the amount of excess air entering a flame is accomplished through burner design and can be optimized through the use of oxygen controls. No additional energy is required, and the method is very easy to implement. Crucially, a low amount of oxygen may result in an incomplete combustion, which in turn leads to the decrease of team temperature, high carbon monoxide emissions, reduction in boiler efficiency. The efficiency of this method varies from 10-45%. [19]

- Fuel switching, which aims at reducing the NOx levels from boilers firing distillate oils. This method uses natural gas or low nitrogen fuel oil that contain a smaller amount of fuel-bound nitrogen. Refined oils contain less than 0.05% of fuel-bound nitrogen, whilst residual oils may contain more than 0.6% of these bounds. When oils are used, the NO_x formed by fuel-bound nitrogen accounts for 20-30% of the total NO_x level. In fact, in order to reduce this effect, the solution is to use natural gas or low nitrogen fuel oil.

- Staged combustion, which involves changing the air and the fuel pattern to reduce the peak flame temperature and oxygen concentrations. This results in lower concentrations of thermal NO_x . Staging can be done internally with the burner body. Furthermore, low NO_x burners may lead to the decrease of NO_x by changing the way the air and fuel are introduced. The application of this method requires changing the burners and the instrument of overfire air. According to the method of low NO_x, burners may be divided into three groups: air staged low NO_x burner (25-35%) [20] flue gas recirculation low NO_x burner (20%), fuel staged low NO_x burners (50%-60%) and new generation of low NO_x burners combining air-staging and flue-gas recirculation.

- Fuel reburning, which consists in the injection of a natural gas after the primary fuel combustion. It is typically used only on large utility power plants that used coal or residual oil. It is a three-stage combustion process based on fuel staging.

- Water/steam injection, consisting in the injection of water or steam into the flame, which decreases the flame temperature and the formation of thermal NO_x levels. There is a limit of water and steam that can be introduced before condensation problems occur.

1.1.7 Secondary methods

Two types of secondary methods are considered [20] :

- Selective non-catalytic reduction (SNCR)
- Selective catalytic reduction (SCR)

The selective non-catalytic reduction is a method involving the reduction of the existing NO_x which formed in the flue gas of a combustion unit. Without the catalyst, the temperatures of 870-1200 °C have been achieved, depending on the reagent used (ammonia, urea or caustic ammonia, other component with high value of nitrogen).[21] When the reagent is ammonia, the main reaction is the reduction of NO_x to N_2:

$$4\,NO + 4\,NH_3 + \,O_2 \rightarrow 4N_2 + 6\,H_2O \qquad (1.10)$$

A side reaction of unwanted oxidation of ammonia may also occur:

$$4\,NH_3 + \,5\,O_2 \rightarrow 4\,NO + 6\,H_2O \qquad (1.11)$$

At temperatures below this range both the reactions have very low efficiencies, whilst at higher temperatures the unwanted one dominates and increases the level of NO_x emission. The application of urea may create high levels of N_2O and induces more carrion problems than ammonia does. There are many different configurations for different industrial areas. The presence of the catalysts is not required by this process. SNCR consists of two main units: the unit for the reducing agent storage and the SNCR unit itself, where there is the injection of the agent and the reduction of NO_x. In order to increase the efficiency of the SNCR (60-80%) , a larger amount of reducing agent is required, although this may be achieved with a release of ammonia (NH_3-slip). [22]

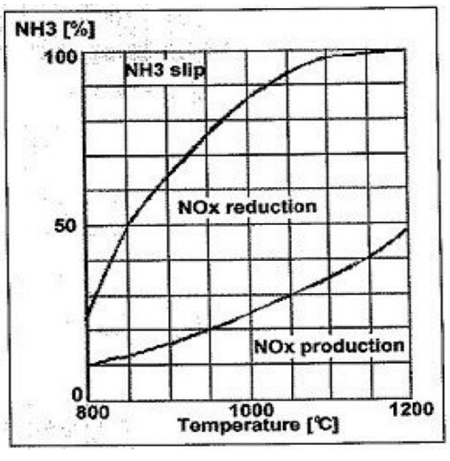

Figure 1.9: NO_x emissions and NH-slip in function of the temperature

Fig.1.9 shows the relation between the temperature, the NO_x emissions and the NH_3 slip. At high temperature the NO_x removal is bigger, and NH_3-slip is lower, while the formation of NO_x for the undesired reaction is increasing. At low temperature the NO_x is less efficient, the NH_3-slip is bigger, but the formation of NO_x is minor. To obtain low NH_3-slip formation and better NO_x removal, the reagent and NO_x should be mixed appropriately. In addition to the distribution and mixing, another important parameter is the size of the reagent drops. Small drops evaporate too fast and react at too high temperatures, with a consequent decrease in the NO_x removal. On the other hand, if the drops are too large, they evaporate too slowly, dragged by fumes, and react at too low temperatures, causing an increase in the NH_3-slip. The costs of this application are relatively low; their installation is easy. High NH_3/NO_x ratio is preferred for the removal, although this also increases the NH_3-slip. In order to neutralize these two opposite effects, it has been found that the optimal ratio varies between 1.5-2.5 as it is shown in the Tab.1.4. [23]

Selective catalytic reduction is similar to SNCR, in that it uses ammonia or urea as reducing agents. SCR introduces the application of catalysts to enable reaction with a smaller activation energy, such that nitrogen oxides reduction occurs on the catalyst surface at lower temperatures (170°C-510°C). This technology was invented in 1974 and introduced commercially in the 1980's. The reactions are similar to the ones in SNCR. [24] The ammonia presents a higher selectivity in the presence of O_2 than with other reducing agents (CO, HC):

$$4\,NO + 4\,NH_3 + \ O_2 \rightarrow 4N_2 + 6\,H_2 \text{ (standard)} \tag{1.12}$$

$$6\,NO + 4\,NH_3 \rightarrow 5\,N_2 + 6\,H_2O\ (\,slow) \tag{1.13}$$

$$6\,NO_2 + 8\,NH_3 \rightarrow 7\,N_2 + 12\,H_2O\ (NO_2) \tag{1.14}$$

$$NO + 2\,NH_3 + \ NO_2 \rightarrow 2\,N_2 + 3\,H_2O\ (fast) \tag{1.15}$$

As in SNCR, some unwanted reactions may occur without the presence of NO_x; the ammonia, for example, may be oxidized to N_2, N_2O and NO:

$$4\,NH_3 + \ 5\,O_2 \rightarrow 4\,NO + 6\,H_2O \tag{1.16}$$

$$4\,NH_3 + \ 3\,O_2 \rightarrow 2\,N_2 + 6\,H_2O \tag{1.17}$$

$$2\,NH_3 + \ 2\,O_2 \rightarrow N_2O + 3\,H_2O \tag{1.19}$$

Catalytic reduction exploits different reduction agents, among which ammonia and urea are the most applied, although other agents are also available, such as hydrocarbons (methane, propylene) Since the homogenous mixture of the flue-gas with the reducing agent is crucial, these are injected through a system of nozzles. In order to minimise the NH_3- slip and to obtain a high removal efficiency, the NH_3/ NO_x ratio has to be homogenous. The NH_3- slip must be contained under a small value, for environmental and economic reasons. Due to its lower cost per kg, the most common agent is ammonia, which shows a higher selectivity compared to other reducing agents.

Ammonia is stored as an aqueous solution or in a liquefied state at a 17 bar pressure at 20 °C. Urea is commonly used in the form of crystal granules dissolved in water before the injection . [23]

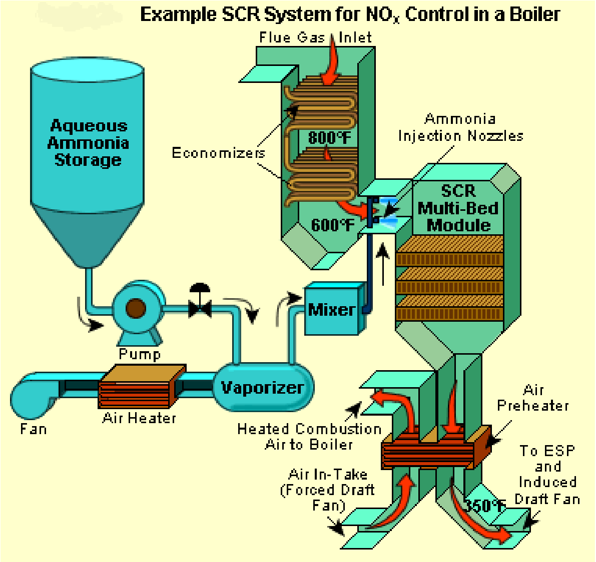

Figure 1. 10: Example SCR for NO_x

Table 1.4 General performance of secondary methods (BAT for large combustion plants, 2006)

Secondary methods	**General NOx reduction**	**Other performance parameters**	
		Parameter	Value
Selective catalytic reduction (SCR)	80-95 %	Operating temperature	350-450 °C (high -dust)
			170-300 °C (tail-end)
			280-510 °C (gas turbines)
			200-510 °C (diesel engines)
		Reducing agent	Ammonia, urea
		NH_3/ NO_x ratio	0.8-1
		NH_3-slip	< 5 mg Nm^3
		Availability	>98%
Selective non-catalytic reduction (SNCR	30- 50%	Operating temperature	850-1050 °C
		Reducing agent	Ammonia, urea
		NH_3/ NO_x ratio	1.5-2.5
		NH_3-slip	< 10 mg Nm^3
		Availability	>97 %

There are three different main configurations for SCR in the depuration of gases, which are listed in the following paragraph. The position of the catalysts is shown in Fig. 1.11. [23]

- High dust: mostly applied in big plants using coal. Here, temperatures are high and there is not the need of reheating the flue-gases thanks to the position of the catalyst. The method is characterized by high dust concentrations, that yields blocking of the monolith channel and its deactivation. Fly ash and corrosion are the main disadvantages of this configuration. Fly ash is a serious problem, due to the reaction of some compounds with the catalyst.
- Low dust: it prevents the limit of the high dust installation by installing the catalysts bed downstream the electrostatic precipitator (ESP). It requires high temperatures of the ESP, since no additional heating of the fumes is needed. Although the mechanical stress on the catalysts is reduced, this configuration may be prohibitively expensive when upgrading the old power plants.
- Tail end: it is a solution in that it overcomes the limitations of the two afore mentioned configurations (high and low dust), due to the abrasion, corrosion and deactivation of the catalyst. Narrow channels may be used without blocking, the catalyst volume is lower and the catalyst is positioned after the ESP and the desulfurization. However, due to their low temperatures, the exhaust gases need to be reheated.

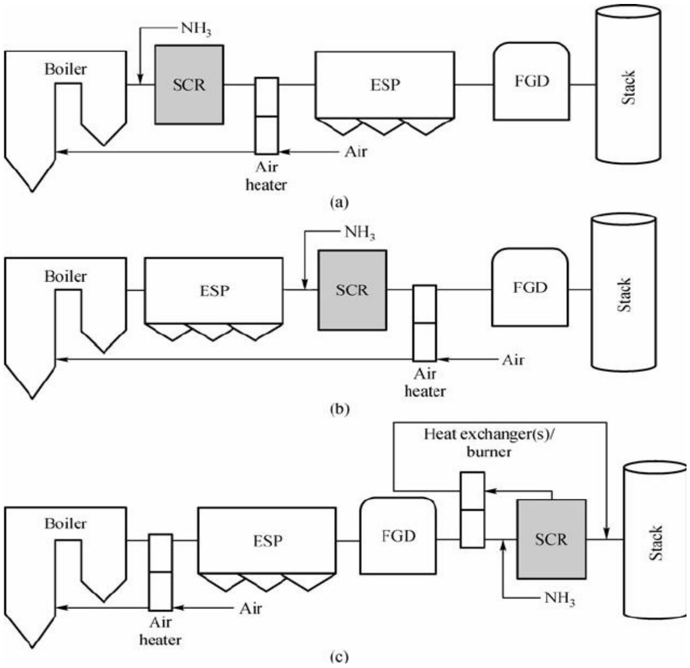

Figure 1.11 Main configurations for SCR

Selective catalytic reduction is used also in some diesel engines, with the injection of a liquid reducing agent directly into the exhaust gases. This is commonly known in Europe under its trade name “AdBlue”. Urea plays an important role and it is called Diesel Exhaust Fluid (DEF), which is classified by the Environmental Protection Agency (EPA) as a non-hazardous substance. The SCR may be connected with a particulate filter and it is generally used worldwide.

Although there are some disadvantages in the SCR method to reduce NO_x, such as the NH_3 -slip and the higher cost compared to the SNCR, this secondary method is still considered the main and most efficient technology to reduce the emission of nitrogen oxygen.

This work it will be investigate the NH_3- SCR application to calculate the efficiency of the catalysts which were prepared in the laboratory of the group for catalytic and adsorption processes in energy and environmental protection at the AGH- University of Science and Technology. Currently the SCR processes using NH_3 have been commercially used in stationary source combustion units. In the United States more than 1000 SCRs have been applied in 2019. SCR needs the application of a catalyst and during the years great efforts have been made to develop highly efficient and poison-resistant SCR catalysts. Strong acidity and redox properties are two crucial and main factors to increase the properties of SCR catalysts, with a huge window of temperatures, which optimize the formation of the desired products (N_2 and H_2O) and influence the adsorption/activation of NH_3 and NO_x. As it is shown in Fig.1.12. modification or doping are aimed at increasing the acidity and the redox circle, through the creation of new nanostructures, the explosion of specific crystalline plans and the improvement of the preparation steps. [25]

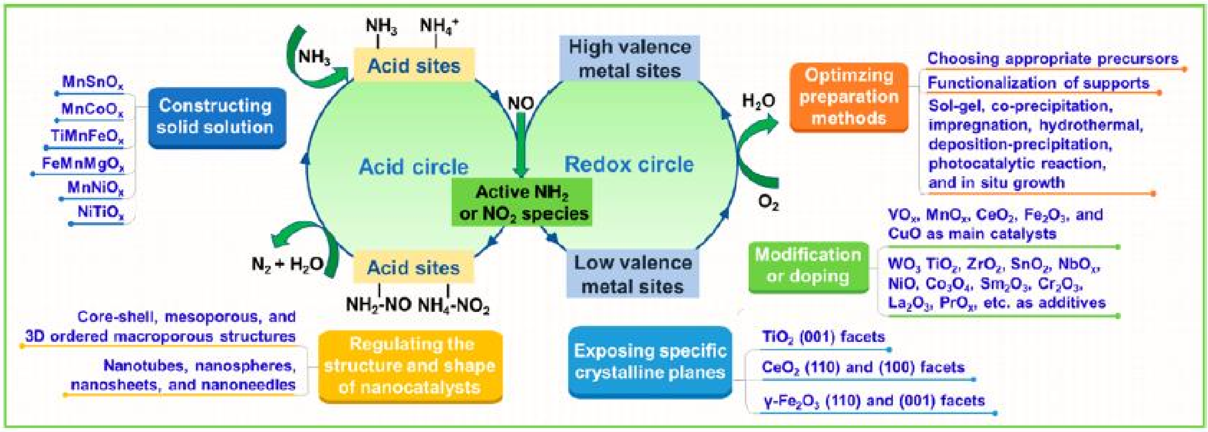

Figure 1. 12 General strategies for improving the acidity circle and redox circle of SCR catalysts.

1.2 Catalysis and catalysts for NO_x removal

Catalysis is defined as a process in which a small amount of substance (catalyst) leads to the increase of the reaction rate. Surface intermediates are created and in the last stage the catalyst returns to its original form.

The first definition was provided by Berzelius in 1835: “a catalyst is a substance that increases the velocity with which a chemical reaction reaches its equilibrium without being appreciably consumed” [1]. Furthermore,

- a catalyst can increase only the reactions that are thermodynamically preferable, it cannot increase the rate of reactions that are not thermodynamically feasible
- a catalyst increases the direct reaction and the inverse one at the same time

- when multiple reaction pathways are possible, the catalyst only increases some of them with increased selectivity of the reaction
- it does not exist a unified theory for catalysis

The choice of the most suitable catalyst is important, as well as the proper conditions of the catalytic reaction, which lead to high selectivity to a certain reaction. Catalysis is a relatively young science. As such, a unified theory which explains a catalytic system regardless of its composition and the specific reaction in which the catalyst is applied has not yet been achieved. In industry, catalysis may be considered as some sort of "art", in that every industry develops its catalytic system with principles based primarily on empirical assessments.

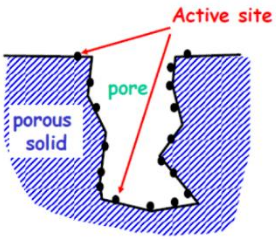

Figure 1.13: Catalyst

The considered catalyst consists mostly of an active phase support on a carrier. The carrier gives stability whilst also allowing a proper dispersion of the active phase material and it usually has a high specific surface area. The carrier, in general, has to be inactive but in some cases it affects the activity of the active phase and it influences the structure and texture.

Catalysts may be classified and divided in two groups, although the distinction is not so strict. The former are the bulk catalysts (metal alloys, co-precipitated catalysts) and the latter are the supported catalysts, in which the active phase is dispersed onto a porous material (support). Catalysis may further be distinguished between heterogenous or homogeneous catalysis. The heterogenous catalysis implies that the catalyst is in a different physical phase than the reagents; usually the catalyst is a solid and the reagents are gaseous or liquid. On the other hand, the homogeneous catalysis requires that both the reagents and the catalyst are in the same physical phase, generally liquid or gas. In general, the diction is 80% heterogeneous catalysts, 15% homogeneous catalysts, and 5% biocatalysts among the catalysts in use.

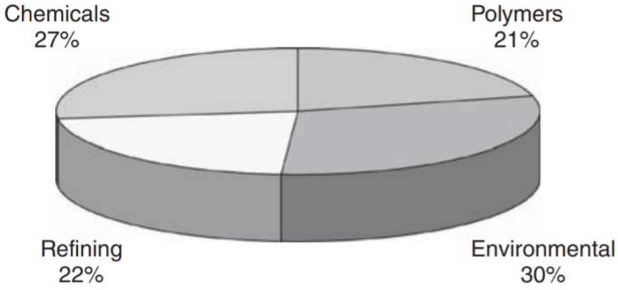

Figure 1.14: Worldwide catalyst market according to application

For over 100 years chemical industry is the main sector where catalysts have been used, since 1880 when the production of sulfuric acid was introduced. From 1970, the environmental catalysis gained more importance, especially within the automobile and the industrial area, because of the purification of off gases from power stations and industrial plants. Environmental catalysis contributes to protect the environment and to guarantee a higher standard of living. As it is shown in Fig.1.14 , the catalyst market is divided into four areas: chemicals, polymers, refining, environmental. From 1995 to 2005 catalysts grew by 4% annually, mostly in North America and Europe. [26]

The work that is reported here focuses on heterogenous catalysis for environmental applications. In particular, in catalytic air pollution controls, the processes employ solid heterogeneous catalysts through which gaseous reactants flow.

The production of NO_x from outgases is one of the most relevant and challenging problems of the 21st century. As it was explained in the previous paragraph, NO_x are still considered one of the most dangerous substances released in the atmosphere by industries and transports. Even if the legislations' targets have become more restrictive and NO_x emissions have decreased in the last decades, the problem of their reduction is still under investigation.

Among the heavy industrial sources, the issue of limiting stationary sources has only been tackled by the SCR-NH_3 method (Selective Catalytic Reduction with ammonia). This method is commonly used in EU, Japan and the USA. It is also one of the solutions to remove NO_x in Diesel engines exhaust. Further investigation is needed in order to introduce a more competitive installation, where the main concern is the choice of the catalyst that is required in SCR.

In NH_3-SCR, the ammonia reacts selectively with NO_x to produce N_2 over three different types of catalysts: Pt type catalysts at low temperatures (175-250°C), zeolites at high temperatures (350-600 °C) and V_2O_5/ WO_3/TiO_2 at intermediate temperatures (300-450 °C) (Fig. 1.15) [27]

Pt catalysts exhibit low selectivity to N_2 at temperature above 300 °C, although V_2O_5 based on Al_2O_3 was first used at higher temperatures. However, $Al_2(SO_4)_3$ may form, which deactivates the catalysts, and introduces problems concerning the presence of sulfur. At this temperature range (250 °- 400 °C), V_2O_5- TiO_2 seem to be the best and most used solution, according to 10-15 years of experience, and they are sulfur tolerant. At high temperatures (345°C -600°C), zeolites are the most effective catalysts. These show high NO_x conversion, very low NH_3-slip and sulfur tolerance above 425 °C.[28]

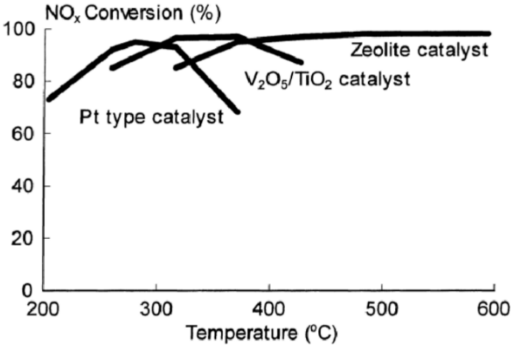

Figure 1.15: Three catalysts for SCR

V_2O_5/ WO_3/TiO_2 is an active and selective catalyst for SCR with ammonia, although its shortcomings prevent it from meeting new requirements. In fact, this catalyst is not ideal for the removal of NO_x in SCR-NH_3, which implies the need to improve some properties such as:

- Higher activity in a wider range of temperature (for lower temperatures < 250°C and for higher temperatures > 400 °C)
- Higher resistance to water and SO_2
- Possibility to employ other reducing agents (hydrocarbons: methane, propane, propene and others)
- Cheaper solutions

1.2.1 New promising catalysts for NO_x removal

Many scientific publications tried to develop other promising supports for NH_3-SCR catalysts. For example: hydrotalcite-derived mixed metal oxides [29], cenosphers [30], activated carbons [31].

Layered clays appear to be good candidates for their application in SCR. For this reason, they are often used in catalysis, but because of the wide variety of different clays, they continue to be studied in order to try to find more and more effective solutions. They represent a large class of abundant materials in the natural environment, they are fairly cheap, and they can also be prepared in the form of monolithic, like V_2O_5/ WO_3/TiO_2 [28] .

It was shown in the literature that some pillared clays may also exhibit a higher activity than the commercial vanadia [28]. Acid-treated layered clays were the first catalysts used for cracking catalysis, although they are no longer used for this application because of their low hydrothermal stability. Nonetheless, they are still being investigated for their use in the organic industry and environmental protection.

Among all the clays and mineral clays, which have been investigated throughout the year as possible solutions to the problem of NO_x removal, particular consideration was given to smectites, mostly montmorillonites. These are interesting since, when treated with different methods, they change their activity, selectivity, acid/basic and textural properties.[32] Therefore, the aim was to recognize which peculiar characteristics resulted in higher performances. The typical preparation steps will be analysed and presented in the following chapters. Montmorillonite was an industrial waste, used for sorption and for cleaning oils from organic compounds. However, after modification of the clay, montmorillonite proved to be active and selective in SCR at low temperatures [32] . Therefore, this represents a source of reusable material and a good alternative to the common V_2O_5/ WO_3/TiO_2 catalysts.

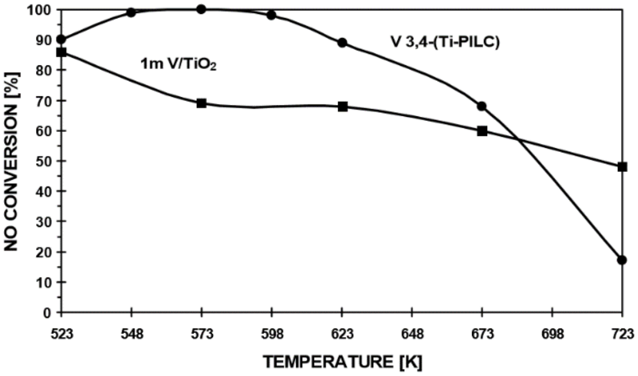

Figure 1.16: Catalytic performance of vanadium catalyst supported on Ti-pillared clay and of conventionally prepared V/TiO2 sample in

Serwicka and Bahranowski showed that titania pillared clay with vanadia has better performance in wide windows of temperatures, compared to the commercial vanadia/TiO_2, as it is shown in Fig 1.16. [33]

The catalyst supported by pillared clays exhibits better performances than it does without the clay. This supports the studies of the application of these new materials for NO_x removal.

The commercial V-based catalyst can also release vanadium in the environment, which leads to some secondary contamination in the soil. [34]

The choice of the support must be well considered: it should have well-developed pores systems to facilitate the access of the molecules, it should have high thermal stability, durability and it should provide active sites itself.

A general agreement has not yet been reached regarding the mechanism of removal of NO_x with layered pillared clays. In fact, the main acidic sites necessary for the reaction and the NO intermediate species have not been satisfactorily identified yet. The design of a corresponding system of V_2O_5/ WO_3/TiO_2, involving clay structures, still represents a great challenge.

This work addresses this issue, in order to find an alternative catalyst which is active at low temperatures, where the V_2O_5/ WO_3/TiO_2 shows the higher activity. The adopted approach is based on different modifications of the layered clays.

There are several possible structural, textural and compositional modifications and also a wide range of preparation variables determining the resulting layered minerals, which may find catalytic applications in particular in the environmental catalysis.

Therefore, the development of low-temperature SCR catalysts that can be located downstream of the desulfurizer and the electrostatic precipitator is a challenging task. Research is currently underway to obtain the best possible catalysts, capable of reducing nitrogen oxides to pure nitrogen and water. Among the zeolite systems enriched with metal ions of transitions, cobalt seems particularly promising. These metal ions of transitions seem to be able to overcome the presence of a low amount of SO_2, which was created after the deactivation of the desulfurizer responsible for the creation of catalysts at low temperatures.

Cobalt has different oxidation states which makes it suitable for redox reactions. It has shown high efficiency in CH_4-SCR of NO_x and Co exchange zeolites show a high catalytic activity. For this reason, the presence of Cobalt is expected to result in a good performance also in NH_3-SCR. Co has widely been used as/to promote the active phase for the support; Zhang and Shen first understood that this element may be used as a modifier for the support, since it has a good catalytic activity at low temperatures and a good resistance to SO_2 and H_2O. [35]

In the work of Carriazo et al., Colombian bentonite was successfully pillared with solutions of Al, Al-Fe or Al-Ce-Fe polyhydroxocations under moderate conditions of synthesis in order to obtain active catalysts. The addition of Ce as a pillar agent allows the increase of the basal spacing and enhances the catalytic activity of the solids.[36]. Unlike the reported studies where cobalt is used as an active phase and ceria as a pillar agent, this work introduces ceria as the active phase and cobalt as the pillar agent, and a discussion is included on whether they are able to increase the removal of NO_x and improve the performances.

1.2.2 Clays science

In the Earth's crust, clay and mineral clays are the youngest members of the minerals' family. Natural clays are irregularly distributed in the lithosphere and they are subjected to spontaneous modification and transformation, they are formed from different rocks under different conditions, varying in the structure, chemical composition and properties. Clay particles are sensitive to mechanical and chemical treatments. The testing conditions can give rise to discrepancies in the results of measurements analysed in different laboratories and with different techniques of investigation. A small sample of material examined may present different ways to react from its bulky counterpart. For this reason, the results of the investigation for these materials are still unknown, they can react in different ways and the analyses do not lead to unique results when the same clays are studied. Clay science has become increasingly significant after decades of studies. [37] This has yielded an extensive examination of the mineral clays that began to tend towards a physico-chemical orientation. Several hundreds of scientific reports on clays and clay materials have been published each year, such as patents, lecture notes, technical reports. The rapid development of clay science is supported by the increasing formation of related scientific communities in several countries. For example, *Clays and Clay Minerals* is the official publication of The Clay Minerals Society. (Fig. 1.17)

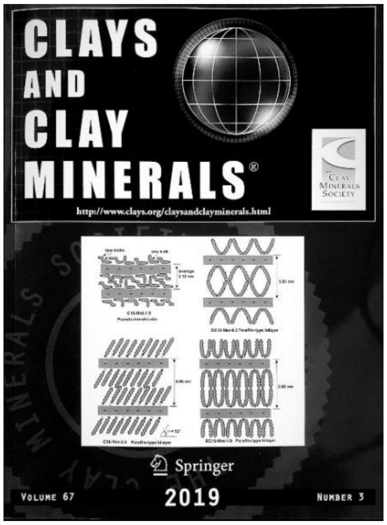

Figure 1.17: The Clay Mineral Society

Although the scientific interest has increased over the years, the practical use of clay dates back to the first ancient agrarian settlements, even if clay is still indispensable to modern living. Therefore, humans have always employed these materials to make utensils or bricks, even before acquiring the knowledge that was only gained decades later and before achieving the level of expertise about the physico-chemical properties of clays, which has only been achieved lately. With time, empirical technologies have been converted into scientific methods based on theoretical studies. Two main features have sparked the increasing interest in and study of these materials:

- Extraordinary properties
- Common availability

In fact, no other group of inorganic materials have as many different species showing a range of reactivity as wide and a capability to be modified as high as these materials. Even if the chemical and mineral composition of clays (variations in crystallinity, presence of impurities, structural imperfections) is much more difficult to quantify than in other materials, the bibliography connected to this subject is rich of references. Clays are still a subject of current investigation that has not yet reached a complete knowledge due to the difficulty in gathering all the aspects of clay science in a single comprehensive text. In fact, the multi-disciplinary nature of clay science creates several different concepts and views on clay and clay mineral species.

Clays and clay minerals are recognized as the materials of the 21st century for these three main features [37]:

- Abundance
- Low cost
- Environment friendly

1.2.3 Differences between clays and clay minerals

- **Clays:**

Georgius Agricola (1494-1555) introduced the first definition of clay. Five centuries later, the Joint Nomenclature Committees (JNCs) of the Association Internationale pour l'Etude des Argiles (AIPEA) and the Clay Minerals Society (CMS) defined 'clay' as 'a naturally occurring material composed primarily of fine-grained minerals, which is generally plastic at appropriate water contents and will harden with (sic) dried or fired'. [38]

Sometimes the term *clay* is used synonymously with the term *soil*. Moore (1996) commented that clay is used in three different ways: as a size term, as a rock term and as a mineral term. Particle size is a key parameter for defining a clay, although there is no established upper limit target. In pedology the size of particles is < 2 µm, in geology and geoengineering is < 4 µm [39]. In terms of clays, plasticity is considered as "the property of a material which allows it to be repeatedly deformed without rupture when acted upon by a force sufficient to cause deformation and which allows it to retain its shape after the applied force has been removed" [39]. Mineralogical composition, particle size distribution, organic substances and additives may affect the plasticity of clays. The presence of water requires more force to deform the clay. The minimum amount necessary to make clay plastic is the "Plastic Limit" (PL). A plastic body can withstand the addition of a huge amount of water, if the content of water is increased then the clay becomes a paste, it gets wet and can no longer maintain a molded shape. This state is represented by the "Liquid Limit" (LL). The difference between LL and PL id the Plasticity Index (PI). A clay with PI > 25 % tends to expand or swell when wet.[40]

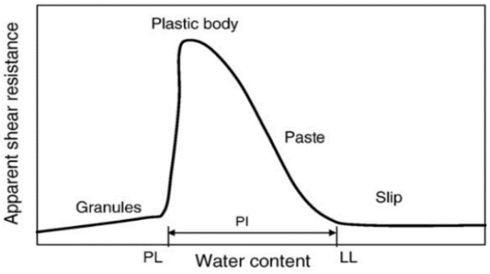

Figure 1.18: Plasticity limits of clays

Tab 1.1 shows the currently adopted clay names, even if four types of clays (bentonite, kaolins, palygorskite and sepiolite and common clays) are mainly investigated for industrial applications. [39].

Table 1.1 Current names of clays

Current names of clays	**Origin**
Ball clay	Sedimentary
Bentonite	Volcanic rock
Bleaching earth	Acid-activated bentonite
Common clay	Sedimentary or by weathering
China clay	Hydrothermal
Fire clay	Sedimentary
Flint clay	Sedimentary with subsequent diagenesis
Fuller's earth	Sedimentary, residual, or hydrothermal
Primary kaolin	Residual or by hydrothermal
Secondary kaolin	Authigenic sedimentary
Refractory clay	Authigenic sedimentary
Laponite	Synthetic

- **Clay minerals**

According to the definition approved by the JNCs, clay minerals "are phyllosilicate minerals and minerals which impart plasticity to clays, and which harden upon drying or firing". [38]

In addition, clay minerals are not distinguished by their size, they can be natural or synthetic and they may contain phyllosilicates or non-phyllosilicates.

Table 1.2 Mineral clays

Mineral class	**Mineral subclass**	**Mineral group**
SILICATE **Contains SiO_4^{-4} tetrahedron as basic structural**	**Phyllosilicate** SiO_4^{-4} tetrahedra are linked together to form two-dimensional sheet like structure	Kaolite (Serpentine-kaolin)
		Smectite (Montmorillonite)
		Illite (Interlayer-deficient)
		Vermiculite
		Palygorskie-Sepiolite
		Mixed Layer (Inter-stratified)

1.2.4 Atomic structure of mineral clays

The atomic structure of mineral clays is made up of two basic units with a different repetition in the space, the octahedral and the tetrahedral sheet. (Fig 1.19) The diversification of mineral clays is based upon the different configuration and arrangement of tetrahedral and octahedral sheets.

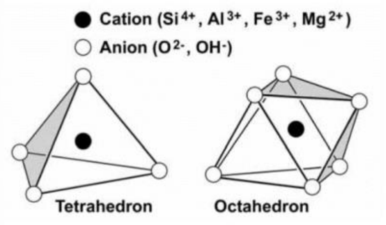

Figure 1.19: Atomic structure of mineral clay

- **Silica tetrahedral sheet**

The basic unit of a tetrahedral sheet is the silicon-oxygen tetrahedron, where each central silicon (Si^{4+}) shares its charge with four oxygen anions (O^{2-}). Along the tetrahedral sheet each Si atom shares three oxygens with the adjacent tetrahedrons, while one oxygen remains unshared. The atoms are dislocated on three levels (Fig. 1.20)

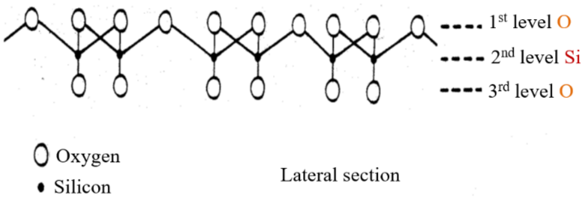

Figure 1.20: Diagrammatic sketch of the tetrahedral sheet

The silicon atoms are equidistant from the four oxygens (or hydroxyls). The tetrahedrons are placed to form a hexagonal network repeated in two dimensional directions, which creates the so-called "Silica tetrahedral sheet". The fourth O^{2-} anion is not shared with the other tetrahedron (apical oxygen); this, in addition to an H^{+} ion, forms hydroxyls, which neutralises the charge. Individual tetrahedral silica sheets do not form stable mineral but they are combined with the octahedral sheets. (Fig. 1.21) [41]

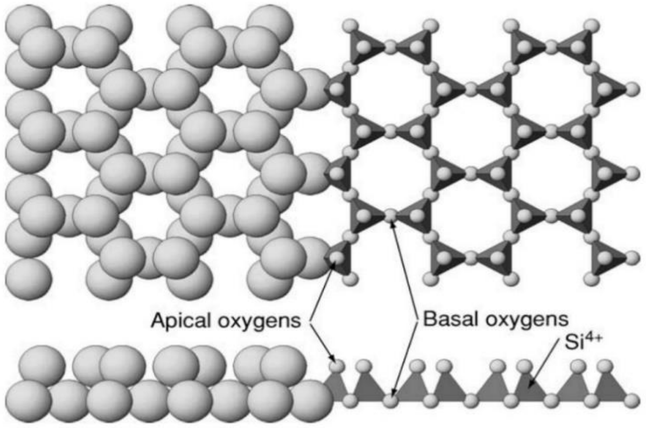

Figure 1.21: The tetrahedral sheet as a sphere-packing model (left half) and a polyhedral model (right half).

- **Octahedral sheet**

The octahedral sheet of clay minerals is usually made up of Al^{3+} ions at the centre, surrounded by 6 hydroxyl (OH^-) anions. Sometimes iron or magnesium ions may be found in place of the central cation with an octahedral. The structure is defined dioctahedral if the cation is Al^{3+} formed by the sequence of 2 Al^{3+} and 6 OH- groups. (Fig. 1.22) Otherwise, it is defined trioctahedral if all the three central positions are filled to balance the structure. (Fig 1.23)

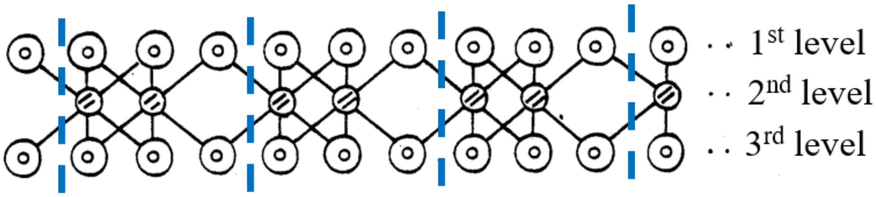

Figure 1. 22: Dioctahedral structure

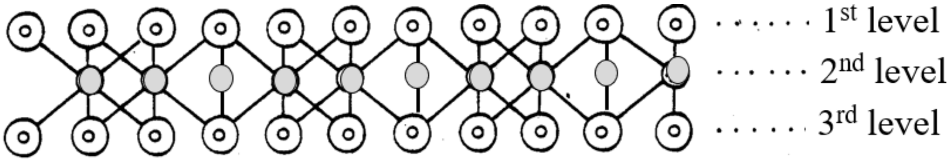

Figure 1.23: Trioctahedral structure

Fig 1.24 shows that in the octahedral sheet with Al^{3+}, each adjacent octahedra shares edges, and a proton (H^+) must be associated with each O^{2-} for charge balance. Each OH^- contributes one-half a negative charge to each cation because each OH^- is shared between two octahedra, which results in a neutral structure. [41]

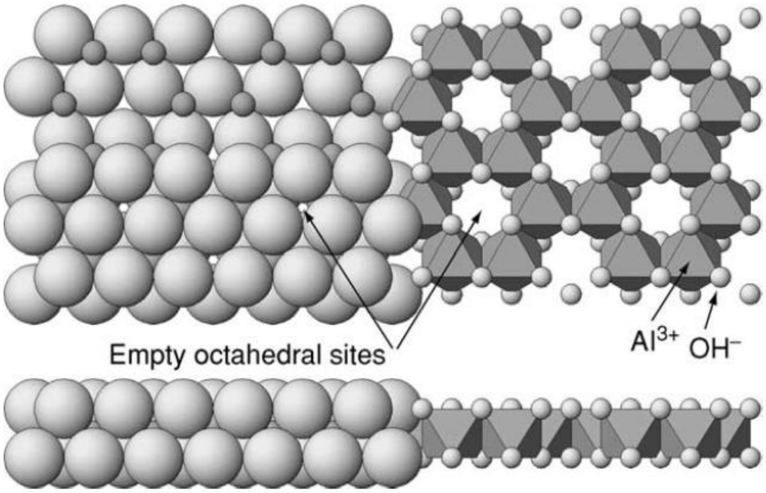

Figure 1.24: The octahedral sheet as a sphere-packing model (left half) and polyhedral model (right half)

The octahedra also shows two different topologies based on the (OH^-) position, corresponding to the cis- and trans-orientation

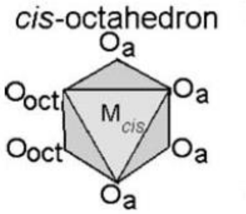

Figure 1.25: Cis-octahedron

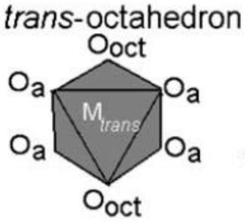

Figure 1.26: Trans-octahedron

O_a represents the apical oxygen, which atoms share with the tetrahedral, while O_{oct} is the anionic site which is shared among adjacent octahedra.

The two basic sheets (the tetrahedral and the octahedral) are assembled and they share the apical oxygens or hydroxyls. From this union two mineral layers may be distinguished: the 1:1 clay mineral layer and the 2:1 clay mineral layer. [41] (Fig. 1.27)

In the 1:1 layer, there are two planes of atoms composed by one tetrahedral sheet and one octahedral sheet. One plane of the sheet is formed only by O_b belonging to the tetrahedral sheet, the second consists of the oxygens (O_a) in common to both the tetrahedral and the octahedral sheets in addition to the hydroxyls belonging to the octahedral sheet, whilst the third consists only of hydroxyls belonging to the octahedral sheet.

In the 2:1 layer, there are four planes of anions composed by two tetrahedral sheets and one octahedral sheet. The two external surfaces are composed of the O_b belonging to the tetrahedral sheets, while the two internal ones are formed by the oxygens (O_a) shared with the octahedral and the tetrahedral sheets, in addition to the hydroxyls belonging to the octahedral sheet.

Several mineral species belong to the 2:1 minerals, which are more structurally different, whereas only two major minerals present 1:1 layer structures.

In addition, there is also the 2:1:1 clay minerals, which are composed of an octahedral sheet adjacent to a 2:1 layer; this is typical of chlorite.

These different types of layers have a given and constant thickness (thickness of the fundamental sheet structure). The combination of the sheets is less thick when one layer is interconnected to another through a shared atom. For instance, the thickness of the tetrahedral layers is almost 3,4 Å and the octahedral is thinner.

- tetrahedral + octahedral layer = 7 Å unit layer, a 1: 1 structure,
- two tetrahedral + octahedral layer = 10 Å unit layer, a 2:1 structure,
- two tetrahedral + two octahedral layers = 14 Å unit layer, a 2:1 + 1 structure

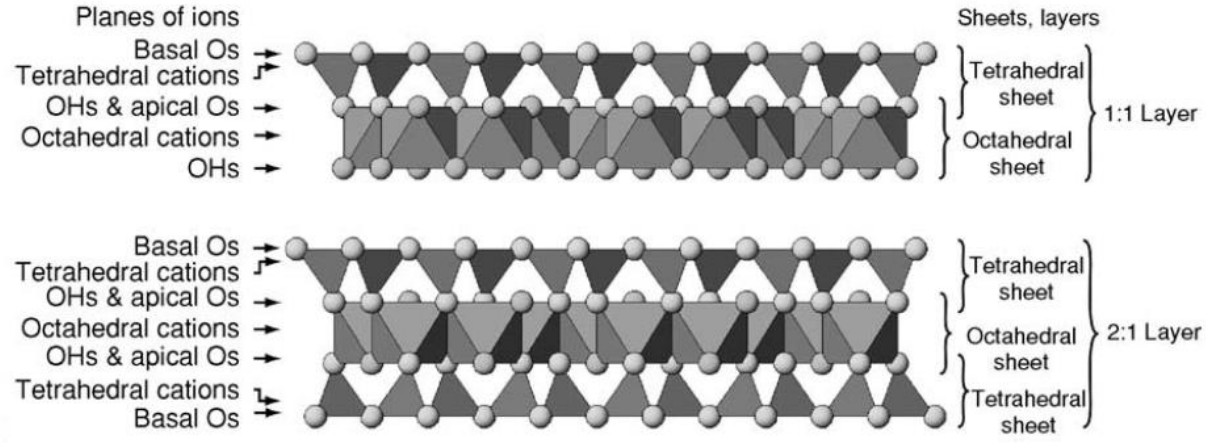

Figure 1.27: 1:1 and 2:1 layer

The thickness of the layers depends on the amount of interlayer water; hence these values are not fixed. [42]. When these layer clay minerals are linked together, the resulting structure is either electrically neutral or negatively charged. Neutral sheets: when the tetrahedral sheet contains Si^{4+} in all the tetrahedra, when there is a trivalent cation present in two octahedral sites and a vacancy in the third octahedra or when there is a divalent cation present in all the octahedral sites. Negative sheets: when there is a substitution of a cation with another with a different charge. There are different types of charge substitution which can create charge imbalance.

Different types of charge imbalance created in the layers:

- Constant ionic site occupation
- Interlayer Substitution
- Non-stoichiometric, di- and trioctahedral substitution

- **Constant ionic site occupation**

The tetrahedral and octahedral cations are brought into electrostatic equilibrium by the substitution of a lower charge in one site and the substitution of a higher charge in the other site. For example, when Al $^{3+}$ substitutes Si^{4+} in the tetrahedral site, a charge imbalance is created in the tetrahedral sheet, therefore, it is necessary to have a charge compensation to create electrostatic balance in the structure. Fig 1.28 shows the 1:1 structure with this type of substitution.

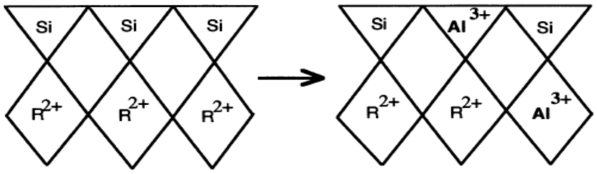

Figure 1.28: Constant ionic site occupation

- **Interlayer substitution**

In the 2:1, the charge imbalance may be compensated by the insertion of an ion between the unit sheets of the structure. If in the tetrahedral sheets Al^{3+} is substituted by Si^{4+}, the charge deficiency of -1 is compensated by the insertion of an ion with a balancing charge of +1 between the two sheets facing one another.

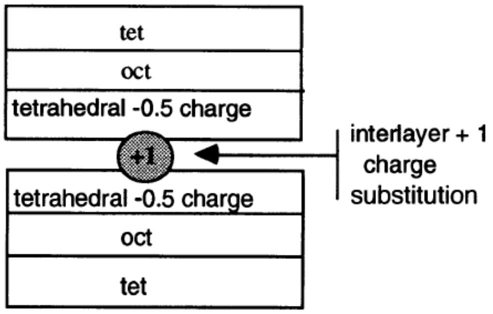

Figure 1.29: Interlayer substitution

- **Non-Stoichiometric, Di- and Trioctahedral Substitution**

In case a charge imbalance occurs in the octahedral sheet, it is possible to fill the three sites, included in a layer silicate unit cell, with three divalent ions (trioctahedral structure) or with two trivalent ions (dioctahedral structure). This is a major subdivision of the clay minerals, defining their composition and their origin.

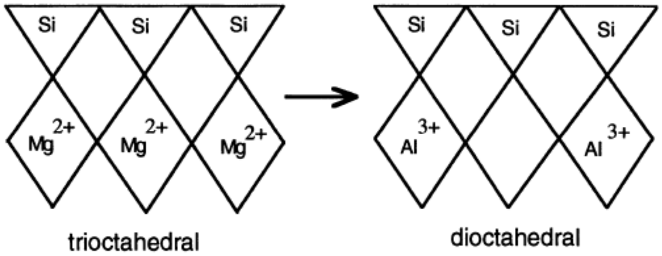

Figure 1.30: Non-Stoichiometric, Di- and Trioctahedral Substitution

1.2.5 Bentonite

The term "bentonite" is ambiguous. Other names are often used instead of bentonite to indicate the same object: bleaching soil, adsorptive soil and adsorptive clay, volcanic clay, soap clay, mineral soap. The term bentonite was first used in1898 by Knight to describe a clay mineral with soapy properties, dating back to the Fort Benton unit of Cretaceous age formations in Wyoming.

In 1917 Wherry and Hewitt defined this clay as an alteration product of volcanic ash. In 1926 Ross and Shannon presented the following definition: "Bentonite is a rock composed essentially of a crystalline clay mineral formed by the devitrification and the accompanying chemical alteration of a glassy igneous material, usually a tuff or volcanic ash". The term bentonite is now well established (Whright, 1968) for any clays whose main composition is a smectite clay mineral, which determines the properties of the bentonite regardless of its origin. It is applied commercially to any clay with similar properties. Fuller's earth is a bentonite. [27]

Bentonite is a geological term for soil materials with high content of swelling minerals, it is highly plastic, it can expand considerably when water is added (up to 12-15 times its dry bulk) and it has high cation exchange capacity. It is a rock made of highly colloidal and plastic clays. It is composed of smectites, mainly montmorillonite. The remaining part of the bentonite may vary substantially in mineralogy, depending on the geochemical conditions during the formation of the bentonite. Quartz, felspars, gypsum, calcite, pyrite, iron oxides and hydroxides are present in bentonite as a typical accessory mineral. The properties of the bentonite are in fact due to the crystal structure of the smectite group. Therefore, bentonite is a mixture of minerals, and no "molecular" formula can describe them.

Variations in interstitial water and exchangeable cations in the interlayer spaces affect the properties of the bentonite. In this project, modification on layered clays is used to increase some properties and to improve the catalysis. Bentonite exhibits the properties of thixotropic gel formation with water, high water adsorption and high exchange capacity (CEC). Among its properties, there are low compression, high shear and compressive strength, sorbent effects, plasticity, lubricity, shrinkage. However, the mentioned properties vary depending on the identity of the absorbent balancing cations. Since it is very easy to exchange the cations, these properties may be easily controlled. Properties are only to be considered in general terms, since they effectively vary from sample to sample even in a given deposit. [27]

1.2.6 Bentonite production

Bentonite derived from ash falls tends to be in beds of uniform thickness (from few mm to 15m) extended in large areas, spanning a huge range of ages. The major producer of bentonite is the USA. 90% of the bentonite which was produced worldwide between 1991-2002 has arrived from the USA, Greece, Turkey, Germany, Italy, Japan, Mexico, South Africa and Australia.

A partial amount of bentonite has been produced synthetically in Europe and in the USA for employment in catalysis. Bentonite has different applications, spanning from agriculture, horticulture, to chemical industry (e.g. sulphur production, catalysis, adsorbent for radioactive materials) and environment technology (e.g. forest and water conservation).

1.2.7 Na -Bentonite and Ca- Bentonite

The distinction between these two types of bentonites is due to the main mineral clays present in the bentonite: montmorillonite. If the basic mineral is Na-montmorillonite, the bentonite is called sodium bentonite (Na-Bent), whereas if the basic mineral is Ca- montmorillonite the bentonite is called calcium bentonite (Ca-Bent). Like in the case of Na-montmorillonite, in the sodium bentonite the suspensions of Na-Bent that have a high swelling property with water have a long lifetime, higher than Ca-bentonite. There exist some bentonites that contain both the swelling and non-swelling bentonites. Meta-bentonite contains both Ca-bentonite and Na-bentonite.

Na- Bentonite was adopted throughout this work. The first step in preparing the samples is therefore to obtain the Na- Bentonite. To this purpose, an exchange with NaCl is carried out. As it was mentioned in the first chapter of this thesis, the presence of exchangeable cations is of crucial importance for the following treatments. [43]

Bentonite has a layered construction which looks like convoluted leaves, which is especially evident in darker spots. Clays minerals occur abundantly in nature and due to their high surface area and ion-exchange properties, they are also widely used as catalysts. [44]

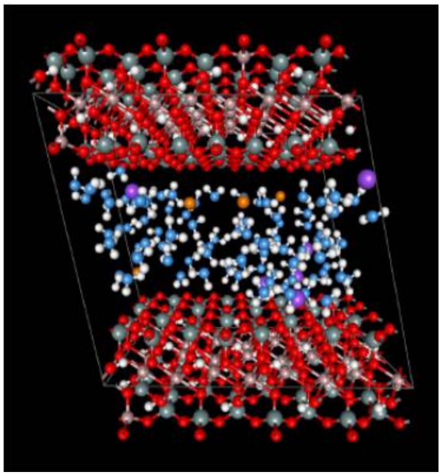

Figure 1.31: Bentonite

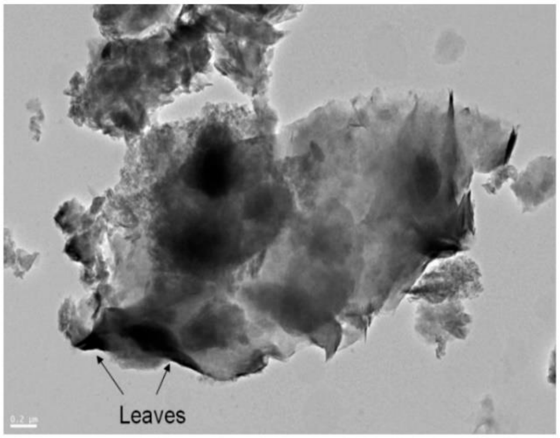

Figure 1.31: convoluted leaves of Bentonite

1.2.8 Montmorillonite

The montmorillonite is part of the dioctahedral smectites group and it is the main component of bentonite. The structural unit of the mineral is a negatively charged layer composed of SiO_4 pyramids and a layer containing Al^{3+} ions. Its structural charge is originated from the partial substitution of Mg^{2+} by Al^{3+} in the octahedral sheet and therefore additional cations are needed in the interlayer space to neutralize the charge. Other ions (e.g. such as Mg^{2+}, Fe^{2+}, Zn^{2+} and Li^{+}) can enter the octahedral sheet structure. However, Si^{4+} cannot enter because of its higher oxidation state, but the Si^{4+} may be replaced by Al^{3+} or Fe^{3+} in the silica layers.

M^{+} is generally cations that can neutralize the negative charge. Depending on the amount of water that enters, the layer thickness changes and the swelling property characteristic of the smectite group is improved by the presence of Na^{+} that attracts a lot of water. For this reason, the Na-montmorillonites are also called "swelling montmorillonites". X- ray diffraction patterns show the difference between the Na- and Ca- montmorillonite, the Na-montmorillonite has an original layer thickness of d (001)= 12 Å and the Ca- Montmorillonite d (001)=15 Å.[45]

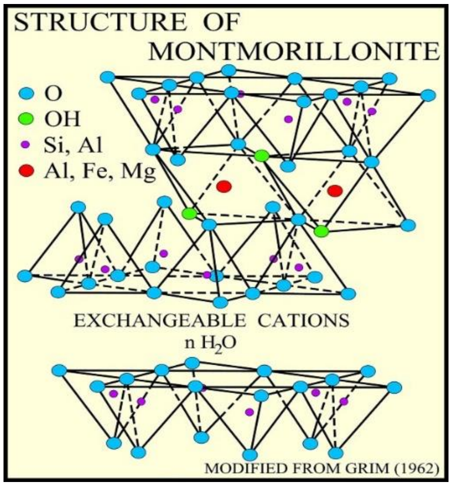

Several octahedral and tetrahedral sheet may be joined in a crystallite by interlayer cations, due to Van der Waals forces, electrostatic forces or hydrogen bondings.

Figure 1.32: Structure of montmorillonite

1.3 The possibilities of modification of layered clays

There are lots of different alternative possibilities for modifying the structure, texture and other physicochemical properties of natural layered clays thanks to their structure expandability, ion exchange properties and flexibility of the layer composition.

This work focuses mainly on three of these modifications:

- Acid treatments
- Pillaring

1.3.1 Acid treatments

Acid modification of minerals is based on the use of an acid solution for a certain amount of time at boiling temperature. The result depends on the type of applied acid, acid-to-clay ratio and the duration of the treatment. Acid activation of clays and clay minerals had been used for decades for many applications, and it has remained the most useful chemical treatment for the future of clay science. The acid activation is one of the most common chemical modification of layered clays employed in industrial and scientific fields. The result of this modification is based on the increasing of the specific surface area, porosity and surface acidity. The most used acid solutions are HCl, HNO_3 and H_2SO [46].The activation force and the number of acidic sites also increases. During the treatment, various number of cations present in the clay are removed, depending on the composition of the clay and on the intensity of the acid treatment. An aggresive treatment may be adopted in order to dissolve the octahedral cations, while the tetrahedral sheet forms free amorphous silica gel, which shows different properties depending on the used clays and on the applied treatments. This change in the structure implies the transformation of ordered silicates to amorphous silica. However, a less acid and hence less aggressive treatment may be adopted, since the maximum efficiency of the acid treatment is obtained at intermediate acidity concentrations. In fact, increasing the acidity results in a decrease in the catalytic performance of the acid treatment. The maximal increase is obtained at intermediate acid concentrations. [47] The term "acid-activated clays" refers to acid activation of bentonites. Na^+ and Ca^{2+} bentonites are industrially treated in order to exchange with the inorganic acid mentioned before, such that the divalent calcium ions or the monovalent sodium ions are substituted with the monovalent hydrogen ions, and ferric, aluminium, magnesium ions are leached out resulting in an alteration of the structure of the original clay. In the first stage of the acid treatment, the protons (H^+) replace the exchangeable cations and attack the layers; this substitution creates instability. [46]. A good exchange occurs when there is an efficient contact between the acid and the clay. To study the properties of H^+-clays, maximal stability and saturation of the protons is required. The treatment with these very strong inorganic acids is known as "acid dissolution" or "acid activation". Acid-dissolution studies demonstrated that there is a faster dissolution of the octahedral sheet than the tetrahedral sheet. However, the analysis carried out by Bergaya showed that the acid he had used dissolved both octahedral and tetrahedral layers with a comparative rapidity.[37]

Furthermore, acid treatment is one of the most common treatments for bentonite. The first step of the acid activation is the dissolution of acid-soluble minerals and organic matter which may be present in the bentonite. It then follows the replacement of the exchangeable cations with the H^+ protons, their penetration into the layer, the attack of the OH groups, the dihydroxylation, the release of the central atoms from the octahedra and the removal of Al. A transformation of the tetrahedral sheet into a three-dimensional framework occurs and an amorphous, partly protonated, silica phase is produced.[48] The ratio between the amorphous and the mixture of smectite layers depends on the acidity of the treatment. This structural alteration depends on the layer-charge and the surface alteration. Acid treatments increase the porosity in clays, the activation force and the number of acid pores. The acid treatment also affects the pillaring, which is the treatment applied to clays following the acid exchange. The presence of some elements that can be realised by the acid treatment before the pillaring increases the efficiency of the pillaring. Different clays have different compositions, and the presence of Fe for acid-base catalysis may reduce the stability. Nonetheless, the presence of Fe is important for the catalytic activity.[49]

Acid treatments remove Fe, Ca, Mg, Na. The presence of this elements may represent a problem for some industrial application of clays, for example Fe_2O_3. Therefore, acid treatments are essential to have a low Fe content. The materials then can be used for the pillared forms. If the concentration of the acid is low, the majority of the cations exchanged are the extralattice ones, such as Na^+ and Ca^{2+}. Only a part of Fe^{3+} is released and remains after the treatment outside the lattice. The analytical test demonstrates that free silica may be seen only with an increase in the concentration of the acid, which means that the acid exchanged cations also with the layers. However, due to the reasons explained in the previous paragraphs, the acid concentration is not necessarily extreme. [47] A passivation effect may also occur, as Pesquera et al. (1992) observed, such that the free silica generated with the increase in the acid concentration may create a barrier which protects the octahedral sheet from the acid attack; as a consequence, a smaller amount of Fe^{3+} and Mg^{2+} is released. The rates of the octahedral cations release is $Mg^{2+} > Fe^{2+} > Fe^{3+} > Al^{3+}$.[50]

In the case of H-clays, specifically H-bentonite, the acid treatment differs from other forms due to the instability that the acid attack creates. Acid treatments have therefore been widely studied and investigated. Acid activated bentonites are in fact applied in the chemical industry, the sulphur production, the mineral oil industry, the forest and water conservation, the foodstuffs industry, the environmental protection and the paper industry [51].

Acid-activated clays have strong acidic centres and their partially amorphous structure allows the formation of mesoporosity. These activated clays are used in the chemical industry (removal of olefins from ethylbenzene or cumene streams, purification of kerosene, jet fuels, dimerization of unsaturated fat acids to dimer acids, decolorization of industrial oils and petroleum oil derivates). In the first stage, the surface of the clay becomes acidic. The acid treatment increases the Bronsted acid sites that allow the formation of a very active acid catalyst. This treatment is applied before the pillaring. The Bronsted acidity is crucial for $DeNO_{x.}$ The use of ammonia increases the efficiency of the SCR process for the removal of $NO_{x.}$ The presence of ammonia prevents the migration of the cations from the interlayer space to the octahedral sheet, while the Bronsted acidity disappears with heating. The protons are attracted by the ammonia and they remain in the interlayer space. Acid treatments have different effects on the different clay minerals where they are applied. Two different characteristics from the acid activation in clays are the swelling properties and the cation exchange (CEC). The CEC decreases with the increase of the acid concentration and the swelling capacity decreases of 20%.

1.3.2 Pillaring

Pillaring of clays allows to create an additional porous structure and increase the specific surface area. This is allowed by the introduction of the inorganic polymer hydroxy-cations whose sizes are bigger than the original exchangeable cations. The calcination that follow the pillaring create a stable formation of pillars, that in contrast to the exchangeable cations do not undergo another exchange but remain stable in the structure. [52] The choice of the pillar agent is related to the final application of the clays. Pioneers in clay pillarization used amines, not stable at high temperature (> 250 °C). So different metals have been used, Al, Fe, Zr, Cr, Ti , Ga, Mn and mix pillar agents such as Al/Ce/Fe, Al/Ga, Al/Fe. The interest of intercalation with mixed solutions is growing, normally the first cation polymerizes easily by the addition of different fraction of another cation seems to improve the thermal, adsorptive and catalytic properties. As it was written in the first chapter the aim of this work is to use also cobalt as a pillar agent. The basal space d_{001} increase when mixed pillars are obtained using Al and other cations larger than Al, such as Co, this is due to the difference in the ionic radii. [13]

Even for pillaring method there are no general rules for the best conditions, different methods and preparations are reported in literature. In this work is followed the pillaring method approved by clay researches within the university AGH. [28] Many factors can influence the intercalation process. Pillared clays were often used as supports for catalytically active materials. There are several active materials described in literature that can give a high activity for the removal of NO_x. From the pillaring there is the separation of the layers by the insertion of inorganic compounds (such as Kegging ions). The pillared materials are thermodynamically stable and present micro and mesoporosity.

The interlayer cations can be replaced by the other cations in a liquid phase. As the starting materials, layered clays with sodium cations are used, for this reason the first step of the work is the exchange with NaCl (Fig. 1.33).[53]

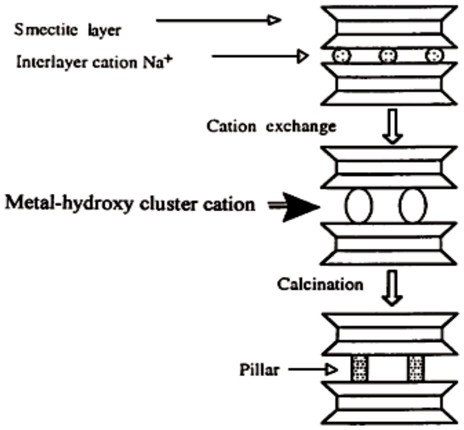

Figure 1.33: Schematic diagram for the preparation of pillared clay minerals (adapted from Moore and Reynods)

Pillared clays (PILC) also can overcome the disadvantages connected to the zeolites. Among these disadvantages the most important is that zeolites have relatively small pores so before their application in the cracking of heavy oil fractions, for example, the big molecules must be pre-treated.

The concept of using intercalation transform a lamellar solid into a porous analog originated more than 55 years ago in the Aberdeen University laboratory of Professor Richard M. Barrer. He published in the Transactions of the Faraday Society an article describing how the "replacement of inorganic cations in montmorillonite by $N(CH_3)_4^+$ and $N(C_2H_5)_4^+$ cations opens up the lamellae and causes profound changes in the sorption and intercalation of organic molecules". [13]

In 1977, George W. Bridley and R.E Sempels discovered that the partial replacement of Na+-exchange cations by hydroxyaluminum cations in the galleries of smectic clay increase the surface area, this lead to the patent invention of David E.W. Vaughan, Roger J. Lussier and John S. Magee on "Pillared Interlayered Clay Materials Useful as Catalysts and Sorbents".[13] From that time there was an increasing interest in porous derivates of lamellar compounds increase and more than 3500 journal publications have been published, with in the twenty first century an addition of more than other 200 journal publications. Since the first introduction of aluminium pillar agents in clays in 1970 the synthesis of pillared interlayered clays has expanding enormously. The calcination is an important step after pillaring giving a thermal stability and the formation of stable metal oxide, with a result in surfaces and area four times bigger than no pillared clays. A stable structure can be obtained by the conversion of hydroxide pillars to stable oxides. Washing, drying and calcination are very important step necessary after the pillaring and have important consequences on the properties of the final structure such as for the porosity. [13]

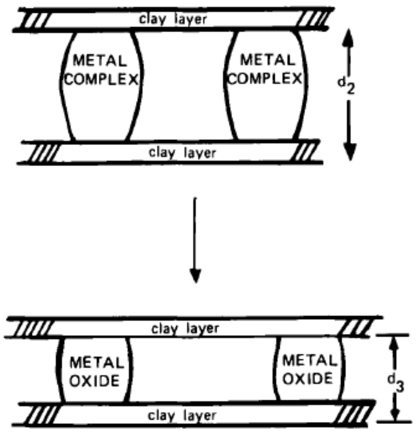

Figure 1.34: Clay structure after calcination

One factor that has to be considered in the pillaring process is the intercalating solution. But other factor has to be considered for the successful of the pillaring, such as the condition of stirring of the clay and the solution, the temperature, time of contact, stirring speed. The thermal history of this process is predominant for this reason the laboratory conditions influence the results. Samples followed the same preparation steps can present different result.

A great effort on studying the pillared-acid activate clays, the final solids are usually called (PAACs= pillared acid-activated clays). The properties of these clays are in the middle of the PILC and the acid activated ones. [54]

PAACs surface area > PILC surface area

PAACs pore diameter > PILC pore diameter

PAACs fixed Al < PILC fixed AL

The results are related to the effect of the acid treatment that create a partial destruction of layers and the formation of an amount of amorphous silica and the development of Bronsted acid sites.

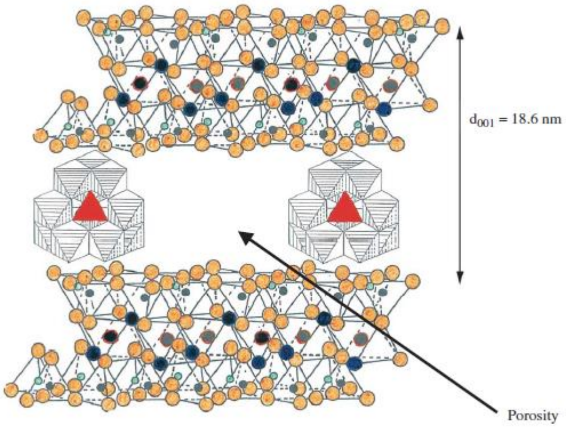

Figure 1.35: PILC

Most of the studied in pillar clays are focused on the Al polyoxocation. Solutions containing this precursor are prepared by the addition of a base to $AlCl_3$ or $Al(NO_3)_3$ since the ratio OH/Al is 2.5. The most important cationic complex formed is the polinuclear $[Al_{13}O_4(OH)_{24}(H_2O)_{12}]^{7+}$, that is called Keggin ion or Al_{13}. The $[Al_{13}O_4(OH)_{24}(H_2O)_{12}]^{7+}$ polycation (Al_{13}) is the most used and Al-PILC are the most widely known.[54] Keggin ions are built with a central aluminium ion in tetrahedral coordination, surrounded by 12 octahedrally coordinated Al^{3+} cations. Tetahedron and octahedra are connected through their corners. After the calcination the metal complex are transformed in metal oxide. The decomposition of oligocations occurs, metal oxides are formed, and they can support the silicate layers. Even if after the calcination the interlamellar distance decrease the pillar metal oxides provide more space for molecules involved in the catalytic processes.

Finally, a ‘pillared material’ must fulfil at least three criteria:

- chemical and thermal stability
- a certain layer ordering that enables at least a d_{001} spacing to be determined (although a rational series of basal reflections is not necessary)
- accessibility of the interlayer space to molecules at least as large as N_2

Chapter 2 – Materials and methods

2.1 Starting material and preparation steps

As starting material, the following layered clay is used: pure bentonite (Fisher Scientific UK), extra pure, CAS: 1302-78-9, EC:215-108-5. Component CID: CID 962 (water), CID 14769 (Alumina), CID 24261 (Silicon dioxide).

Table 2.1 Bentonite properties

Bentonite	
Physical state	solid
Appearance	Light grey granulates
Odour	none
Physical state	6.5-8
Flammability	non flammable
Bulk density	700-900 kg/m

Pure bentonite contains only interstitial water. For this reason, the first step of the modification of the clay is the exchange with a solution of NaCl to obtain the Sodium Bentonite. Variations in interstitial water and exchangeable cations in the interlayer space affect the properties of bentonite and thus the commercial uses of different types of it.

Steps follow for the treatment of pure bentonite

- Na-Bentonite preparation
- Acid treatment with HNO_3 and HCl
- Intercalation (pillaring) by Al and Co-hydroxycations
- Deposition of active component (Fe or Ce species)

2.1.1 Sodium Bentonite preparation

Pure bentonite is firstly ion-exchanged with a solution of 1M of NaCl to obtain Na-Bentonite (Fig.2.2) from the pure one (Fig 2.3). The solution of NaCl is ion-exchanged with pure bentonite for 24h at ambient temperature. 20 g of raw bentonite and 200 ml of NaCl solution. The separation of the phases in the solution occur by centrifugation, the material is filtered, dried for 24h in the oven and then calcined for 2h at 450°C.

Figure 2.1: Sodium Bentonite (NaB)

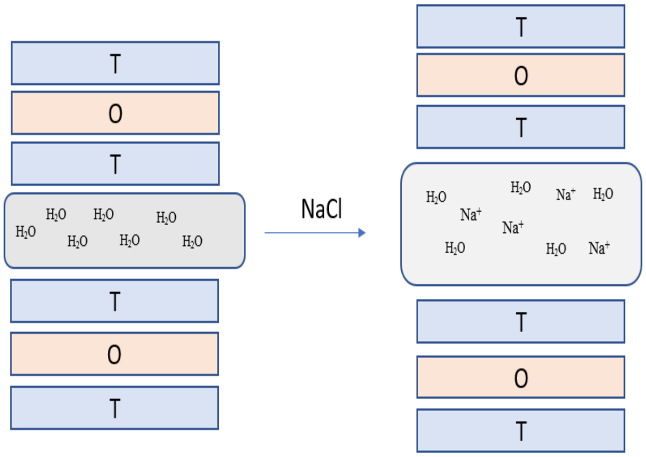

Figure 2.2: Pure bentonite (B) and Sodium Bentonite (NaB)

2.1.2 Acid treatment with HNO_3 and HCl

Different solution of HNO_3 and HCl are prepared: 0.4M, 0.6M, 0.8M, 1M of HNO_3 and 0.4,0.6,0.8, 1 M of HCl. Acid treatment is conducted with pure bentonite and Na-Bentonite obtained in 2.2.1. All the samples are exchanged with both the two acids with different concentration, but only the samples exchanged with 0.6 and 0.8 of HNO_3 and HCl will be mainly analysed. This choice is carried out consulting the studies of Pushpalatha et al., 1995 which consider the maximum increase of the number of acid sites only for intermediate concentration of acid. [47] If the acid treatment is too much aggressive there is a decrease of the catalytic activity of the clay due to the impairment of the octahedral layers, with a decrease in the Bronsted acidity that is higher in material previous treated with lower concentration of acid solution. The acid treatment lasts for 24 hours at 100 °C. 20 g of the sample are introduced into 200 cm^3 of acid. After the treatment the samples are washed with distillate water, dried for 24 h at 110°C and calcined for 2h at 450°C to enrich the catalysts with Lewis acid sites and to remove any organic impurities. Another acid treatment is carried out with oxalic acid to stabilize the structure. 20 g of the sample are introduced into 200 cm^3 of acid solution (0.12 M) for 1 hour. After filtration the sample is dried at 110°C for 24 h and calcined at 450°C for 2 h.

Figure 2.3: Acid treatment

2.1.3 Preparation of the pillaring solution

After calcination and acid treatments all the samples prepared are pillared. The pillaring solution is prepared from aluminium chloride and sodium hydroxide. The starting material for preparing the aluminium chloride solution was aluminium chloride hexahydrate ($AlCl_3 \cdot 6H_2O$). The concentration of the two solutions of $AlCl_3 \cdot 6H_2O$ and NaOH is 0.4 M. The molar ratio of OH/Al in the final solutions is 2.5.

The solution of NaOH (0.4 M) is slowly added to $AlCl_3 \cdot 6H_2O$ (0.4 M) mixed with a magnetic stirrer at 70°C. The low speed of the addition of NaOH favourites the formation of $Al(OH)_3$. It takes some days to end this preparation, the solution has been hydrolysed in order to polymerize a multivalent cation. The same procedure is carried out for the mixed pillar agent solution. A solution of $CoCl_2 \cdot 6H_2O$ is introduced (0.4 M) and $AlCl_3 \cdot 6H_2O$ and NaOH (0.4 M). NaOH solution is dripped slowly into Al and Co solutions under constant stirring at 70°C. This is the same procedure as for the first pillaring solution prepared but with a substitution of Al with Co (50% Co and 50% Al).

Figure 2.4: Preparation of pillaring solution

2.1.4 Intercalation (pillaring) by Al and Co-hydroxycations

After the preparation of pillaring solution, all the samples are pillared, both the samples without a first exchange with NaCl (B) and the samples firstly exchanged with NaCl (NaB). According to the procedure described by Chmielarz, alumina pillars are introduced in the solution. The ratio of 12 mmol Al/1 g sample was used for the pillaring, stirring for 24h at 70°C. Pillaring solution is added dropwise to the 3 wt. % suspension of the Na-bentonite until the ratio 12 mmol/g is reached. The same procedure for the pillaring solution contained 50% of cobalt. Same ratio 12 mmol cations/1 g of sample stirring for 24h at 70°C.

With Buchner funnel the separation of the modified bentonite from the solution takes place. For the removal of chlorine ions, the precipitate is cleaned with distillate water.

Pillaring is done for all the samples. Only the samples exchanged with 0.6M of HNO_3 and HCl are also pillared with the solution of Al and Co.

After the filtration, the samples are dried at 120 °C for 24h and after calcined for 2h at 450 °C.

Figure 2.5: Pillaring step

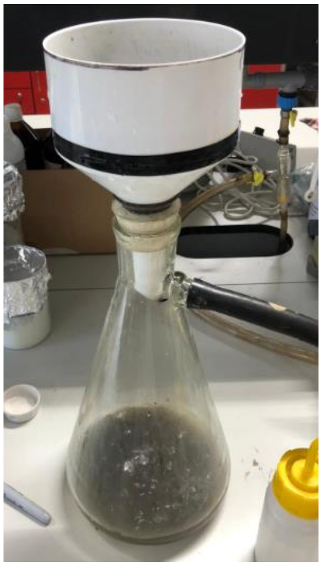

Figure 2.6: Filtration

2.1.5 Deposition of the active phase

Active materials are introduced by Incipient Wetness Impregnation (IWI) which provides a greater dispersion of the metals on the support. The sources of Fe and Ce species are respectively aqueous solutions of $Fe(NO_3)_3 \cdot 9\ H_2O$ and $Ce(NO_3)_3 \cdot 6\ H_2O$. In a concentration of 4 wt% of Fe and 0.12 wt% of Ce. The calculated amount of the solution of nitrate is added to a suitable amount of bentonite (1g). The sample is dried for 24 hours at 120°C and calcined at 450°C for 2 hours.

Figure 2.7: Sample impregnated with Fe

Figure 2.8: Samples calcined after pillaring (white samples) and Fe-impregnation (orange samples)

After each preparation step (Na-Bentonite formation, acid treatment with HNO_3 and HCl, pillaring and deposition of the active phase) drying (120°C for 24 h) and calcination (450°C for 2 h) processes are carried out. The list of samples prepared is reported in Tab2.2.

Table 2.2 Lists of samples

N°	Sample	NaCl exchange	Acid	Pillaring	Active material
1	B	No	No	No	No
2	NaB	Yes	No	No	No
3	B0.4HNO3AlFe	No	HNO_3 0.4 M	Al oligocations	Fe
4	B0.6HNO3AlFe	No	HNO_3 0.6 M	Al oligocations	Fe
5	B0.6HNO3AlFeCe	No	HNO_3 0.6M	Al oligocations	Fe & Ce
6	B0.6HNO3Al/CoFe	No	HNO_3 0.6 M	Al and Co oligocations	Fe
7	B0.8HNO3AlFe	No	HNO_3 0.8 M	Al oligocations	Fe
8	B1HNO3AlFe	No	HNO_3 1 M	Al oligocations	Fe
9	B0.4HClAlFe	No	HCl 0.4 M	Al oligocations	Fe
10	B0.6HClAlFe	No	HCl 0.6 M	Al oligocations	Fe
11	B0.6HClAlFeCe	No	HCl 0.6 M	Al oligocations	Fe & Ce
12	B0.6HClAl/CoFe	No	HCl 0.6 M	Al and Co oligocations	Fe
13	B0.8HClAlFe	No	HCl 0.8 M	Al oligocations	Fe
14	B1HClAlFe	No	HCl 1 M	Al oligocations	Fe
15	NaB0.4HNO3AlFe	Yes	HNO_3 0.4 M	Al oligocations	Fe
16	NaB0.6HNO3AlFe	Yes	HNO_3 0.6 M	Al oligocations	Fe

17	NaB0.6HNO3AlFeCe	Yes	HNO_3 0.6M	Al oligocations	Fe & Ce
18	NaB0.6HNO3Al/CoFe	Yes	HNO_3 0.6 M	Al and Co oligocations	Fe
19	NaB0.8HNO3AlFe	Yes	HNO_3 0.8 M	Al oligocations	Fe
20	NaB1HNO3AlFe	Yes	HNO_3 1 M	Al oligocations	Fe
21	NaB0.4HClAlFe	Yes	HCl 0.4 M	Al oligocations	Fe
22	NaB0.6HClAlFe	Yes	HCl 0.6 M	Al oligocations	Fe
23	NaB0.6HClAlFeCe	Yes	HCl 0.6 M	Al oligocations	Fe & Ce
24	NaB0.6HClAl/CoFe	Yes	HCl 0.6 M	Al and Co oligocations	Fe
25	NaB0.8HClAlFe	Yes	HCl 0.8 M	Al oligocations	Fe
26	NaB1HClAlFe	Yes	HCl 1 M	Al oligocations	Fe

In Tab 2.2 the designations represent:

- B= Bentonite
- NaB = Na-Bentonite
- Al-intercalated with $AlCl_3$ (oligocations), Al/Co-intercalated with $CoCl_2$ and $AlCl_3$
- Wet impregnation- from aqueous solutions of $Fe(NO_3)_3 \cdot 9\ H_2O$ and $Ce(NO_3)_3 \cdot 6\ H_2O$

Chapter 3 – Catalyst characterization

In this chapter XRD, FT-IR, UV-vis and TG characterization techniques are reported with the analysis and discussion of the results for the samples investigated.

3.1 X-ray diffraction (XRD)

X-ray diffraction (XRD) allows to identify the crystalline phases in powder specimens, poly crystalline aggregate solids and thin-film samples and to determine the size of crystals. XRD is used to study only solids, totally or at least partially crystalline. This technique is used to identify the chemical composition and crystalline phases of any compounds. It offers therefore the possibility to provide both quantitative and qualitative information.

It is one of the first test that can be done after having synthesize a new catalyst. It is based on Bragg's law, on the interaction between a monochrome X-ray beam and a crystalline solid with certain crystalline planes ordered. There is a constructive interference (peak) only when Bragg's law is satisfied:

$$n\lambda = 2\, d \sin\theta \tag{3.1}$$

- n = positive integer
- λ = the wavelength of the incident wave
- θ = the glancing angle
- d = the crystal plane separation

XRD instrument is called an X-ray diffractometer. Diffracted X-ray intensity is reported as a function of the diffraction angle. The pattern obtained is analysed by comparing the position of the peaks with those known of metals and oxides present in database containing over 60000 diffraction spectra of known crystalline substances.

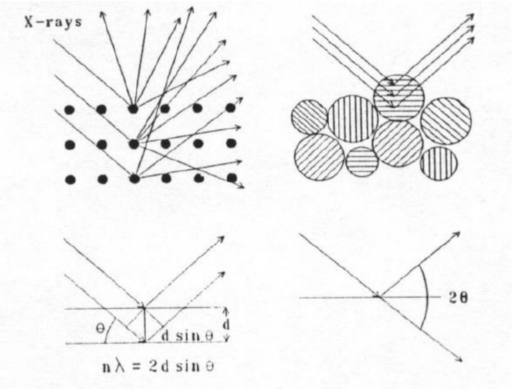

Figure 3.1: Bragg diffraction

2θ is varied and the intensity of the reflected rays is recorded. Each peak corresponds to a numerical tern representing a geometry of a planar configuration. This term is described by Miller notation in which *h,k,l* are the crystallographic planes of the crystalline lattice.

Debye-Scherrer equation is used to determine the size of the crystals:

$$D = \frac{K\lambda}{B\ \cos\theta} \tag{3.2}$$

- B = line broadening at half the maximum intensity (FWHM)
- K = dimensionless shape factor

Clays and minerals clays are identified by X-ray diffraction. *Hkl* peaks are not very diagnostic because the structures are very similar in X and Y directions. The atomic pattern in *Z* is the most different from mineral to mineral. [55]

The X-ray diffraction patterns are obtained using Empyrean (Panalytical) diffractometer. The instrument consists in a copper-based anode (Cu-Kα LFF HR, λ = 0.154 nm). Patterns are represented by 2θ range of 2.0-80.0° (2θ step scans of 0.02° and a counting time of 1 s per step).

Figure 3.2: XRD diffractometer

3.1.1 Preparation of samples for XRD

In powder or polycrystalline diffraction, it is important to have a sample with a smooth plane surface. If possible, it is necessary to grind the sample down to particles of about 0.002 mm to 0.005 mm. The sample is pressed into a sample holder to have a smooth flat surface. The patterns are analysed by HighScore Plus 2012.

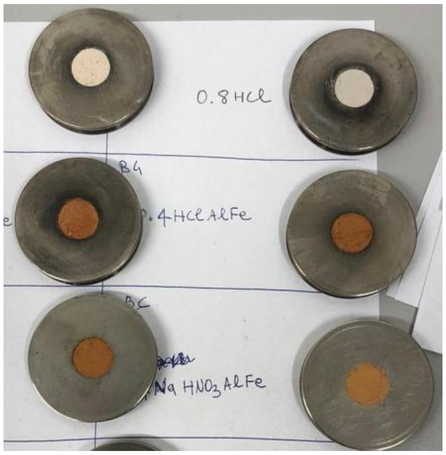

Figure 3.3: Sample holders

3.2 Fourier Transform Infrared Spectroscopy (FT-IR)

3.2.1 Infrared spectroscopy

Infrared spectroscopy is a useful technology used to investigate chemical properties, bonds and the structure of compounds such as clay minerals. Transmission spectroscopy is the eldest and most used method in the clays' studies. Clays in nature can be found as powders or solids, grounded into powders, and easily analyse with IR analyses.

IR spectroscopy is an analytical technique based on the interaction between electromagnetic radiation and the samples. Infrared radiation is included in the area of the electromagnetic spectrum between the visible and microwave region. (Fig 3.4)

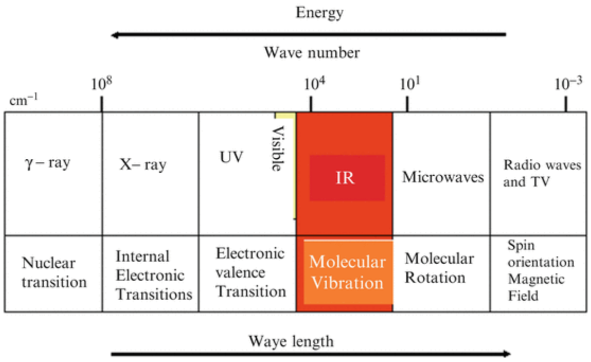

Figure 3.4: Infrared radiation

The energy released by the radiation at a certain frequency (expressed as wave number, 1/λ, in cm^{-1}) is converted into rotational and vibrational energy, so the molecule can vibrate and rotate. This does not happen for all the molecules, but the vibration occurs only if the frequency of radiation has a very precise value that depends on the chemical characteristics of the molecule. If in the spectrum of an unknown compound there is a signal at a certain frequency the compound has a specific functional group.[56]

The peaks of the same functional groups have almost the same frequencies or narrow ranges. An infrared spectrum is presented as a series of absorption bands in function of the wave number.

The IR absorption bands are characterised by:

- The shape (sharp or broad)
- The intensity (strong, medium, weak)
- The position expressed as wave number ν max

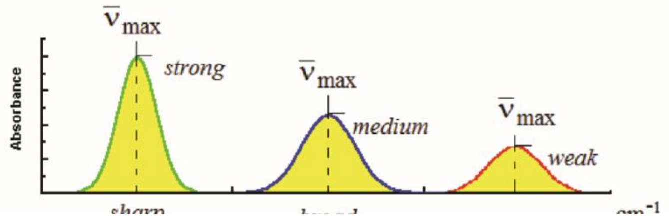

Figure 3.5: IR absorption bands

The infrared electromagnetic radiation generated by a source may or may not be absorbed by the sample. The radiation (I) that goes out from the sample can be equal to the radiation that goes in the sample (I_0), this means that there is no absorption or I can be less than I_0 and this means that there is absorption:

- Absorption: $I < I_0$
- No absorption: $I = I_0$

The IR spectrum results may be as a function of Transmittance (Fig.3.6) or Absorbance (Fig 3.7). For the transmittance T ($T = \frac{I}{I_0}$) the minimum value is 0 (max absorption) and the maximum is 100% (no absorption). For the absorbance A ($A = \frac{1}{logT}$) the minimum value is 0 (no absorption) and the maximum is +∞ (max absorption)

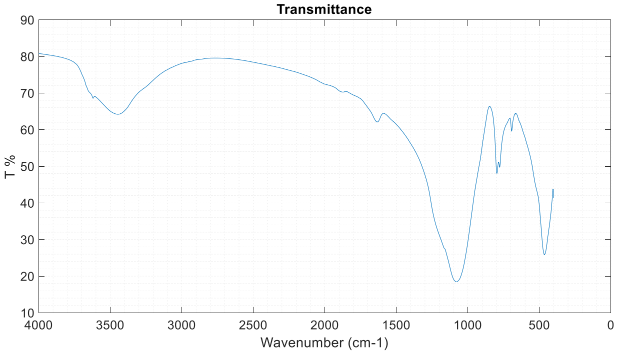

Figure 3.6: Transmittance

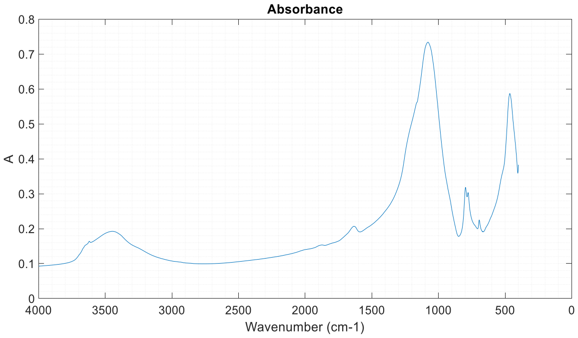

Figure 3.7: Absorbance

The first generation of infrared instruments consisted of CW-IR dispersion spectrometers consisting of an IR radiation source, an optical system (dividing IR radiation through a series of mirrors), a monochromator (decomposing radiation into its spectral components) and a detector capable of converting IR radiation into an electrical signal sent subsequently to the data processing and spectrum recording system. In recent decades, a new generation of interference spectrophotometers (FT-IR) was introduced without the monochromator but with a mechanical device called Michelson interferometer.

3.2.2 Fourier-Transform Infrared Spectrometers

Fourier-Transfom infrared spectroscopy is based on the idea of the interference of radiation between two beams to yield an interferogram, a signal produced as a function of the change of pathlength between the two beams. The mathematical method of Fourier-transformation can interconvert the domains of distance and frequency. The radiation from the source is passed through an interferometer to the sample then it reaches the detector. Upon amplification of the signal, the data are converted to digital form by an analogue-to-digital converter and transferred to the computer for Fourier-transformation.

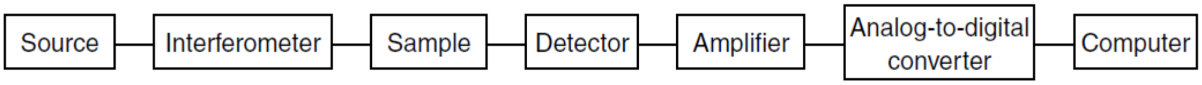

Figure 3.8: basic components of FT-IR

The IR beam can be absorbed by the sample or pass through it. The information about the IR beams, that pass through the sample is collected by the set of mirrors. The most common interferometer used in FTIR is the Michelson interferometer. [57]

3.2.3 Preparation of samples for FT-IR

The concentration of the sample in KBr should be in the range of 0.2% to 1%. A homogeneous mixture gives the best results, excessive grinding is not required. The finely powdered potassium bromide absorbs humidity (it is hygroscopic) from the air and therefore lead to an increased background in certain ranges. Before each measurement, the sample is mixed with KBr at the ratio of 1:100 and pressed into a disk using the hydraulic press.
For the analysis it is used PerkinElmer Frontier FT-IR spectrometer, these spectrometers are built to the highest ISO-9001 manufacturing standards. Data analysis is done by assigning the observed absorption frequency bands in the sample spectrum and the region used for infrared absorption spectroscopy is generally 4000-400 cm^{-1} with a resolution of 4 cm^{-1}. The absorption radiation of most organic compounds and inorganic ions is within this region.

Figure 3.9: KBr disks

Figure 3.10: PerkinElmer Frontier FT-IR spectrometer

3.3 Ultraviolet-visible spectroscopy (UV-vis)

Ultraviolet-visible spectroscopy or ultraviolet-visible spectrophotometry is abbreviated to UV-vis. It is a known method for the identification and characterization of metal ion frameworks, it useful to consider the coordination and aggregation of transition metals present in modified clays.

Incipient wave lengths from 200 to 1000 nm are applied. It is a method of absorption or reflectance spectroscopy in the ultraviolet (near and middle range) and visible region.

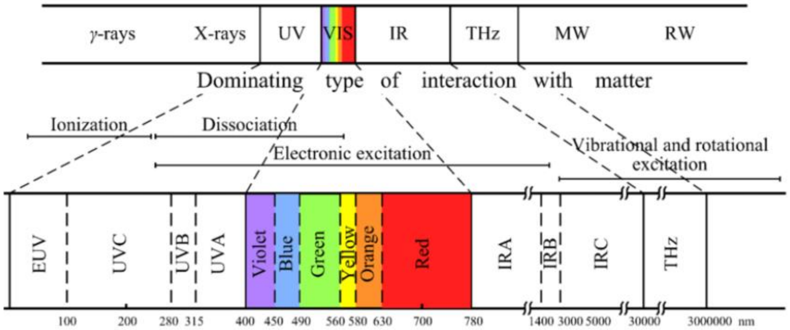

Figure 3.11: Ultraviolet and visible range

The waves used in the UV-vis induce the transition of the electronic state from the fundamental to an excited level. The spectrum is the combination of the electronic absorption, oscillation, rotational spectrum. In the spectrum the wavelengths is reported in function of the absorbance. The absorbance (A) is the relation between the intensity of incident radiation (I_0) and the transmitted radiation (I):

$$A = \log\left(\frac{I_0}{I}\right) \tag{3.3}$$

The UV-vis spectrum can also be calculated with the Beer-Lambert equation: where c is the concentration, l is the path length of the radiation trough the sample and ε is the absorptivity.

$$\varepsilon = \frac{A}{cl} \tag{3.4}$$

- c= concentration (M)
- l= path length
- ε = absorptivity

3.3.1 Preparation of the samples for UV-vis

Perkin Elmer Lambda 35 UV/Vis Spectrophotometer is used with a resolution of 1 nm and 240nm per minute scan speed. Lambda 35 is used for measurements on liquids, solids, pastes and powder samples and regulatory tests requiring variable bandwidths. Features of Perkin Elmer Lambda 35 UV/vis are: true double-beam operation, sealed and quartz-coated high-throughput optics, fast scanning and prealigned deuterium and tungsten halogen lamps. The first step was the preparation of the barium sulphate (VI) cell as the background for following measurements. Then, the samples have been prepared introducing the powder of the sample that has to be tested on the cuvette of barium sulphate (VI) analysed as the background. The powder of the sample is introduced in the centre of the cuvette forming a circle of about 1 cm of diameter.

The prepared sample was placed in the spectrophotometer and the measurement started after the appropriate parameters were set in the computer program (measuring range = 200-1000 nm).

Na-bentonite has strong absorption in nearly the whole range of visible light, the result of the UV-vis analysis even if the Na-Bentonite does not have any interesting pattern for UV-vis analysis.

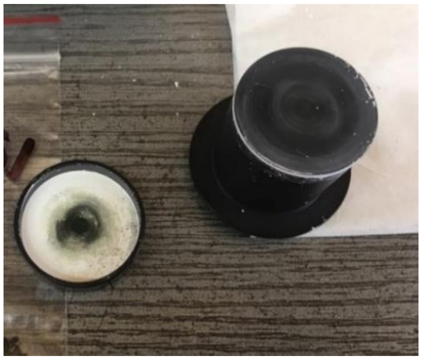

Figure 3.12: Preparation of the sample.

Figure 3.13: Perkin Elmer Lambda 35 UV/Vis Spectrophotometer

3.4 Thermogravimetric analysis (TG)

Thermal gravimetric analysis (TG) is considered as a characterization technique for measuring the mass variation of the sample during time. The mass decrease can be express in function of time or temperature at control atmosphere. Temperature range of analysis starts from ambient temperature and it reaches 500°C. 0.30 mg of sample are used and the analysis last 16h. The main components in the TG system are: balance, ventilation and gas recirculation system, control system.

Figure 3.14: TG system

Figure 3.15: TG balance

3.5 X-ray diffraction (XRD) results and discussion

3.5.1 Reference and experimental patterns

The first step of the analysis is the comparison with a reference pattern to confirm the formation of Na-Bentonite, after the exchange with the mentioned solution of NaCl (1 M). A successful conclusion can be carried out comparing Na-Bentonite pattern found in literature with the pattern of Na-Bentonite obtained. [58]

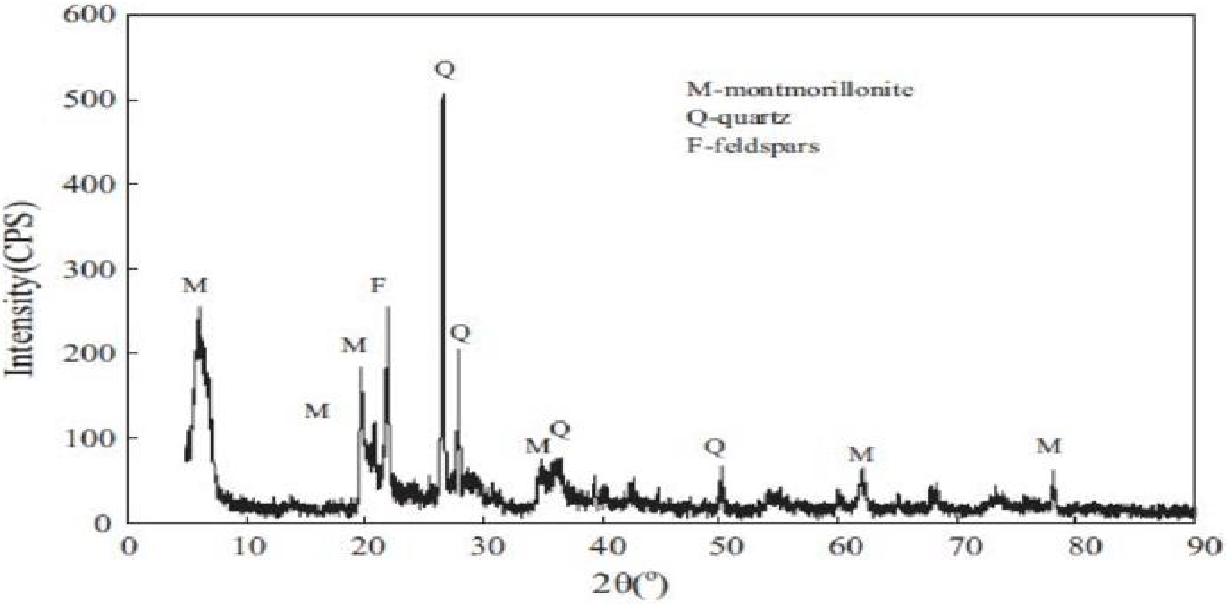

Figure 3.16: XRD of natural Na-Bentonite (Reference pattern)

The main components of Na-Bentonite are: Montomorillonite (M), Quartz (Q) and Feldspars (F). Na- Bentonite is mainly composed of montmorillonite and the other reflections represent the presence of impurities (such as quartz and feldspars) (Fig 3.16).

Fig 3.17 shows the pattern of the experimental NaB. The main components are: Montmorillonite (M), Quartz (Q) and Feldspar (F).

Further discussion will focus the attention mainly in Z direction, all the other reflections in X and Y directions will remain almost unchanged during the following steps of clay modification. NaB is composed primarily of montmorillonite (M). Reference pattern of Na-Montmorillonite is reported in Tab 5.1.

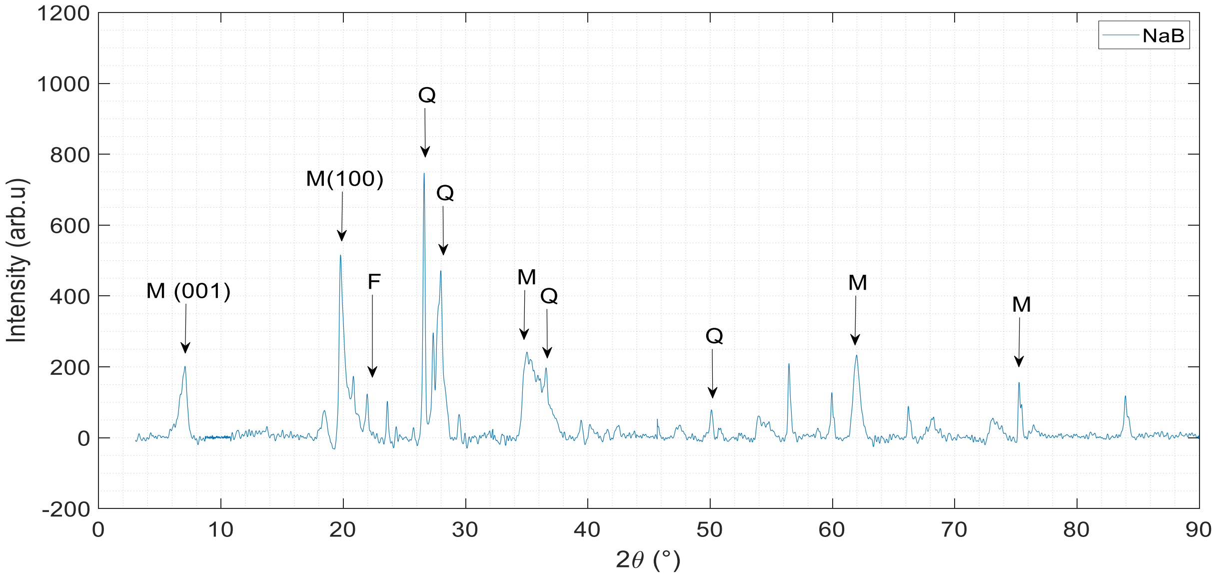

Figure 3.17: XRD of NaB (Experimental Pattern)

Table 3.1. Reference Pattern of Na-Montmorillonite

Name and formula
Reference code: 00-003-0019
Mineral name: Bentonite (Na-Montmorillonite)
Compound name: Sodium Aluminium Silicate Hydroxide Hydrate
Chemical formula: Na_ Al _ Si _ O _ OH _ H_2O
d_{001} (Å) = 11.28, 2θ (°) = 7.75°, Intensity (arb.u) =192.25, FWHM (°) = 0.51

Other reflections of montmorillonite have been identified in Fig 3.17 such as *100* (M) at 2θ (°) = 19.77 (Intensity (arb.u.) = 501.02 and FWHM (°) = 0.43) and *060* (M) at 2θ (°) = 61.97 (Intensity (arb.u.) = 222.11 and FWHM (°) = 0.59) . Reflections of quartz and feldspar agree with the reference pattern. Quartz (Reference code: 01-089-1961) mainly and most intense reflection at 2θ (°) = 26.59° (Intensity (arb.u.) = 733.46 and FWHM (°) = 0.19).

3.5.2 Increasing in the intensity of acid treatments

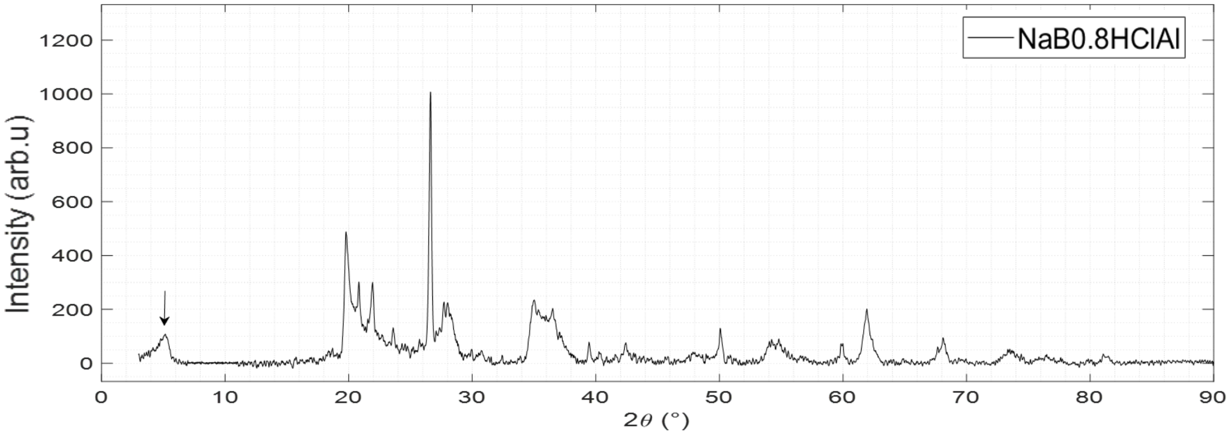

Figure 3.18: XRD of NaB0.8HClAl

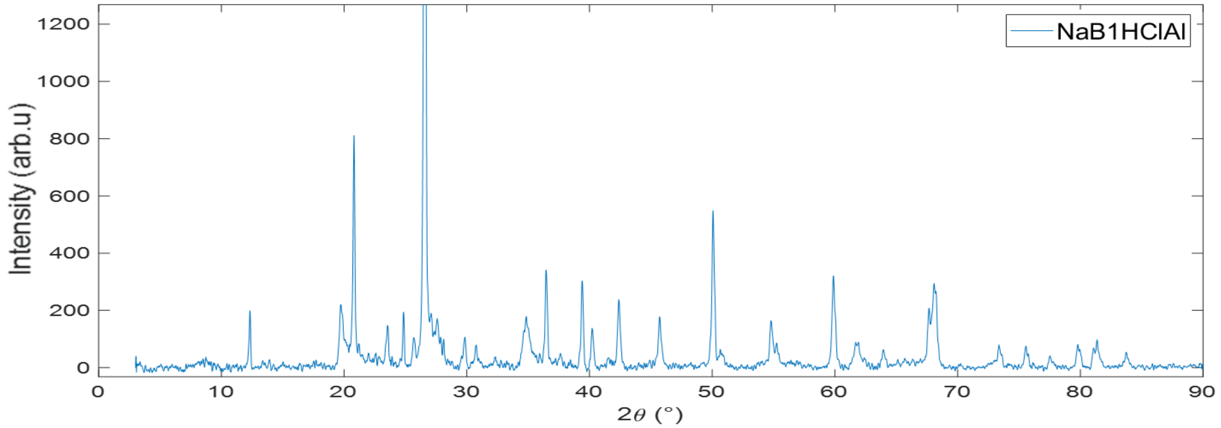

Figure 3.19: XRD of NaB1HClAl

The increase in the intensity of acid treatments may result in a loss of crystallinity, Al present in the layer structure may be taken out with an increase of acidic sites. The collapse of the structure may occur with the formation of amorphous SiO_2 not visible in x-ray. The acid treatment does not have to be too aggressive otherwise the structure of clay is going to collapse completely, and the amorphous concentration increases dramatically.[59]

Fig 3.18 shows XRD pattern of NaB0.8HClAl, acid treatment did not change the main reflections of montmorillonite and quartz. Only a slightly decrease in the crystallinity is confirmed and the structure did not collapse completely. X direction remained unchanged (*100* (M): 2θ (°) = 19.77°, Intensity (arb. u.) = 510, FWHM (°) = 0.43) and in Y direction only small changes are visible. They can possibly be connected to a slight partial collapse of Al (*060* (M): 2θ (°) = 61.97°. Intensity (arb.u.) = 222.30, FWHM (°) = 0.31). In Z direction changes in the structure due to acid treatments and pillaring are more visible. Due to the acid treatment the intensity of 001 peak is lower (114.11 abs.u.) and the shape of the peak is broader (0.58 °) compared to NaB pattern. Pillaring moves to lower value the position of 001 at 2θ = 5.11°.

In Fig 3.20 is shown a schematic representation of the structure of the sample, no high visible changes in X and Y directions, slightly lower crystallinity, pillaring occurred and changed only the position of *001* reflection.

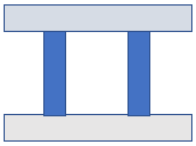

Figure 3.20: Scheme of the final structure of NaB0.8HClAl

Fig 3.19 shows XRD pattern of NaB1HClAl. The formation of a delaminated structure is suggested. 001 peak has been completely destroyed and the structure maintained only order in X and Y directions. The impossibility to calculate d_{001} and the way in which the pillaring was fixed suggest only the formation of possible pseudo pillars. The catalytic test will give more information about the activity of this sample. Reflections in X and Y directions change in intensity and FWHM (*100* (M): 2θ (°) = 19.77°, Intensity (arb. u.) = 210, FWHM (°) =0.33 and M *060* (M): 2θ (°) = 61.97° Intensity (arb.u.) = 100, FWHM (°) = 0.30). Quartz mainly reflection in 2θ = 26.59°, Intensity= 4707.11 and FWHM= 0.16°.

A decrease in the intensity of the typical reflections of montmorillonite agrees with the exchange in the structure due to acid modification. In Fig 3.21 is shown a schematic representation of the structure of the sample: a delaminated structure is visible, pseudo pillars are formed, higher number of acidic sites and higher S_{BET} may give better accessibility to the molecules with an increase in the catalytic performances of the sample. Order in X and Y direction is preserved.

Figure 3.21 Scheme of the final structure of NaB1HClAl

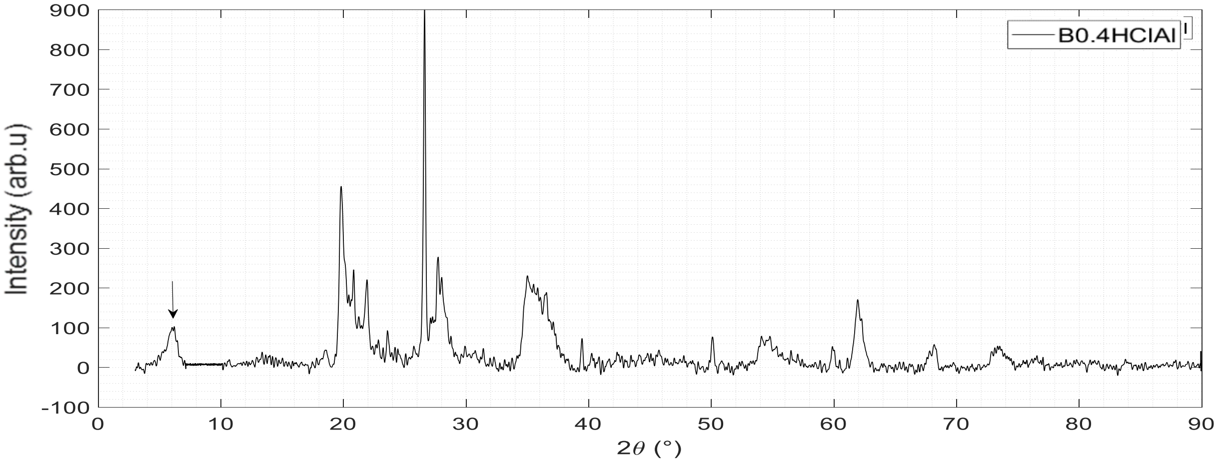

Figure 3.22: XRD of B0.4HClAl

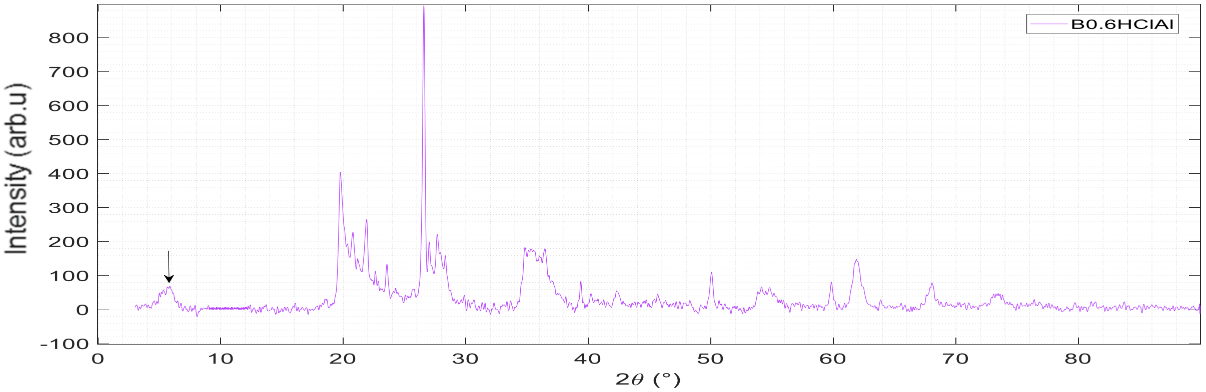

Figure 3.23: XRD of B0.6HClAl

Fig 3.22 and 3.23 show the pattern of B0.4HClAl and B0.6HClAl respectively. Pillaring occurred in both the samples but there is not distinction in the position of d_{001}. Both 001 have been shifted at 2θ = 6.00°, the intensity of the peak is different (respectively 100 arb.u. and 80 arb.u.) and the shape of the first reflection due to the increase of the acid treatment becomes broader. X and Y directions remained completely unchained all the reflections of montmorillonite are visible and the samples did not lose its crystallinity, visible changes emerged only in Z direction thanks to the acid treatments and the pillaring.

Acid treatments affect less pure bentonite than Na-Bentonite, in fact for pure bentonite the structure in not going to collapse even with the increasing of acid concentration. After acid treatments FWHM increases and the shape of *001* peak becomes broader. For an acid solution 1M of HCl the acid treatment affects the structure and 001 disappeared. Loss of intensity occurs for the lamellar distortion which creates a decomposition of the original structure. It is visible that acid treatments with different concentrations of acid (0.4, 0.6, 0.8 M of HCl) retained the crystalline character of samples, only for NaB1HClAl the structure is collapsed. Fig 3.24 from literature studies shows the influence of HCl concentration on x-ray analysis. Curve 1 corresponds to the area under the peak corresponding to *001* reflection, curve 2 corresponds to the smectite bands relate to *h* and *k* directions. The value is almost constant with the increasing of the acid concentration. Curve 3 corresponds to the area under the diffusion peak corresponding to the amorphous structure. The minimum value for which corresponds the total collapse of the first peak is for HCl concentration > 2,5 M. [60] In this work bentonite treated with HCl show the disappearance of *001* reflection for 1M HCl. The presence of Na$^+$ favourites the acid effect of the acid treatment at lower value of acid. The concentration of acid solution can be lower to have the same result.

- *001* (M) reflection appears broader after acid activation due to the partial destruction of the layered structure of smectite. All the other reflection remained almost unchanged.
- Activation shows that acid treatments influenced mainly *001*-order (basal) reflections. The non- basal reflection (prismatic reflections) does not significantly change after the treatment. (100, 060). [60]

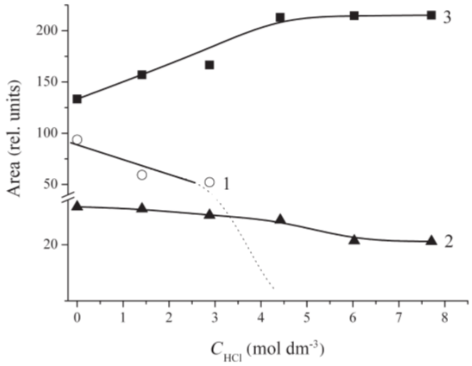

Figure 3.24: Dependence of the cation oxide contents in acid treated samples on the HCl concentration employed

3.5.3 Results of pillaring and deposition of the active phase

Changes in 001 have been explained in 3.5.2 due to acid treatments, changes in its position are explained in this subsection caused by pillaring.

The list of samples is reported in Tab 3.2. The impregnation with cerium and iron species after pillaring did not change the position of *001* peak for all the samples. The deposition of the active phase did not result in any structural changes.

Table 3.2: List of samples for pillaring consideration

Sample	**2θ (°)**	**d (Å)**	**Pillaring**
NaB	7.75	11.28	*
NaB1HClAl	-	-	Delaminated structure
B0.4HClAl	6.00	14.55	+
B0.6HClAl	6.00	14.55	+
B0.6HClAlFe	6.00	14.55	+
B0.6HClAlFeCe	6.00	14.55	+
B0.6HNO3Al	8.10	10.80	x
B0.6HNO3AlFe	8.10	10.80	x
B0.6HNO3AlFeCe	8.10	10.80	x
NaB0.8HClAl	5.11	17.07	+
NaB0.8HClAlFe	5.11	17.07	+
NaB0.8HNO3Al	4.19	20.81	+
NaB0.8HNO3AlFe	4.19	20.81	+
NaB0.6HClAlFe	4.25	20.52	+
NaB0.6HClAlFeCe	4.25	20.52	+
NaB0.6HNO3AlFe	4.20	20.77	+
NaB0.6HNO3AlFeCe	4.20	20.77	+
B0.6HClAl/CoFe	8.10	10.80	x
B0.6HNO3Al/Co	7.41	11.80	+
B0.6HNO3Al/CoFe	7.41	11.80	+

* : pillaring not carried out

\+ : pillaring succeded

x : pillarind did not succed

Fig 3.25 shows the pattern of B0.6HNO3Al, acid treatment did not change reflections in X directions (*100*(M): 2θ=19.776°, Intensity (arb. u.) = 501.92 FWHM (°) = 0.43), and in Y only a small decrease in the FWHM (*060* (M): 2θ=61.97°, Intensity (arb.u.) = 222.111, FWHM= 0.41). Presence of quartz are confirmed. The crystallinity retained and the position of the first reflection it is not shifted compared to pure B. For this sample pillaring went completely wrong, there is not a formation of the wanted pillared structure.

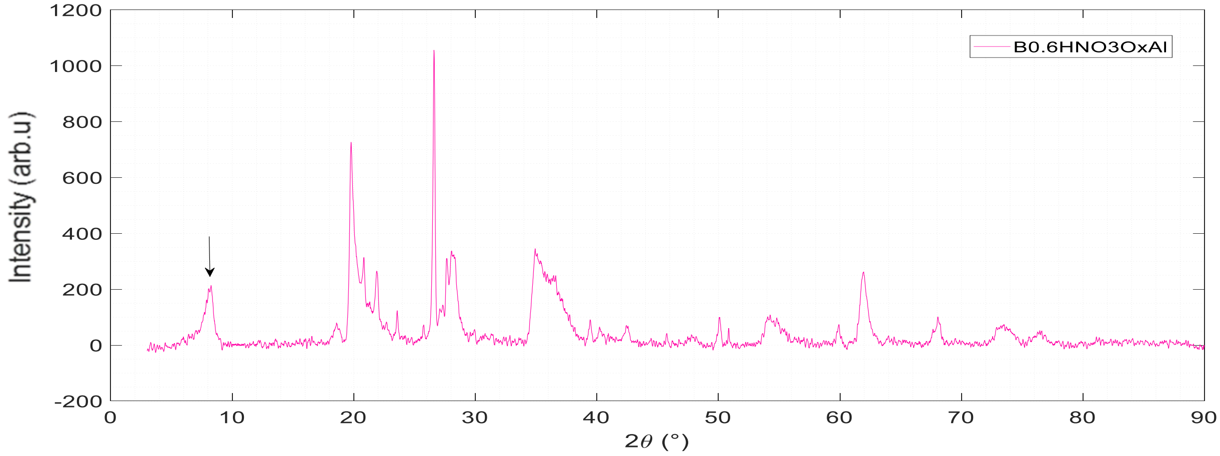

Figure 3.26: XRD of B0,6HNO3Al

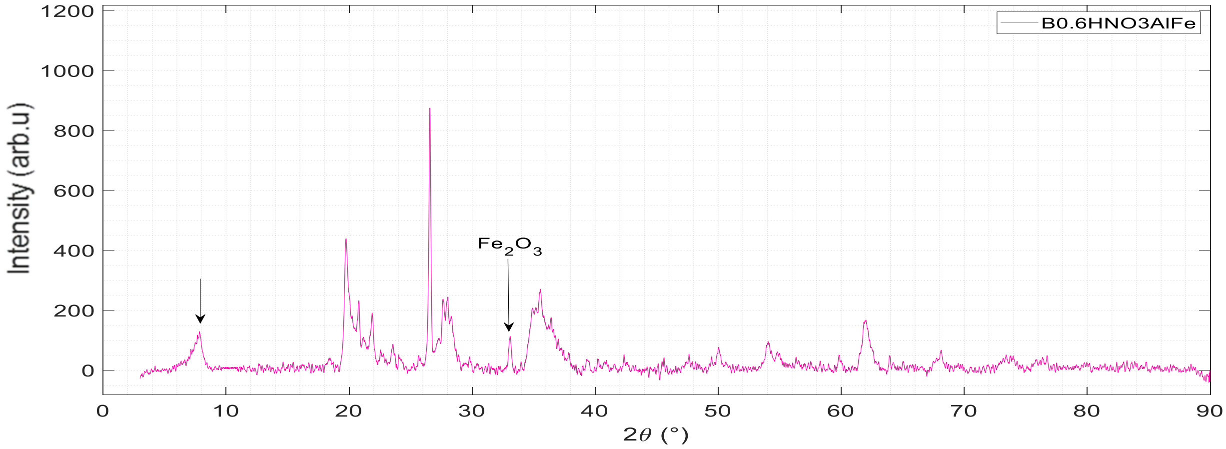

Figure 3.27: XRD of B0.6HNO3AlFe

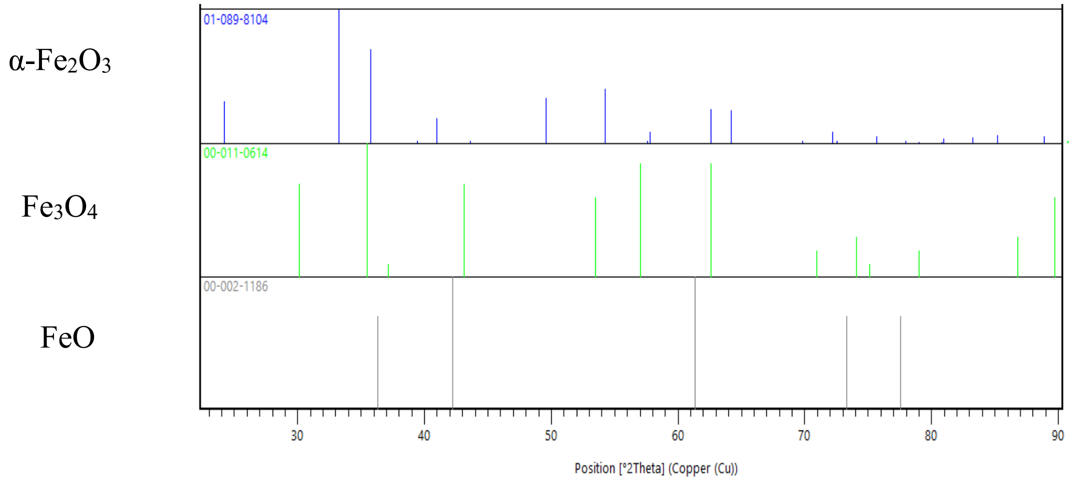

Figure 3. 28: Reference Patterns of iron oxides

Three main possible iron oxide compounds are found on High Score Plus data base: α-Fe_2O3 (Reference code: 01-089-8104), Fe_3O_4 (Reference code: 00-011-0614) and FeO (Reference code: 00-002-1186). Fe_3O_4 and FeO positions are overlapped by other reflections come from the main reflections present in the sample such as montmorillonite or quartz. For this reason, amorphous forms of iron oxides cannot be excluded, x-ray analysis gives only information about totally or partially crystalline structure. To assure that iron species have been successfully introduced in the sample other characterization techniques will be carried out such as UV-vis. The only crystalline form identify in this sample is the α-Fe_2O_3. The highest position reflection has been identified at 2θ= 33.12 °. Second most intense position would have been at 2θ= 35.56° but this reflection is overlapped by other positions come from montmorillonite (Fig. 5.9) or reflections come from other iron oxide species.

The crystallite size of the reflection at 2θ= 33.12° can be calculated. Intensity (abs. u) = 100.48 and FSWH (°) = 0.25. By the equation 3.2 it is calculated D= 5.70 Å

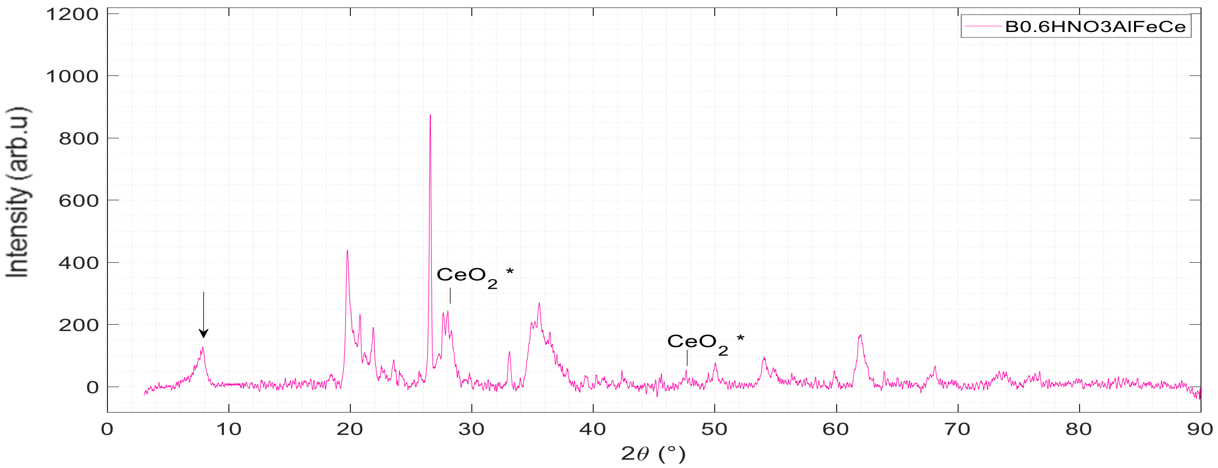

Figure 3.29: XRD of B0.6HNO3AlFeCe

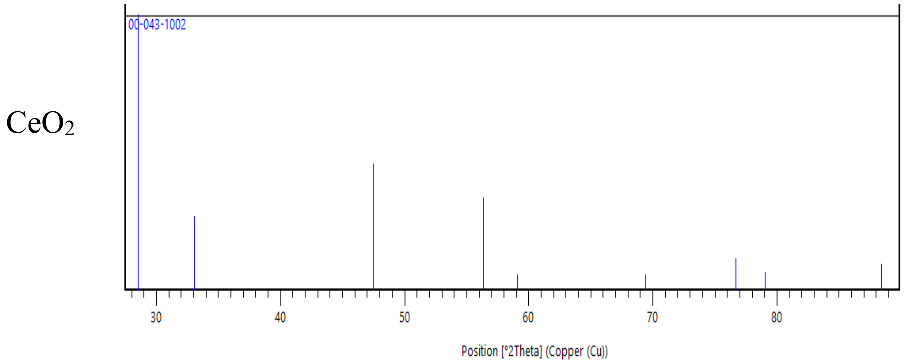

Figure 3.30: Reference Pattern of cerium oxide

In Fig 3.29 the presence of (*) represents the possible positions of CeO_2 but not a clear identification is possible because of:

- Very low amount of cerium species

- Presence of other reflections that overlap with CeO_2.

Crystallite sizes of oxide cerium are not confirmed. Presences of CeO_2 forms cannot be excluded, cerium oxides may be present in a totally amorphous phase.

The impregnation with cerium and iron species after previous steps of preparation of the samples did not shift the position of 001 peak after pillaring. Pillaring went wrong, Na^+ cations present in the interlayer space are very small and there is not a serious different between d_{001} of B and NaB.

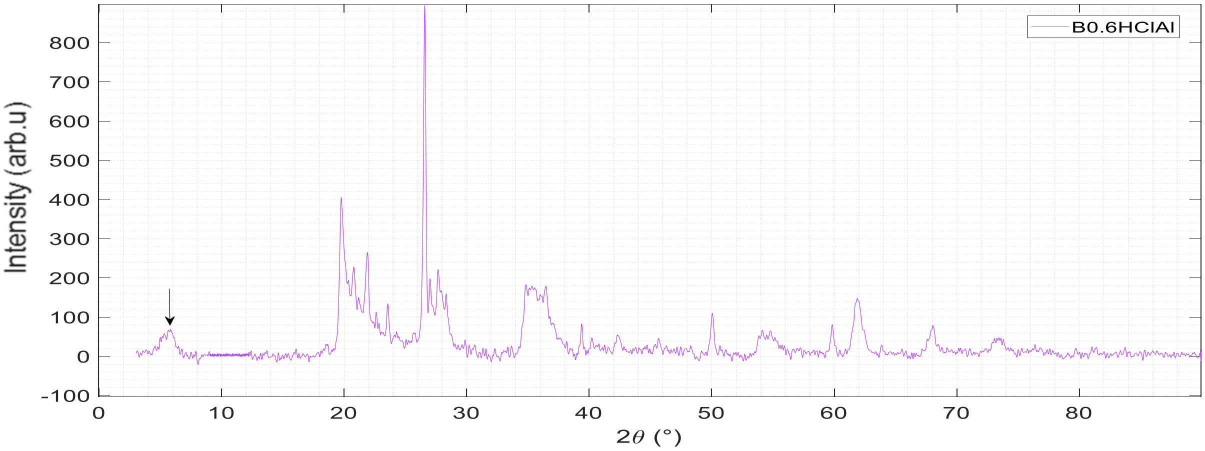

Figure 3.31:. XRD of B0.6HClAl

Fig 3.31 shows the pattern of B0.6HClAl, considerations on this sample have been done in 3.5.1 for acid treatment. Also, in this case as for B0.6HNO3AlFe and B0.6HNO3AlFe the impregnation after pillaring did not shift at lower values *001* reflection. Differently from B0.6HNO3 the pillaring succeeded.

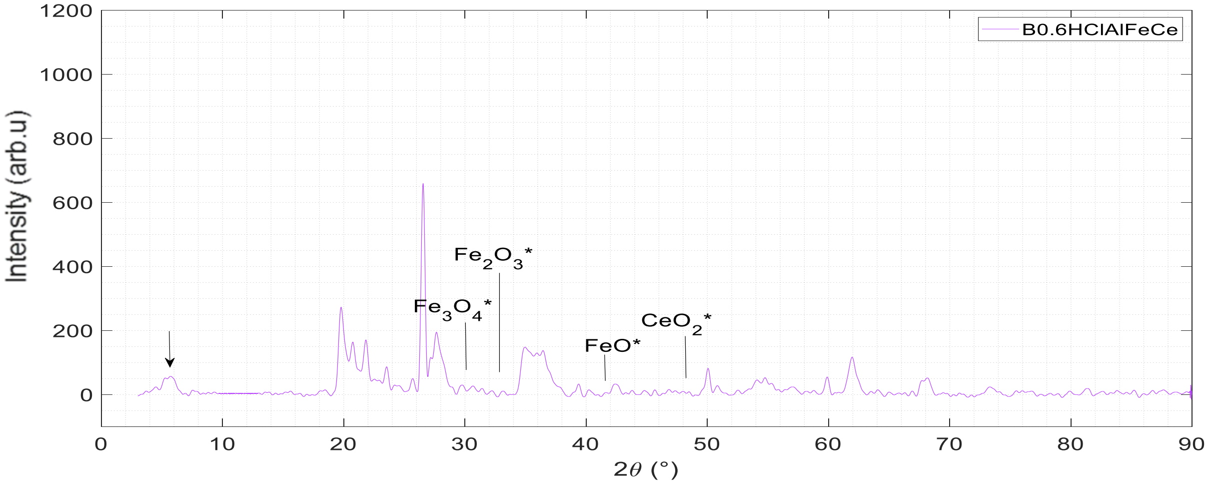

Figure 3.32 XRD of B0.6HClAlFeCe

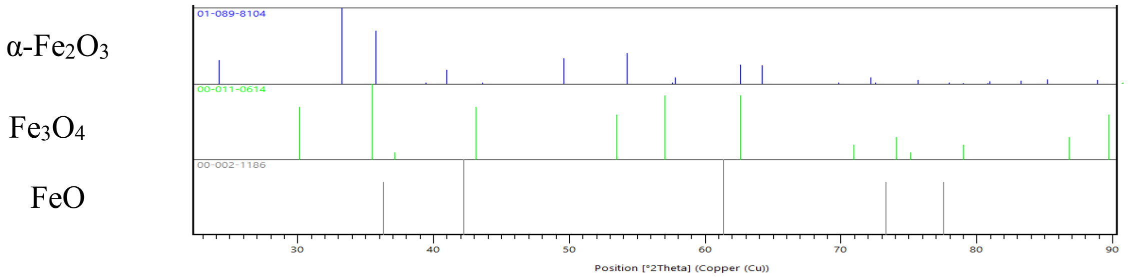

Figure 3.33: Reference Patterns of iron oxides

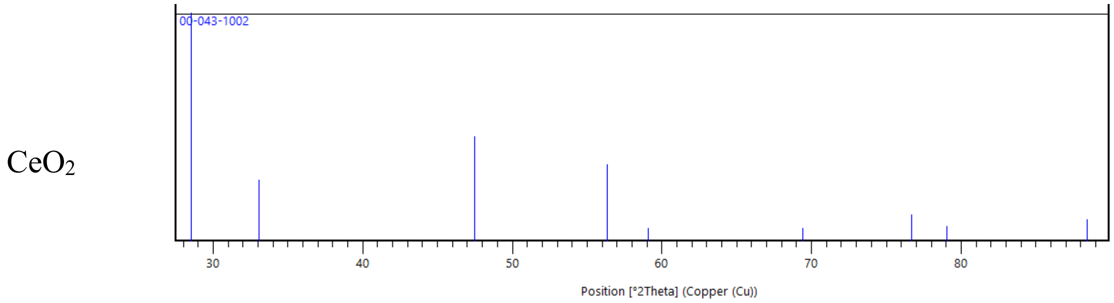

Figure 3.34: Reference Pattern of cerium oxide

In Fig 3.32 the presence of (*) represents the possible positions of cerium and iron oxides but no positive identifications are possible for the same reason as for B0.6HNO3AlFe. Cerium oxide (Reference code: 00-043-1002), α-Fe2O3 (Reference code: 01-089-8104), Fe3O4 (Reference code: 00-011-0614) and FeO (Reference code: 00-002-1186). Fe3O4, FeO, Fe_2O_3, CeO_2 positions are overlapped by other positions come from the main reflections present in the sample such as montmorillonite or quartz. For this reason, amorphous forms of iron oxides cannot be excluded, x-ray analysis gives only information about totally or partially crystalline structure. To assure that iron and cerium species have been successful introduced in the sample as the active phase other characterization techniques will be carried out such as UV-vis. Possible iron and cerium oxide forms may be well dispersed and totally amorphous. Impregnation did not change the structure.

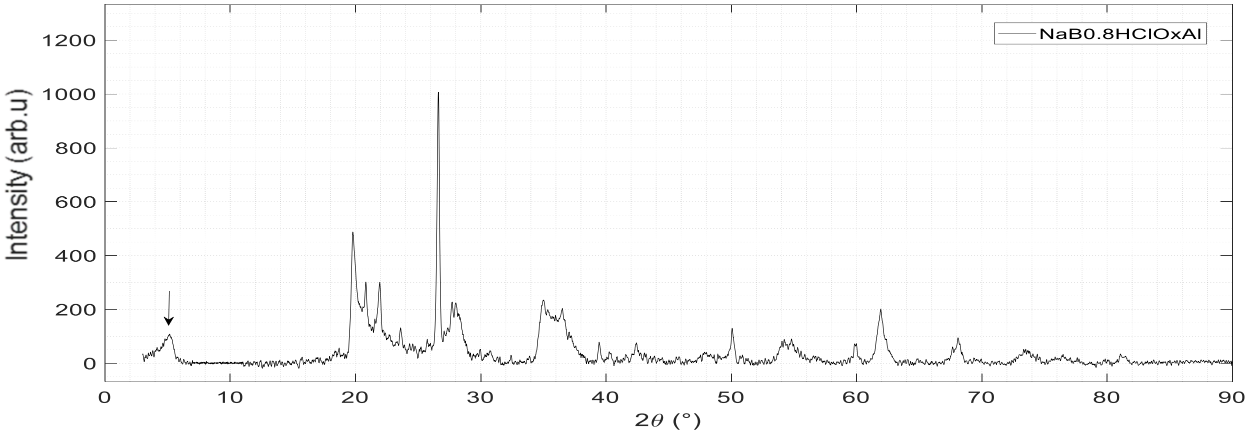

Figure 3.35: XRD of Na0.8HClAl

Fig. 3.35 has been discussed in 5.3.1. In this chapter the attention is paid on the comparison between the pattern of Na0.8HClAl and Na0.8HClAlFe. No differences in X, Y and Z directions, the impregnation step does not change d_{001}.

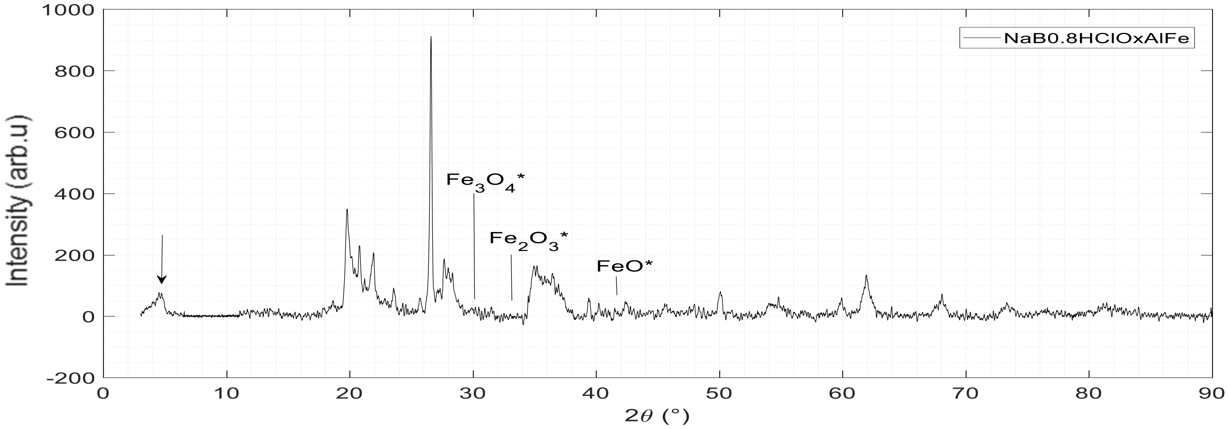

Figure 3.36: XRD of NaB0.8HClAlFe

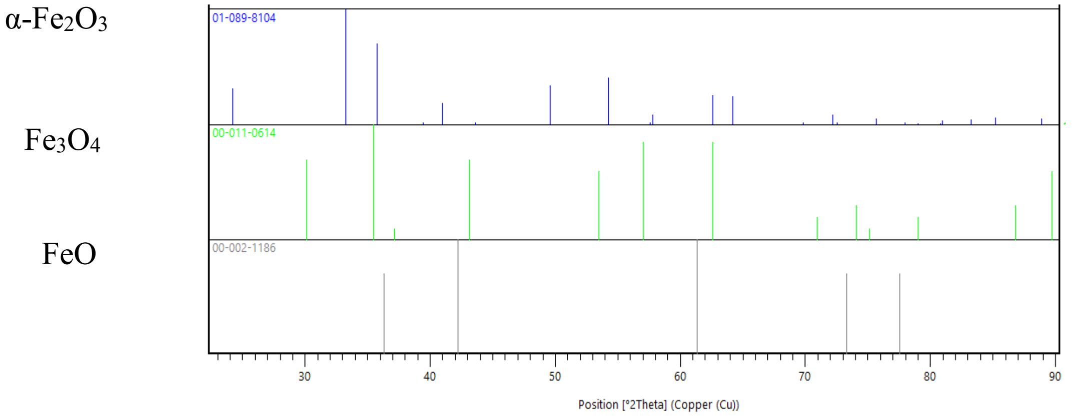

Figure 3.37: Reference Patterns of iron oxides

No forms of iron oxides may be identified. Comparison between Fig 3.35 and Fig 3.36 cannot confirm the presences of crystallite sites of iron oxides. All the typical reflections are overlapped by other reflections present in NaB. Amorphous forms of iron oxides cannot be excluded. It must be remembered that the presence of amorphous forms should increase the catalytic activities and has a positive effect on the performances. The impossibility to identify any crystalline forms does not give bad consideration on the dispersion of the active phase.

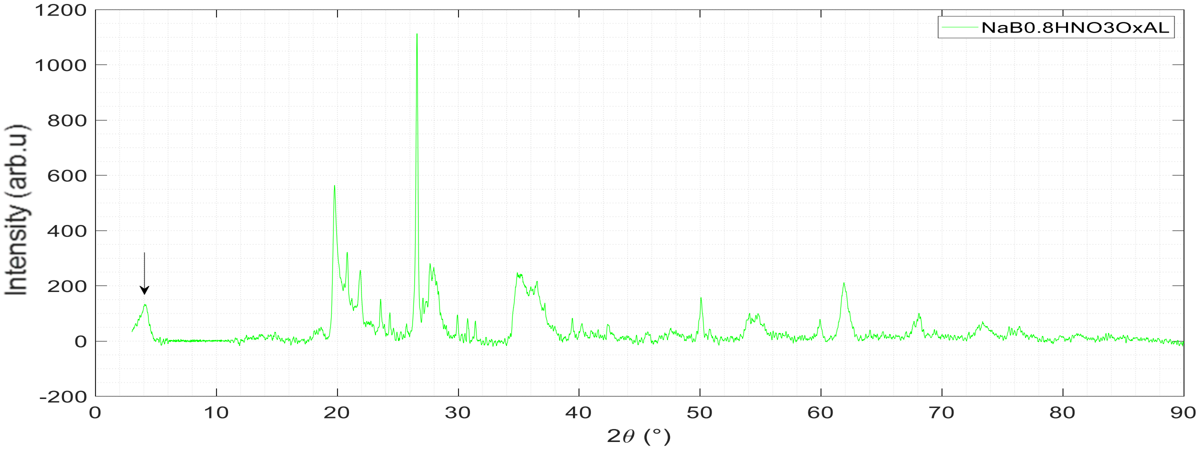

Figure 3.38: XRD of Na0.8HNO3Al

In Fig 3.38 pillaring occurred and the crystallinity retained. Visible changes only in *Z* direction due to the increase of d_{001} after pillaring, 001 peak at 2θ= 4.19°. Treatment with HNO_3 and pillaring has been more efficient and successfully. In NaB0.8HClAl *001* reflection was shifted at 2θ= 5.11°. Intensity of *001* reflection decreased compared to NaB (Intensity =125 abs. u.) and its shape remained sharp (FWHM= 0.54°). Other reflections remained unchanged in X direction (*100* (M): 2θ (°) = 19.77° Intensity (arb. u) = 530, FWHM (°)= 0.42), only some small changes are visible in Y direction (*060* (M): 2θ (°) = 61.97° Intensity(a. u) = 230, FWHM (°)= 0.31). The structure of pillars is ordered also in Z direction, the pillars have been introduced between the layer structures which remained parallel to each other.

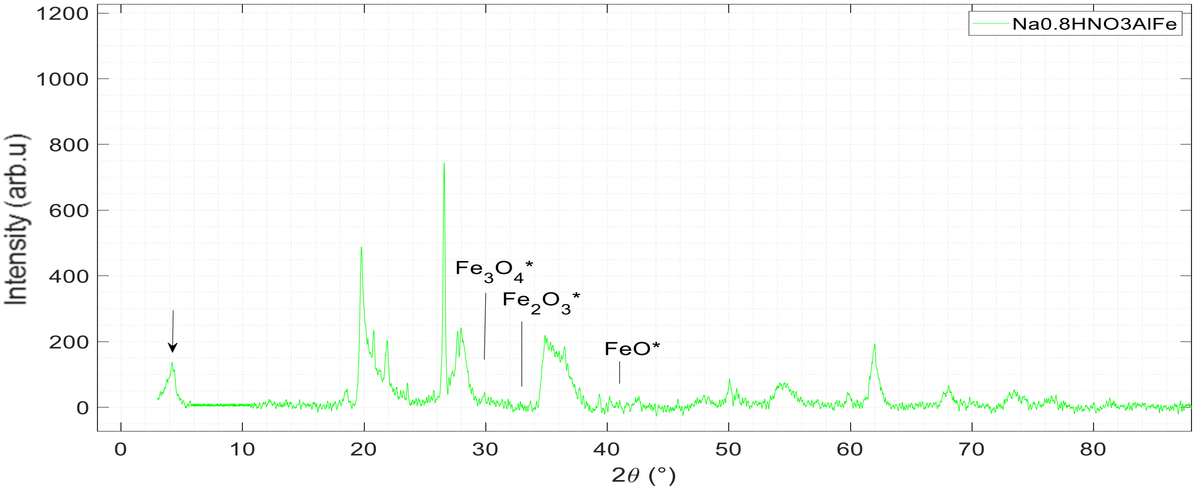

Figure 3.39: XRD of Na0.8HNO3AlFe

In Fig 3.39 the presence of (*) represents the possible positions of iron oxides. As for the samples already analysed no positive identifications are confirmed for Fe_3O_4, FeO, Fe_2O_3. Their positions are overlapped by other positions come from the main reflections present in bentonite.

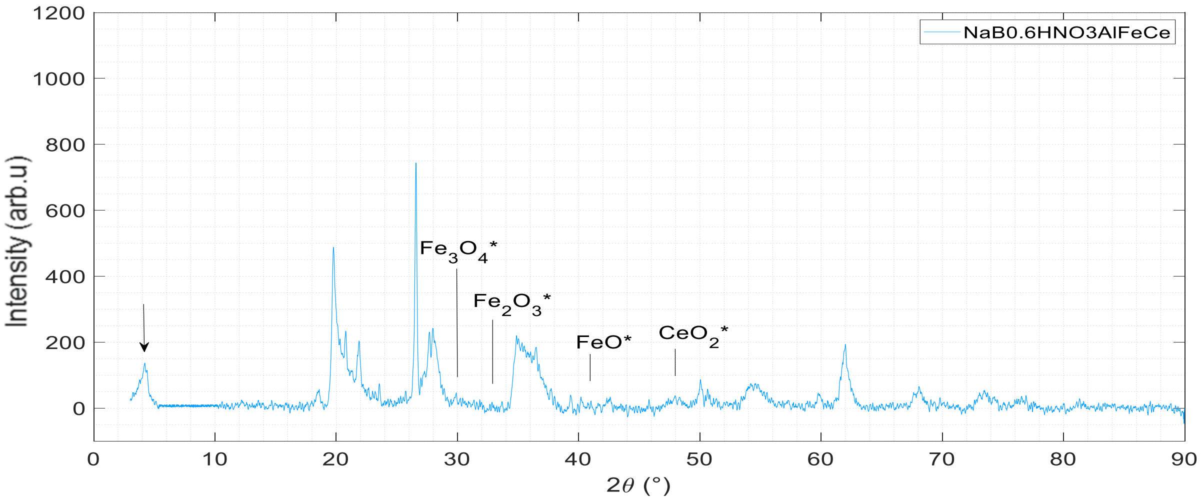

Figure 3.40: XRD of Na0.6HNO3AlFeCe

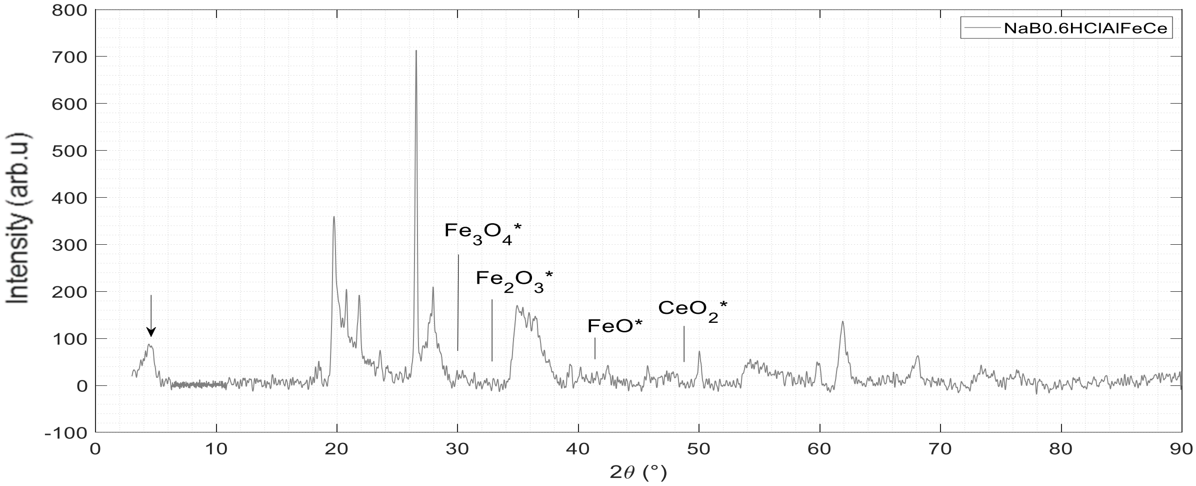

Figure 3.41: XRD of NaB0.6HClAlFeCe

In Fig 3.40 the presence of (*) represents the possible positions of iron and cerium oxides. As for the samples already analysed no positive identifications can be confirmed, there is an overlap of reflections. For Fig 3.39 and Fig 3.40 possible oxide species are reported, their reference codes are the same shown in Fig 3.33 and Fig 3.34 respectively for iron and cerium oxides. Comparing the effect of pillaring for difference acid treatments 0.6 M and 0.8 M for both acids (HNO3 and HCl), there are not huge differences: the shift of 001 peak at lower 2θ is almost the same. No differences in HNO3 and HCl: pillaring has been successful for both the samples. Well dispersed and amorphous forms of FexOy and CeOx cannot be excluded. 001 peak for NaB0.6HClAlFeCe at 2θ= 4.25° and for NaB0.6HNO3AlFeCe at 2θ= 4.20°. For a solution 0.8M of acid the differences in 001 peak position between the sample treated with HNO_3 and the sample with HCl was higher.

3.5.4 Introduction of cobalt as a pillar agent

The amount of cobalt introduced is too low to be confirm in XRD. Radius of cobalt is bigger than the radius allumium and d_{001} has to increase. As for the sample without cobalt as a pillar agent but only with aluminium the impregnation with iron has not to change the main reflections in X, Y, Z directions.

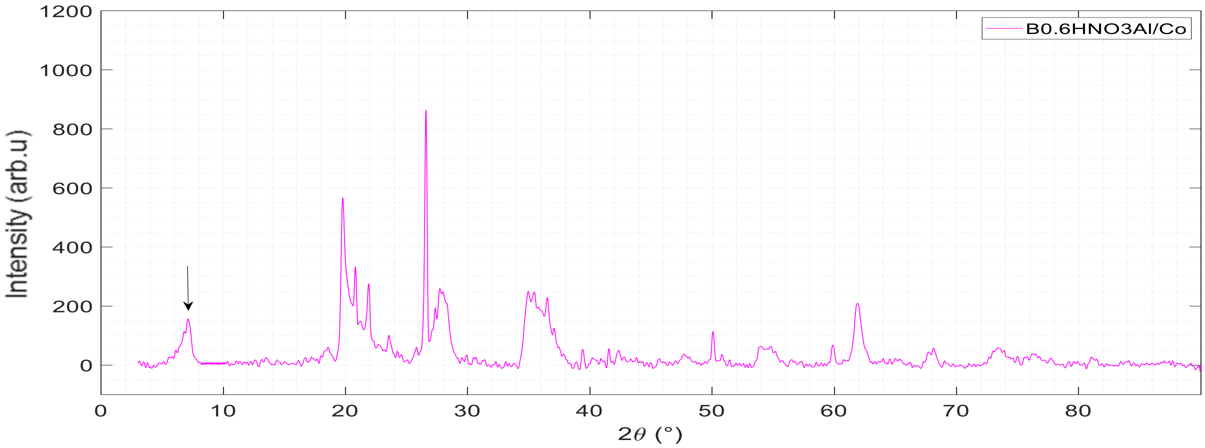

Figure 3.42: XRD of B0.6HNO3Al/Co

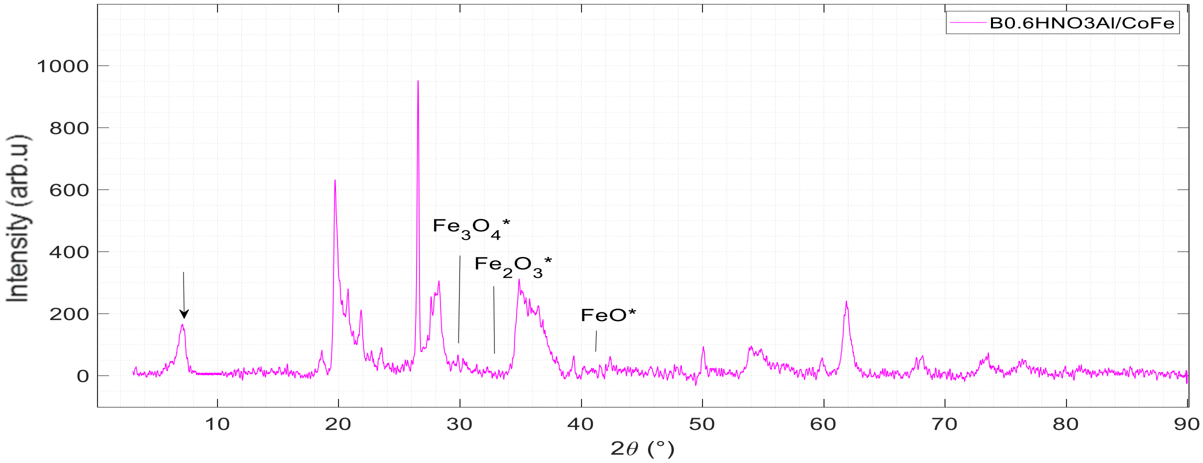

Figure 3.43: XRD of B0.6HNO3Al/CoFe

Fig 3.42 shows the pattern of B0.6HNO3Al/Co, pillaring increases d_{001} . 001 peak is shifted at 2θ=7.41°. The first reflection after acid treatment does not lose its sharp shape related to the absence of loss in crystallinity still visible after the impregnation with iron species. The possible iron oxides formed are reported in Fig 3.43 with (*). Overlaps of reflections with the ones present in the pattern of B0.6HNO3Al/Co cannot identify Fe_2O_3, Fe_3O_4 and FeO. Amorphous forms of iron may be hypothesized as cobalt oxide species as separate phases such as CoO or Co_3O_4.

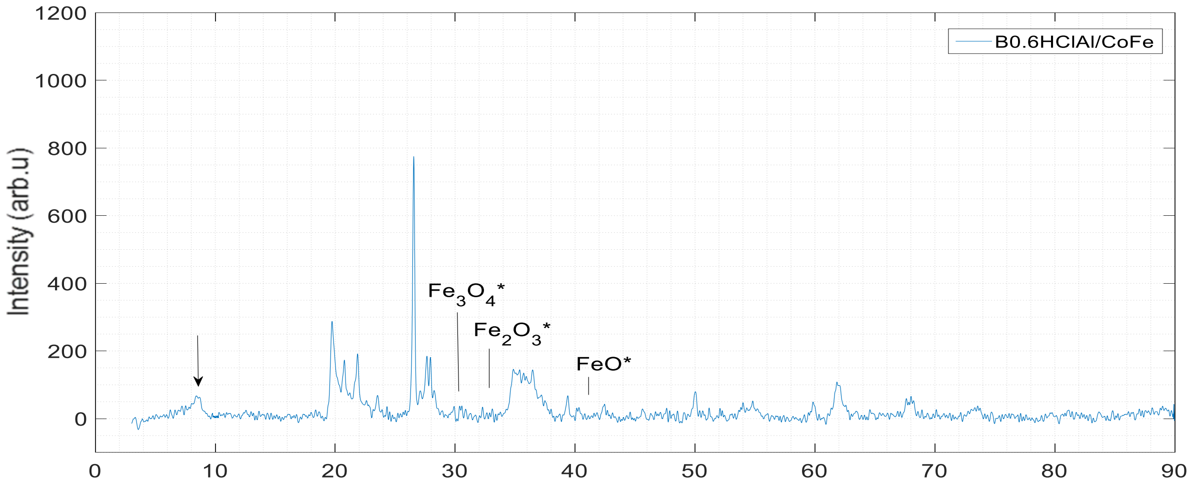

Figure 3.44: XRD of B0.6HClAl/CoFe

Fig 3.44 shows the pattern of B0.6HClAl/CoFe, pillaring did not occur , 001 peak is located at 2θ= 8.10°. The shape of *001* reflection is broader than at the beginning in pure bentonite this is due to the acid treatment that decrease the crystallinity. The structure is not delaminated, pillars have not been introduced to increase d_{001} and all the other reflections in X and Y directions retained their crystallinity. The possible iron oxides formed are reported in Fig. 3.44 with (*). The presence of amorphous forms of iron oxides may give good catalytic activities to the sample even if the pillaring was not successful.

Table 3.3 : The value of the BET surface area for raw bentonite and pillared bentonite.

Sample	Surface Area (m^2/g)
Na-Bentonite (raw)	31.38
Al-Bentonite	40.62
Al-Co/Bentonite rasio 0,1	90.49
Al-Co/Bentonite rasio 0,2	98.19
Al-Co/Bentonite rasio 0,3	105.65

From literature studies if the pillaring occur the surface area increases, Na-Bentonite shows a surface area of about 31.23 m^2 /g, Al-Bentonite presents a higher surface area thanks to pillaring process, but the presence of mixed pillar agents increases it at higher values. Table 3.3 shows the increase of the surface area Al-Co/bentonite with different ratio of Al-Co and represents the formation of stable pillar bonds in the interlayer spaces. More Cobalt is added more the surface area is going to increase. Increased surface area will extend the reaction area. If the pillaring was successful samples with mixed pillar agents present values of d_{001} higher than the samples pillared only with aluminium which suggest a smaller surface area.

3.6 Fourier Transform Infrared Spectroscopy (FT-IR) results and discussion

3.6.1 Reference and experimental spectra

By FT-IR method it is possible to focus the attention on the consequences of the acid treatments that create a depopulation of the octahedral sheet and the formation of amorphous silica.

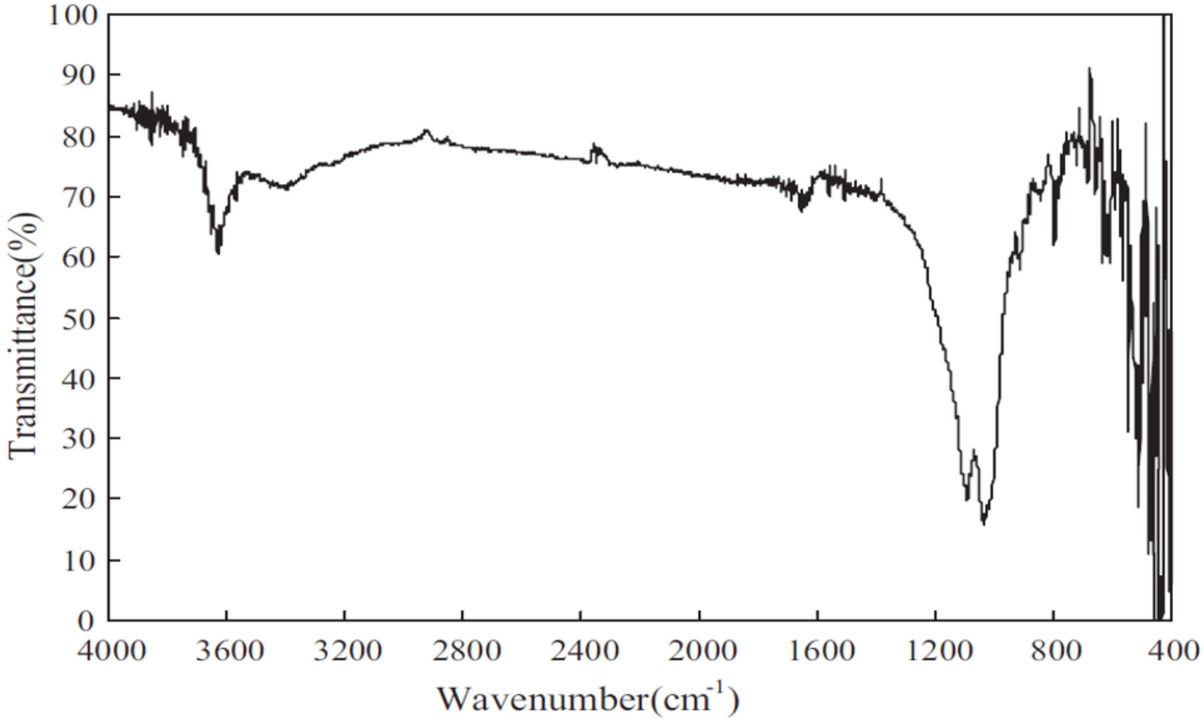

Figure 3.45: FT-IR of natural Na-Bentonite (Reference spectra)

Treated bentonite with the mentioned solution of NaCl (1 M) has formed Na-Bentonite. It is possible to compare the pattern of Na-Bentonite treated in this work with the result found in literature and effectively accepted the formation of the wanted form. [58] As it is resumed in Tab. 3.4 with the corresponding connection between the wavenumber (cm^{-1}) and the different bonds present in the mineral clays. 3633 cm^{-1} relate to the adsorption of O-H stretching vibrations of non-hydrogen-bonded and 3446 cm^{-1} to the adsorption of O-H stretching vibrations of hydrogen-bonded water region. 1643 cm^{-1} relate to the adsorption of H-O-H bending vibration. 915 cm^{-1} is related to Al–O(OH)–Al deformation adsorption band. The absorption bands corresponding to Fe–O–Fe vibration of Fe-bentonite were not detected; this agrees with all the first consideration of having a pure bentonite without any substitution in the layers. This is also in agreement considering the absence of absorption band in the range 875 cm^{-1} and 836 cm^{-1} related to hydroxyl bending vibration of AlFeOH, AlMgOH [61]. Absorption bands at 1118, 1046, 797, 524 and 462 cm^{-1} related to the stretching and bending vibrations of silica bonds. In general, Si–O bands are strongly evident in the silicate structures, they exhibited a very strong absorption bands in 1100-1000 cm^{-1} and from the result of the spectrum of Na-B analysed this is confirmed. 525 and 462 cm^{-1} bands absorption are related to Al-O-Si and Si-O-Si bending vibrations. The band with 621 cm^{-1} is related to Al-O and Si-O out of plane vibration. 797 cm^{-1} related to the presence of impurities such as quartz. Another conclusion is the absence of the band in 1430 cm^{-1} relate to calcite impurities.[62][63]

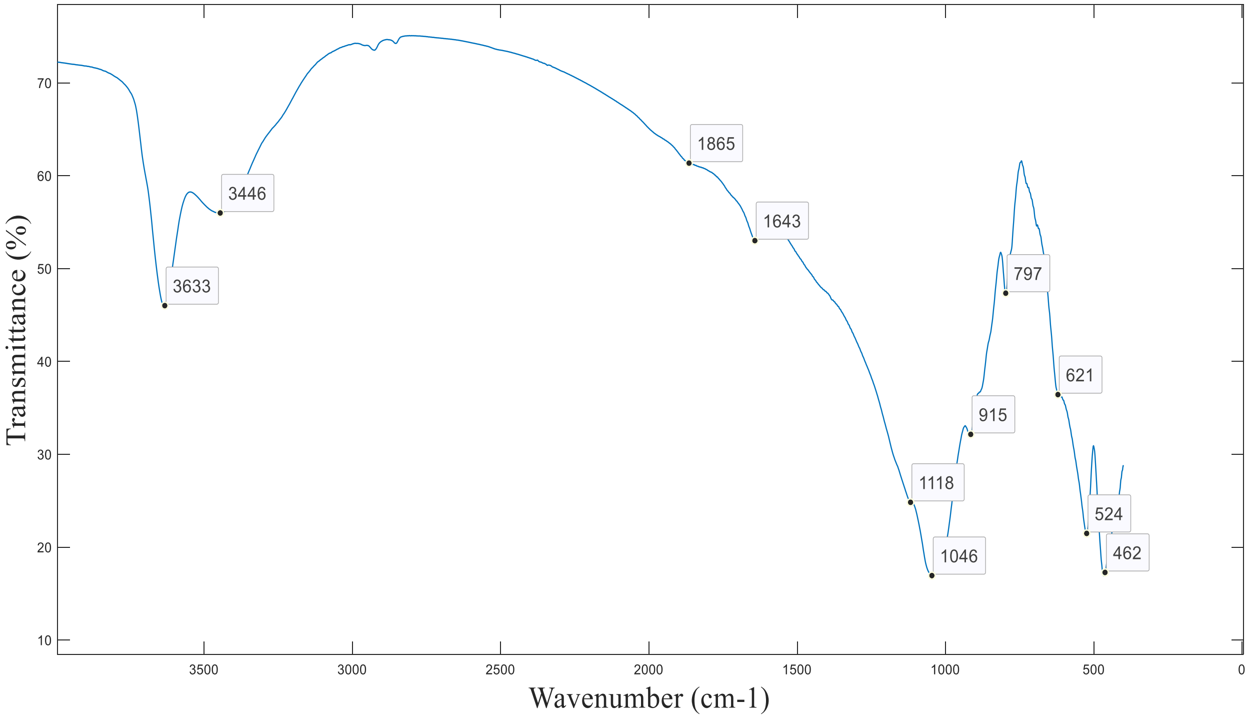

Figure 3.46: FT-IR of Na-Bentonite (Experimental spectra)

Table 3.4: Bonds present in Na-Bentonite

Wavenumber (cm^{-1})	**Bonds**
3633	O-H
3446,1865,1643	H-O-H
11846,1046, 621	Si-O
915	Al-Al-OH
797	Quartz

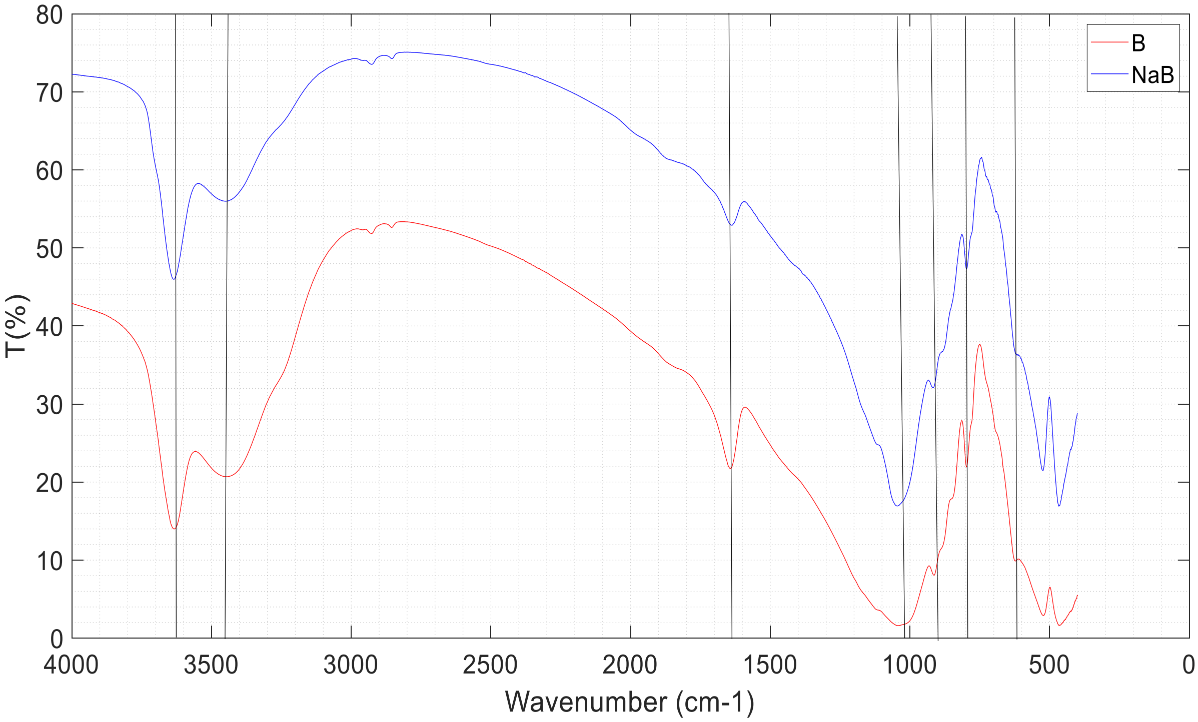

Figure 3.47: FT-IR of B and NaB

Exchange with NaCl 1M did not change the spectra of pure bentonite, the pattern of NaB and B are the same, Na^+ has been successfully introduced to obtain Na-Bentonite but it does not change the main bonds in the mineral clay. (Fig. 3.47)

3.6.2 Influence of the introduction of the active phases (iron and cerium species)

There are not considerations that can be done for the active phases in FT-IR. Iron and cerium oxides mentioned in XRD analysis are not visible in the range 4000-500 nm. FT-IR confirmed that the introduction of iron and cerium species did not introduce any visible differences in the spectra compared to the ones without the impregnation preparation. This conclusion has also been done by x-ray analysis.

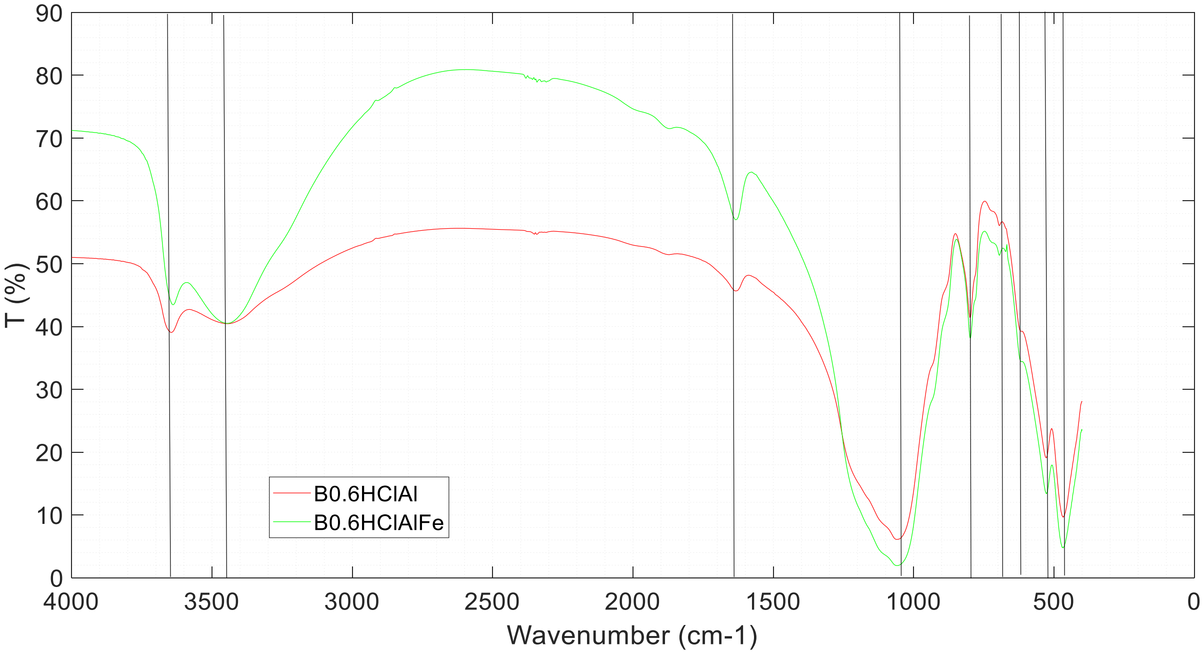

Figure 3.48: FT-IR of B0.6HClAl and B0.6HClAlFe

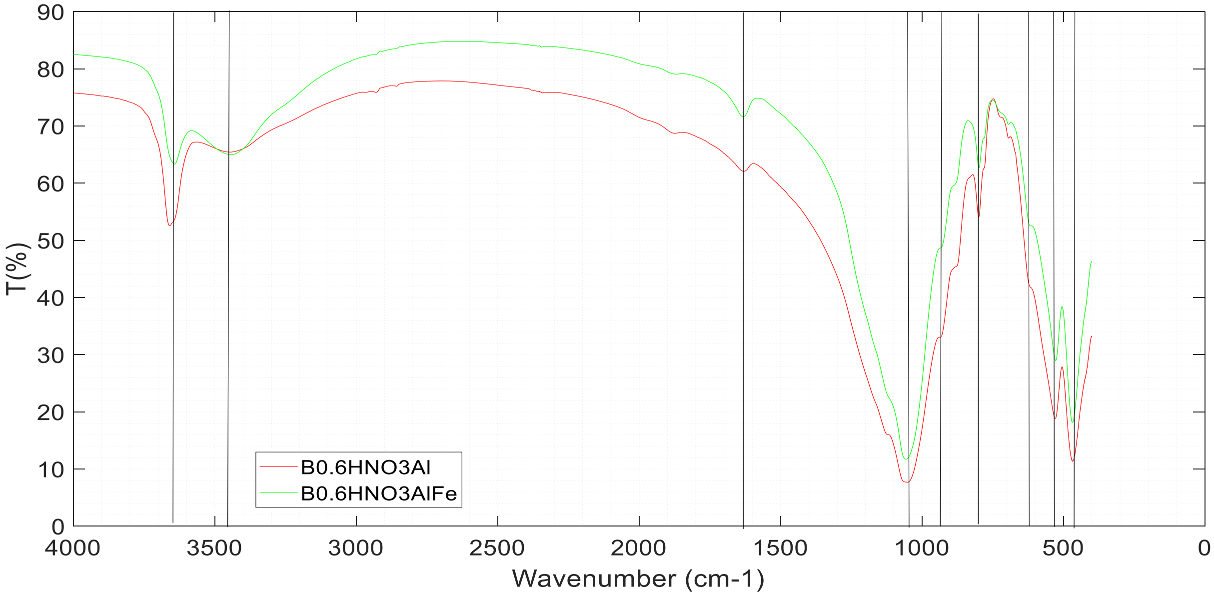

Figure 3.49: FT-IR of B0.6HNO3Al and B0.6HNO3AlFe

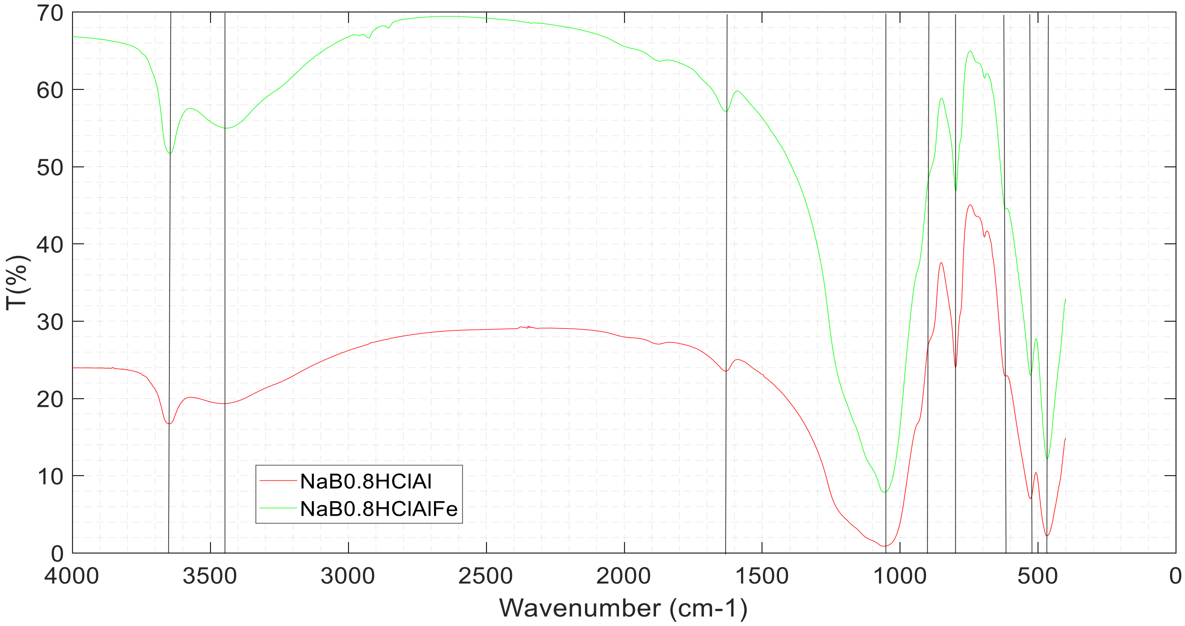

Figure 3.50: FT-IR of NaB0.6HNO3Al and NaB0.6HNO3AlFe

Fig 3.48, 3.49 and 3.50 show the spectra of B0.6HClAlFe, B0.6HNO3AlFe, NaB0.6HNO3AlFe compared respectively to their supports. In all the three figures the active phase (iron species) does not change the wavenumber of absorption of the main bonds.

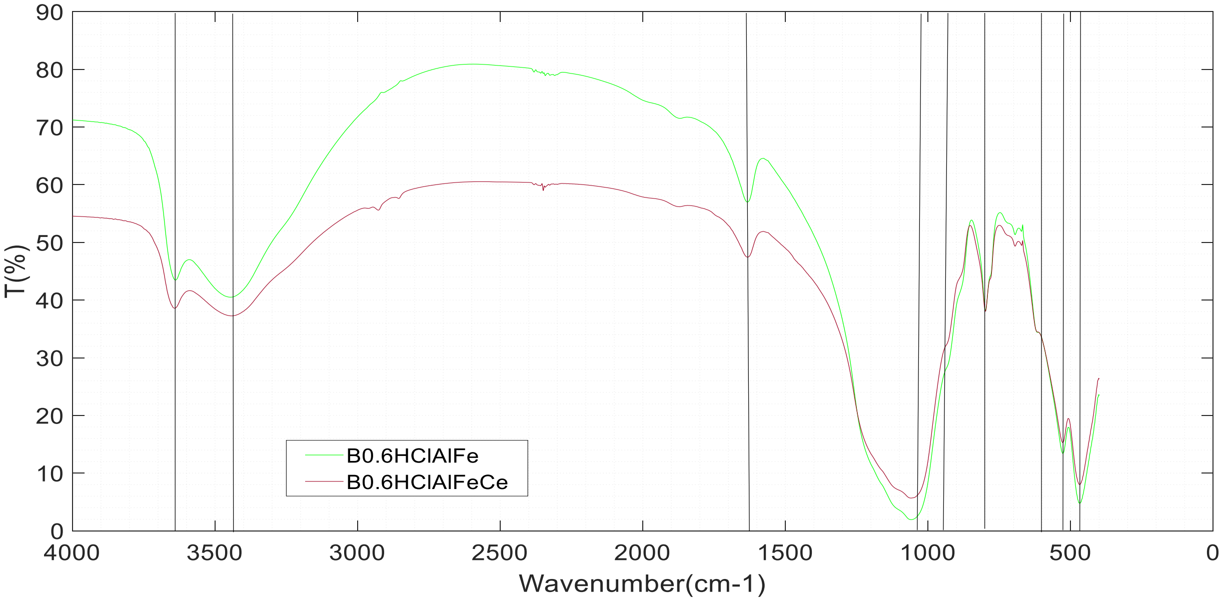

Figure 3.51: FT-IR of B0.6HClAlFe and B0.6HClAlFeCe

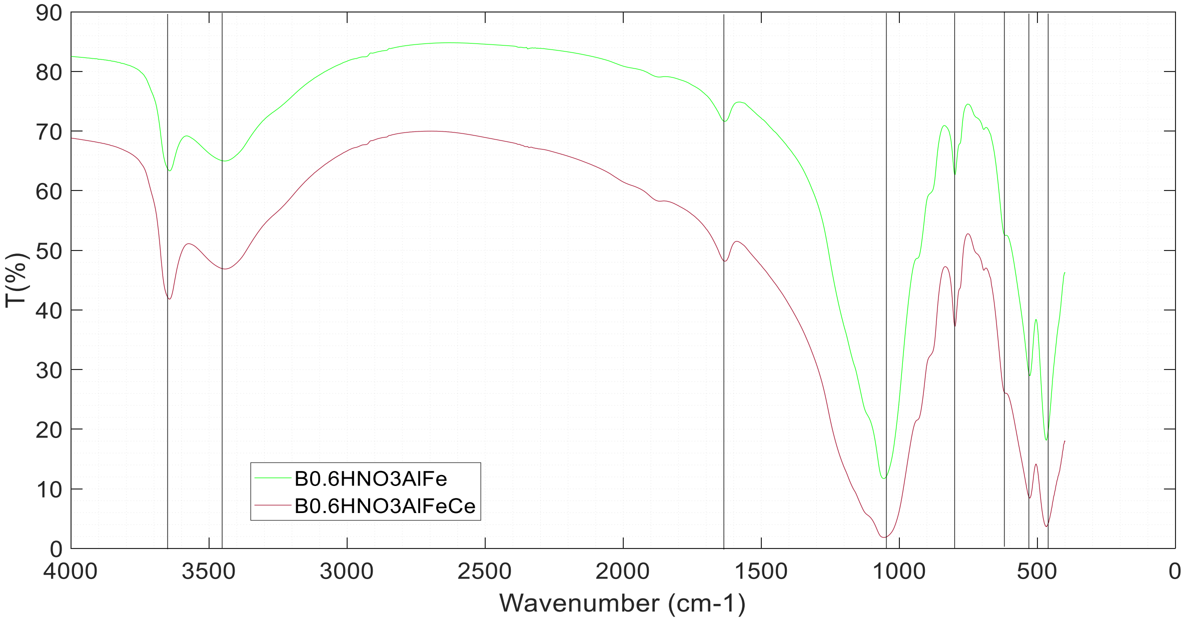

Figure 3.52: FTIR of B0.6HNO3AlFe and B0.6HNO3AlFeCe

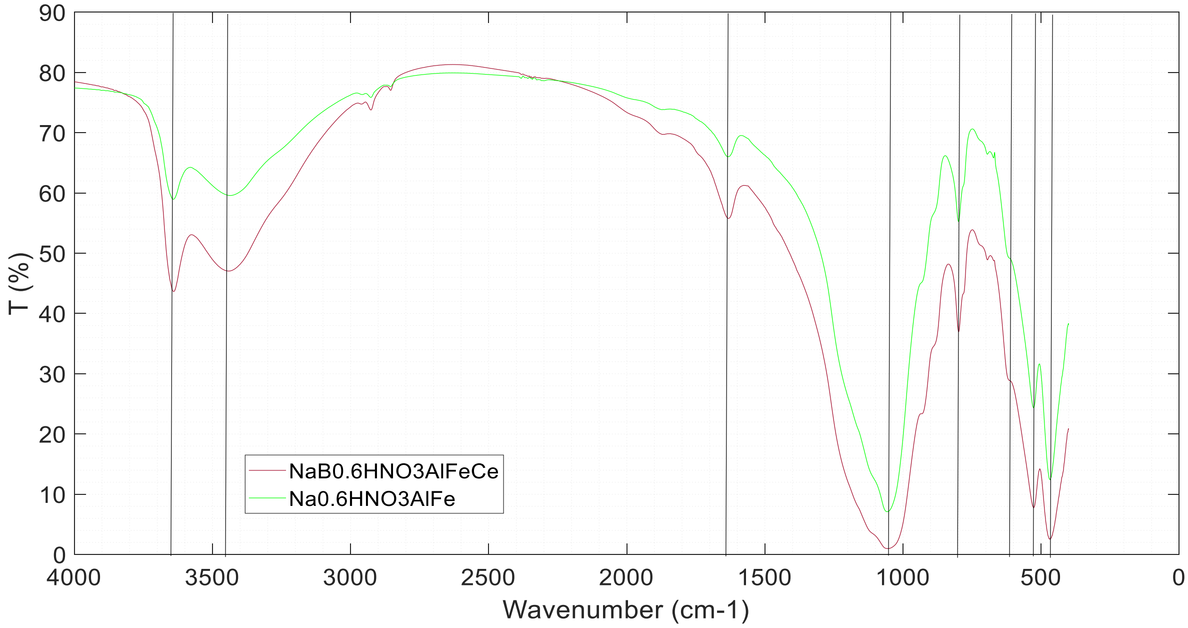

Figure 3.53: FT-IR of NaB0.6HNO3AlFe and NaB0.6HNO3AlFeCe

Fig 3.51,3.52, 3.53 show the spectra of B0.6HClAlFeCe, B0.6HNO3AlFeCe, NaB0.6HClAlFeCe compare to the respectively samples only impregnated with iron species. The impregnation with ceria is the following step after calcination and impregnation with iron species. The structure of the samples has not been changed after impregnation with iron species and the same conclusion can be done also for ceria.

3.6.3 Influence of the type of acid used (HNO3 or HCl)

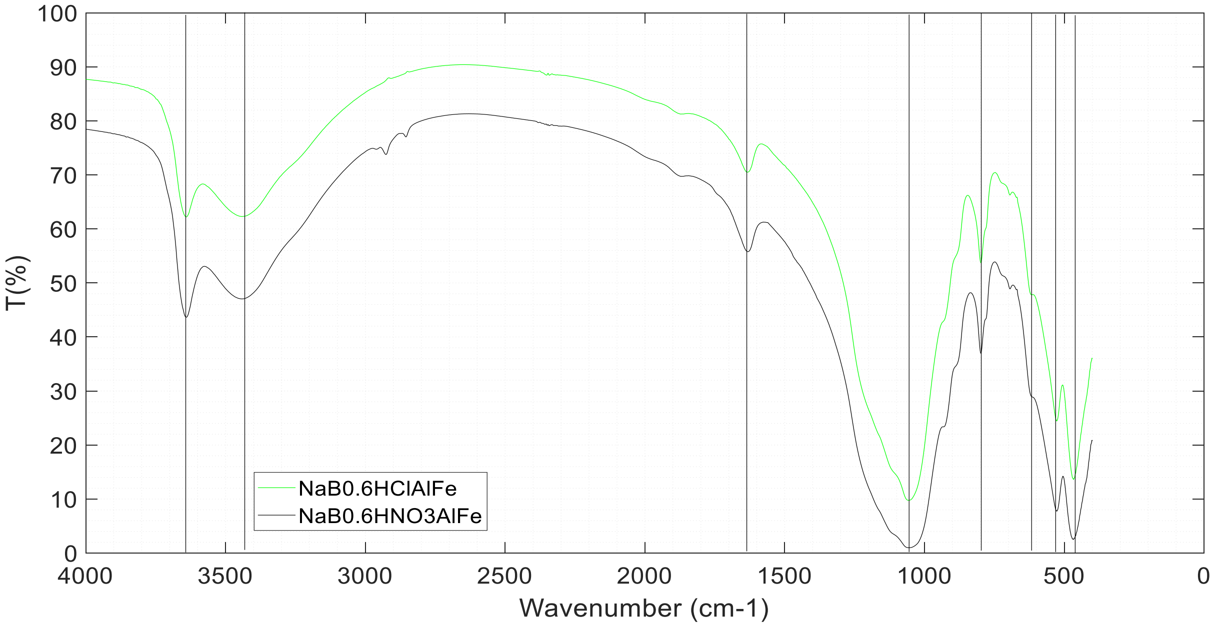

Figure 3.54:. FT-IR of NaB0.HClAlFe and NaB0.6HNO3AlFe

Fig. 3.54 and Fig. 3.55 show the patterns of NaB0.6HClAlFe, NaB0.6HNO3AlFe, B0.6HClAlFe and B0.6HNO3AlFe. The spectra have been compared to show that there are not visible differences in the spectra (HNO_3 or HCl). Presence of NO_3^- may be visible in the range 1500-1300 cm^{-1} for samples treated with HNO_3, their absence suggested that the samples have been completely washed after acid treatment. Cl^- are not visible in this range.

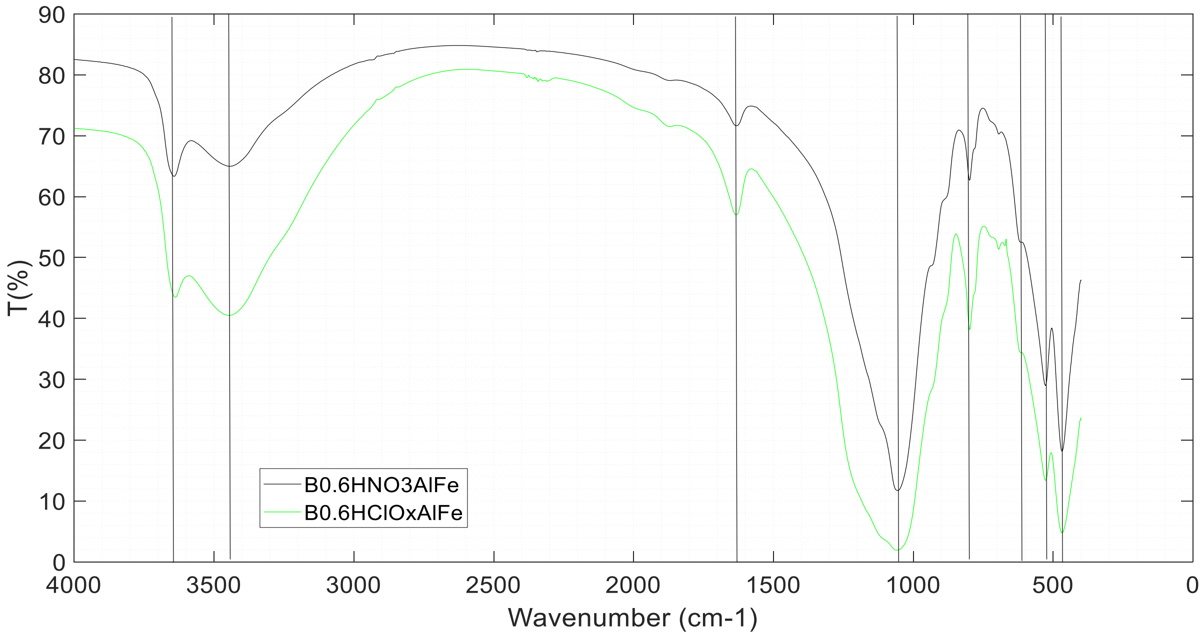

Figure 3.55: B0.6HClAlFe and B0.6HNO3AlFe

3.6.4 Influence of the increase of acid concentration

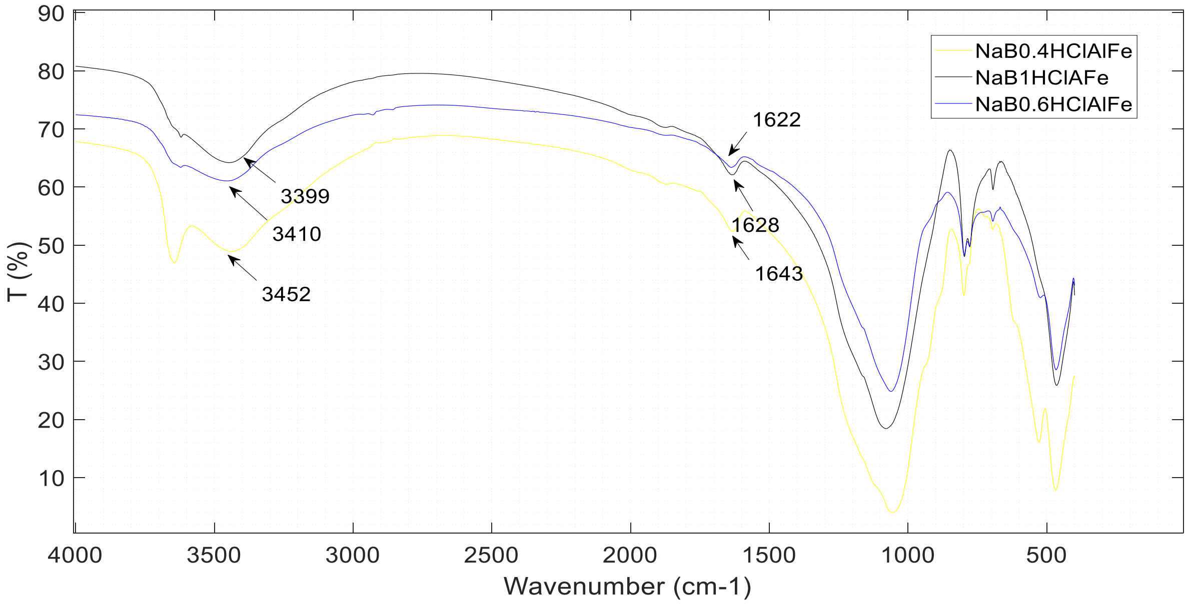

Figure 3.56: Increase of acid concentration of HCl range 4000-1500 cm^{-1}

The bands close to 3446 and 1643 correspond to absorbed water. Drying and calcination have been carried out after every preparation step. Bands corresponding to water face a loss of intensity with the increase of the acid concentration. They seem to disappear, and they are shifted at lower values.

The difference concentration of acid decreases the intensity of these mentioned bands and the molecules have less water interaction. Three different sample NaB0.4HClAlFe, NaB0.6HClAlFe, NaB1HClAlFe are reported in Fig. 3.56. The absorbance intensity decreases with the intensification of the acidity. 3452, 3410 and 3399 cm^{-1} and 1643, 1628 and 1622 respectively for NaB0.4HClAlFe, NaB0.8HClAlFe, NaB1HClAlFe.

The decrease of the absorption bands for the water of hydration is related to the removal of the octahedral cations causing loss of water and hydroxyl groups coordinated to them.

These considerations agree with literature, but the presence of water is very sensitive, powdered potassium bromide used for the test absorbs more humidity (it is hygroscopic) from the air and therefore lead to an increased background in certain ranges. Furthermore, calcination and dried steps are not enough to remove water. The absence of evacuation of water makes the peaks broader and interferes with the bands.

The range from 3000 to 4000 cm^{-1} is influenced by many parameters and it may be considered with attention, the results can be more reliable and not influenced by the content of water in lower range (1500- 500 nm) as it presented in Fig 3.57.

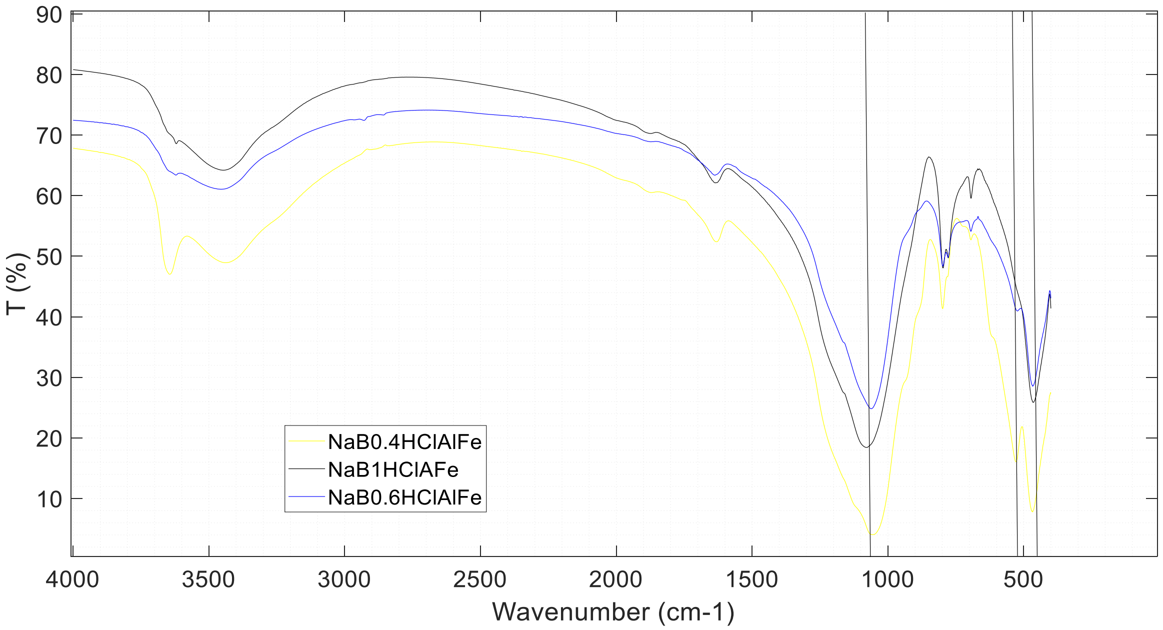

Figure 3.57: Increase of acid concentration of HCl range 1500- 500 cm^{-1}

Intensity of Si-O out of plane and Si-O-Si in plane stretching bands have not been influenced by the increase of the acid treatments. Pure bentonite and modified bentonites present almost the same pattern with the increase of acid concentrations. Acid treatment hardly affect the structure of bentonites, this has also been confirmed with x-ray analysis. Only changes in Z direction are visible, the order in X and Y directions remained even when a delaminated structure is formed. There are not any strong differences in the typical reflections of montmorillonite and quartz, and in FT-IR this is confirmed. Vibrations of Si-OH groups with increasing in the acid attack increase slightly, modest alteration of the structure during increasing of acid attack are visible.

3.6.5 Influence of pillaring

Fig 3.58 shows the comparison between raw bentonite and bentonites pillared with different elements. It can be seen in fact that pillaring did not change the structure of raw bentonite. There are not significant differences between the pattern of bentonite and pillared ones. Pillaring in fact do not affect the main bonds present in the mineral clay. [64] Decrease of the peaks at 3623 cm^{-1} and in the range 400 to 100 cm^{-1} with a higher decrease for the mixed oxide pillar agents implying the interaction of pillar agents with Si-O group in the silica tetrahedron plates and Al-OH in the octahedral layers.

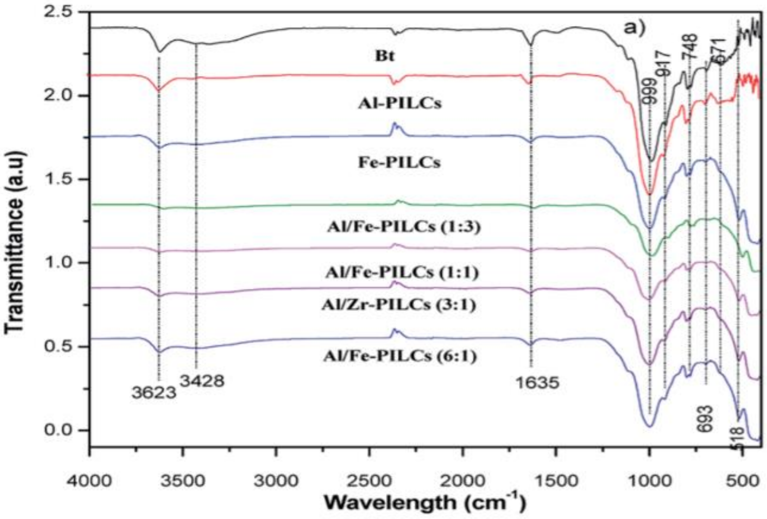

Figure 3.58: FT-IR spectra of natural bentonite and pillared bentonite

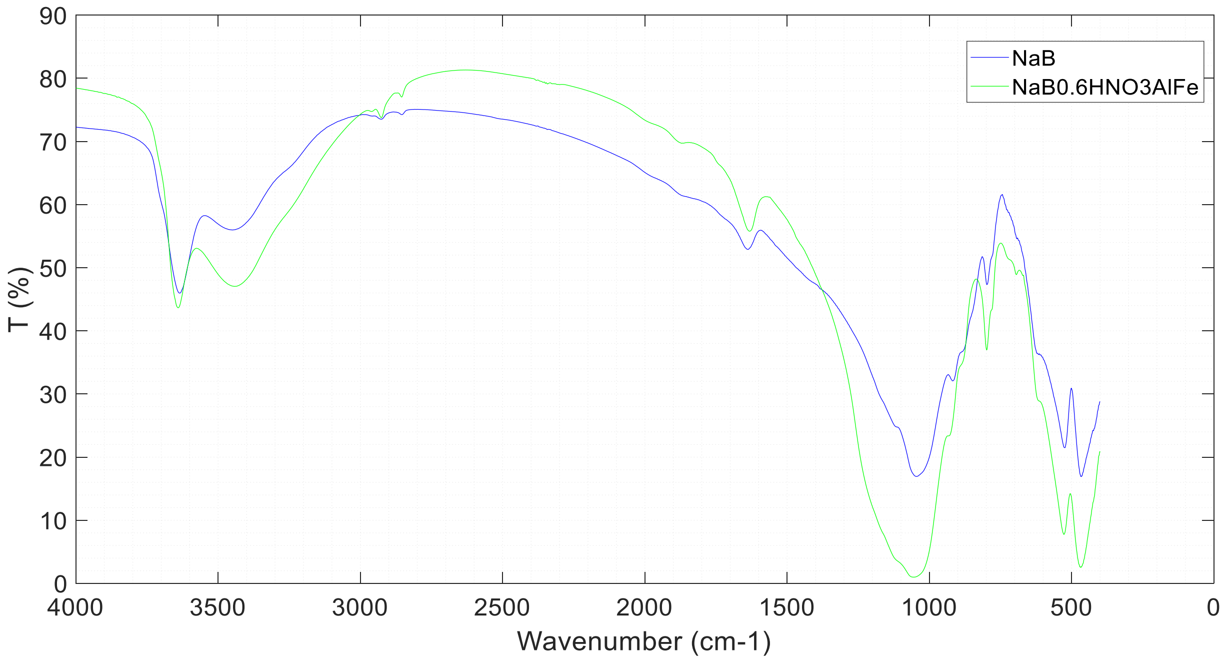

Figure 3.59: FT-IR of NaB and NaB0.6HNO3AlFe

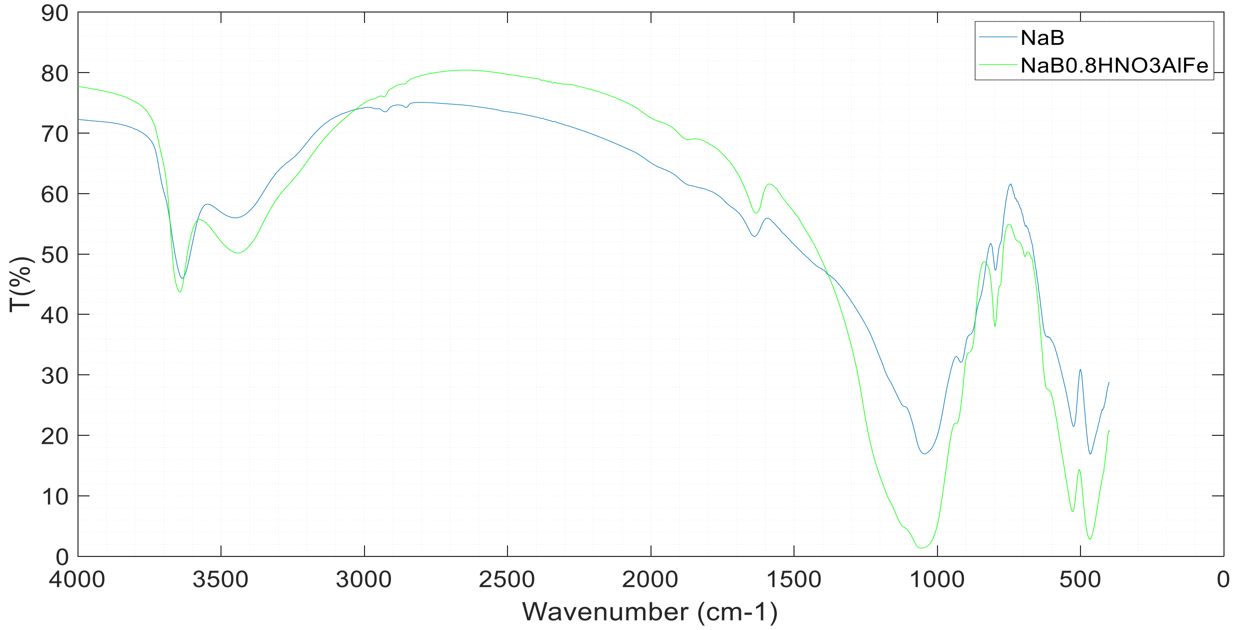

Figure 3.60: FT-IR of NaB and NaB0.8HNO3AlFe

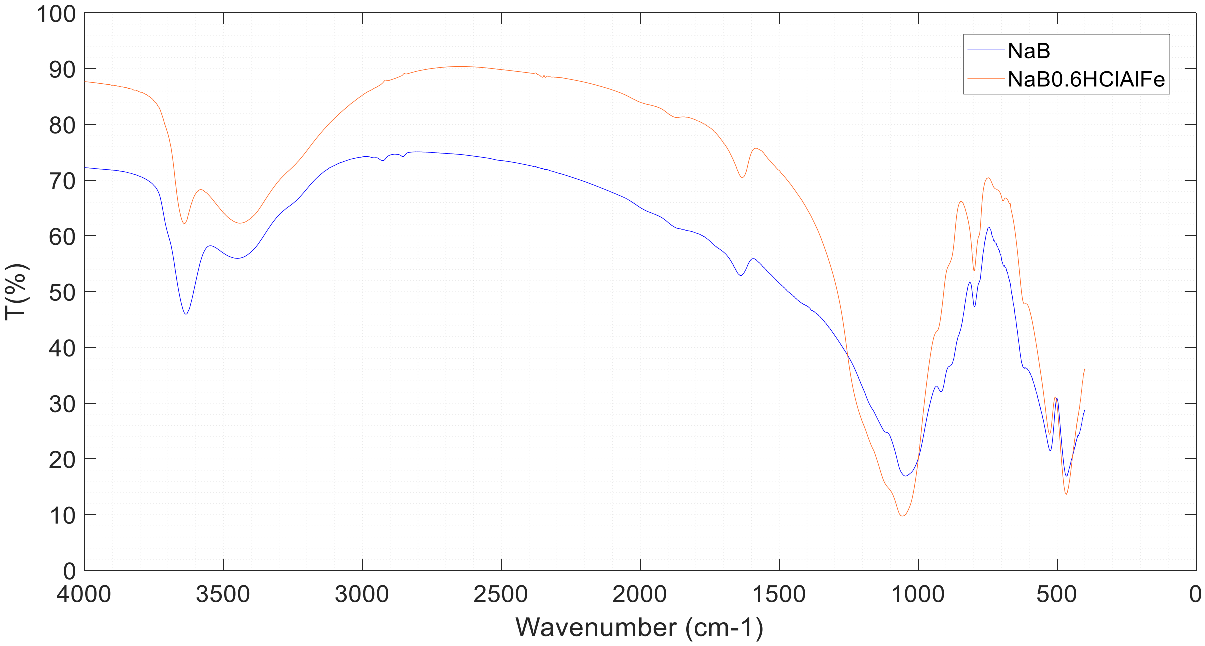

Figure 3.61: FT-IR of NaB and NaB0.6HClAlFe

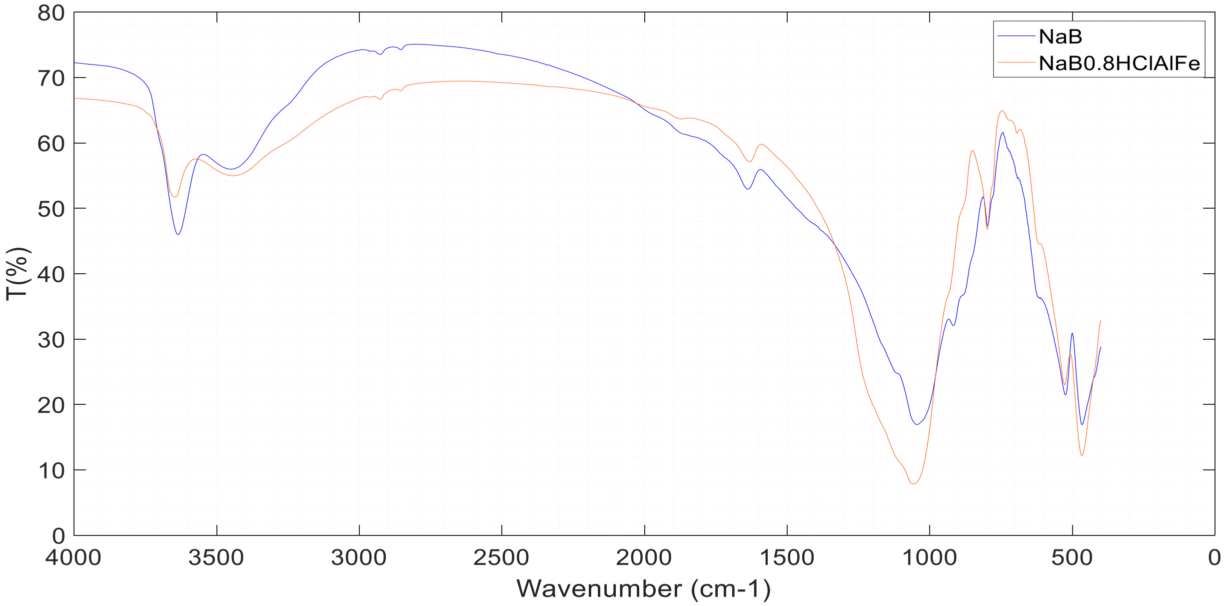

Figure 3.62: FT-IR of NaB and NaB0.8HClAlFe

Fig 3.59, 3.60, 3.61, 3.62 show the spectra of NaB compare to NaB0.6HNO3AlFe, NaB0.8HNO3AlFe, NaB0.6HClAlFe, NaB0.8HClAlFe. Pillaring did not influence the structure of the spectra, there are not visible differences from NaB and pillared-NaB without mainly changes in the structure as it was also confirmed for acid treatments. Little changes in the shape of the peaks in the range 1500-500 cm^{-1} agree with the conclusion of Moma.[64] X-ray confirmed that pillaring has been successful for all the samples reported in figures. Small changes in the area 1500-500 cm^{-1} imply the interaction of pillar agents with Si-O group in the silica tetrahedron plates and Al-OH in the octahedral layers.

3.6.6 Influence of pillaring with mixed pillar agents

From literature differences with the presence of cobalt as a pillar agent are not such visible [65]. Different concentrations of cobalt do not influence the main bonds. However, some changes can be observed for higher concentration of cobalt, a band appeared at 662 cm^{-1} due to presence of the cobalt compounds.

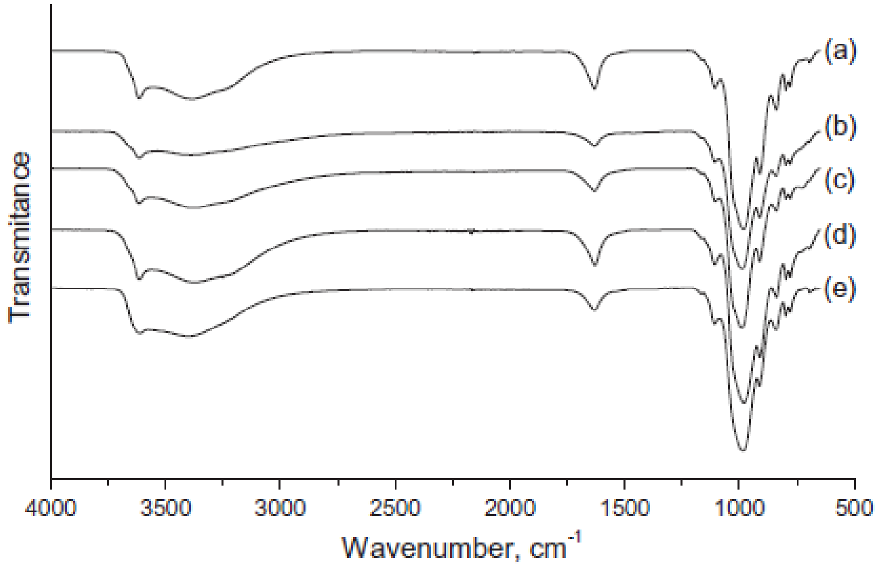

Figure 3.63: Infrared spectrum of the natural (a), 10% (b), 25% (c), 50% (d) and 75% (e) Co pillared clays.

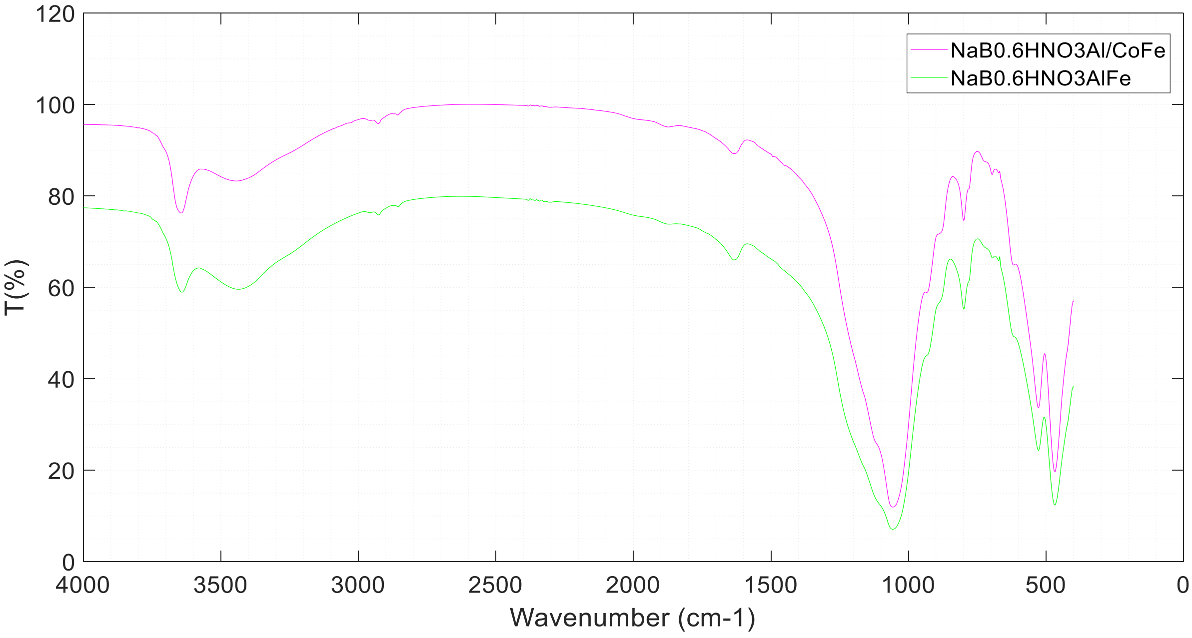

Figure 3.64: FT-IR of NaB0.6HNO3Al/CoFe and Na0.6HNO3AlFe

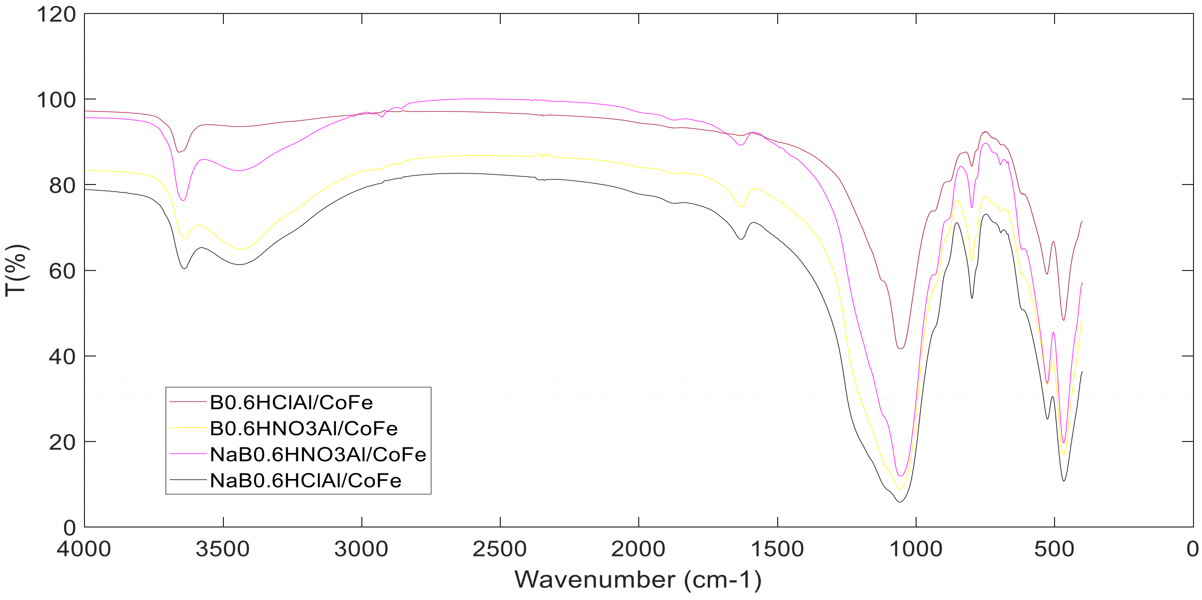

Figure 3.65: FT-IR of B0.6HClAl/CoFe, NaB0.6HClAl/CoFe, B0.6HNO3Al/CoFe and NaB0.6HNO3Al/CoFe

Fig 3.64 and Fig. 3.65 show the spectra of mixed pillar agents (cobalt and aluminium) for all the samples that have been pillared with cobalt in this work. Comparing with literature information some visible changes in the spectra are related only to 75%- 100% Co pillared clays. In this work the percentage is 50% Co-pillared bentonite and the spectra for all the samples remained unchanged. Fig. 3.64 shows that there are not changes between the spectra of NaB0.6HNO3Al/CoFe and Na0.6HNO3AlFe.

3.7 Ultraviolet-visible spectroscopy (UV-vis) results and discussion

In this work the only useful consideration with UV-vis analysis is the determination of various forms of iron species introduced with the impregnation by the observation of typical bands characteristic of these species, coordination and aggregation of $Fe^{3+} \leftarrow O$ charge transfer.

3.7.1 Literature consideration and NaB spectra

X-ray analysis could not give more information than the possible presence of a totally amorphous distribution of iron oxides. Only for one sample it was identified a crystallite size of Fe_2O_3. UV-vis may give more information about the introduction of the active phase on the support of the catalyst.

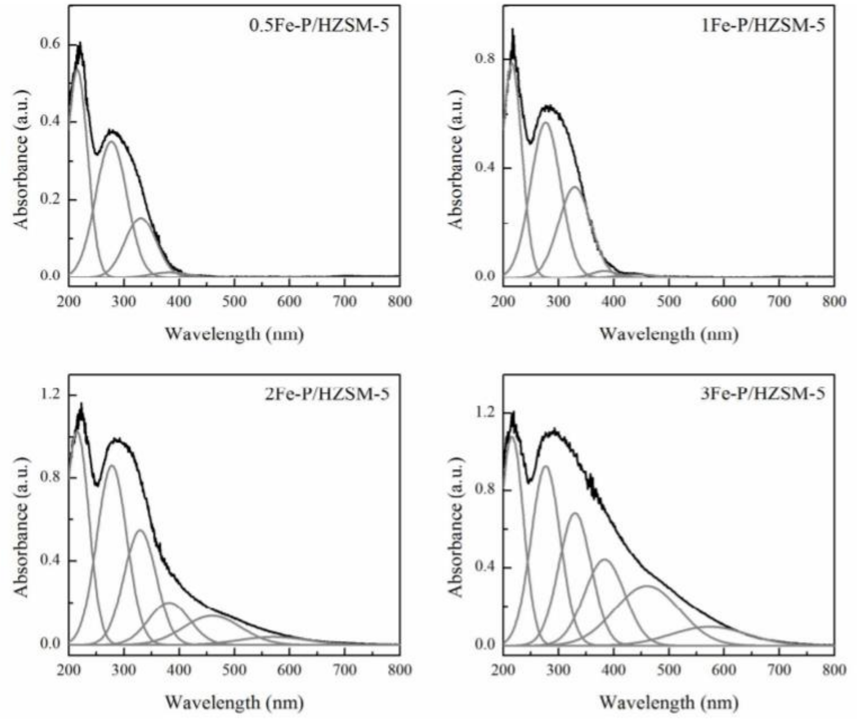

Figure 3.66: UV-vis diffuse reflectance spectra of xFe-P/HZSM-5 (x= 0.5,1,2,3)

In UV-vis the presence of iron in fact is confirmed by the absorption peak in different wavenumbers. From literature it is possible to synthesize that the intensities of bands in spectra increase with the iron content. Fig. 3.66 shows UV-vis analysis of xFe-P/HZSM-5 for x = 0.5, 1, 2, 3) [66]. The spectra have been deconvoluted into Gaussian sub-bands with lowest numbers.

Bands at 215 and 278 nm relate to isolated tetrahedrally coordinated Fe^{3+} ions in or close to the framework and isolated octahedrally coordinated Fe^{3+} in extra framework. Bands in 333 and 384 nm relate to oligonuclear Fe_xO_y clusters and additional bands over 400 nm relate to dispersed and bulky Fe_2O_3 particles. As it is visible in Fig. 3.66 for 0.5Fe-P/HZSM-5 there is not a band over 400 only bands in 215, 278 and 333 nm are visible and a weak band in 384 nm: the catalyst present only Fe^{3+} ions and small clusters. Adding more percentage of iron also bands over 400 nm are clearly visible relating to the presence of Fe_2O_3 particles. Catalysts containing more than 2 wt% of iron present iron species as isolated ions and Fe_2O_3 bulky particles.

Fig 3.67 shows semiquantitative estimation for the distribution of iron species in xFe-P/HZSM-5 (x= 0.5, 1, 2, 3). Results show that the predominant species for all iron species presented are isolated ions, when the iron content increases the contribution of Fe_xO_y and Fe_2O_3 increase and the contribution of isolated Fe^{3+} ions decreases from 80.6 % to 43.7%. The increase of the agglomerated particles of not isolated iron can block the micropores and reduce the micropore areas with negative impact in the catalytic activity. [66]

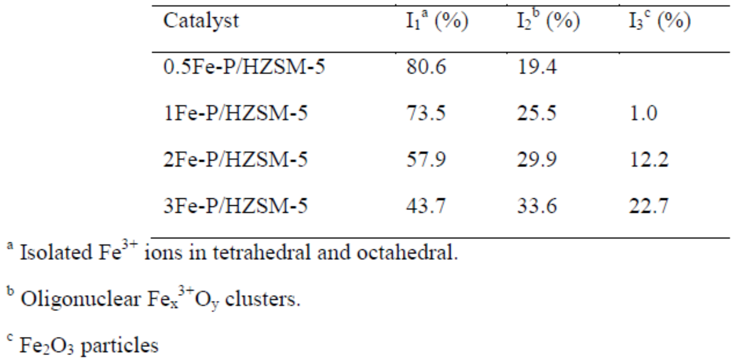

Catalyst	I_1[a] (%)	I_2[b] (%)	I_3[c] (%)
0.5Fe-P/HZSM-5	80.6	19.4	
1Fe-P/HZSM-5	73.5	25.5	1.0
2Fe-P/HZSM-5	57.9	29.9	12.2
3Fe-P/HZSM-5	43.7	33.6	22.7

[a] Isolated Fe^{3+} ions in tetrahedral and octahedral.

[b] Oligonuclear $Fe_x^{3+}O_y$ clusters.

[c] Fe_2O_3 particles

Figure 3.68: Percentage of the area of sub-bands (I_1 at $\lambda < 300$ nm, I_2 at $300 < \lambda < 400$ nm. I_3 at $\lambda > 400$ nm) of UV-vis spectra of xFe-P/HZSM-5 (x=0.5,1,2,3)

Pérez-Ramírez turned up that the absorption coefficients for bands of various iron species are of the same order of magnitude. For iron species the typical bands that allow to do some consideration are 200-350 nm, increasing the intensity demonstrates the presence of isolated Fe^{3+} cations and the formation of Fe-O-Si bonds. 350-450 nm referred to small oligonuclear Fe_xO_y clusters. Above 450 nm represents the formation of dispersed Fe_2O_3 particles. [67]

The deposition of the active phase influences UV-vis spectra, initial modification and impregnation changed the shape of the untreated bentonite. Na- Bentonite doesn't present any typical absorption bands.

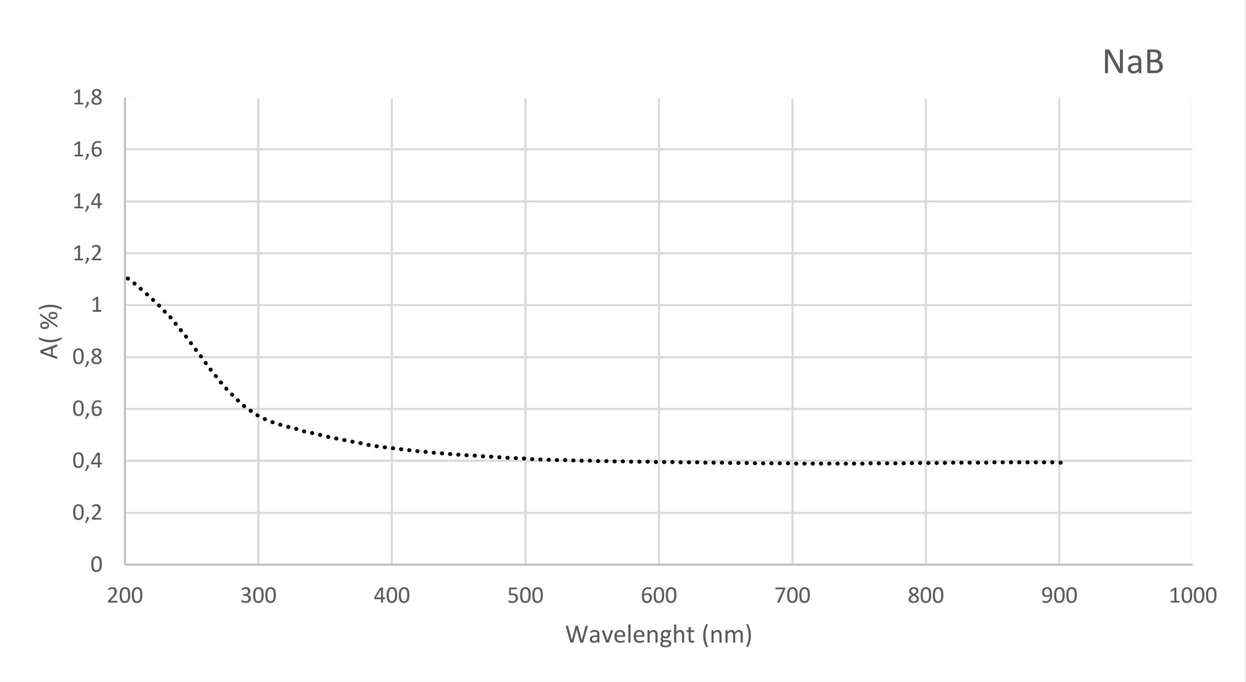

Figure 3.69: UV-vis of NaB

The absence of any typical absorption bands of metal species such as iron agree with the starting consideration to have a completely pure bentonite without any presences of iron as substitution species in the layers. Na^+ does not influence the absorption bands. (Fig. 3.69)

3.7.2 Iron species absorption bands

To identify the position of Fe^{3+}, UV–vis spectra are analysed. The possible ranges for iron species are:

- Isolated Fe^{3+} (mononuclear Fe^{3+} ions) in tetrahedral coordination
- Isolated Fe^{3+}(mononuclear Fe^{3+} ions) in octahedral coordination and small oligonuclear Fe_xO_y clusters
- Dispersed Fe_2O_3 particles.

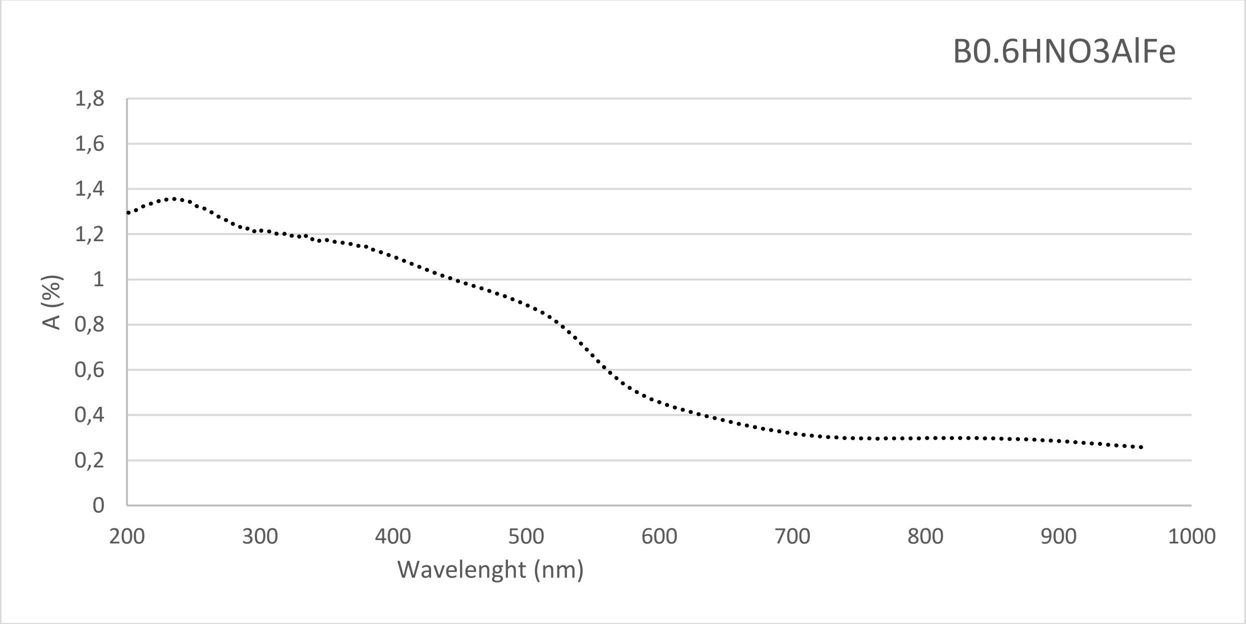

Figure 3.70: UV-vis of B0.6HNO3AlFe

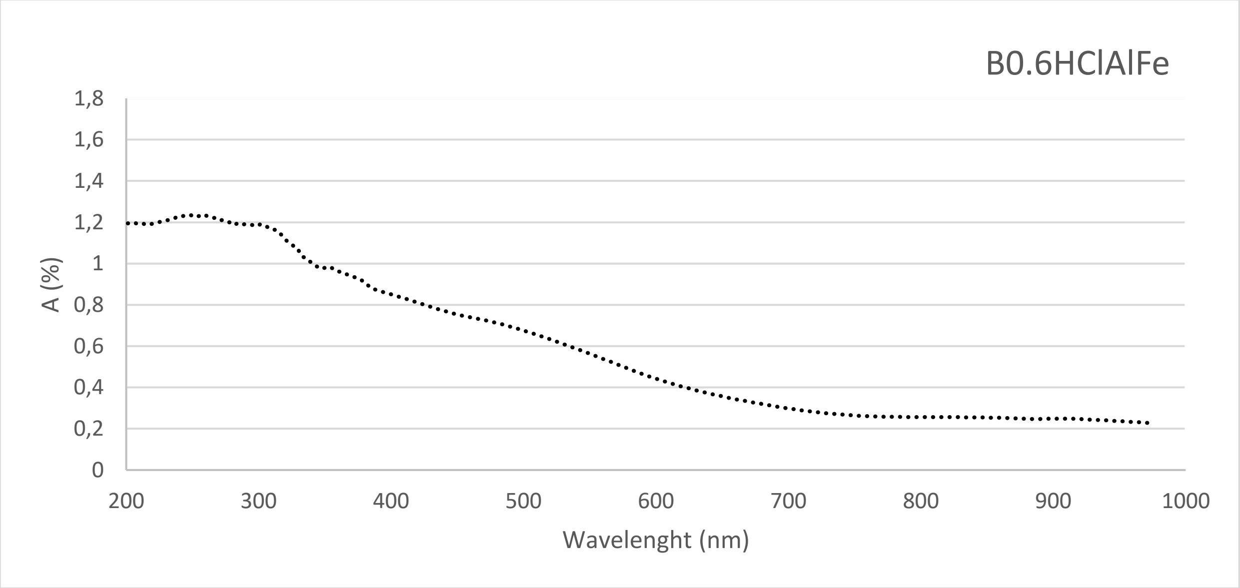

Figure 3.71: UV-vis of B0.6HClAlFe

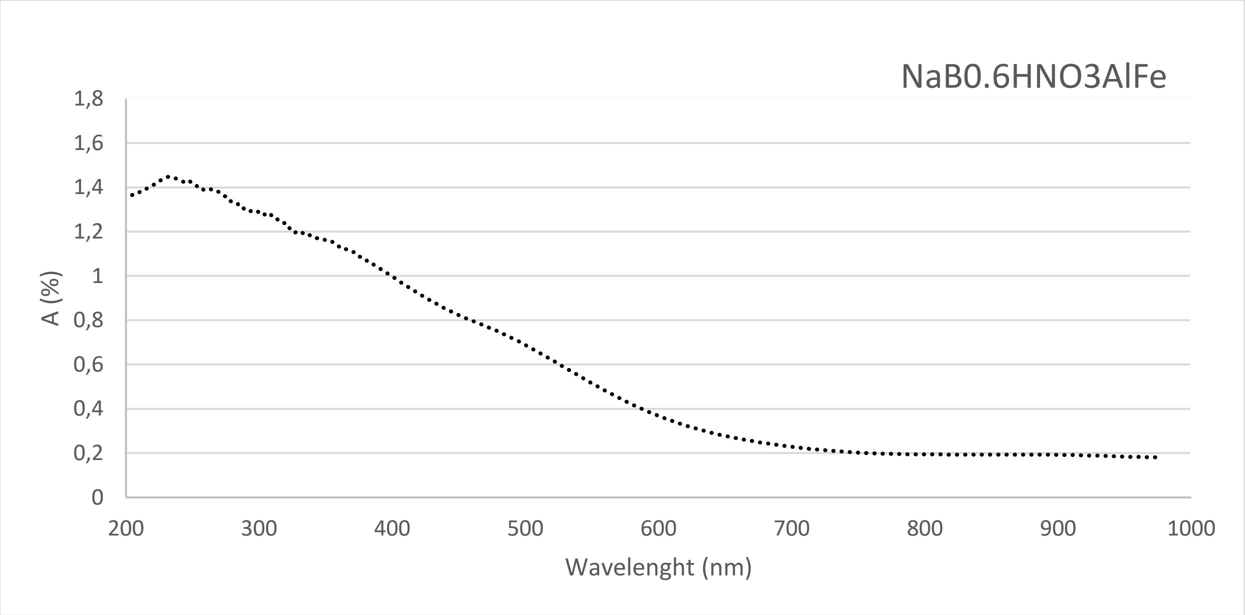

Figure 3.72: UV-vis of NaB0.6HNO3AlFe

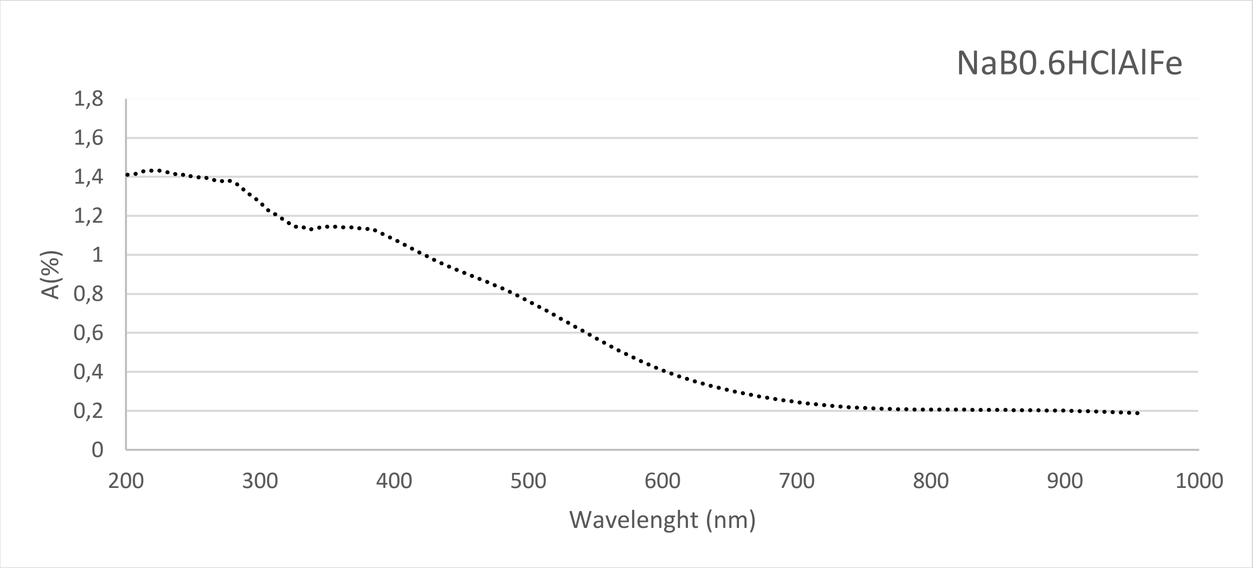

Figure 3.73:. UV-vis of NaB0.6HClAlFe

Differences from NaB (Fig. 3.69) are visible, all the four figures present an absorption in the typical bands of iron species.(Fig. 3.70, 3.71, 3.72, 3.73)

Presences of Fe^{3+} isolated ions in the range below 300 nm are present, for the samples with HCl the shape is broader than for B0.6HNO3AlFe and NaB0.6HNO3AlFe. There are not visible differences from the sample treated with pure bentonite or the samples treated with Na-Bent as in the analysis in FT-IR. B0.6HClAlFe and NaB0.6HNO3AlFe present almost the same patterns. Presence of isolated Fe^{3+} ions (200/300 nm), oligonuclear Fe_xO_y clusters (300/400 nm) and Fe_2O_3 particles are confirmed.

Differences in the pattern are visible in B0.6HNO3AlFe where in the range above 450 nm the intensity is higher than in the other samples, this sample has more Fe_2O_3 particles dispersed in the sample. Furthermore, for this sample the pillaring went wrong and the presence of Fe_2O_3 particles can block the micropores and reduce the micropore areas with negative impact in the catalytic activities.

A more intense band is also visible for NaB0.6HClAlFe indicating the presence of a bigger amount of Fe_xO_y cluster in the interlayer space or at the surface of the material. From the catalytic activity between all these four samples considering the conclusion from the analysis with x-ray and UV-vis NaB0.6HClAlFe is supposed to have the highest catalytic activities, but only with SCR-NH_3 test it can be confirmed.

In all the samples the presence of little amount of Fe_2O_3 particles is visible comparing to their total absence in the pattern of NaB. UV–vis results showed that Fe^{3+} ions are present in a bigger amount compare to other iron forms.

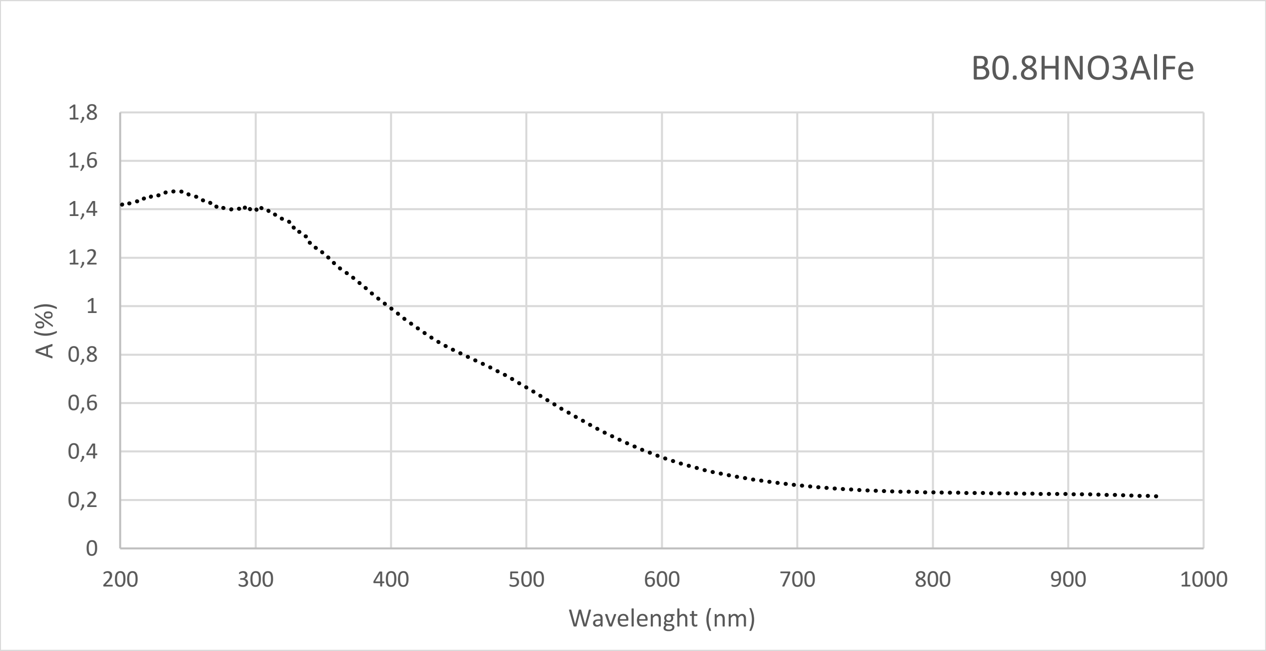

Figure 3.74: UV-vis of B0.8HNO3AlFe

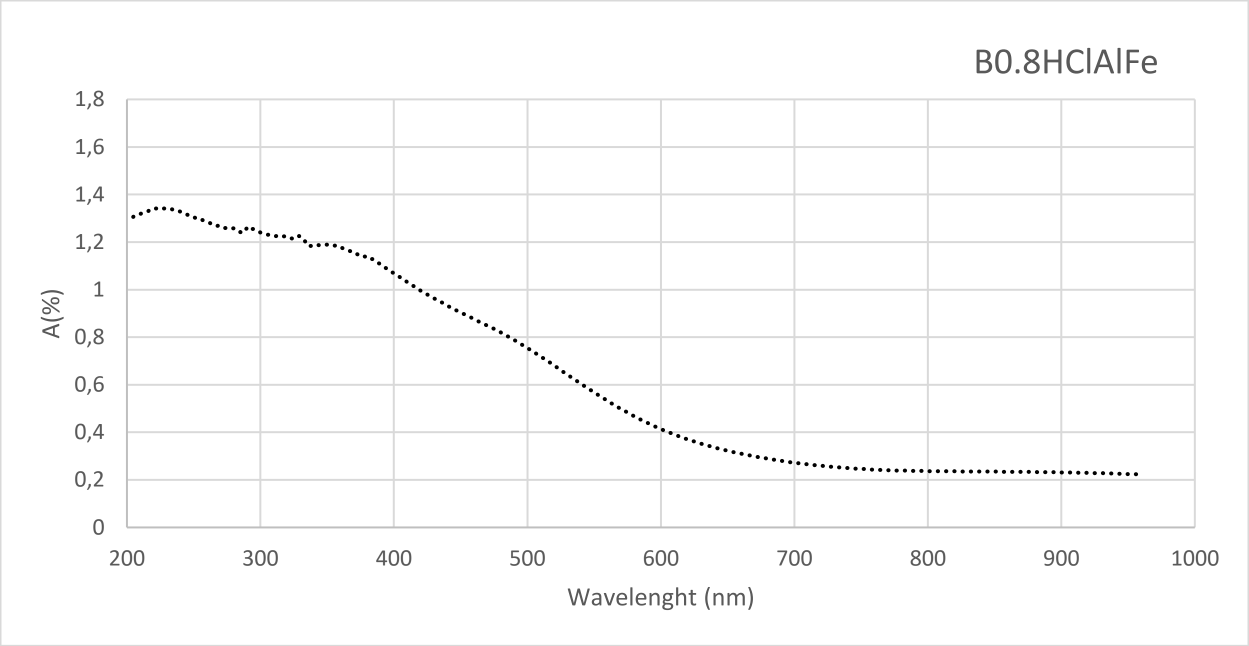

Figure 3.75: UV-vis of B0.8HClAlFe

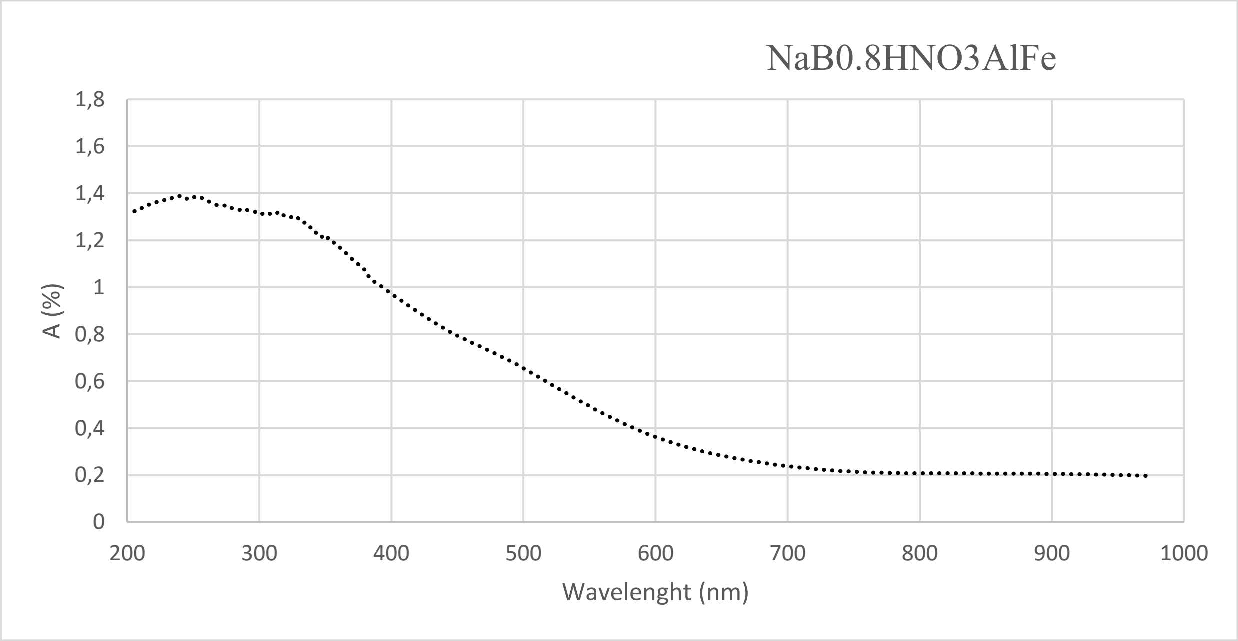

Figure 3.76: UV-vis of NaB0.8HNO3AlFe

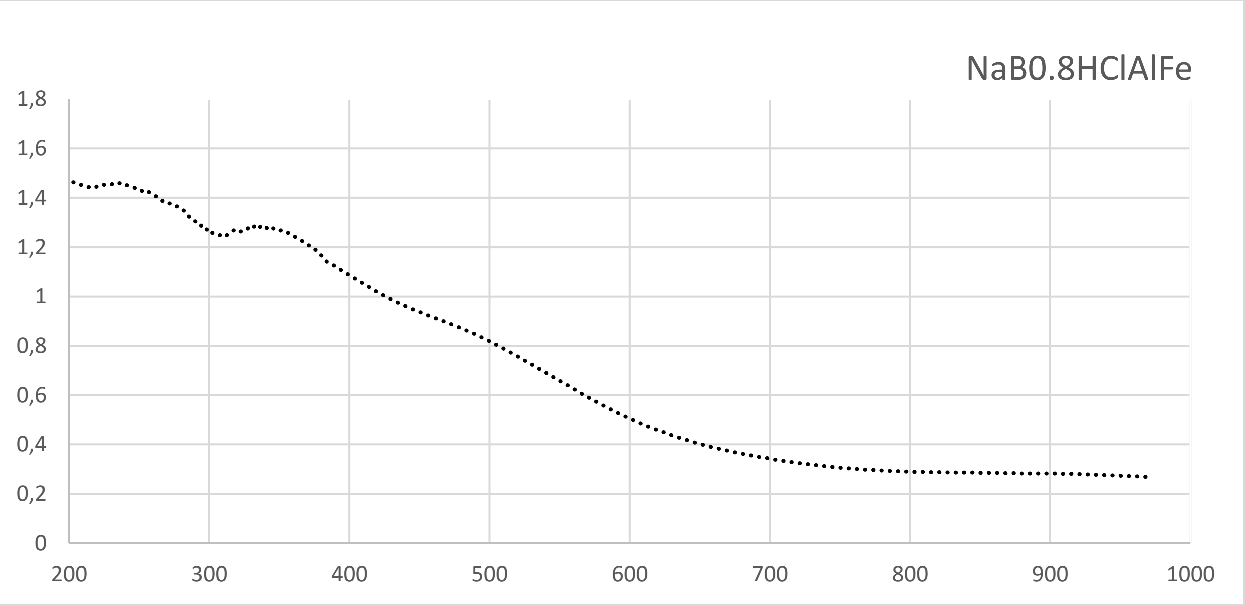

Figure 3.77: UV-vis of NaB0.8HClAlFe

Fig 3.74, 3.75, 3.76, 3.77 show the spectra of the same samples compared before but with an increase of the acid concentration during the preparation (0.6 M → 0.8 M of acid solution for HNO_3 and HCl). The patterns are the same to the ones exchanged with 0.6 M of acid solutions. There are not visible changes for NaB and B. For all the samples (B0.8HNO3AlFe, Na0.8HNO3AFe, B0.8HClAlFe, NaB0.8HClAlFe) the presence of isolated Fe^{3+} ions (200/300 nm), oligonuclear Fe_xO_y clusters (300/400 nm) and Fe_2O_3 particles are confirmed. Broader shapes for samples treated with HNO_3 and NaB0.8HCl present the highest concentration of Fe_xO_y clusters in the range 300/ 400 nm and also confirms the presence of Fe_2O_3 particles. The amount of Fe_2O_3 particles is bigger for B0.8HClAlFe.

3.7.3 Cerium species absorption bands

The presence of different metal species can change the oxidation state of iron species explained in 3.7.2.

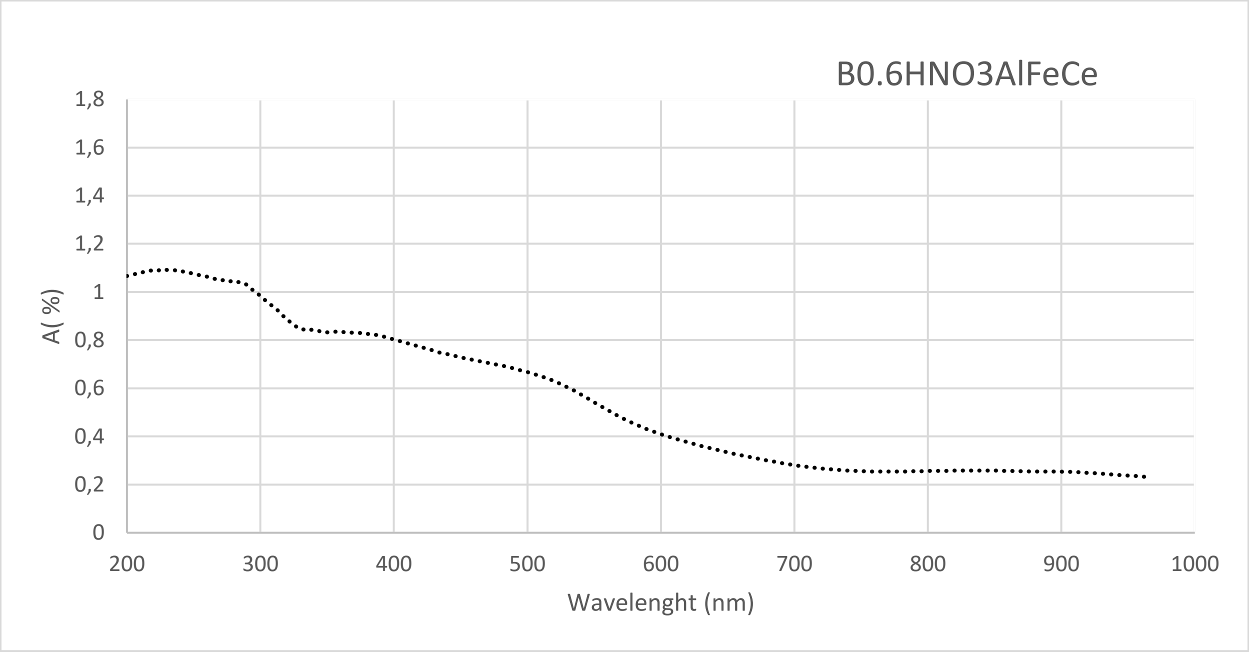

Figure 3.78:. UV-vis of B0.6HNO3AlFeCe

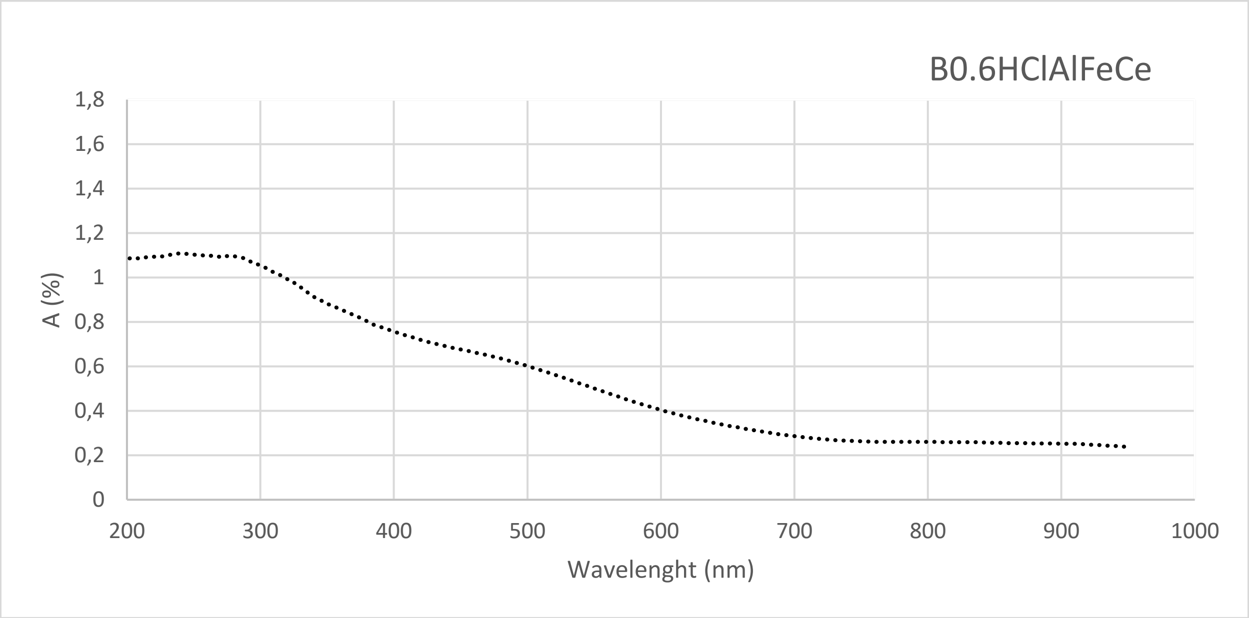

Figure 3.79: UV-vis of B0.6HClAlFeCe.

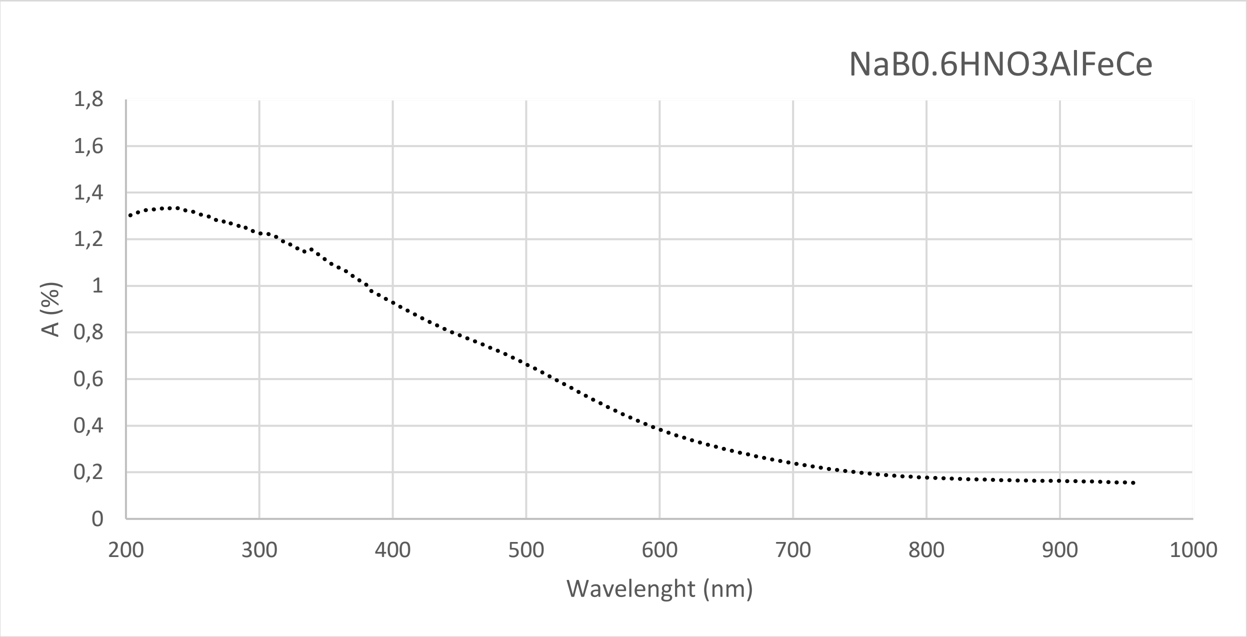

Figure 3.80: UV-vis of NaB0.6HNO3AlFeCe

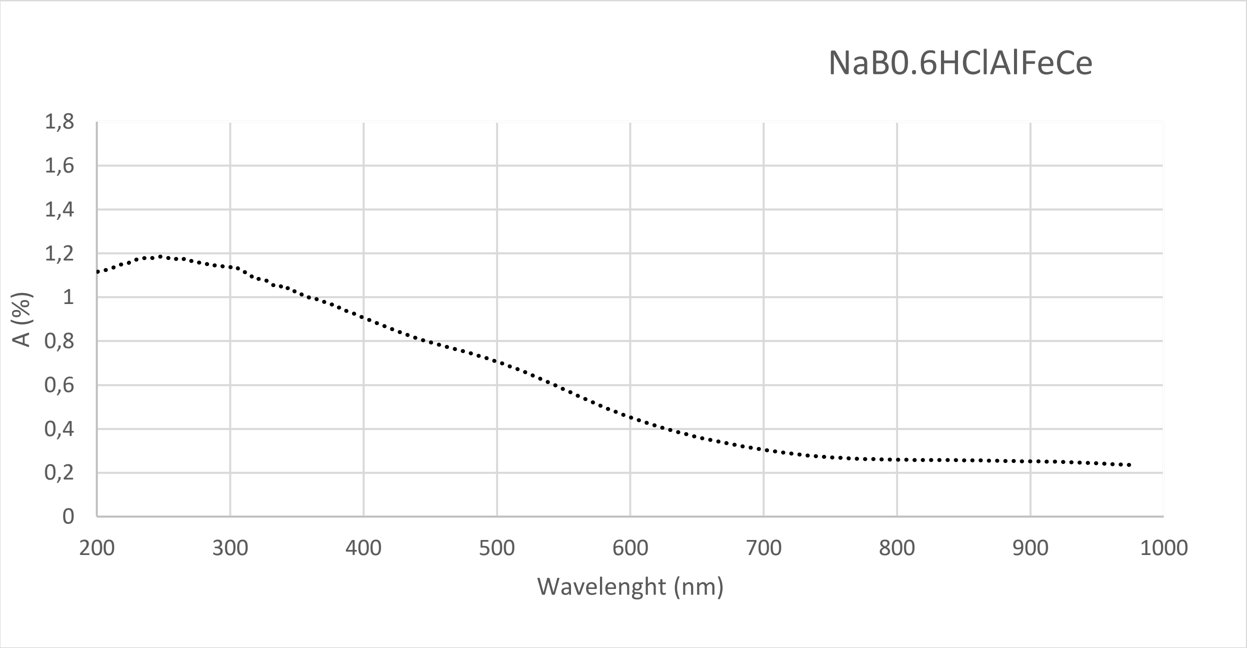

Figure 3.81: UV-vis of NaB0.6HClAlFeCe

For cerium species according to literature researches an absorption edge occurring at <375 nm can imply the presence of fine crystallite size (8.5-4.5 nm) that are not visible with x-ray. [68] Values above 375 nm shows correspond to determined crystallite sizes by XRD. From the x-ray studies for samples impregnated with cerium species in this work there is not a formation of any crystallite sizes of CeO_2. The only range that has to be consider for UV-vis for Ce is the range < 375 nm.

For all the samples B0.6HNO3AlFeCe, NaB0.6HNO3AlFeCe, B0.6HClAlFeCe, NaB0.6HClAlFeCe the introduction of cerium over the metal active phase of iron does not change the pattern too much. All the ranges in which the iron species have been identified are still visible.

The addition of cerium mainly influences the range under 375 nm, above 375 nm crystallite sizes of cerium are not confirmed as in x-ray analysis and the shape of sample impregnated only with iron has not been changed.

On the other hand, the maximum in the range from 200 nm and 375 nm have been slightly suppressed of intensity for all the samples with the addition of cerium, its influenced needs more in-depth analysis, the effect of cerium overlaps with the absorption of iron species. Absorption bands of cerium are sensitive to the environment. From literature bands close to 263 nm relate to $Ce^{3+} \leftarrow O$ charge transition and 305 nm inter band transitions. $Ce^{4+} \leftarrow O$ and inter band transitions in 300-350 nm. [69]

The same considerations are made for cobalt. Cerium and cobalt overlap and their states cannot be recognised. Further analysis can be carried out.

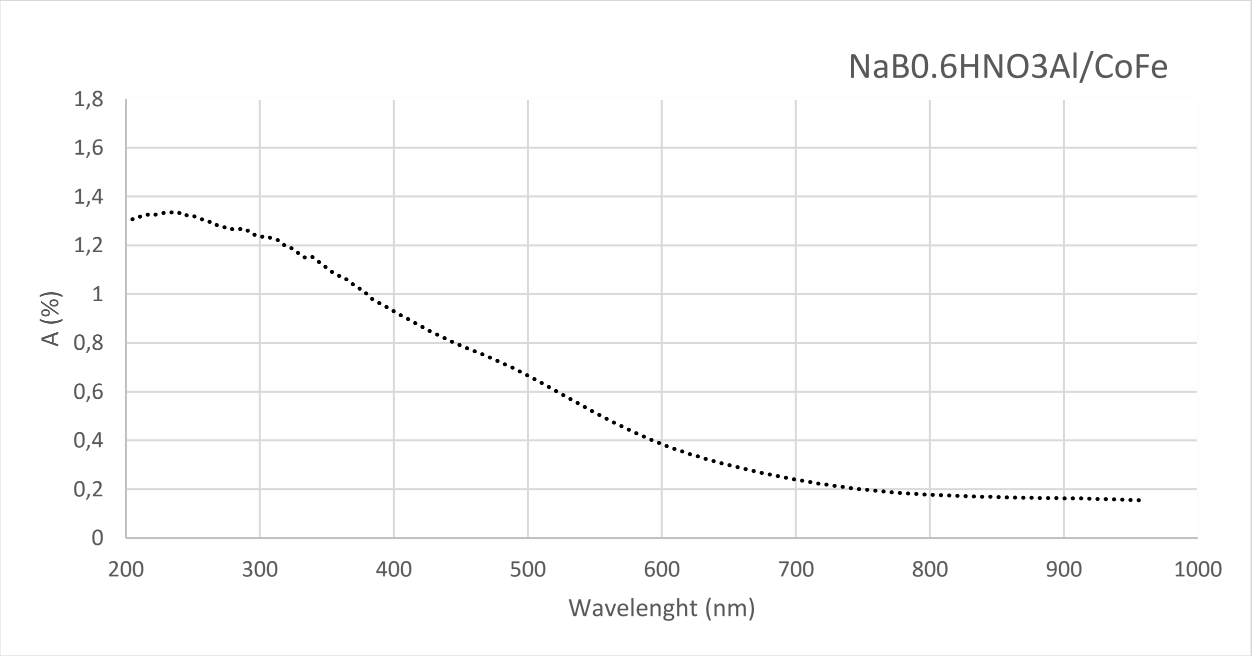

Figure 3.82: NaB0.6HNO3Al/CoFe

3.8 Thermogravimetric analysis (TG) results and discussion

High temperature thermal treatment to clay minerals gives information about the evolution of physical properties of clays. Studies have been carried out to show that some properties are correlated to thermal damage (mass, mechanical strength, porosity, permeability, chemical and mineral composition and wave velocity) [70]. Variation of mass is considered during TG analysis identifying two main regions of weight loss of water.

3.8.1 TG curves of NaB and B

TG curve of natural bentonite shows a steep weight loss in the range below 180°C and a slight decrease above 180 °C.[71]

In Fig. 3.8 TG curves of NaB and B are reported. Two well- defined weight loss regions are visible. The first below 180°C due to the loss of physiosorbed water and the dehydroxylation of coordinated and structural water above 180 °C.

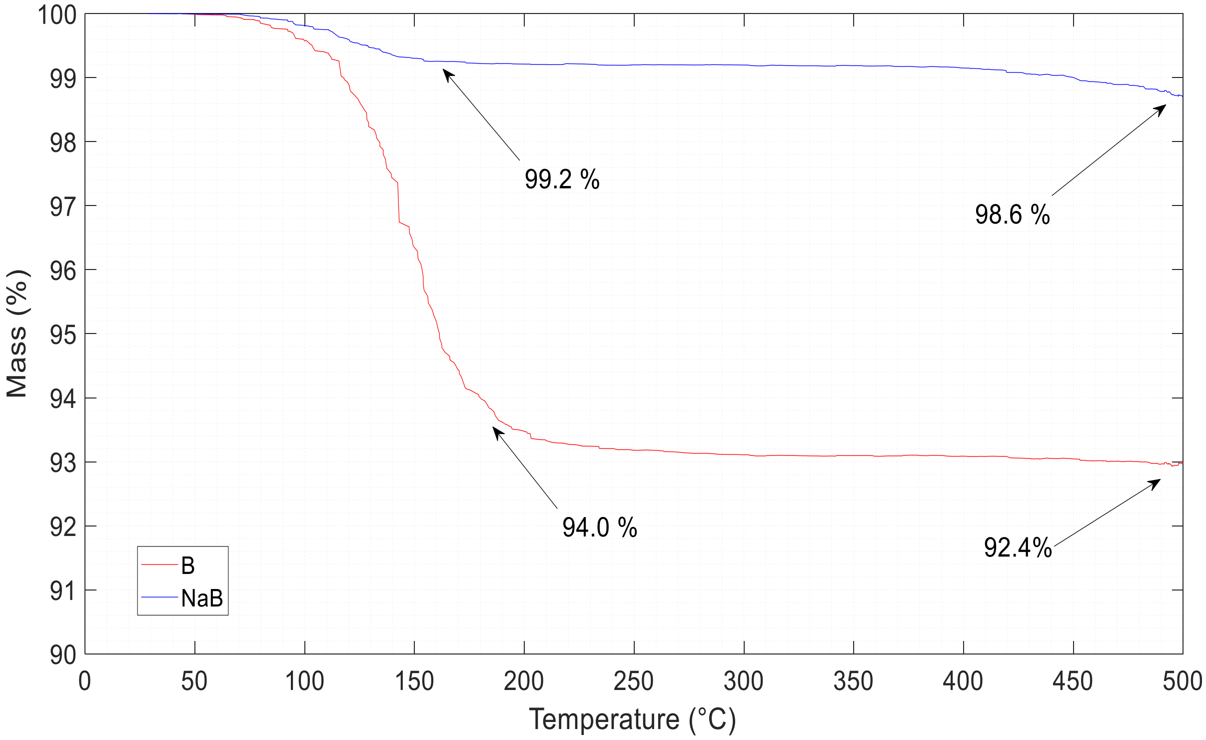

Figure 3.83: TG of NaB and B

Clays in their structure contain three kinds of water molecules [72]:

- Interlayer and physiosorbed water
- Water molecules present in the first coordination sphere of the interlayer ions
- Structural hydroxyl groups

In this work two main ranges of weight loss are identified: low temperature water loss (Δm_l (%)) for the physiosorbed water and the high temperature water loss (Δm_h (%)) for the dehydration and dehydroxylation of clay layers.

TG curves of NaB and B show the high stability of bentonites during the thermal treatment, the percentage of loss weight is very low mainly at higher temperatures. For pure bentonite Δm_l (%) is 6 % while for NaB is 0.8 %. This difference may be due considering the interlayer and physiosorbed water that is removed during the NaCl exchange step treatment.

Tab 3.5 reports the lists of samples that have been analysed by TG and the distinction of the main two areas of weight loss of water. Percentage of weight loss are very low for all the samples and there are not such visible differences. Otherwise it is possible to give some explanations comparing the samples.

Table 3.5: Lists of samples analysed with TG

Sample	Δm_l (%)	Δm_h (%)
NaB	0.8	0.6
B	6	1.6
B0.6HNO3AlFe	1.8	1.6
NaB0.6HNO3AlFe	1.5	0.9
B0.8HNO3AlFe	1.2	0.9
NaB0.8HNO3AlFe	1.2	0.6
B0.8HClAlFe	2.2	2.5
NaB0.8HClAlFe	1	0.5
B0.6HNO3Al/CoFe	1	0.8
B0.6HNO3AlFeCe	1.6	1.4
NaB0.6HNO3Al/CoFe	0.9	0.5
NaB0.6HClAlFe	1.4	0.8
NaB0.6HClAl/CoFe	1.3	0.5

3.8.2 Influence of acid treatments

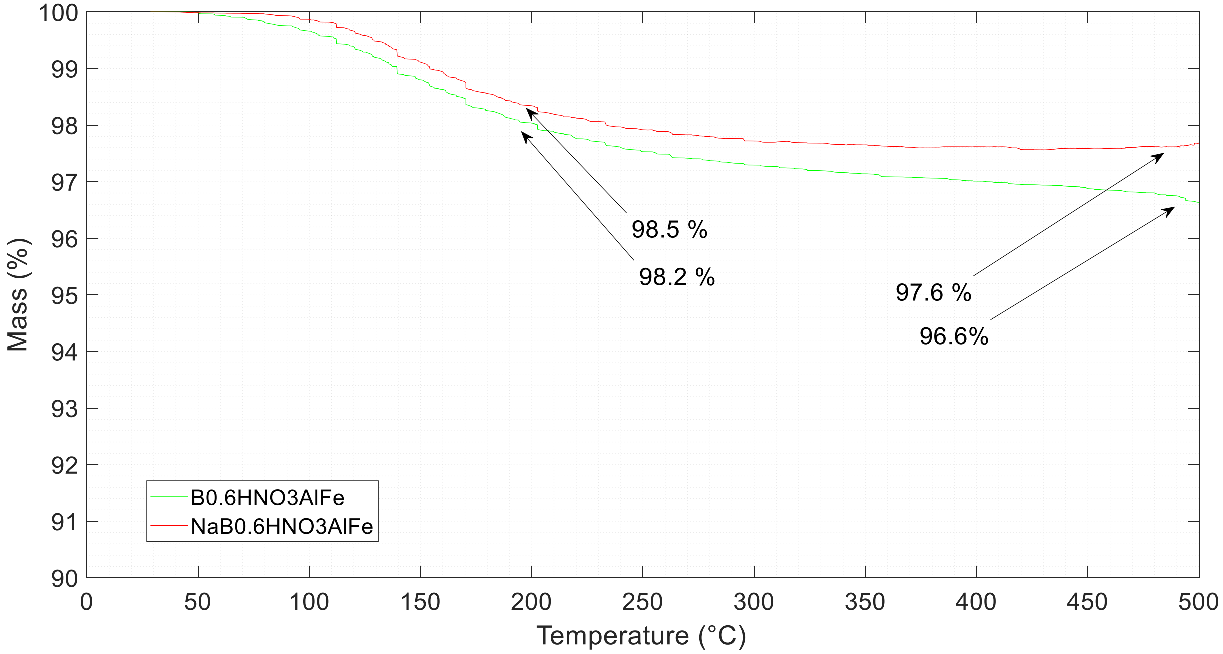

Figure 3.84: TG of B0.6HNO3AlFe and NaB0.6HNO3AlFe

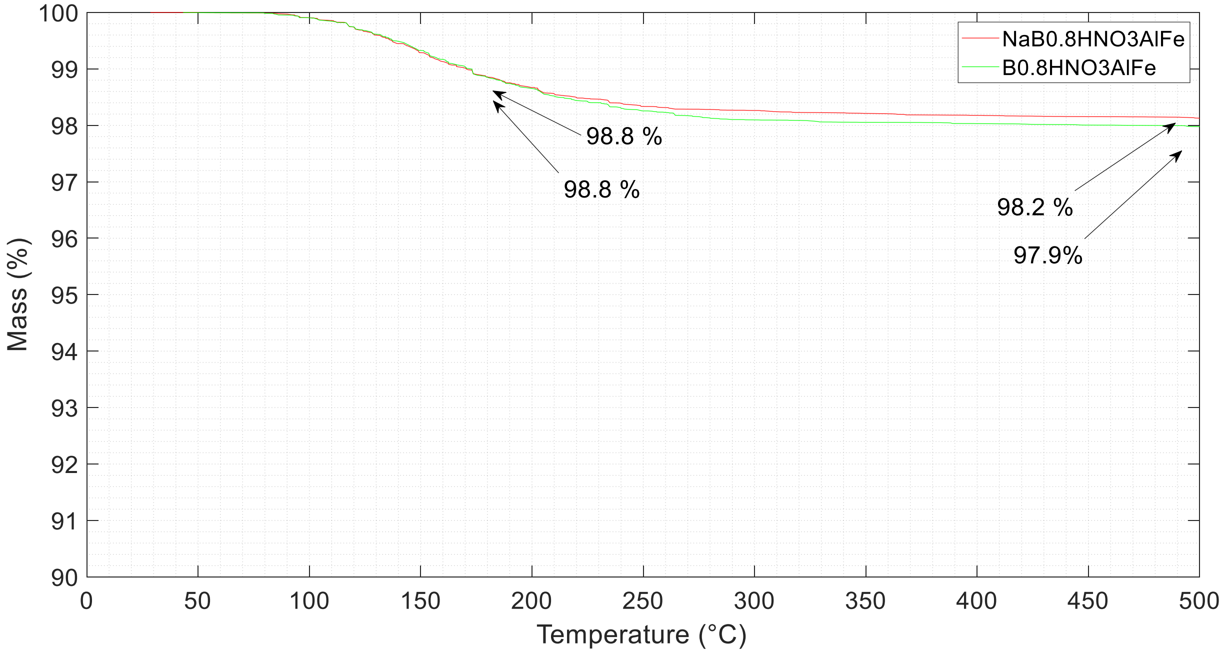

Figure 3.85: TG of B0.8HNO3AlFe and NaB0.8HNO3AlFe

Fig 3.84 and Fig 3.85 show the curves of B0.6HNO3AlFe, NaB0.6HNO3AlFe, B0.8HNO3AlFe and NaB0.8HNO3AlFe. Increasing the acid concentration of the treatment result with a decrease in percentage loss at higher temperature. This is correlated to the octahedral Al ions removal with the concurrent removal of structural hydroxyl groups removal. Δm_h (%) for B0.6HNO3AlFe is 1.6% and for B0.8HNO3AlFe is 0.9%, for NaB0.6HNO3AlFe is 0.9 % and for NaB0.8HNO3AlFe is 0.9 %. The area of the interlayer water peak remains essentially unchanged with the increase of the severity of treatment.

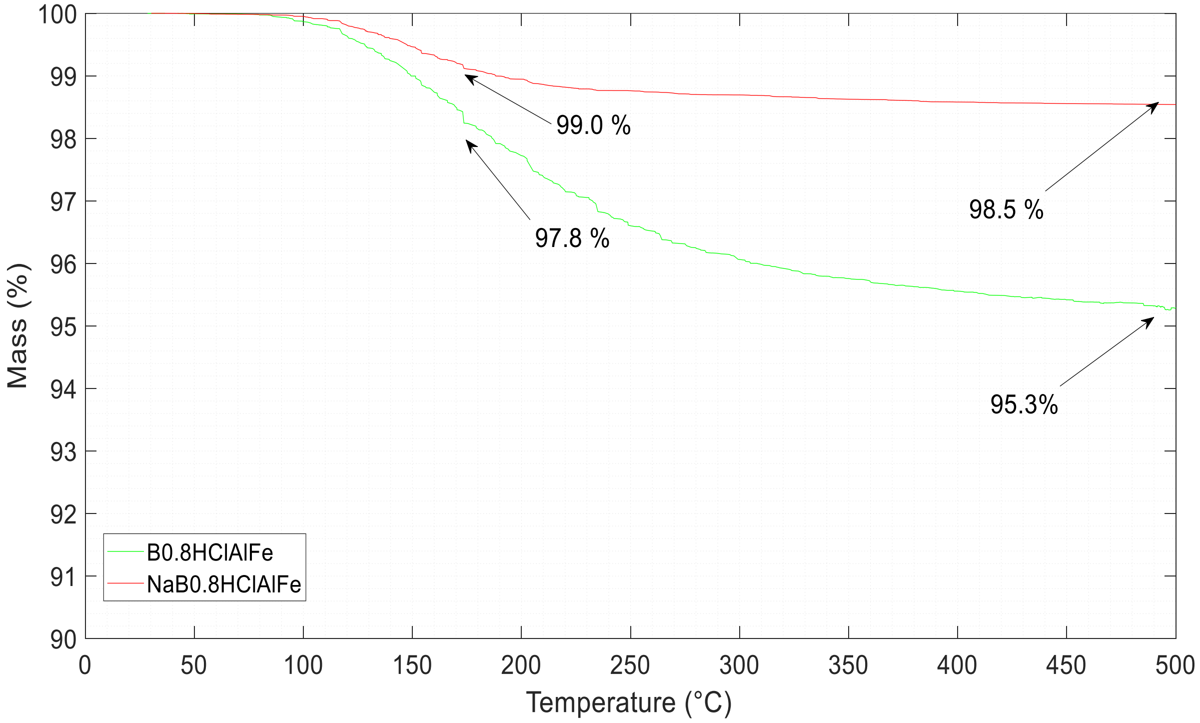

Figure 3.86: TG of B0.6HClAlFe and NaB0.6HClAlFe

Fig. 3.86 shows TG curves of B0.6HClAlFe and NaB0.6HClAlFe. For NaB0.6HClAlFe there are not differences from the corresponding sample treated with 0.6M of HNO_3. While in the range above 180°C, B0.6HClAlFe is less stable to thermal treatment. The stability of the sample structure is lower compared to N0.6HNO3AlFe. From the list of samples reported in Tab 3.5 B0.6HClAlFe has the higher value of Δm_h (2.5 %).

3.8.3 Influence of the introduction of metal species

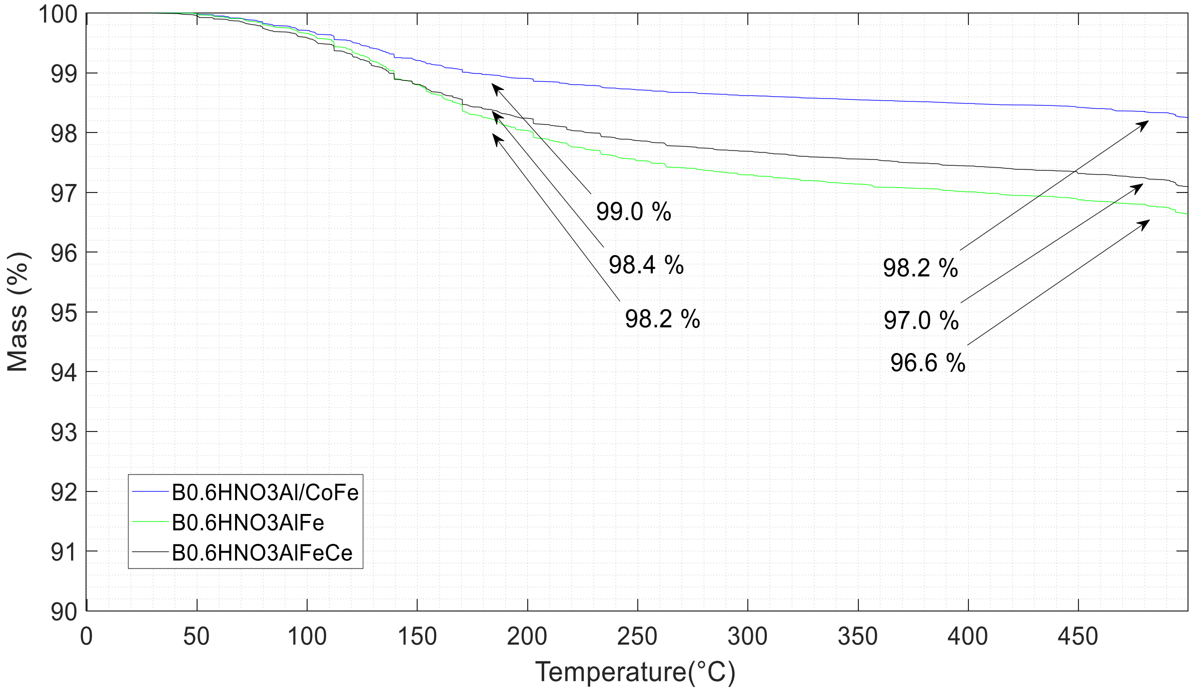

Figure 3.87: TG of B0.6HNO3Al/CoFe, B0.6HNO3AlFe, B0.6HNO3AlFeCe

Fig 3.87 shows the pattern of B0.6HNO3Al/CoFe, B0.6HNO3AlFe and B0.6HNO3AlFeCe. The curves present almost the same percentage of weight loss. For B0.6HNO3AlFe and B0.6HNO3AlFeCe, Δm_l (%) are respectively 1.8% and 1.6 % and Δm_h (%) are 1.6% and 1.4 %. There are any differences in both the ranges between the sample only impregnated with iron species and the sample impregnated with iron and cerium species. The addition of cerium did not change the thermal stability of the sample.

The addition of iron and cerium with the possible formation of iron or cerium hydroxyl groups can interfere with the hydroxyl groups present in the structure of the clay. However, all the samples present high stability of the structure very low percentages of weight loss have been calculated. No significant changes in the structure occur for all the preparation steps followed in this work. The presence of cobalt is investigated in the following figures.

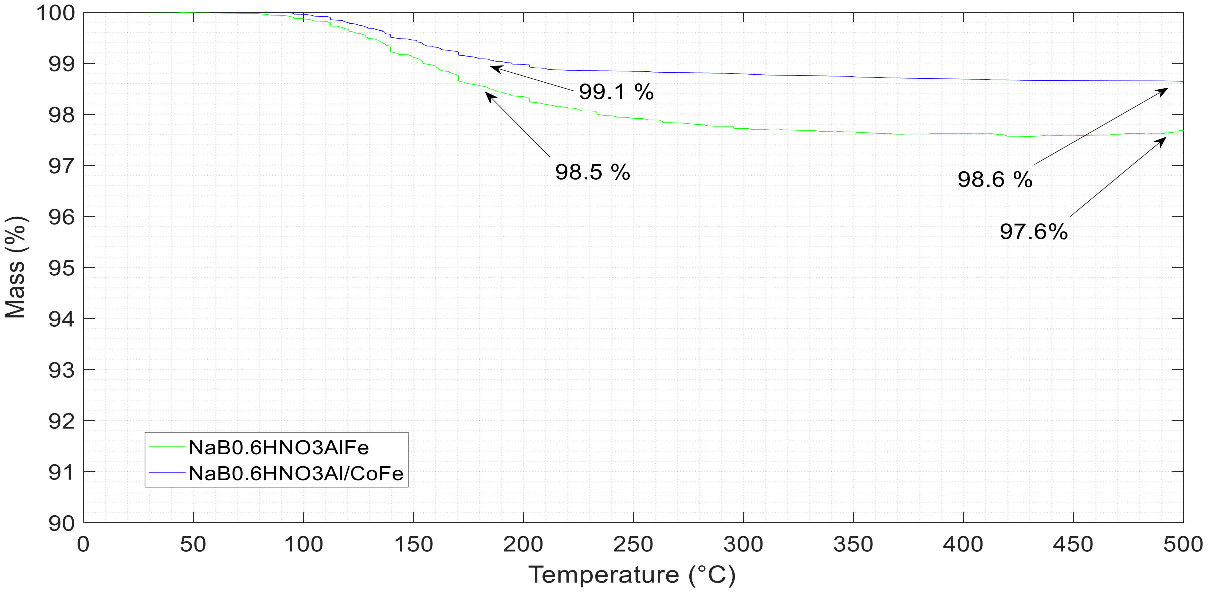

Figure 3.88: TG of NaB0.6HNO3AlFe and NaB0.6HNO3Al/CoFe

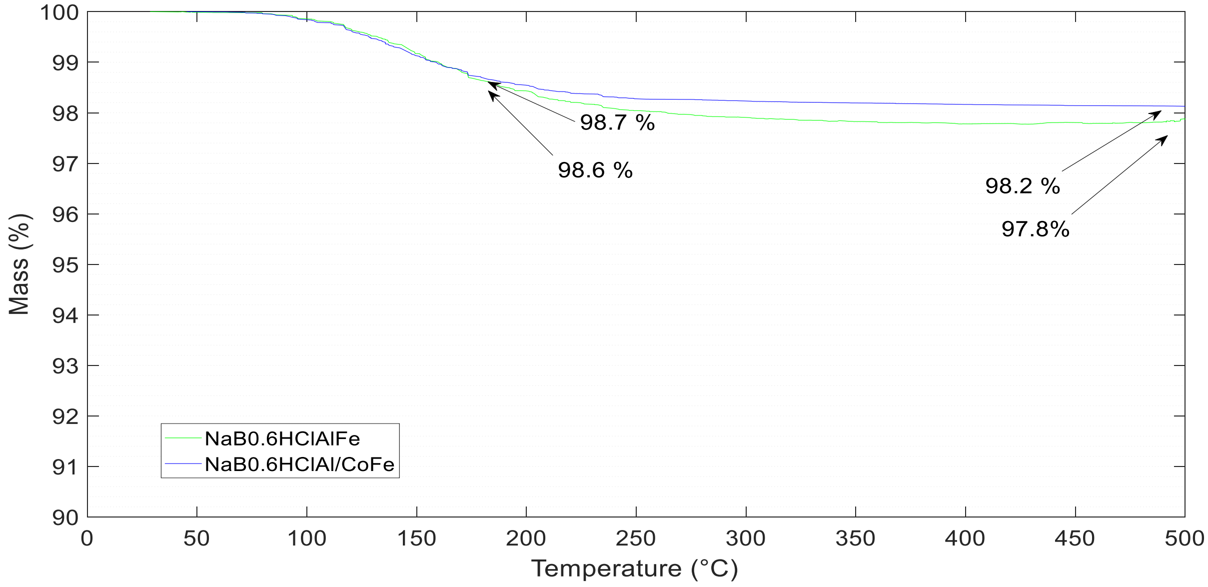

Figure 3.89: TG of NaB0.6HClAlFe and NaB0.6HClAl/CoFe

A consequence of the introduction of mixed pillared oxides is the improvement of the thermal stability of the samples. This is confirmed from the results of TG visible in Fig 3.88 and in Fig. 3.89. Δm_h (%) for NaB0.6HNO3Al/CoFe and NaB0.6HClAl/CoFe is 0.5%. Both the samples have a very stable structure with the increase of temperature.

Chapter 4 – Catalysts performances

4.1 Selective catalytic reduction of NO with ammonia (SCR-NH_3)

Different ways for testing the efficiency of the removal of NO_x can be used. In this work the catalytic test was followed in a fixed-bed flow microreactor system under atmospheric pressure. The formula for the NO conversion is:

$$\%\, NO_{conversion} = \frac{NO_{inlet} - NO_{outlet}}{NO_{inlet}} \cdot 100$$

Catalytic performances are studied for all the catalysts prepared with the presence of the active phase after impregnation and compared with the supports: samples after pillaring and acid treatment without the active phase.

For the catalytic test 200 mg of each sample are used, NO initial concentration= 800 ppm, O_2= 3,5 vol.%, Balance He and total flow of the gas mixture =100 $cm^3 \cdot min^{-1}$

4.2 Selective catalytic reduction of NO with ammonia (SCR-NH_3) results and discussion

4.2.1 Catalytic performances of NaB and B

The first step of the catalytic test is to consider if pure bentonite or bentonite treated with NaCl (1 M) present any catalytic activities. Results are reported in Fig. 4.1 and Tab 4.1.

Table 4.1: NO Conversion (%) of B and NaB

Temperature (°C)	**NO Conversion (%)**	
	B	Na-B
150	4	4
200	4	4
250	5	5
300	5	5
350	6	7
400	7	7
450	4	4

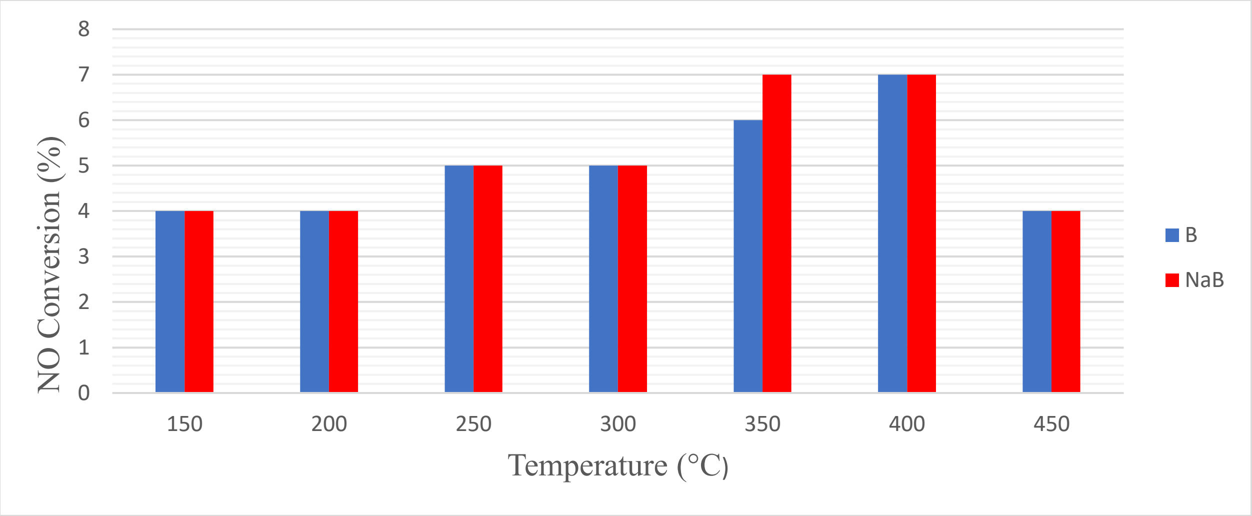

Figure 4.1: NO Conversion (%) of B and NaB

NaB and B do not present any catalytic activities in all the range of temperatures. They present very low values of NO conversions and they cannot be considered as catalysts themselves. Values of NO conversion in Tab. 4.1 are reported within experimental errors related to the analysers (± 3%). For this reason, there are any distinctions between the performances of NaB and B in all the range. The treatment of pure bentonite with the solution of NaCl (1 M) did not increase catalytic performances.

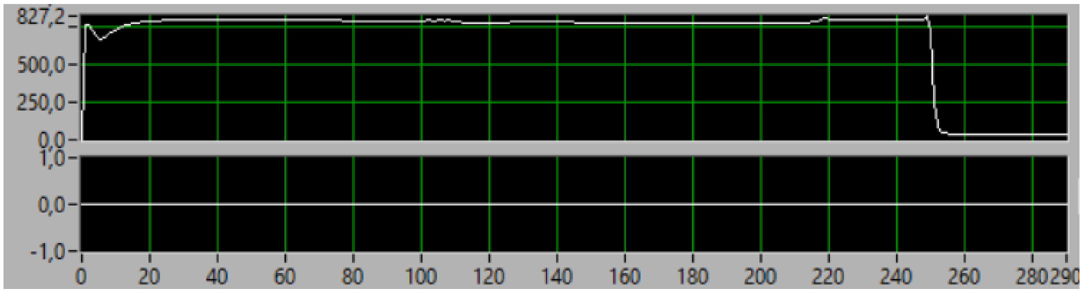

Figure 4.2 NO flow in ppm for NaB

4.2.2 Catalytic performances of modified B0.6HNO$_3$

In this subsection a comparison between B0.6HNO3AlFe, B0.6HNO3AlFeCe and B0.6HNO3Al/CoFe is investigated. The aim is to compare pure bentonite treated with the same concentration of HNO$_3$ (0.6 M) pillared with aluminium or aluminium and cobalt and impregnated with iron species or iron and cerium species. The results are reported in Fig. 4.3 and Tab 4.2. It might be remembered the addition of experimental errors (± 3%).

Table 4.2: NO Conversion (%) of B0.6HNO3AlFe, B0.6HNO3AlFeCe and B0.6HNO3Al/CoFe

Temperature (°C)	**NO Conversion (%)**		
	B0.6HNO3AlFe	B0.6HNO3AlFeCe	B0.6HNO3Al/CoFe
150	11	10	8
200	16	14	11
250	26	39	20
300	38	67	43
350	52	82	70
400	45	76	78
450	28	60	60

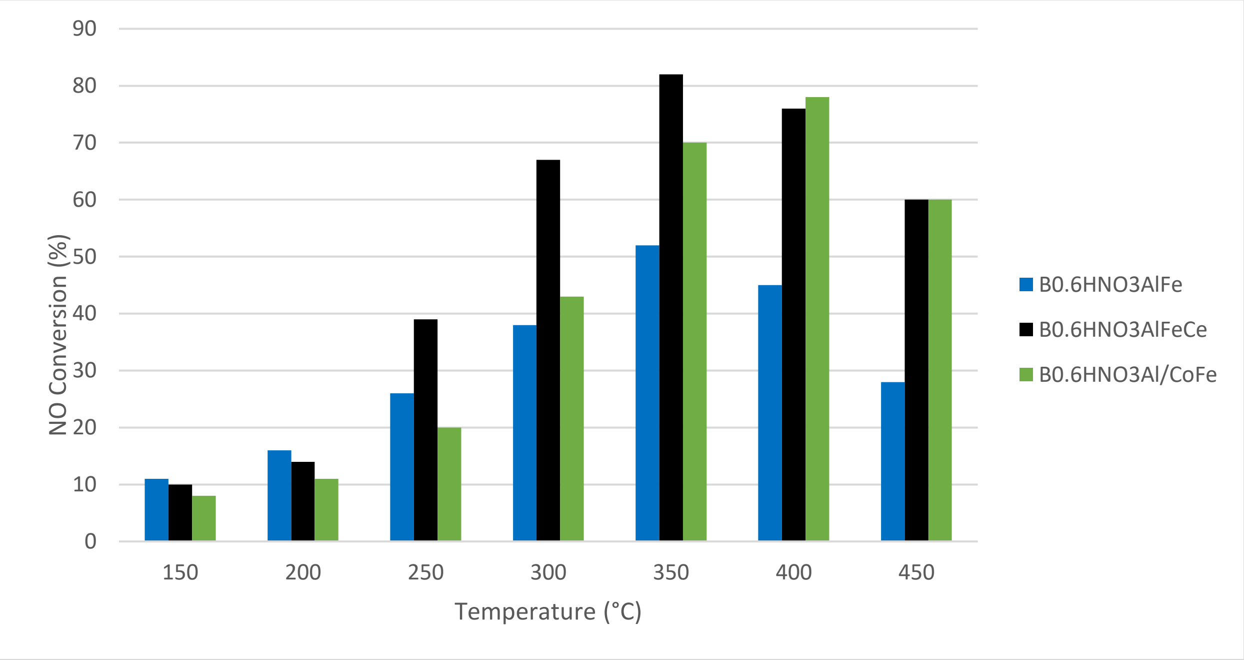

Figure 4.3: NO Conversion (%) of B0.6HNO3AlFe, B0.6HNO3AlFeCe and B0.6HNO3Al/CoFe

Catalytic activities of B0.6HNO3AlFe are lower than B0.6HNO3AlFeCe and B0.6HNO3Al/CoFe in all the window of temperatures. Different trend for lower temperatures (around 150 °C) where there are not differences in the activity for all the three samples considering the experimental errors (± 3%). The range with the maximum activity is around 350 °C, even if for B0.6HNO3AlFe the maximum value is only 52 % of NO conversion. Low activities can be related to the failure of pillaring discovered with x-ray analysis. *001* reflection remained in the same position and the activation with the first modification was not successful. Otherwise, the increase of activity with temperature is caused by the presence of the active phase (iron species) identified also by UV-Vis analysis. Impregnation with cerium species increase the activities of B0.6HNO3AlFe in all the ranges, from 52% to 82 % of NO conversion. B0.6HNO3Al/CoFe exhibited quite good activities comparable to the ones of B0.6HNO3AlFe at lower temperatures and to B0.6HNO3AlFeCe at higher temperature. All the samples in the range of 450 °C decrease their catalytic activities, possible reason is due to the NH_3 oxidation (unwanted reaction).

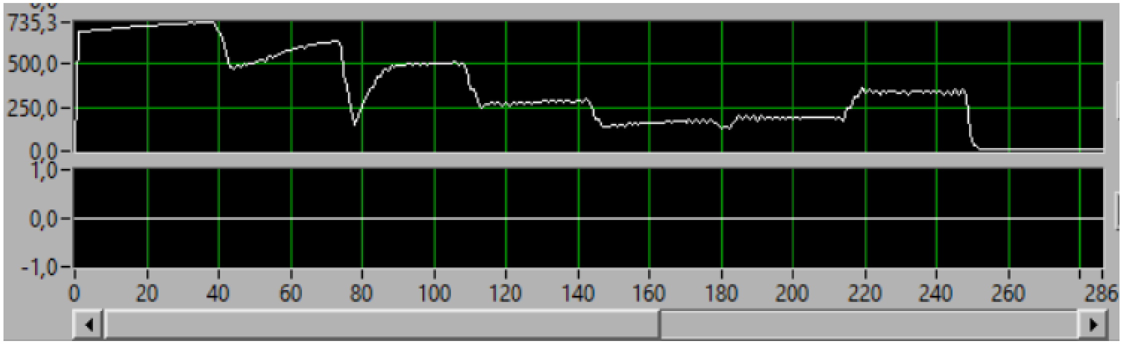

Figure 4.4: NO flow for B0.6HNO3AlFeCe

4.2.3 Catalytic performances of modified NaB0.6HNO$_3$

In this subsection a comparison between NaB0.6HNO3AlFe, NaB0.6HNO3AlFeCe and NaB0.6HNO3Al/CoFe is investigated. The aim is to compare Na-Bentonite treated with the same concentration of HNO_3 (0.6 M) pillared with aluminium or aluminium and cobalt and impregnated with iron species or iron and cerium species. The results are reported in Fig 4.5 and Tab 4.3. It might be remembered the addition of experimental errors (± 3%). Each result is compared to each reported in Tab 4.2 (numbers in brackets). The aim is to show if there are any differences between NaB and B.

Table 4.3: NO Conversion (%) of NaB0.6HNO3AlFe, NaB0.6HNO3AlFeCe and NaB0.6HNO3Al/CoFe

Temperature (°C)	**NO Conversion (%)**		
	NaB0.6HNO3AlFe	NaB0.6HNO3AlFeCe	NaB0.6HNO3Al/CoFe
150	6 (11)	8 (10)	10 (8)
200	10 (16)	15 (14)	18 (11)
250	23 (26)	40 (39)	27 (20)
300	43 (38)	79 (67)	57 (43)
350	66 (52)	93 (82)	82 (70)
400	76 (45)	86 (76)	86 (78)
450	57 (28)	68 (60)	64 (60)

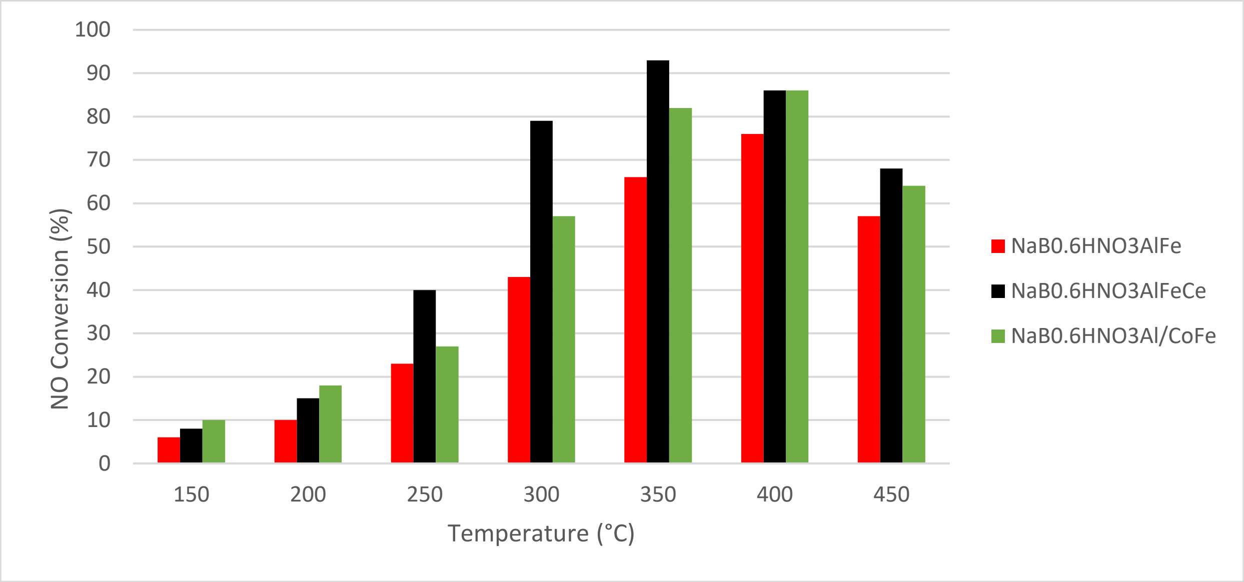

Figure 4.5: NO Conversion (%) of NaB0.6HNO3AlFe, NaB0.6HNO3AlFeCe and NaB0.6HNO3Al/CoFe

Same conclusions done in 4.2.1 can be reported also for NaB0.6HNO3AlFe, NaB0.6HNO3AlFeCe and NaB0.6HNO3Al/CoFe. The trends are similar for all the three samples at lower temperatures (150 °C and 200 °C). No evident differences in NO conversion. The sample with ceria presents the best catalytic activities in the range 250/ 450 °C with the highest NO conversion at 350 °C (93%). This value is higher than the conversion of B0.6HNO3AlFe at the same temperature. Cobalt increases the catalytic activity compared to NaB0.6HNO3AlFe and gives the same catalytic activity of sample impregnated with ceria at 400°C with 86% of NO conversion. NaB0.6HNO3AlFe has higher activity compare to the sample with pure bentonite mostly at higher temperature. The pillaring for NaB0.6HNO3AlFe succeeded. The treatment with NaCl (1 M) was efficient and all the trends of NO conversions for samples with NaB are higher than the ones with pure bentonite.

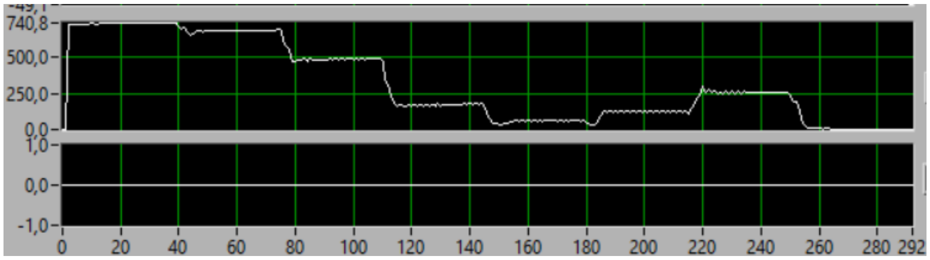

Figure 4.6: NO flow of NaB0.6HNO3AlFeCe

4.2.4 Catalytic performances of modified B0.6HCl

In this subsection a comparison between B0.6HClAlFe, B0.6HClAlFeCe and B0.6HClAl/CoFe is investigated. The aim is to compare pure bentonite treated with the same concentration of HCl (0.6

M) pillared with aluminium or aluminium and cobalt and impregnated with iron species or iron and cerium species. The results are reported in Fig 4.7 and Tab 4.4. It might be remembered the addition of experimental errors (± 3%).

Table 4.4: NO Conversion (%) of B0.6HClAlFe, B0.6HClAlFeCe and B0.6HClAl/CoFe

Temperature (°C)	**NO Conversion (%)**		
	B0.6HClAlFe	B0.6HClAlFeCe	B0.6HClAl/CoFe
150	4	6	4
200	10	15	15
250	19	43	19
300	40	74	40
350	63	86	66
400	72	81	73
450	60	64	61

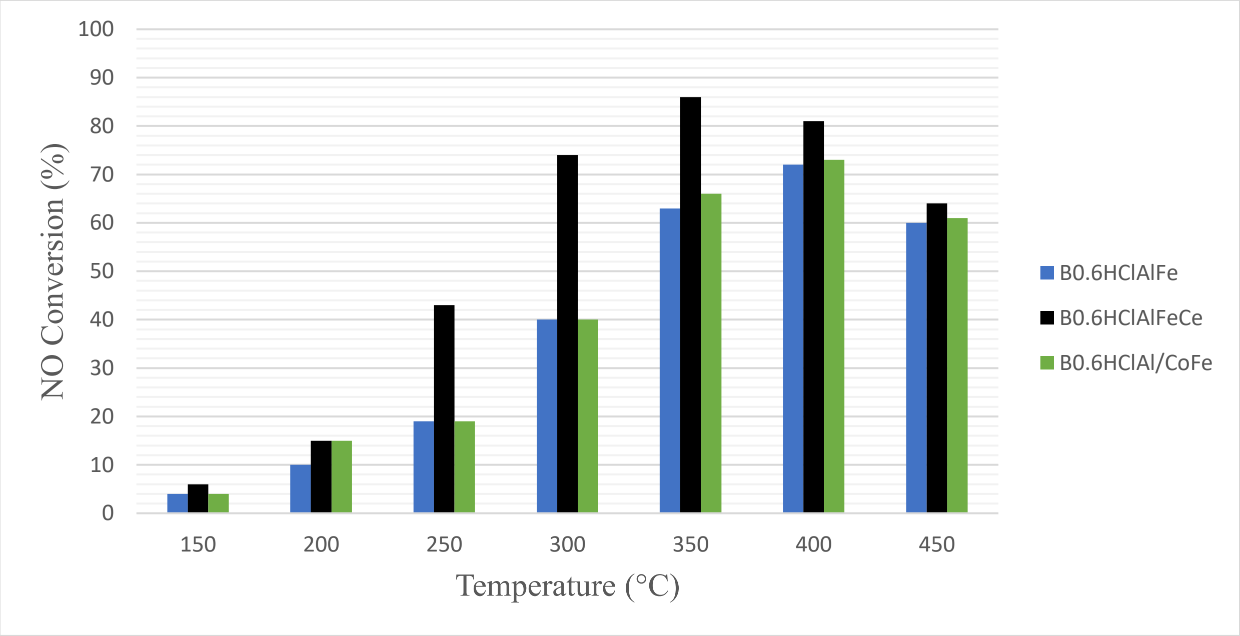

Figure 4.7: NO Conversion (%) of B0.6HClAlFe, B0.6HClAlFeCe and B0.6HClAl/CoFe

Same conclusions done in 4.2.1. and 4.2.2 can be reported also for B0.6HClAlFe, B0.6HClAlFeCe and B0.6HClAl/CoFe. The trends are similar for all the three samples at lower temperatures (150 °C and 200 °C). No evident differences in NO conversion considering also experimental errors. Pillaring of B0.6HClAlFe was successfully confirmed by x-ray. The catalytic activity of this sample has a maximum of 86% at 350°C. It is higher than B0.6HNO3AlFe in which the pillaring failed. Pillaring of B0.6HClAl/CoFe was not such efficient as the pillaring of B0.6HNO3Al/CoFe.

The presence of cobalt does not increase too much the activity considering experimental errors (± 3%). At 350 °C, 66% for B0.6HClAl/CoFe and 63% for B0.6HClAlFe. The presence of cerium increases the activities from 250°C compared to the other two samples without ceria. In the range at 300 °C, NO conversion of B0.6HClAlFeCe is 74 % almost twice that of the conversion of B0.6HClAl/CoFe and B0.6HClAlFe at the same temperature. The decrease of the catalytic activity at 450°C is due to the presence of NH_3 oxidation for the unwanted products.

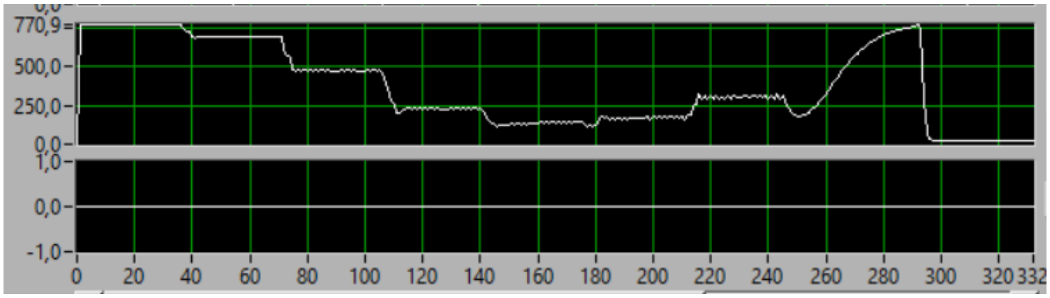

Figure 4.8: NO flow of B0.6HClAlFeCe

4.2.5 Catalytic performances of modified NaB0.6HCl

In this subsection a comparison between NaB0.6HClAlFe, NaB0.6HClAlFeCe and NaB0.6HClAl/CoFe is investigated. The aim is to compare Na-Bentonite treated with the same concentration of HNO_3 (0.6 M) pillared with aluminium or aluminium and cobalt and impregnated with iron species or iron and cerium species. The results are reported in Fig. 4.9 and Tab 4.5. It might be remembered the addition of experimental errors (± 3%). Each result is compared to each reported in Tab. 4.4 (numbers in brackets). The aim is to show if there are any differences between NaB and B.

Table 4.5: NO Conversion (%) of NaB0.6HClAlFe, NaB0.6HClAlFeCe and NaB0.6HClAl/CoFe

Temperature (°C)	**NO Conversion (%)**		
	NaB0.6HClAlFe	NaB0.6HClAlFeCe	Na0.6BHClAl/CoFe
150	5 (4)	6 (6)	9 (4)
200	9 (10)	15 (15)	11 (15)
250	24 (19)	39 (43)	28(19)
300	51 (40)	71 (74)	55(40)
350	75 (63)	89 (86)	78(66)
400	80 (72)	84 (81)	84(73)
450	59 (60)	63 (64)	52(61)

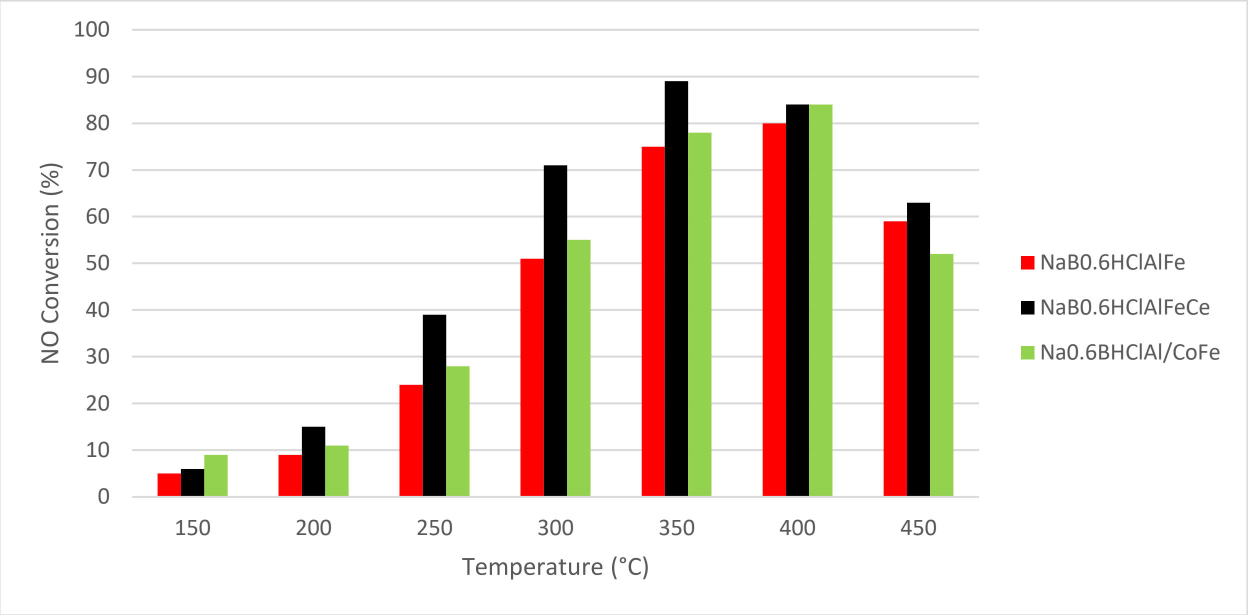

Figure 4.9: NO Conversion (%) of NaB0.6HClAlFe, NaB0.6HClAlFeCe and NaB0.6HClAl/CoFe

Same conclusions for the results of samples treated with HNO_3 are done for samples treated with HCl. For treatments with HNO_3 the samples with NaB presented higher catalytic activities at higher temperatures. In this case the increase of NO removal is not so evidenced. Only small percentages relate to an increase with NaB compare to B (numbers in brackets). Best results are visible for BNa0.6HClAlFeCe with a maximum of 89% of NO conversion at 350 °C. The ceria did not increase too much the activities as it was explained in 6.5.3. Activities of the sample pillared with cobalt presents only a bit higher activity than the sample NaB0.6HClAlFe. The promotion with cobalt does not change the performances significatively in all the temperature window. Maximum at 400°C with 84% of conversion while NaB0.6AlFe is 80 % at 400 °C.

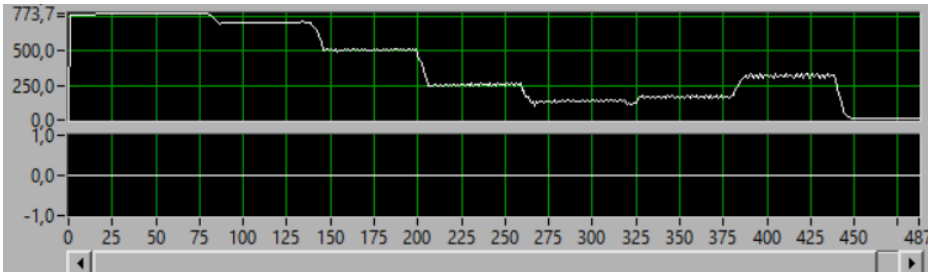

Figure 4.10: NO flow for NaB0.8HClAlFeCe

As a conclusion for samples presented in 4.2.2, 4.2.3, 4.2.4 and 4.2.5. the range of temperatures with higher catalytic activity is at 350°C. For this range all samples present:

B0.6ACIDAlFe/NaB0.6ACIDAlFe<B0.6ACIDAl/CoFe/NaB0.6ACIDAl/CoFe<B0.6ACIDAlFeCe/NaB0.6ACIDAlFeCe

4.2.6 Catalytic performances for samples impregnated with iron species

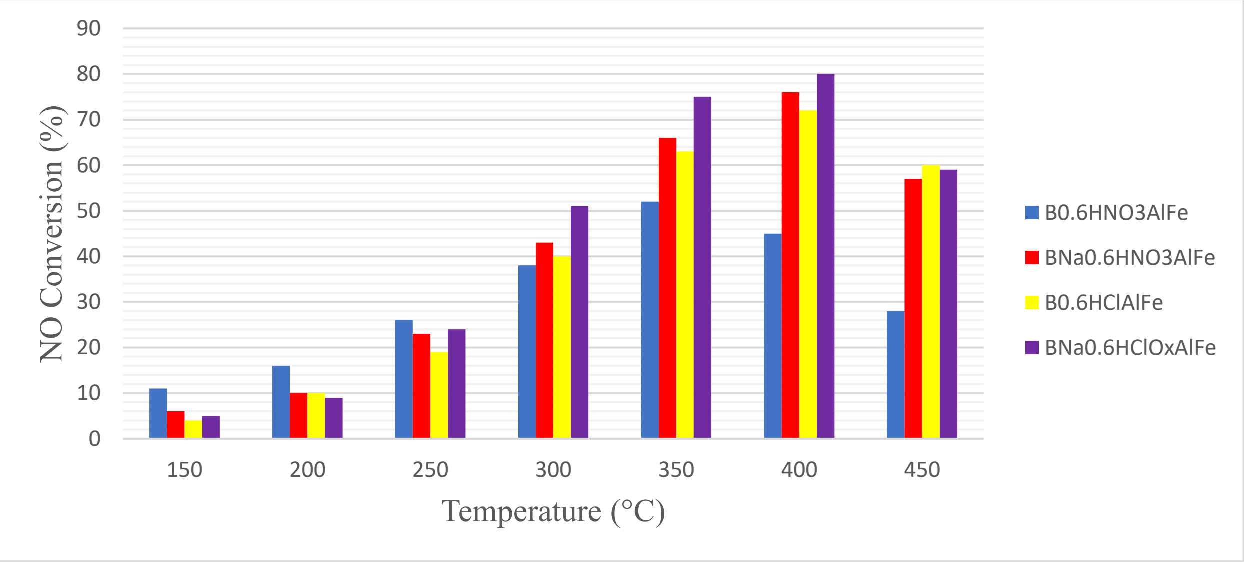

Figure 4.11: NO conversion (%) for samples impregnated with iron species

Fig 4.11 shows NO conversion (%) for B0.6HNO3AlFe, NaB0.6HNO3AlFe, B0.6HClAlFe and NaB0.6HClAlFe. It is visible that all the samples exchanged with NaCl (1 M) present higher activities in the range from 300°C to 400°C. In this range all the catalysts exchanged with HCl present higher activities than the sample with HNO_3. This has been confirmed by x-ray for pillaring and by UV-vis for the presence of iron species. NaB0.6HClAlFe presents a bigger amount of Fe_xO_y clusters in the interlayer space or at the surface of the material while B0.6HNO3AlFe a higher amount of Fe_2O_3 that can block the pores. B0.6HNO3AlFe presents the lowest activities, pillaring went wrong. It presents higher activity only at 150°C but in this range SCR-NH_3 test can have some settings problems so it is not such reliable and the experimental errors must always be considered.

4.2.7 Catalytic performances with the increase of acid concentration

In this subsection the results of B0.8HNO3AlFe, NaB0.8HNO3AlFe, B0.8HClAlFe and NaB0.8HClAlFe are reported in Fig 4.12 and Tab 4.6.

Table 4.6: NO Conversion (%) of B0.8HNO3AlFe, NaB0.8HNO3AlFe, B0.8HClAlFe and NaB0.8HClAlFe

Temperature (°C)	**NO Conversion (%)**			
	B0.8HNO3AlFe	NaB0.8HNO3AlFe	B0.8HClAlFe	NaB0.8HClAlFe
150	9	10	9	10
200	12	22	10	17
250	23	33	24	34
300	43	59	29	58
350	69	79	46	79
400	75	79	60	83
450	55	60	52	69

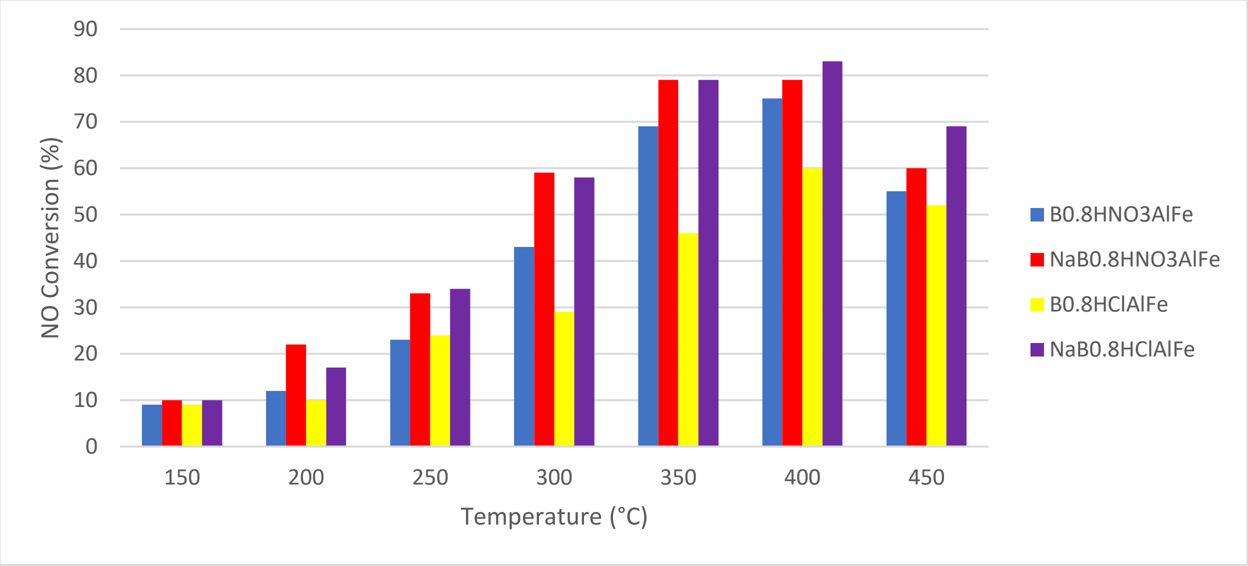

Figure 4.12: NO Conversion (%) of B0.8HNO3AlFe, NaB0.8HNO3AlFe, B0.8HClAlFe and NaB0.8HClAlFe.

The conclusion reached for samples treated with 0.6M of HNO_3 and HCl are the same with the increase of acid treatment (0.8M). All the samples treated with NaCl (1M) have higher catalytic activities. This difference is more visible for HCl in all the window of temperature. For HNO_3 treated bentonite the differences from NaB and B are very low. With the increase of acid concentration there are not such differences in the activities compared to the samples treated with 0.6 M of acid. The maximum value for 0.6 M of acid is 80% of NO conversion for NaB0.6HClAlFe at 400°C and in this case is 83% for NaB0.8HClAlFe at the same temperature.

The influence of the type of acid is different, not all the samples exchanged with HCl present higher activities, this means that there is not the possibility to give any conclusion about which acid gives better activities. B0.8HClAlFe resulted as the less stable with the increase of temperature by TG and it is also the catalysts with the lower catalytic performances.

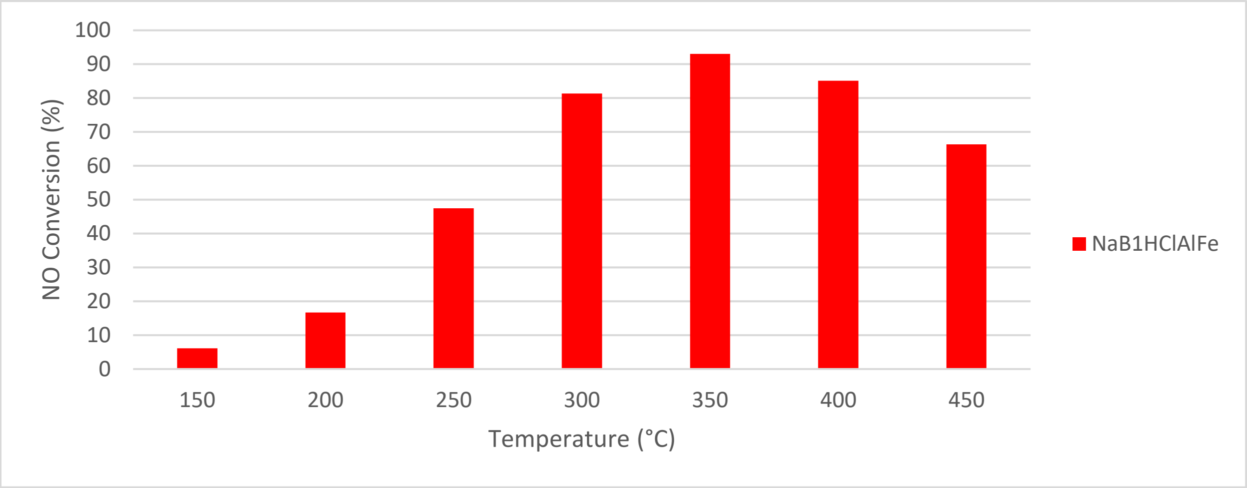

Figure 4.13: NO Conversion (%) of NaB1HClAlFe

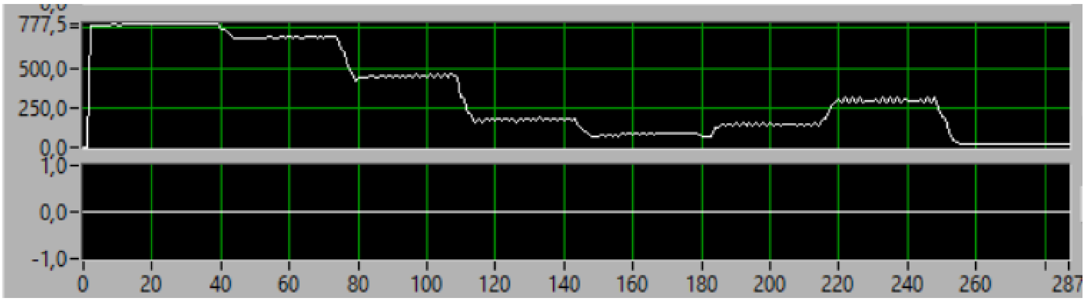

Figure 4.14: NO flow of NaB1HClAlFe

Fig. 4.13 shows the catalytic activities of NaB1HClAlFe. In this case the increase of the acid treatment (1 M of HCl) has good consequences on the catalytic test. X-ray of this sample explained the formation of a delaminated structure.

4.2.8 Catalytic performances for samples without the active phase

The activity of the support has also been analysed after pillaring and acid activation for B0.6HNO3Al, B0.6HClAl, NaB0.8HNO3Al and NaB0.8HClAl

Table 4.7: NO Conversion (%) for B0.6HNO3Al, B0.6HClAl, NaB0.8HNO3Al and NaB0.8HClAl

Temperature	**NO Conversion (%)**			
	B0.6HNO3Al	B0.6HClAl	NaB0.8HNO3Al	NaB0.8HClAl
150	4 (4)	5	6 (4)	6

200	4 (4)	6	8 (4)	7
250	5 (5)	6	13 (5)	12
300	10 (5)	10	19 (5)	16
350	14 (6)	18	25 (7)	22
400	21 (7)	25	30 (7)	26
450	24 (4)	25	32 (4)	27

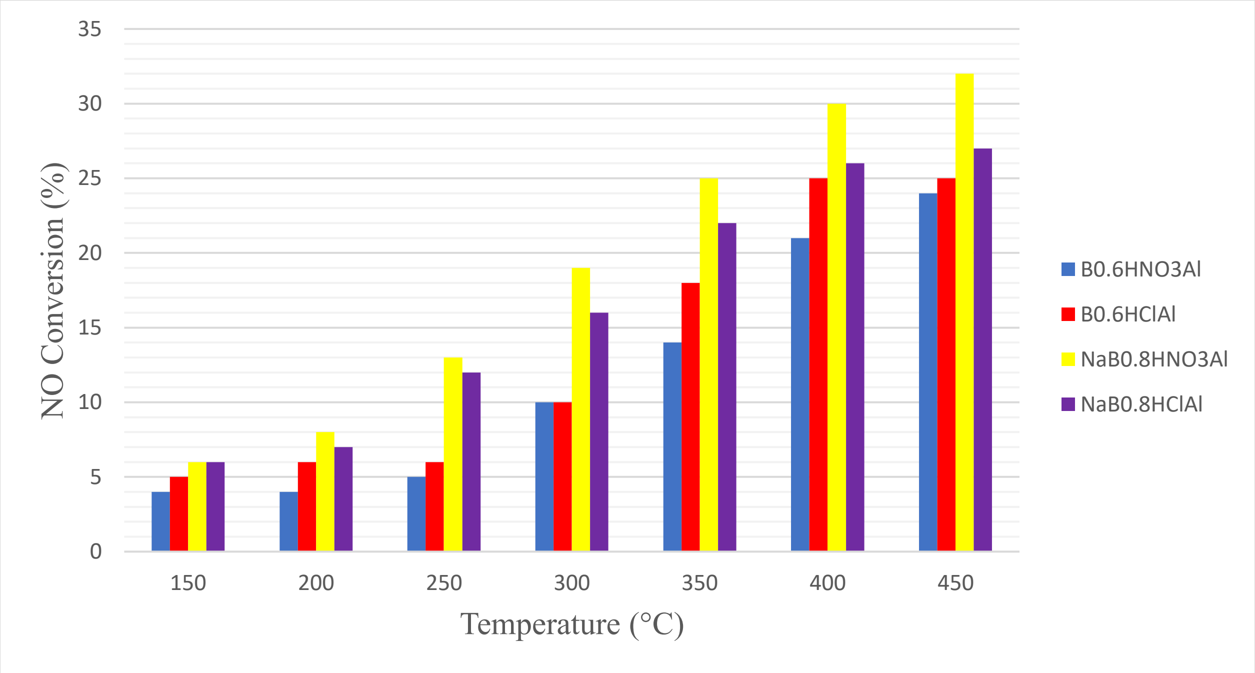

Figure 4.15: NO Conversion (%) for B0.6HNO3Al, B0.6HClAl, NaB0.8HNO3Al and NaB0.8HClAl

Modifications steps for B and NaB have increased the catalytic activities. The values are among 20% and 30% of NO conversion in the ranges 350 /400 /450 °C, without the decrease of activity in the range 450 °C due to the oxidation of NH_3.

However, without the active phase modified and treated supports cannot be considered as good and efficient catalysts, even though modifications changed the properties of bentonite and gave some higher catalytic efficiencies. (from 7 % of B). Higher catalytic activities are shown for NaB0.8HNO3Al, the surface area of this sample is bigger, the pillaring shifted 001 peak at 2θ= 4.2°. Lower activity trends instead are reported for B0.6HNO3Al the pillaring did not occur, and the acid activation does not change the structure the presence of acidic sites can increase the efficiency of NO removal. The effects of the treatments are compared to the NO conversion of B and NaB (number in brackets). At lower temperatures the modified support does not present any changes from B and NaB conversion.

4.2.9 N_2O Formation

The selectivity to N_2 is confirmed by the amount of N_2O emitted are very low (the experimental error is ca. 30 ppm).

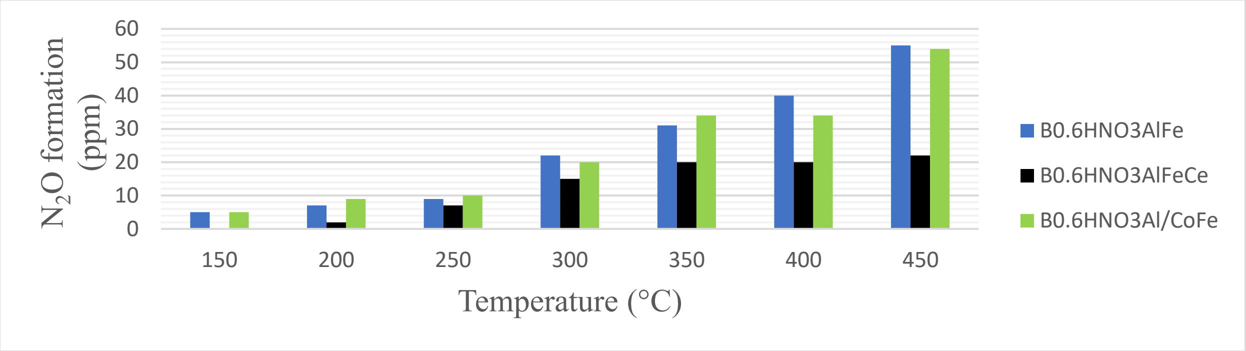

Figure 4.16: N_2O formation (ppm) for B0.6HNO3AlFe, B0.6HNO3AlFeCe and B0.6HNO3Al/CoFe

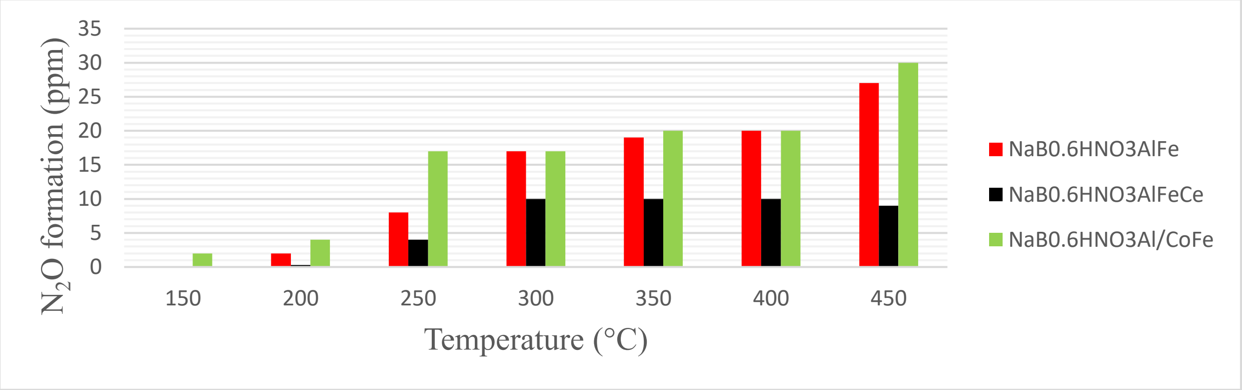

Figure 4.17: N_2O formation (ppm) for NaB0.6HNO3AlFe, NaB0.6HNO3AlFeCe and NaB0.6HNO3Al/CoFe

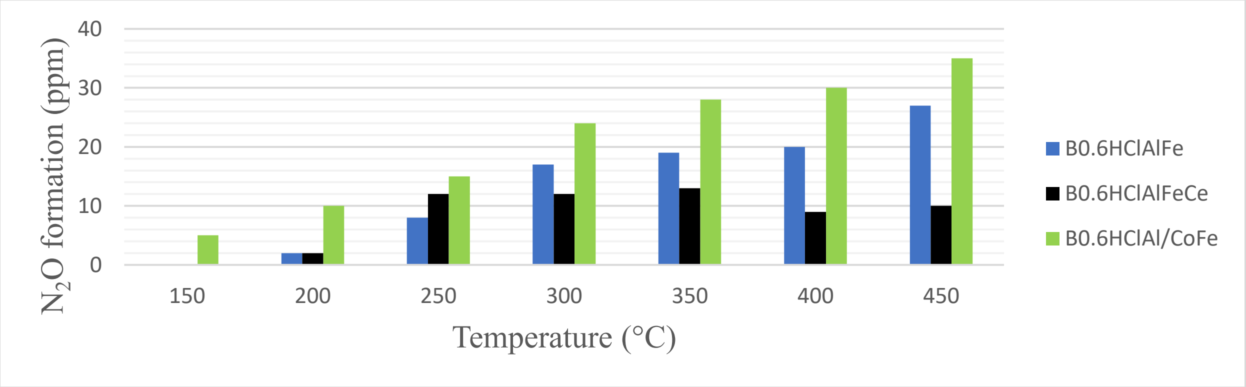

Figure 4.18: N_2O formation (ppm) for B0.6HClAlFe, B0.6HClAlFeCe and B0.6HClAl/CoFe

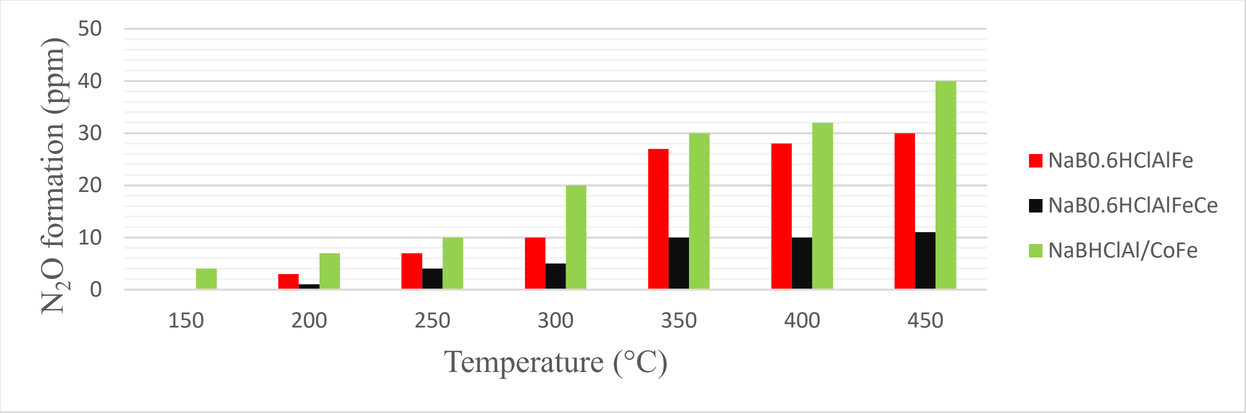

Figure 4.19: N_2O formation (ppm) for NaB0.6HClAlFe, NaB0.6HClAlFeCe and NaB0.6HClAl/CoFe

Amount of N_2O are very low considering 30 ppm of experimental error, only at 450° there are some visible of N_2O. 24 ppm for B0.6HNO3Al/CoFe, 3 ppm for B0.6HClAl/CoFe and 10 ppm for NaB0.6HClAl/Co at 450 °C. 25 ppm for B0.6HNO3AlFe at 450 °C. All the other samples are present values of N_2O lower than the experimental value (30 ppm).

Chapter 5 – Conclusions

The aim of this work has been the preparation of active catalysts for the removal of NO in SCR-NH_3. A natural layered clay such as bentonite has been modified following the preparation steps reported in Chapter 2 and tested as NH_3- SCR catalyst.

The impregnation with iron and cerium species has been investigated by XRD and UV-vis, which provided the introduction of Fe- and Ce- active phases. By the way, the amount of these species is very low and XRD cannot confirmed any crystallite form of iron (only for B0.6HNO3AlFe it was confirmed the presence of Fe_2O_3). For all the other samples, all the reflections of iron and cerium oxides are overlapped by the reflections of the main components of Bentonite visible in the pattern without the impregnation step. Amorphous forms of iron and cerium oxides cannot be excluded. XRD gives information about pillaring step considering the increasing of $d_{001.}$ If the pillaring went wrong 001 peak remains in the same position otherwise its value decrease. By increasing the acid concentration during acid treatment, a delaminated structure is formed with the presence of possible pseudo pillars, higher numbers of acidic sites which give better accessibility to the molecules and an increase in the catalytic performances of the sample. This is confirmed for NaB1HClAlFe.

UV-vis spectra identify the position of Fe^{3+}, for all the samples all the possible ranges for iron species have been confirmed (isolated Fe^{3+} in tetrahedral coordination, isolated Fe^{3+} in octahedral coordination and small oligonuclear Fe_xO_y clusters and dispersed Fe_2O_3 particles). The spectra of the starting material did not confirm any presences of iron species and the addition of cerium species by impregnation cannot be recognized due to its overlap with the absorption of iron species in the same ranges. By FT-IR analysis the spectra of NaB and B have been compared with the spectra of bentonite found in literature studies. All the main bonds in the starting materials have been identified. FT-IR analysis shows that the following steps of the preparation of samples (acid treatment, pillaring and impregnation) did not influence the main bonds of pure bentonite.
TG analysis reports two main ranges of weight loss of water: low temperature water loss (Δm_l (%)) for the physiosorbed water and the high temperature water loss (Δm_h (%)) for the dehydration and dehydroxylation of clay layers. All the sample present very high thermal stability, Δm_h% is closed to 1 % for all the samples. Only for B0.8HClAlFe is higher (2.5 %). A consequence of the introduction of mixed pillared oxides is the improvement of the thermal stability of samples. This is confirmed from the results. Δm_h (%) for NaB0.6HNO3Al/CoFe and NaB0.6HClAl/CoFe is 0.5%.

By the catalytic test, all the samples treated with NaCl solution (1 M) present higher catalytic activities. Na^+ has higher CEC. For the preparation of an “acid” saturated clay is important the pre-saturation of the clay with Na^+. H^+ of the acid replaced easily Na^+, a high degree of Na saturation is in fact important for a better dispersion of bentonite and efficient acid treatments. The saturation with Na^+ in fact allows better results in the H^+ saturation. The treatment with two types of acid (HNO_3 and HCl) did not result in any bigger differences in the catalytic activity. FT-IR spectra of samples treated with HNO_3 does not show any presences of NO^-_3. This means that the sample have been completely washed from the anions of the acid, soluble in water. Samples treated with HCl (0.6 M) present higher catalytic activities at 350°C than the samples treated with HNO_3 (0.6 M).

On the other hand, samples treated with HCl (0.8 M) do not present higher catalytic activities than the samples treated with HNO_3 (0.8 M). These differences depend only on the modification steps (acid treatments, pillaring and impregnation) which can be affected by experimental conditions. Different conclusion could have been carried out if starting material (bentonite) has not been pure. Bentonite can be substituted in the octahedral coordination by different cations such as iron species. The removal of iron in the raw material is more efficient with HCl than with HNO_3, but for the catalytic activity may be the opposite. Raw bentonites that have more concentration of iron present higher catalytic activity. For this reason, the treatment with HNO_3 could have been more efficient if the starting material was not extra pure.[73]

The introduction of cobalt as a mixed pillared agent increases the thermal stability and the catalytic activities mostly at 400°C compared to the samples pillared only with Al. Cobalt has different oxidation states (suitable for redox reactions), the presence of Cobalt gives a good performance in NH_3-SCR.

The addition of Ce can increase the accumulation and exchange of oxygen at low temperatures. CeO_2 has prominent oxygen storage capacity, the addition of CeO_x improved catalytic activity of the pillared layered clay impregnated also with iron. The beneficial effect of Ce is explained by its ability to store oxygen and redox rection : $CeO_2 \leftrightarrow CeO_{2-x} + \frac{x}{2} O_2$. All the sample impregnated with cerium species present the highest catalytic activities. The best catalysts prepared in this work is NaB0.6HNO3AlFeCe at 350°C with 93 % of NO conversion.

This work has demonstrated that, with different modifications, pure bentonite and Na-Bentonite, which do not present any catalytic activities (7% of NO removal as the maximum value), can be transformed into good catalysts for the removal of NOx, reaching NO conversions above 90%. The materials chosen are active in NO conversion and selective to N_2 and they have big potentials to replace commercial catalysts in SCR-NH_3.

References

[1] Russo; Piumetti, “Notes on Catalysis for Environment and Energy.” C.L.U.T - Politecnico di Torino.

[2] B. LÜBKERT-ALCAMO, “The update and revision of the 1987 WHO air quality guidelines (WHO european centre for environment and health),” *Pollut. atmosphérique*, vol. 36, no. 144, pp. 95–101, 1994.

[3] C. Ernst, “The New England Journal of Medicine Downloaded from nejm.org at GALTER HEALTH SCIENCES LIBRARY on August 9, 2011. For personal use only. No other uses without permission. Copyright © 1993 Massachusetts Medical Society. All rights reserved.,” *N. Engl. J. Med.*, vol. 328, pp. 1167–1172, 1993.

[4] M. Ivanova, “Designing the United Nations Environment Programme: A story of compromise and confrontation,” *Int. Environ. Agreements Polit. Law Econ.*, vol. 7, no. 4, pp. 337–361, 2007, doi: 10.1007/s10784-007-9052-4.

[5] B. Ostro, A. Prüss-üstün, D. Campbell-lendrum, C. Corvalán, and A. Woodward, “Outdoor air pollution: Assessing the environmental burden of disease at national and local levels,” *World Heal. Organ. Prot. Hum. Environ. Geneva*, no. Environmental Burden of Disease Series, No. 5, 2004.

[6] E. European Environment Agency, “National Emission Ceilings Directive,” pp. 5–12, 2018.

[7] J. Li, Suyoulema, W. Wang, and Sarina, “A study of photodegradation of sulforhodamine B on Au-TiO2/bentonite under UV and visible light irradiation,” *Solid State Sci.*, vol. 11, no. 12, pp. 2037–2043, 2009, doi: 10.1016/j.solidstatesciences.2009.09.012.

[8] X. Q. Jiang, X. D. Mei, and D. Feng, “Air pollution and chronic airway diseases: What should people know and do?,” *J. Thorac. Dis.*, vol. 8, no. 1, pp. E31–E40, 2016, doi: 10.3978/j.issn.2072-1439.2015.11.50.

[9] Marshall James L, M. J. L, and M. V. R, “Rediscovery of the Elements: Paracelsus,” *Hexag. Alpha Chi Sigma*, no. Winter, pp. 71–8, 2005.

[10] H. A. Bernthsen, “The Synthesis of Ammonia from its Elements-II,” *Sci. Am.*, vol. 74, no. 1930supp, pp. 410–411, 1912, doi: 10.1038/scientificamerican12281912-410supp.

[11] M. Zajemska, A. Poskart, and D. Musiał, “The kinetics of nitrogen oxides formation in the flame gas,” *Econ. Environ. Stud.*, vol. 15, no. 4, pp. 445–460, 2015.

[12] J. F. Rohr, “Control of Nitrogen Oxides Emissions Control of Nitrogen Oxides Emissions Student Manual,” vol. 19090, no. x.

[13] Herdiana, *Pillared Clays and Related Catalysts*, vol. 53, no. 9. 2013.

[14] E. Environment Agency, “Emissions of the main air pollutants in Europe,” *Https://Www.Eea.Europa.Eu/Data-and-Maps/Indicators/Main-Anthropogenic-Air-*

Pollutant-Emissions/Assessment-4, 2019.

[15] I. Assessment, “Nitrogen Oxides (NOx),” pp. 247–325, 2003, doi: 10.1201/9780203912782.pt2.

[16] M. Skrętowicz, L. Sitnik, A. Kaźmierczak, and M. Magdziak-Tokłowicz, “Evaluation Methods of the Impact of Motorization on the Quality of the Atmospheric Air,” *J. KONES. Powertrain Transp.*, vol. 21, no. 4, pp. 445–452, 2014, doi: 10.5604/12314005.1130507.

[17] Ministry of Energy, “Extract from the draft of Energy of Poland until 2040 (EPP2040),” vol. 2040, 2018.

[18] W. Cycles, F. Wave, and R. Core, “USUWANIE TLENKÓW AZOTU ZE SPALIN KOTŁÓW PYŁOWYCH,” *Aerosp. Eng.*, p. 128, 1993.

[19] Environmental Protection Agency (EPA), “Nitrogen oxides (NOx), why and how they are controlled,” *Epa-456/F-99-006R*, no. November, p. 48, 1999, doi: EPA 456/F-99-006R.

[20] B. M. D. Tillman, “combustion engineering issues,” *J. Chem. Inf. Model.*, vol. 53, no. 9, pp. 1689–1699, 2013, doi: 10.1017/CBO9781107415324.004.

[21] K. Skalska, J. S. Miller, and S. Ledakowicz, *Nitrogen Oxides Removal by SCR Process – State of The Art*, vol. 7, no. 7. 2013.

[22] C. Locci, L. Vervisch, B. Farcy, P. Domingo, and N. Perret, “Selective Non-catalytic Reduction (SNCR) of Nitrogen Oxide Emissions: A Perspective from Numerical Modeling,” *Flow, Turbul. Combust.*, vol. 100, no. 2, pp. 301–340, 2018, doi: 10.1007/s10494-017-9842-x.

[23] M. Armitage, “Integrated pollution prevention and control (IPPC),” *Foundryman*, vol. 91, no. 6, pp. 193–195, 1998.

[24] G. Busca, L. Lietti, G. Ramis, and F. Berti, “Chemical and mechanistic aspects of the selective catalytic reduction of NO(x) by ammonia over oxide catalysts: A review,” *Appl. Catal. B Environ.*, vol. 18, no. 1–2, pp. 1–36, 1998, doi: 10.1016/S0926-3373(98)00040-X.

[25] L. Han *et al.*, “Selective Catalytic Reduction of NOx with NH3 by Using Novel Catalysts: State of the Art and Future Prospects,” *Chem. Rev.*, vol. 119, no. 19, pp. 10916–10976, 2019, doi: 10.1021/acs.chemrev.9b00202.

[26] D. L. Trimm, “Economic Importance of Catalysts,” *CEA, Chem. Eng. Aust.*, vol. ChE 5, no. 3, pp. 31–36, 1980, doi: 10.1038/122802b0.

[27] M. Mladenović, M. Paprika, and A. Marinković, “Denitrification techniques for biomass combustion,” *Renew. Sustain. Energy Rev.*, vol. 82, no. September, pp. 3350–3364, 2018, doi: 10.1016/j.rser.2017.10.054.

[28] T. Grzybek, “Layered clays as SCR deNOx catalysts,” *Catal. Today*, vol. 119, no. 1–4, pp. 125–132, 2007, doi: 10.1016/j.cattod.2006.08.006.

[29] D. Wierzbicki, R. Debek, M. Motak, T. Grzybek, M. E. Gálvez, and P. Da Costa, “Novel Ni-La-hydrotalcite derived catalysts for CO2 methanation,” *Catal. Commun.*, vol. 83, pp. 5–8, 2016, doi: 10.1016/j.catcom.2016.04.021.

[30] B. Samojeden, T. Grzybek, A. Szymaszek, O. Ligęza, W. Kowalczyk, and M. Motak, “The application of modified cenospheres in DeNOx process,” *E3S Web Conf.*, vol. 108, 2019, doi: 10.1051/e3sconf/201910802019.

[31] B. Samojeden and T. Grzybek, “The influence of the promotion of N-modified activated carbon with iron on NO removal by NH3-SCR (Selective catalytic reduction),” *Energy*, vol. 116, pp. 1484–1491, 2016, doi: 10.1016/j.energy.2016.04.059.

[32] M. Motak, “Montmorillonites modified with polymer and promoted with copper as DeNOx catalysts,” *Catal. Today*, vol. 137, no. 2–4, pp. 247–252, 2008, doi: 10.1016/j.cattod.2008.02.001.

[33] E. M. Serwicka and K. Bahranowski, “Environmental catalysis by tailored materials derived from layered minerals,” *Catal. Today*, vol. 90, no. 1–2, pp. 85–92, 2004, doi: 10.1016/j.cattod.2004.04.012.

[34] A. Aihemaiti *et al.*, “Review of plant-vanadium physiological interactions, bioaccumulation, and bioremediation of vanadium-contaminated sites,” *Sci. Total Environ.*, vol. 712, p. 135637, 2020, doi: 10.1016/j.scitotenv.2019.135637.

[35] X. Zhang, B. Shen, K. Wang, and J. Chen, “A contrastive study of the introduction of cobalt as a modifier for active components and supports of catalysts for NH3-SCR,” *J. Ind. Eng. Chem.*, vol. 19, no. 4, pp. 1272–1279, 2013, doi: 10.1016/j.jiec.2012.12.028.

[36] J. Carriazo, E. Guélou, J. Barrault, J. M. Tatibouët, R. Molina, and S. Moreno, “Synthesis of pillared clays containing Al, Al-Fe or Al-Ce-Fe from a bentonite: Characterization and catalytic activity,” *Catal. Today*, vol. 107–108, pp. 126–132, 2005, doi: 10.1016/j.cattod.2005.07.157.

[37] F. Bergaya, B. K. G. Theng, and G. Lagaly, *Handbook of Clay Science*, vol. 1, no. 2. 2006.

[38] s. Guggenheim and R. T. Martin, “Definition of clay and clay mineral: joint report of the AIPEA and CMS Nomenclature Committees,” *Clay Miner.*, vol. 30, no. 3, pp. 257–259, 1995, doi: 10.1180/claymin.1995.030.3.09.

[39] Assessment and Teaching of 21st Century Skills, “Clays, Clay Minerals, and Clay Science,” *J. Chem. Inf. Model.*, vol. 53, no. 9, pp. 1689–1699, 2013, doi: 10.1017/CBO9781107415324.004.

[40] F. A. Andrade, H. A. Al-Qureshi, and D. Hotza, “Measuring the plasticity of clays: A review,” *Appl. Clay Sci.*, vol. 51, no. 1–2, pp. 1–7, 2011, doi: 10.1016/j.clay.2010.10.028.

[41] J. Wimpenny, “Clay minerals,” *Encycl. Earth Sci. Ser.*, pp. 265–275, 2018, doi: 10.1346/ccmn.1982.0300513.

[42] *Origin and Mineralogy of Clays*. 1995.

[43] “Preparation of Na saturated montmorillonites.” University of California, California.

[44] B. Samojeden and M. Motak, “The characteristics of modified layered aluminosilicates as catalysts for VOC oxidation,” p. 166183, 2011.

[45] V. V. Krupskaya *et al.*, “Experimental study of montmorillonite structure and

transformation of its properties under treatment with inorganic acid solutions," *Minerals*, vol. 7, no. 4, pp. 1–15, 2017, doi: 10.3390/min7040049.

[46] P. Komadel and J. Madejová, "Chapter 7.1 Acid Activation of Clay Minerals," *Dev. Clay Sci.*, vol. 1, no. C, pp. 263–287, 2006, doi: 10.1016/S1572-4352(05)01008-1.

[47] P. Pushpaletha, S. Rugmini, and M. Lalithambika, "Correlation between surface properties and catalytic activity of clay catalysts," *Appl. Clay Sci.*, vol. 30, no. 3–4, pp. 141–153, 2005, doi: 10.1016/j.clay.2005.03.011.

[48] J. Madejová *et al.*, "Characterization of products obtained by acid leaching of Fe-bentonite," *Clay Miner.*, vol. 42, no. 4, pp. 527–540, 2007, doi: 10.1180/claymin.2007.042.4.09.

[49] P. Falaras, F. Lezou, G. Seiragakis, and D. Petrakis, "Bleaching properties of alumina-pillared acid-activated montmorillonite," *Clays Clay Miner.*, vol. 48, no. 5, pp. 549–556, 2000, doi: 10.1346/CCMN.2000.0480507.

[50] M. S. Barrios, L. V. F. González, M. A. V. Rodríguez, and J. M. M. Pozas, "Acid activation of a palygorskite with HCl: Development of physico-chemical, textural and surface properties," *Appl. Clay Sci.*, vol. 10, no. 3, pp. 247–258, 1995, doi: 10.1016/0169-1317(95)00007-Q.

[51] E. L. Foletto, G. C. Colazzo, C. Volzone, and L. M. Porto, "Sunflower oil bleaching by adsorption onto acid-activated bentonite," *Brazilian J. Chem. Eng.*, vol. 28, no. 1, pp. 169–174, 2011, doi: 10.1590/S0104-66322011000100018.

[52] P. Salerno and S. Mendioroz, "Preparation of Al-pillared montmorillonite from concentrated dispersions," *Appl. Clay Sci.*, vol. 22, no. 3, pp. 115–123, 2002, doi: 10.1016/S0169-1317(02)00133-3.

[53] F. R. V Días and S. P. S., "Studies on the acid activation of brazilian smectitic clays," *Quim. Nova*, vol. 24, no. 3, pp. 345–353, 2001.

[54] A. Gil, L. M. Gandía, and M. A. Vicente, "Recent Advances in the Synthesis and Catalytic Applications of Pillared Clays," *Catal. Rev. - Sci. Eng.*, vol. 42, no. 1–2, pp. 145–212, 2000, doi: 10.1081/CR-100100261.

[55] "D. M. Moore, R. C. Reynolds, X-Ray Diffraction and the Identification and Analysis of Clay Minerals. Oxford University Press, Oxford.," vol. 322. p. 321, 1997.

[56] J. Madejová, "FTIR techniques in clay mineral studies," *Vib. Spectrosc.*, vol. 31, no. 1, pp. 1–10, 2003, doi: 10.1016/S0924-2031(02)00065-6.

[57] B. H. Stuart, *Infrared Spectroscopy: Fundamentals and Applications*. 2005.

[58] L. Zhirong, M. Azhar Uddin, and S. Zhanxue, "FT-IR and XRD analysis of natural Na-bentonite and Cu(II)-loaded Na-bentonite," *Spectrochim. Acta - Part A Mol. Biomol. Spectrosc.*, vol. 79, no. 5, pp. 1013–1016, 2011, doi: 10.1016/j.saa.2011.04.013.

[59] Q. Huang, S. Zuo, and R. Zhou, "Catalytic performance of pillared interlayered clays (PILCs) supported CrCe catalysts for deep oxidation of nitrogen-containing VOCs," *Appl. Catal. B Environ.*, vol. 95, no. 3–4, pp. 327–334, 2010, doi: 10.1016/j.apcatb.2010.01.011.

[60] Z. Vuković, A. Milutonović, L. Rožić, A. Rosić, Z. Nedić, and D. Jovanović, “The influence of acid treatment on the composition of bentonite,” *Clays Clay Miner.*, vol. 54, no. 6, pp. 697–702, 2006, doi: 10.1346/CCMN.2006.0540605.

[61] B. Tyagi, C. D. Chudasama, and R. V. Jasra, “Determination of structural modification in acid activated montmorillonite clay by FT-IR spectroscopy,” *Spectrochim. Acta - Part A Mol. Biomol. Spectrosc.*, vol. 64, no. 2, pp. 273–278, 2006, doi: 10.1016/j.saa.2005.07.018.

[62] J. Madejová, J. Bujdák, M. Janek, and P. Komadel, “Comparative FT-IR study of structural modifications during acid treatment of dioctahedral smectites and hectorite,” *Spectrochim. Acta - Part A Mol. Biomol. Spectrosc.*, vol. 54, no. 10, pp. 1397–1406, 1998, doi: 10.1016/S1386-1425(98)00040-7.

[63] J. Temuujin, T. Jadambaa, G. Burmaa, S. Erdenechimeg, J. Amarsanaa, and K. J. D. MacKenzie, “Characterisation of acid activated montmorillonite clay from Tuulant (Mongolia),” *Ceram. Int.*, vol. 30, no. 2, pp. 251–255, 2004, doi: 10.1016/S0272-8842(03)00096-8.

[64] J. Moma, J. Baloyi, and T. Ntho, “Synthesis and characterization of an efficient and stable Al/Fe pillared clay catalyst for the catalytic wet air oxidation of phenol,” *RSC Adv.*, vol. 8, no. 53, pp. 30115–30124, 2018, doi: 10.1039/c8ra05825c.

[65] F. Bertella and S. B. C. Pergher, “Pillaring of bentonite clay with Al and Co,” *Microporous Mesoporous Mater.*, vol. 201, no. C, pp. 116–123, 2015, doi: 10.1016/j.micromeso.2014.09.013.

[66] J. Li, T. Li, H. Ma, Q. Sun, W. Ying, and D. Fang, “Effect of impregnating Fe into p-modified hzsm-5 in the coupling cracking of butene and pentene,” *Ind. Eng. Chem. Res.*, vol. 54, no. 6, pp. 1796–1805, 2015, doi: 10.1021/ie504629p.

[67] J. Pérez-Ramírez *et al.*, “Evolution of isomorphously substituted iron zeolites during activation: Comparison of Fe-beta and Fe-ZSM-5,” *J. Catal.*, vol. 232, no. 2, pp. 318–334, 2005, doi: 10.1016/j.jcat.2005.03.018.

[68] A. Bensalem, F. Bozon-Verduraz, M. Delamar, and G. Bugli, “Preparation and characterization of highly dispersed silica-supported ceria,” *Appl. Catal. A, Gen.*, vol. 121, no. 1, pp. 81–93, 1995, doi: 10.1016/0926-860X(95)85012-0.

[69] C. hai WEI, X. hu TANG, J. rong LIANG, and S. ying TAN, “Preparation, characterization and photocatalytic activities of boron- and cerium-codoped TiO2,” *J. Environ. Sci.*, vol. 19, no. 1, pp. 90–96, 2007, doi: 10.1016/S1001-0742(07)60015-1.

[70] Q. Sun, W. Zhang, and H. Qian, “Effects of high temperature thermal treatment on the physical properties of clay,” *Environ. Earth Sci.*, vol. 75, no. 7, 2016, doi: 10.1007/s12665-016-5402-2.

[71] H. Ma, Q. Ya, Y. Fu, C. Ma, and X. Dong, “Synthesis of zeolite of type a from bentonite by alkali fusion activation using na2co3,” *Ind. Eng. Chem. Res.*, vol. 49, no. 2, pp. 454–458, 2010, doi: 10.1021/ie901205y.

[72] A. K. Panda, B. G. Mishra, D. K. Mishra, and R. K. Singh, “Effect of sulphuric acid treatment on the physico-chemical characteristics of kaolin clay,” *Colloids Surfaces A*

Physicochem. Eng. Asp., vol. 363, no. 1–3, pp. 98–104, 2010, doi: 10.1016/j.colsurfa.2010.04.022.

[73] L. Bieseki, F. Bertella, H. Treichel, F. G. Penha, and S. B. C. Pergher, “Acid treatments of montmorillonite-rich clay for fe removal using a factorial design method,” *Mater. Res.*, vol. 16, no. 5, pp. 1122–1127, 2013, doi: 10.1590/S1516-14392013005000114.

Ringraziamenti

È difficile sintetizzare in una pagina i miei ringraziamenti, tante sono le persone che sono entrate nella mia vita universitaria, a cui vorrei dedicare un pensiero e grazie alle quali sono arrivata oggi fino a qua.

Dedico questa laurea in primis alla mia famiglia, a mia mamma, a mio papa e a mia sorella, che mi hanno da sempre sostenuto in tutte le scelte, anche in quelle che mi hanno portato ad allontanarmi fisicamente sempre di più, ma mai con il cuore.

A mia nonna e a mio nonno, che saprebbero raggiungermi anche nel più lontano angolo sperduto del mondo, a cui devo la persona che sono oggi, i quali mi hanno trasmesso la passione di esplorare e viaggiare.

A tutta la mia famiglia, così forte e unita: ai miei zii, all'altra mia nonna e ai miei cugini.

E poi alla mia famiglia per scelta: i miei amici.

A Susanna, la mia migliore amica, alla nostra amicizia che riesce a superare qualunque distanza spaziale e temporale.

A Michela e ad Agnese, all'aver trasformato una semplice convivenza in un rapporto tra sorelle.

A Sara, alle nostre pazzie, al nostro essere sincronizzate a distanza di chilometri e a tutti i bicchieri condivisi.

A Tintin, a cui devo il suo aiuto nei momenti di crisi universitari, all'aver condivido le nostre ansie esistenziali.

A Giulia, mia 38, a Stefano e ai nostri kebab, a Valentina, Roberta e Andrea, coloro che sono gli amici di sempre.

Alla mia coinquilina Mihaela (big sister), mio grande conforto nei mesi di stesura della tesi.

E a tutte le persone che hanno condiviso con me la quotidianità nei mesi di Erasmus, le quali sono sparse per l'Europa, ma che porterò sempre nel cuore.

A Torino, a Lione e a Cracovia, tre città che mi hanno aiutato a crescere e ho percepito come casa.